UK-RAS
CONFERENCE: *'ROBOTS WORKING FOR & AMONG US'* PROCEEDINGS
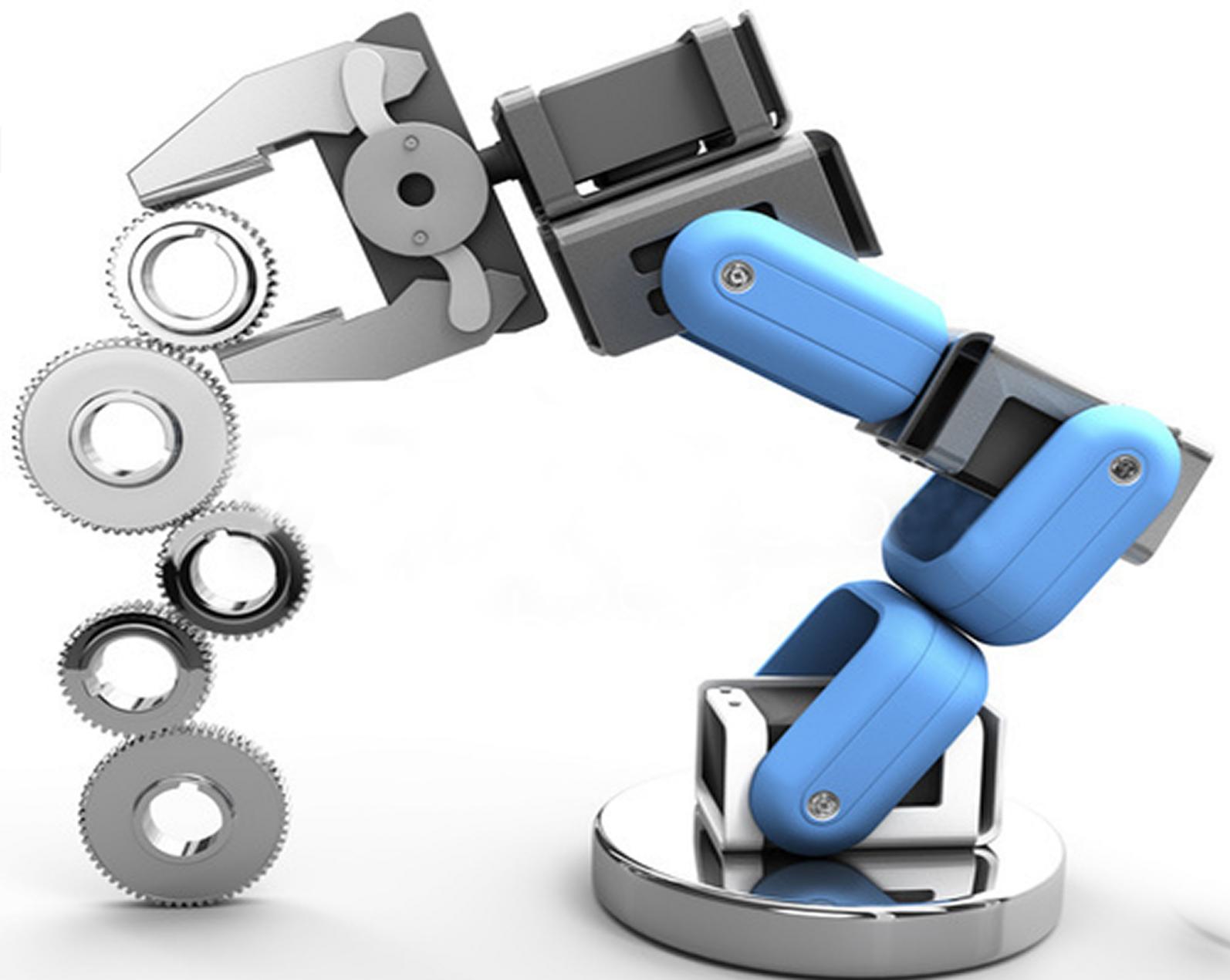
Table of Contents

Research Papers

Poster Papers

PREFACE

In mid-December 2017 around 120 attendees gathered in the Exhibition Centre adjacent to the Bristol Robotics Laboratory for the first UK-RAS Network (www.ukras.org) supported conference on Robotics and Autonomous Systems.

The primary goal of the event was to provide a forum, for early-stage researchers, many of whom were PhD students studying independently or in one of the EPSRC-funded Centres for Doctoral Training, to present their work to peers and more senior academics. As such, this event was designed to fit into an emerging UK niche that has arisen from the increasing scope and maturity of the UK's prime conference event TAROS.

Approximately 60 papers were accepted, and the standard was very high. A set of very wide-ranging application domains for advanced Robotics and Autonomous Systems and devices was presented and discussed at the meeting. The event format allowed either for a conventional podium presentation of the work, or a lunchtime poster session. In either case the written presentation was a two-page extended abstract.

To make the TAROS link explicit, the authors of the best of the papers presented at this event were each invited to develop their extended abstract into a full paper submission to be presented in a special UK-RAS conference session at TAROS 2018 (http://www.brl.ac.uk/taros2018.aspx from 25th to 27th July 2018).

A secondary goal of the conference was to expose these predominantly early-stage researchers to the complex debate around research and development Technology Readiness Levels (TRLs). As the RAS community matures, this is becoming a more and more pressing debate. Of course, fundamental low-TRL work is essential in order to "feed the innovation pipeline" but getting across the mid-TRL "Death Valley" is a more and more immediate problem in terms of creating and sustaining research impact.

To directly support this secondary goal, the four invited speakers were asked to refer, during their presentation, to their experiences in this respect. The four invited speakers were:

Dr. Praminda Caleb-Solly, Associate Professor at UWE/Head of Electronics & Computer Systems, Designability. Praminda talked about working in healthcare research and development at the boundaries between academia and industry with an emphasis on the deep involvement of the stakeholders and end-users of the services to be developed.

Dr. Lester Russell, Senior Director EMEA Scale Team, Intel Corporation. Lester drew on his combined skills and experience in clinical, commercial and health service roles to talk about the ways in which "the black box" of AI can be used for social good. By adopting ICT to improve healthcare he will highlight not only the potential applications for artificial intelligence in health and life sciences, but also the barriers to its adoption and practical implementation.

A

Prof. Rustam Stolkin, Chair in Robotics, Royal Society Industry Fellow, Birmingham University. Rustam talked about the challenges facing our community as it takes on the use of robotics in the nuclear industries, including making the connection between low Technology Readiness Level (TRL) fundamental academic research and high TRL R&D in close association with this very conservative industry.

Prof. Jim Scanlan, Professor in Design, Department of Engineering & Environment, Southampton University. Jim talked about his experiences in carrying out research in Extreme Environments Robotics, with a special focus on Emergency Response, Disaster Relief and Resilience. Similarly, Prof. Scanlan included dealing with the challenges of ascending the TRLs.

The event was a resounding success, with plans already in place for a second event in the Winter of 2018.

We would like to take this opportunity to express our special thanks to Profs. Sanja Dogramadzi and Manuel Giuliani for their great support throughout the preparations, and especially in carrying out many first stage reviews of the 60+ submitted papers. We would also like to express sincere thanks to the Executive Committee of the UK-RAS Network and all those who have supported the general organisation of the conference. Lastly, we would like to express our special thanks to Prof. Guang-Zhong Yang, Chairman of the UK-RAS Network and Director & Founder of the Hamlyn Centre, Imperial College London for devising the original ideas for this event and for his ongoing support for it.

Professor Tony Pipe (Bristol Robotics Laboratory) & Marianne Knight, UK-RAS Network Manager

Assessing Pose Features for Predicting User Intention during Dressing with Deep Networks

Greg Chance, Aleksandar Jevtić, Member, IEEE, Praminda Caleb-Solly, Guillem Alenyà, Member, IEEE, Carme Torras, Senior Member, IEEE, Sanja Dogramadzi

ABSTRACT

In an ageing population the need for assistive robotics has a great potential to address issues around the increasing demand for nursing and caregiving. Areas that robots may play a role are in helping with the activities of daily living (ADL) and dressing is the focus of this paper. Successful integration of these robots into society will require careful consideration of factors such as safety and interaction. We believe that these systems should be able to predict the user's intention for maximum safety and task efficiency. Using data collected from human-human interaction (HHI) experiments, features were prepared and assessed for importance and models were trained to classify the dressing task segment and which end effector to move; left, right or both simultaneously. Long short term-memory networks (LSTM) were explored to predict these outcomes one time-step ahead. The networks were assessed against a variety of hyper-parameters including the depth of the hidden layers. The models show promise for correctly classifying task segment based on user pose, with the best test accuracy >95%.

1. INTRODUCTION

ROBOTIC assisted dressing for those with mobility issues or cognitive impairment is an area of research gaining interest. It is estimated that by 2050, the proportion number of people aged 60 years and over is expected to total around 2 billion [11] accounting for nearly a quarter of the worlds population. With this ageing population comes an increase in the incidence and prevalence of diseases and disabilities which will require additional nurses and caregiving support workers which are in decline [2]. In the present paper we discuss analysis of our human- human interaction (HHI) data in order to predict intention of the user during the dressing task from information about their pose. The data was collected during a dressing task, where a user was given assistance from another human posing as a robot, see Fig. 1a.

Previous studies on robotic dressing have used vision systems as the primary modality of interaction using reflective markers [10], stereo cameras [9] and depth cameras [8, 7, 12, 5]. There are groups that have worked on reacting to changes in the state space in order to improve interaction and safety, such as [3] and Gao et al. who argues that force feedback combined with vision can be used to update robot trajectories [4]. Our argument is that if the intention of the user can be anticipated, the robot control can be optimised to ensure safety and fluidity of interaction. Although no groups have so far used this technique to anticipate a dressing sequence, predictive models for dressing a hospital gown have been proposed [6], based on just the force feedback without the use of vision in a simple single arm experiment. In our previous work [1] we used postural cues such as arm angle and head orientation (yaw) to resolve verbal ambiguity and detect dressing errors, such as garment snagging.

G. Chance, P. Caleb-Solly & S. Dogramadzi, Bristol Robotics Laboratory, University of the West of England
e-mail: greg.chance@brl.ac.uk, praminda.caleb-solly@brl.ac.uk, sanja.dogramadzi@brl.ac.uk
A Jevtić, G. Alenya & Carme Torras, Institut de Robòtica i Informàtica Industrial, CSIC-UPC Spain
email: ajevtic@iri.upc.edu, galenya@iri.upc.edu, torras@iri.upc.edu

(a) HHI experiment   (b) Feature importance   (c) Deep network accuracy
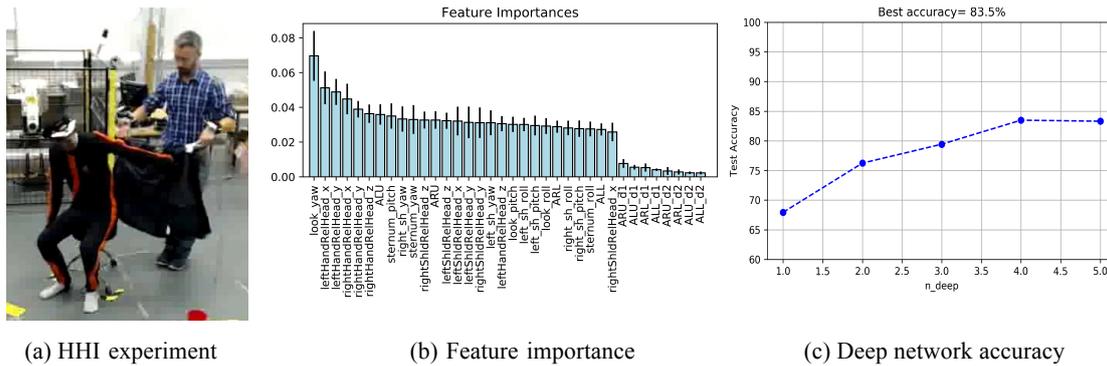
Fig. 1. Showing (a) Human-human interaction experiment where a user is receiving assistance with putting on a jacket whilst wearing a motion tracking suit, (b) normalized feature importance from random forest sub-sampling for dressing segment, and (c) exploring the number of hidden layers in the ANN model.

2. HUMAN INTENTION RECOGNITION

The data from our HHI experiments has provided sufficient information about the postural differences that people assume during the different stages of dressing, which were coded from observing video footage using Boris[1]. During implementation it is unlikely that this level of pose detail will be available. An RGB-D camera will most likely be used in a real system to determine user pose. A focus of this work was to establish features that could be tracked reliably when the user becomes partially occluded during dressing. Whilst exploring the experimental data several observations were made about user pose during the jacket dressing task. The user tended to look at the arm that was the focus of dressing (end effector selection) and often looked forwards if both arms were being dressed simultaneously. If dressing *one arm at a time* strategy, the user might exhibit a *torso roll* away from the arm being dressed and move the associated hand closer to the head, noted by *hand relative to head*. If dressing both arms simultaneously, the user may exhibit a *torso pitch* away from the robot initially (segment 1) and towards the robot during segment 3 (near the shoulders). Switching the dressing focus from left or right was usually preceded with a change in head orientation in the floor plane, termed here as *look yaw*.

A. Data Features and Deep Networks

An assessment of these features was undertaken using a random forest classifier for determining the dressing segment, Fig.1b. A number of sub-samples of the data are fitted to a decision tree and the results are averaged out to minimise issues of over-fitting. Features are assessed relative to their impact on the weighted impurity resulting in an approximation of feature importance. Look yaw (head orientation in XY plane) appears as the highest ranked feature along with the relative distance between the hand and the head (HandRelHeadx/y/z). Positively, some of the features designed for minimal occlusion during dressing (sternum, shoulder) appear in the top 20. Features based on the head, shoulders and sternum were most suitable to avoid occlusion issues. Dynamic features such as *ARU d1* which is the first order differential (d1) of the Upper Right arm Angle (ARU) with respect to time, i.e. angular velocity, and those of the other arm joints were of little importance to the overall feature set and were removed. This is probably as they are dynamic and may be better predictors of a change in the user's state rather than an indication of what it currently is.

As the dressing task can be considered a sequence of events in a particular order, such as a time series, then a recurrent model was hypothesised to perform well. A stacked Long Short-Term Memory (LSTM) network was trained to assess this hypothesis and was tuned for optimal hyperparameters such as L2 regularisation, batch size, epoch, hidden layer depth, and the type of loss mechanism and optimiser. Optimal performance was found for a network, 4 layers deep using the Adam optimiser and mean squared error loss, see Fig.1c.

III. RESULTS & CONCLUSION

Features of a dressing task based entirely on pose have been engineered and assessed. Features that do not suffer from occlusion during dressing have been found and used to build a stacked LSTM network for predicting user intention during jacket dressing. Accuracy of the model on validation data was >95% although this should be further assessed with cross validation and then user testing.

REFERENCES

1. G. Chance, A. Jevtić, P. Caleb-Solly, and S. Dogramadzi. "What's "up"? - Resolving interaction ambiguity through non-visual cues for a robotic dressing assistant". In: *Robot and Human Interactive Communication (RO-MAN), 2017 26th IEEE International Symposium on*. 2017, In Press.
2. Christie & Co. *The UK Nursing Workforce*. 2015.
3. Colome, A. Planells, and C. Torras. "A Friction-model-based Framework for Reinforcement Learning of Robotic Tasks in Non-rigid Environments". In: 1 (2015), pp. 5649–5654.
4. Y. Gao, H. J. Chang, and Y. Demiris. "Iterative path optimisation for personalised dressing assistance using vision and force information". In: *2016 IEEE/RSJ International Conference on Intelligent Robots and Systems (IROS)*. IEEE, Oct. 2016, pp. 4398–4403.
5. Y. Gao, H. J. Chang, and Y. Demiris. "User Modelling for Personalised Dressing Assistance by Humanoid Robots". In: (2015), pp. 1840–1845.
6. Kapusta, W. Yu, T. Bhattacharjee, C. K. Liu, G. Turk, and C. C. Kemp. "Data-driven haptic perception for robot-assisted dressing". In: *Robot and Human Interactive Communication (RO-MAN), 2016 25th IEEE International Symposium on* (2016), pp. 451–458.
7. S. D. Klee, B. Q. Ferreira, R. Silva, P. Costeira, F. S. Melo, and M. Veloso. "Personalized Assistance for Dressing Users". In: *International Conference on Social Robotics (ICSR 2015)*. Vol. 9388. 2015, pp. 359–369.
8. N. Koganti, T. Tamei, T. Matsubara, and T. Shibata. "Estimation of Human Cloth Topological Relationship Using Depth Sensor for Robotic Clothing Assistance". In: *Proceedings of Conference on Advances In Robotics*. New York, New York, USA: ACM Press, 2013, 36:1–36:6.
9. T. Matsubara, D. Shinohara, and M. Kidode. "Reinforcement Learning of Motor Skills with Non-rigid Materials using Topology Coordinates". In: *Advanced Robotics* 27.7 (2013), pp. 513–524.
10. T. Tamei, T. Matsubara, A. Rai, and T. Shibata. "Reinforcement learning of clothing assistance with a dual-arm robot". In: *2011 11th IEEE-RAS International Conference on Humanoid Robots*. IEEE, Oct. 2011, pp. 733–738.
11. WHO. *Facts about ageing*. 2014.
12. K. Yamazaki, R. Oya, K. Nagahama, K. Okada, and M. Inaba. "Bottom dressing by a life-sized humanoid robot provided failure detection and recovery functions". In: *2014 IEEE/SICE International Symposium on System Integration, SII 2014* (2014), pp. 564–570.

---

[1]http://www.boris.unito.it/

Learning-based Robotic Task Planning for Endovascular Catheterization

Wenqiang Chi[1] , Giulio Dagnino[1] and Guang-Zhong Yang[1]

I.INTRODUCTION

Endovascular intervention is a minimally invasive treatment to cardiovascular diseases - the major cause of deaths in the Western world. Current endovascular repair involves guiding catheters and guidewires to a specific target in the aorta and auxiliary vessels (cannulation) combined with treatment options such as stenting, embolization and ablation. This requires accurate control as unintentional contacts between wires and catheters with the vessel wall have the potential for perforation and dissection, with potentially catastrophic consequences (fatal haemorrhage, stroke, organ failure) [1]. Moreover, the current intra-operative imaging (2D fluoroscopy) adds up difficulty as it lacks the required 3D spatial information making the navigation even more difficult. Therefore, successful endovascular navigation hugely relies on the experience and skills of the clinicians. Recently, there has been a growing interests in promoting robot-assisted catheter navigation platforms. Clinical studies have shown their advantages over conventional approaches such as improved stability and accuracy of catheterization, added operators' comfort and reduced radiation doses to the clinicians [2]. Commercial devices such as the Sensei and Magellan systems (Hansen Medical, Mountain View, CA, USA) provide enhanced control strategies (e.g. steerable catheters with extra DoFs) and force feedback to improve the navigation. However, these systems use control interfaces (e.g. joystick, touch screen) that largely change the surgeons' natural manipulation patterns. Hence, experience-related skills - obtained over ages of practice - cannot be exploited in these robotic systems.

There is a trend in developing robotic devices with ergonomic master controller that can replicate the way as manipulating standard devices, thus exploiting the skills and experience of the operator [3] [4]. Few studies have explored operator-tool motion patterns as well as catheter-tissue interactions by Learning from Demonstration (LfD), [5] [6] [7]. A semi-automatic, collaborative platform was developed for robot-assisted catheterization based on LfD [5] [8]. Such robotic platforms could bring benefits such as improved quality of catheterization (smoother catheter motions, lesser tissue contacts) and reduced operators' workloads. However, these LfD frameworks have several limitations: 1) Prior knowledge is needed to segment human demonstrated trajectories; 2) Lack of generalization of skills, fail to transfer and reproduce in different tasks; 3) Only represent skills of a specific procedure in a specific type of anatomy, unable to adapt to patient-specific geometries; and 4) The model cannot be improved though practice, and fails to update in real-time in dynamic environment. The purpose of this paper is to propose an improved LfD framework to address the issues identified above. This work also provide a pilot study for task planning of robotic endovascular catheterization.

II. EXPERIMENTS AND RESULTS

Six demonstrations of a cannulation task to the Innominate artery from one expert surgeon were collected on absilicone-based, anthropomorphic phantom of aortic arch. Catheter proximal motions were collect by customized motion sensors (as reported in [5]) and catheter tip motions were collect by an EM sensor which was attached to the tip of the catheter. Beta Process Autoregressive Hidden Markov Model (BP-HMM) was used to segmented the demonstrated trajectories.

[1]Wenqiang Chi, Giulio Dagnino & Guang-Zhong Yang, Hamlyn Centre for Robotic Surgery, Imperial College London

This method directly infers the number of modes from the data, and also facilitates the sharing the modes across demonstrations in multivariate time series. Reusable subtasks were segmented from the complex cannulation tasks, then Dynamic Movement Primitives (DMPs) were used to capture the essential motion patterns of those segmented trajectories. LfD is then used to learn from the input trajectories after the segmentation in order to calculate the weights for multiple nonlinear functions of the DMP. DMPs can be grouped in the order which represents a complex cannulation task to a specific artery. Robotic trajectories can be generated from DMPs for the robotic manipulators.

Robotic manipulators for conventional catheters and guidewires were developed based on previous works [5]. A new guidewire manipulator was added to the previous platform. Translation of the catheter and the guidewire is achieved by friction-wheel based mechanism. The manipulator rotates the catheter body by steering the friction wheels that are clamped to the catheter. Fig. 1(a) shows the experimental setup. Pulsatile and continuous pumps were used to simulate cardiac motions for the phantom. Catheter tip motions trajectories were registered into the 3D CT scans of the vascular models by using CT markers and EM sensors. Segmented subtasks were temporally matched to corresponding catheter tip paths and their relative positions to the anatomy. These were used to define a higher level skills that attribute to procedural phases in the cannulation task. By comparing the differences in task scale and orientations across different anatomies, the learned models can be modified and adapted to new geometries and tasks.

The learned policies from the proposed LfD framework can be further optimized by model-free, trajectory based Path Integral Reinforcement Learning (PI2 RL). This is achieved by optimizing the shape parameters in each DMP of a cannulation task through practice. The design of the cost functions could depends on quality metrics of the catheter path as well as task scales. Preliminary results of segmentation are presented in Fig. 1(b).

The proposed LfD framework was used to automatically discover the reusable skills in the proximal catheter motion data. The color labels in Fig. 1(b) represents motion primitives such as push, pull and twist of the catheter or any combinations of them. Those skills were also identified from other demonstrations in the same group. It is worth noting that in order to capture all delicate skills obtained from expert surgeon's demonstrations, several over-fitting skills were consequently identified. Future works include pre-processing the raw data in order to remove extra skills. By referencing the catheter tip motions in the anatomy (Fig. 1(c)), the skills discovered from previous step can be grouped into higher level sub-tasks.

III.CONCLUSIONS

The proposed LfD framework for endovascular navigation allows automatic segmentation of unstructured human demonstrations without prior inference. A hierarchical structure of the learned skills can be represented by the segmented lower-level skills and higher level skills with considering anatomical geometries. Low-cost robotic manipulators were developed to perform endovascular tasks with on-the-shelf devices. Furthermore, RL is implemented to optimize the trajectories generated from the learned policy. Future works include incorporating dynamical shape instantiation for compensating tissue motions caused by cardiac cycle, and active constraints into a cooperative human-robot controller.
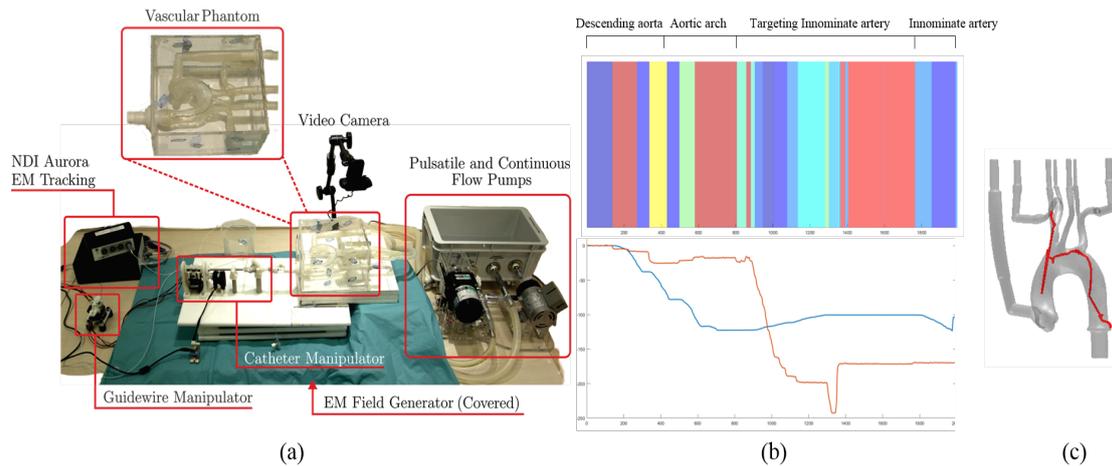
Fig. 1. (a) Experimental setup with robotic manipulators, vascular phantom, and EM tracking. (b) Catheter proximal motions (bottom) of both translation and rotation in time series, skills labels (middle) at each time step are indicated by unique colors, procedural phases that represent higher level skills (top) are labeled above the skills chart. (c) 3D mesh of a vascular phantom with catheter tip motions (red lines).

REFERENCES

1. K. A. Hausegger, P. Schedlbauer, H. A. Deutschmann, and K. Tiesenhausen, Complications in endoluminal repair of abdominal aortic aneurysms, Eur. J. Radiol., vol. 39, no. 1, pp. 2233, 2001

2. Riga, C. D. Bicknell, A. Rolls, N. J. Cheshire, and M. S. Hamady, "Robot-assisted fenestrated endovascular aneurysm repair (FEVAR) using the Magellan system," J Vasc Interv Radiol, vol. 24, pp. 191-6, Feb 2013.

3. Y. Thakur, D. W. Holdsworth and M. Drangova, "Characterization of Catheter Dynamics During Percutaneous Transluminal Catheter Procedures," in IEEE Transactions on Biomedical Engineering, vol. 56, no. 8, pp. 2140-2143, Aug. 2009. Eng. 56(8), 21402143 (2009)

4. H.-J. Cha, B.-J Yi, J.Y Won "An assembly-type mastelave catheter and guidewire driving system for vascular intervention" Proceedings of the Institution of Mechanical Engineers, Part H: Journal of Engineering in Medicine Vol 231, Issue 1, pp. 69 - 79, 2016

5. H. Rafii-Tari, J. Liu, S.-L. Lee, C. Bicknell, and G.-Z. Yang, "Learning-Based Modeling of Endovascular Navigation for Collaborative Robotic Catheterization," MICCAI, 2013, pp. 369-377.

6. Rafii-Tari, C. J. Payne, J. Liu, C. Riga, C. Bicknell and G. Z. Yang, "Towards automated surgical skill evaluation of endovascular catheterization tasks based on force and motion signatures", ICRA, Seattle, WA, 2015, pp. 1789-1794.

7. W. Chi, H. Rafii-Tari, C.J.Payne, J. Liu, C. Riga, C. Bicknell, and G.-Z. Yang, "A learning based training and skill assessment platform with haptic guidance for endovascular catheterization" ICRA, 2017, pp. 2357-2363.

8. Rafii-Tari, J. Liu, C. J. Payne, C. Bicknell, and G.-Z. Yang, "Hierarchical HMM Based Learning of Navigation Primitives for Cooperative Robotic Endovascular Catheterization," in Medical Image Computing and Computer-Assisted Intervention, 2014, pp. 496-503.

Parallel Task Planning for Multi-Robot Coordination

Bidan Huang, Yiming Yang, and Guang-Zhong Yang, Fellow, IEEE

ABSTRACT

This paper presents a framework for task planning of multi-robot cooperation. A task is firstly demonstrated by a human. After extracting the subtasks from human demonstration, a critical path analysis is employed to optimize the timing of the subtasks of each robot. A customized sampling-based planning method is used to generate collision free paths. Preliminary experimental results show that by using this method, the multi-robot system can coordinate with high efficiency and be free from collisions. The proposed approach is generalizable to other manipulation tasks, where bimanual or multi-robot cooperation is required.

I. INTRODUCTION

Multiple robot system have many applications in industrial and medical environment. To ensure the system performance, many constraints need to be taken into account, such as the task constraints, robot velocity, accuracy and collisions. Programming such a system is time consuming. In this paper, we propose a method for multiple robot task planning, which offers a easy-to-use interface for motion planning, and generating optimized and collision free trajectories for all the robots.

Fig. 1: Bimanual sewing system for stent graft manufacturing

Without loss of generality, our approach is framed in the context of a bimanual sewing task for the purpose of personalized stent graft manufacturing [1]. This task is challenging as it involves intricate movements and fine cooperation between robots, e.g. handing over a sewing needle. In our previous work [2], robots move in a sequential order, i.e. only one robot move at a time. With the approach proposed in this paper, multiple robots can move concurrently and hence the task duration can be largely reduced.

II. METHODOLOGY

A bimanual sewing task is firstly, demonstrated by a human and hence a reference trajectory for robot sewing is generated. The demonstrated trajectory is segmented into 10 subtasks for the two robots [2]. The timing of the subtasks are then optimized by the critical path analysis

method. The sum of the durations of the subtasks on the critical path is hence the shortest possible task duration. The subtasks that are not in the critical path are run concurrently with those in the critical path. This maximizes the concurrence of the multiple robots' motion and allows them to cooperate seamlessly. A collision avoidance technique is applied to ensure the robots can move simultaneously without collisions.

A. Critical path analysis

Critical path analysis (CPA) is a method that identifies the critical activities to complete a task and optimize the task planning to achieve good performance. It is commonly used in many areas such as project management and circuit design optimization. To model a task, four steps are taken in CPA:

1) Identify all the subtasks;
2) Estimate the shortest duration of each subtask;
3) Identify the dependencies between subtasks;
4) Identify the critical path.
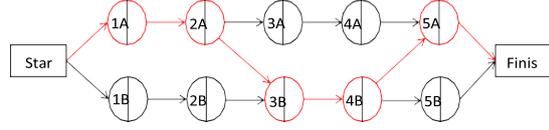
Fig. 2: CPA of bimanual sewing (critical path marked in red).
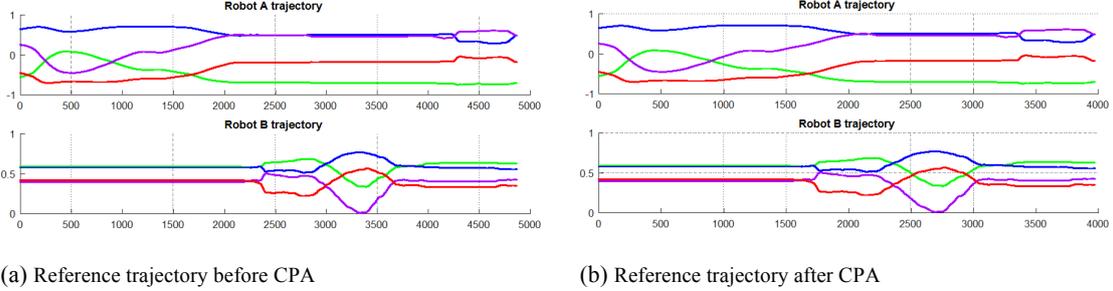
(a) Reference trajectory before CPA

(b) Reference trajectory after CPA

Fig. 3: Bimanual sewing motion trajectory (end effector rotation in quaternion). (a) Before CPA, robot A and B move sequentially. (b) After CPA, robot A and B move concurrently to reduce task duration.

In the bimanual sewing task, we have identified 10 subtasks for both of the robots. The duration of each subtask is decided according to the task context as described in our previous work [2]. When prioritizing the subtasks between the robots, we make the robot contacting the target object, i.e. needle in this case, has higher priority than the others. Based on these analyses above, the CPA graph of the sewing task can be represented as in Fig. 2

B. Collision-free motion planning

The CPA changes the execution window of the robot trajectories, which leads to potential collision, though the original reference trajectories are collision-free. Thus, collision avoidance needs to be taken into account to ensure safe execution. Let $\mathcal{A}$ and $\mathcal{B}$ denote the robots A and B. Let $\mathbf{q}_t^r \in \mathcal{C}_r$, be the robot configuration of robot $r \in \{\mathcal{A}, \mathcal{B}\}$, where $\mathcal{C}_r$ is the configuration space of robot r. Upon CPA, the time for each robot to reach a critical pose is fixed. Let $\mathbf{y}_t^{r*} \in \mathcal{Y}_r$ be the critical end-effector pose that robot r must achieve at time t, where $\mathcal{Y}_r$ is the set of all critical poses of robot r. The motion planning problem can be formed as follows,

$$\mathbf{q}_{[0:T]}^{\mathcal{A}}, \mathbf{q}_{[0:T]}^{\mathcal{B}} = \text{MotionPlan}(\mathbf{q}_0^{\mathcal{A}}, \mathbf{q}_0^{\mathcal{B}}, Environment, \mathcal{Q}_{\mathcal{A}}, \mathcal{Q}_{\mathcal{B}})$$
$$s.t. \quad \mathbf{q}_{[0:T]}^r \subset \mathcal{C}_{free}^r, r \in \{\mathcal{A}, \mathcal{B}\} \tag{1}$$
$$\Phi(\mathbf{q}_t^r) = \mathbf{y}_t^{r*}, \forall \mathbf{y}_t^{r*} \in \mathcal{Y}_r, r \in \{\mathcal{A}, \mathcal{B}\}$$

where $\mathbf{q}_0^{\mathcal{A}}, \mathbf{q}_0^{\mathcal{B}}$ are the current states of the robots, $\mathcal{C}_{free}^r$ is the collision-free manifold of the configuration space of robot r, and $\Phi(\cdot)$ is the forward kinematics mapping. Such a problem can be solved by weighted or biased sampling planning methods such as [3] with an extra sampling dimension representing the time.

III. EXPERIMENTS

According to the graph, the critical path of the bimanual sewing task is 1A-2A-3B-4B-5A. During the execution of the critical path, the subtasks out of the critical path, i.e. 1B, 2B, 3A, 4A, 5B are run in parallel. A new motion plan is generated according to this CPA result and we tested this plan in a simulated environment. The experiment shows that the duration of one cycle of sewing can be reduced to from 41 to 31 seconds.

IV. CONCLUSION

We propose a method for planning concurrent and collision-free motion for multi-robot system. Preliminary result shows that with this approach the duration of the task can be reduced. We have also noticed that, with the current setup where the two robots are placed on separated tables in distance, the new trajectory directly after CPA modification is already collision-free. In our future study, this approach will be implemented to optimize the performance of a multi-robot system, i.e. number of robot more than two, where collision-avoidance will be essential to ensure a safe operation.

REFERENCES

1. Huang, A. Vandini, Y. Hu, S.-L. Lee, and G.-Z. Yang, "A vision-guided dual arm sewing system for stent graft manufacturing," in Intelligent Robots and Systems (IROS), 2016 IEEE/RSJ International Conference on. IEEE, 2016, pp. 751–758.
2. Huang, M. Ye, S.-L. Lee, and G.-Z. Yang, "A vision-guided multi-robot cooperation framework for learning-by-demonstration and task reproduction," arXiv preprint arXiv:1706.00508, 2017.
3. Y. Yang, V. Ivan, W. Merkt, and S. Vijayakumar, "Scaling sampling-based motion planning to humanoid robots," in Robotics and Biomimetics (ROBIO), 2016 IEEE International Conference on. IEEE, 2016, pp. 1448–1454.

Geographies of Robotization and Automation

Dr Mateja Kovacic, & Dr Andy Lockhart, Urban Institute, University of Sheffield

I. INTRODUCTION

Despite a proliferating critical literature on the development of robotics and automated systems (RAS) in a variety of societal settings (e.g. Danaher et al., 2017; Wajcman, 2017; Bissell & Casino, 2017; Del Casino, 2016; Royakkers & Est, 2015), the urban arena remains a relatively unexplored context for the rollout and testing of these technologies.

Cities across the world serve as testbeds for a range of autonomous vehicle trials, including the competitive race to develop 'self-driving' cars. Automated ports and other logistical spaces are increasingly prominent aspects of urban development strategies, while the testing of delivery robots and drones is gathering pace beyond the warehouse gates. Automated control systems are monitoring, regulating and optimising traffic flows and infrastructural systems. Automated vertical farms are being erected in urban areas around the world, and new mobile health technologies carry promise of healthcare 'beyond the hospital'.

Meanwhile, forms of citizen sensing, monitoring and activist projects using automated technologies are gathering pace at the urban scale, challenging official measures of air quality and other environmental indicators. Social robots in many guises – from police officers to restaurant waiters – are appearing in urban public and commercial spaces. Encompassing a variety of different domains and sites of experimentation and application, there is not a singular rationality underpinning urban automation. A multiplicity of logics, processes and effects is unfolding, with uneven geographies and temporalities. These are being driven and contested by contingent groupings of local and extra-local actors, trying to meet different objectives, under the constraints of particular political, material

and path dependent circumstances. This paper discusses how robotization and automation are reconfiguring urban contexts andurban life in response to opportunities and challenges in economic, social, political and healthcare domains. To provide a comprehensive, comparative understanding of these rationales and processes, we offer an overview of the global state of RAS with respect to specific sociocultural and politico-economic contexts. We examine how cities including Tokyo, Singapore, and Dubai are being reconfigured materially and discursively through real-life urban experimenting, to provide a comparative analysis of how RAS are being situated and fused with the urban.

We argue the two key rationales for such intensive proliferation of UAR across the globe are: i) urban governance via experimentation with city systems to maintain the system's increasing complexity and heterogeneity while demonstrating the capability to govern by rearranging and organizing the new urban technological 'nature' and ii) visions of the future, fuelled by the explosion in available technologies, hardware and software, in a global innovation and RAS race.

Through several distinct case studies, we present our comprehensive mapping project of RAS applications and experimentations globally, and discuss how RAS unfolds and transforms work and life in different contexts. Current 54% of the world's population living in urban areas is expected to increase to 66% by 2050 (UN, 2014). Traffic congestion (time waste, traffic accidents), safety on roads, environmental pollution, crowds, crime, time deficit, labour-deficit, control-deficit, aging and shrinking population, increased consumption (of products, healthcare) are seen as specifically

urban problems in an increasingly urbanised global landscape. RAS have thus emerged across national contexts as the primary and privileged solution for the urban issues. Recognising that there is a multiplicity of robotics landscapes constituting different domains, objectives, and modes of experimentation with RAS, this paper provides only a few of many examples to open up a societal debate on robotics as a solution to urban issues as national priorities.

National governments increasingly see RAS as the key to (better) urban futures, due to which cities are becoming test beds for national and local governments for symbolic and programmatic robotisation. National and urban mix together as national strategies unfold in urban contexts including Japan's 2014 New Industrial Revolution Driven by Robots, Smart Dubai, and RIE 2020 Plan Singapore. In the UK, a market-driven, non-programmatic initiative includes Innovate UK and Industrial Strategy Challenge Fund. Both UK and US RAS contexts differ from the above cases by nonprogrammatic approach driven predominantly by the market and corporate-private interests.

In sum, locally specific national plans, political and economic systems govern the unfolding of RAS across global urban contexts, either systematically innovating cities or creating disconnected islands of innovation. This paper briefly introduces three cases of the former character: Tokyo, Dubai and Singapore. The convergence between RAS and Tokyo Olympics 2020, demonstrates how RAS reconfigures the urban through systematic large-scale ubiquitous experimentation. RAS in Japan is discursively legitimised by societal issues (i.e. shrinking population), but the objectives are in line with the economic domestic and global interests of government, including economic reinvigoration, cultural branding and international demonstration. Tokyo Olympics point to how sports mega-events introduce and influence global technology trajectories, with planned ubiquitous robotising of the urban and transforming urban life comprehensively and systematically through robot, automated, digital and AI technologies. This heralds a

new scale of technologizing life and configuring cities. In the government vision for the Olympics, robot taxis transport tourists across the city, smart wheelchairs greet Paralympians at the airport, ubiquitous Peppers greet customers, and interactively augmented foreigners speak with the local population in Japanese. By redefining urban phenomenology, Tokyo Olympics are creating a futurescape through which RAS circulate and provide new form of interactive urban infrastructure.

The case studies of Singapore and Dubai, on the other hand, show a close link between RAS and smart city whereby both governments understand and implement RAS as (physical) extension of the smart and digital to improve operability, management and control of the urban (governance) systems. This rematerializing of the (smart) city is a form of tangible governance where robotization and automation are controlled by the government.

In Singapore, the techno-futuristic smart city national narrative sees robots and automated systems as a 'natural' extension of the existing nationalised smart urban ecosystem. This vision is unfolding through the Panasonic autonomous delivery robots HOSPI, the Singapore Post's delivery drone trial in partnership with AirBus helicopters, and driverless bus shuttles from Easymile, EZ10. Singapore hotels are employing state-subsidised service robots, to clean rooms and deliver linen and supplies, while robots for early childhood education have also been piloted by the Infocomm Development Authority to understand how robots can be used in pre-schools in future (Chin, 2016). Health and social care is one of the fastest growing industries for RAS globally: examples are the Outpatient Pharmacy Automation System that prepares medications for patients and a smart wheelchair system deployed in 2016.The introduction of RAS in Dubai reveals how the established governance regime is finding innovative ways to reproduce its conservative values and norms of the centralised state gaze, management and control. In September 2017, a test flight of a flying taxi developed by the German drone firm Volocopter was

staged to 'lead the Arab world in innovation.' (Reuters, 2017) While national governments aim to position themselves on the global landscape through robotics, they also utilise the narrative to position themselves as regional leaders. Dubai's objective is to automate 25% of transport system by 2030 and is currently also testing robots for surveillance and patrolling: the Barcelona-based PAL Robotics' humanoid police officer and Singapore-based vehicle OUTSAW. Should the experiments prove successful, the government has announced it will robotise 25% of the police force by 2030. By comparatively analysing these case studies, we aim to produce a theoretical and methodological framework for understanding the heterogenous and multiple geographies of automation and robotization in order to address the issues of life, death, work, governance, economies and politics in the increasingly growing ecosystems reconfigured and defined through RAS. Urban is increasingly constituted for learning and demonstration of RAS and the abovementioned case studies demonstrate the attempts to constitute RAS experiments in a

systematic and long-term way in the urban context. Based on the ongoing mapping of the global robotics landscape, there are three main but differing modes of experimenting, emerging from specific national, economic and sociocultural contexts:
1) state directed vs. market-led,
2) open vs. enclosed and 3) local vs. global.
As to the observed consequences of urban robotisation, it is either systemic and city-wide (Tokyo, Dubai, Singapore) or it is creating islands of innovation and automation (UK, US) which has two consequences:
1) fairer cities or
2) intensification of social/economic disparities.
The ongoing research aiming to clarify the consequences of robotising cities includes fieldwork, global mapping and surveying to create a comparative global perspective of the RAS localities that demonstrates how the urban global landscape is being constituted through particular, local and national robotisation plans, and how the locally specific urbanisms constitute robotics.

REFERENCES

1. Bissell, D. & Casino, V. J. D. (2017). Whither Labor Geography and the Rise of the Robots? Social & Cultural Geography, 18(3), 435–442.

2. Chin, Charlene. Exclusive: Singapore is using robots to teach social skills. GovInsider. 16 November 2016. https://govinsider.asia/innovation/exclusive-how-are-robots-teaching-social-skills-in-singapore/.

3. Danaher, J., Hogan, M. J., Noone, C., Kennedy, R., Behan, A., De Paor, A., Felzmann, H., Haklay, M., Khoo, S.-M., Morison, J., Murphy, M. H., O'Brolchain, N., Schafer, B. & Shankar, K. (2017). Algorithmic Governance: Developing a Research Agenda through the Power of Collective Intelligence. Big Data & Society, 4(2), 2053951717726554.

4. Del Casino, V. J. (2016). Social Geographies II: Robots. Progress in Human Geography, 40(6), 846–855.

5. Reuters, New York Post. Dubai completes

first flying taxi test flight. 26 September, 2017. http://nypost.com/2017/09/26/dubai-completes-first-flying-taxi-test-flight/.

6. Reuters, The Express Tribune. Dubai starts tests in bid to become first city with flying taxis. 26 September, 2017. https://tribune.com.pk/story/1516508/dubai-starts-tests-bid-become-first-city-flyingtaxis/.

7. Royakkers, L. & Est, R. van. (2015). A Literature Review on New Robotics: Automation from Love to War. International Journal of Social Robotics, 7(5), 549–570.

8. United Nations. World's population increasingly urban with more than half living in urban areas. 10 July 2014. http://www.un.org/en/development/desa/news/population/world-urbanization-prospects-2014.html.

9. Wajcman, J. (2017). Automation: Is It Really Different This Time? The British Journal of Sociology, 68(1), 119–127.

Robin: An Autonomous Robot for Diabetic Children

Matthew Lewis and Lola Cañamero, Embodied Emotion, Cognition and (Inter-)Action Lab, University of Hertfordshire, UK

ABSTRACT

We describe the cognitively and motivationally autonomous robot toddler Robin, designed as a tool to help children learn about diabetes management. The design of Robin follows an Embodied Artificial Intelligence approach to robotics, to create a robust social interaction agent, friendly but independent. We have used Robin in autonomous interactions with diabetic children in a scenario designed to give them mastery experiences of diabetes management in order to in- crease their self-efficacy.

I. INTRODUCTION

Robin (ROBot INfant) is a cognitively and motivationally autonomous affective robot toddler with \robot diabetes" that we have developed to support (perceived) self-efficacy, self-confidence and emotional wellbeing in children with diabetes, by providing them with positive mastery experiences in diabetes management in a playful but realistic and natural interaction context. Children with Type 1 diabetes mellitus (T1DM) are invited to play with Robin and look after it, including taking care of its diabetes. The children are thus given an opportunity of apply the knowledge they have acquired about diabetes and its management to manage someone else's diabetes in a playful non-stressful environment, with the aim to help them consolidate their knowledge, think how they would apply it to the management of their own diabetes, and develop a sense of responsibility towards self-management of their condition.

The design of Robin follows an Embodied Artificial Intelligence (EAI) or Behaviour-Based approach to robotics [1, 2], relatively little-used by the Human-Robot Interaction (HRI) and Child-Robot Interaction (CRI) communities [3]. However, this approach is well suited to create a robust social interaction agent, friendly but independent, that is believable and engaging, and can be used in a real-world situation to interact autonomously with a wide variety of different children and interaction styles.

II. TYPE I DIABETES

T1DM is an incurable disease caused by the loss of insulin-producing beta cells in the pancreas, resulting in the body being unable to produce insulin naturally [4]. This leads to chronically raised blood glucose levels (hyper-glycemia) that needs to be corrected artificially by injecting insulin and balancing it with carbohydrate consumption. T1DM is often diagnosed in childhood and, if poorly managed, the high glucose levels lead to devastating complications such as blindness, limb amputations or organ failure. Childhood diabetes is a very challenging condition for the children, who have to learn about the condition as they grow, and the family, who will do the bulk of management for young children. In addition to the complex task of management, the emotional burden of chronic illness during childhood, accepting the responsibility for long-term health management in everyday life, and the impact of inevitable failures during the learning period, is associated with mental health problems [5, 6].

III. ROBIN

The Robin character has been designed [7, 8] as a tool to complement diabetes education for children. Robin is implemented in a Nao robot, controlled by our custom software that makes it behaves like a human toddler. It will autonomously make decisions based on its immediate motivations of hunger (resulting in it seeking the toy food objects provided), desire to socialize (it seeks and approaches

human faces), desire to rest (it sits down), and desire to play (it dances). Robin also has an internal model of diabetes which results in its simulated blood sugar level fluctuating as it eats" different foods, moves around or rests, as well as on its current blood insulin level. High and low blood sugar levels will result in the robot becoming increasingly tired until it sits down and complains about feeling sleepy".

The robot's blood sugar levels can be monitored by the child using a wireless glucometer device that we implemented using a LEGO Mindstorms controller, and insulin can be administered using the same device. This allows the child (or anyone caring for Robin) to manage Robin's diabetes with insulin (to reduce blood sugar) and appropriate foods (e.g. glucose tablets to increase blood sugar). Robin was designed to be autonomous in order that it could be used in different scenarios, and it would respond in an appropriate way. It was first used in a scenario conceived to improve children's perceived self-efficacy [9, 10] { briefly, perceived self-efficacy can be considered as the child's belief that they can succeed in learning how to manage their own diabetes; self-efficacy is considered as a key element in behaviour change, necessary for the good management of T1DM.

In this scenario, the diabetic child, who already has theoretical knowledge about diabetes management, but who was not yet independent in their management, is first introduced to Robin by an adult, and shown how to manage Robin's diabetes. The child is then left alone to look after and play with Robin in the robot's \playroom" (a controlled environment, friendly-looking and familiar to the child). During this period, the robot would have a hyper- or hypo-glycemia (induced by the experimenters if it did not happen during the available interaction time). The child is then free to act as they felt appropriate, and could call for assistance if required. Since the aim here is to increase self-efficacy, it is important that the child could not fail.

Therefore, if they failed to take appropriate action to manage Robin's diabetes, an adult

could return and prompt them, or Robin could recover as though the sleepiness was not diabetes related.

I.V. INTERACTIONS

Interactions with Robin have been run with diabetic children (aged 8{12) at a hospital and a diabetes summer camp in Italy (with partners in the EU-funded ALIZ-E project1, under which Robin was initially developed). Results from these interactions are reported in [11, 8]. Briefly, while self-efficacy was not seen to increase (it was not expected to, this is expected only from long-term or repeated interactions) the interactions were considered successful. The children engaged with Robin, and Robin acted appropriately as the scenario played out differently with each child. The \toddler" character successfully acted as a cover for the shortcomings in the robot (limited speech, no speech comprehension, occasional falls, and occasional behaviour that was difficult to understand for those interacting).

Several children showed spontaneous behaviour, such as hiding sweets from Robin, or making a bed. We view this as important because it is useful for the child to be able explore their own concerns related to diabetes, and an overly scripted interaction may limit this. Some of the interactions were done with two children looking after Robin together. Again, even though it had not been programmed for this specific scenario, Robin behaved appropriately, and the children acted together to manage Robin's diabetes.

A number of observations were made concerning the children's relating of their own diabetes with Robin's, such as checking their own glucometer in parallel with Robin's, or verbally relating their own experiences with diabetes in the context of Robin's. We view this as important since Robin was designed as an agent that the child could relate to emotionally, potentially forming a bond. This motivates the child to care for Robin, and in the process to learn about caring for themselves.

V. FUTURE WORK

Robin is currently a research prototype. We are working with healthcare researchers and a

local NHS Trust, in order to explore future development (not limited to self-efficacy). To this end, a number of PPI (Patient and Public Involvement) interactions have been run with diabetic children and members of their families, in order to gather feedback towards further developing Robin so that it can be effectively used by health practitioners to support education in T1DM in children.

REFERENCES

1. R. A. Brooks, \New approaches torobotics," Science, vol. 253, no. 5025,pp. 1227{1232, 1991.

2. R. Pfeifer and C. Scheier, UnderstandingIntelligence. Cambridge, MA: MIT Press,2001.

3. A, Thomaz, G. Ho_man, M. Cakmak, et al.,\Computational human-robot interaction," Foundations and Trends in Robotics, vol. 4, no. 2{3, pp. 105{223, 2016.

4. National Health Service, UK, \Type 1 diabetes."https://www.nhs.uk/conditions/type-1-diabetes/. Page last reviewed: 2016-09-05.

5. B,J. Anderson and J. Brackett, \Diabetes in children," in Psychology in Diabetes Care (F. J. Snoek and T. C. Skinner, eds.), pp. 1{25, John Wiley & Sons, Ltd, 2nd ed., 2005.

6. K. S. Bryden, R. C. Peveler, A. Stein, A, Neil, R. A. Mayou, and D. B. Dunger,\Clinical and psychological course of diabetes from adolescence to young adulthood: A longitudinal cohort study," Diabetes Care, vol. 24, no. 9, pp. 1536{1540, 2001.

7. M. Lewis and L. Canamero, \An affective autonomous robot toddler to support the development of self-e_cacy in diabetic children," in Proc. 23rd Annual IEEE Intl. Symp. on Robot and Human Interactive Communication (IEEE RO-MAN 2014), pp. 359{364, 2014.

8. L. Ca~namero and M. Lewis, \Making new \New AI" friends: Designing a social robot for diabetic children from an embodied AI perspective," International Journal of Social Robotics, vol. 8, pp. 523{537, 2016.

9. A, Bandura, \Self-e_cacy: Toward a unifying theory of behavioral change," Psycho-logical Review, vol. 84, no. 2, pp. 191{215, 1977

10. A, Bandura, Self-E_cacy: The Exercise of Control. Worth Publishers, 1997.

11. M. Lewis, E. Oleari, C. Pozzi, and L. Ca~namero, \An embodied AI approach to individual di_erences: Supportin self-efficacy in diabetic children with an autonomous robot," in Proc. 7th International Conference on Social Robotics (ICSR-2015) (ATapus, E. Andr_e, J.-C. Martin, F. Ferland, and M. Ammi, eds.), (Paris), pp. 401{410, Springer, 2015.

On Decision-making for Computation Offloading in Cloud-assisted Autonomous Vehicle Systems

Y. Lu[1], C. Maple[1], T. Sheik[1], M.Dianati[1], A. Mouzakitis[2]

[1]Cyber Security Centre, WMG, University of Warwick, Coventry, UK.

[2]Jaguar Land Rover, Coventry, UK

{y.lu.16, cm, t.sheik, m.dianati} @warwick.ac.uk, amouzak1@jaguarlandrover.com

I. INTRODUCTION & CONTEXT

In recent years, governments and industry from many countries, including USA, China, Japan and various countries in Europe, have invested millions of pounds in the research and development of connected and autonomous vehicles (CAVs) as well as supporting wide-scale introduction of electric vehicles to the market [1]. Although at its initial stage of realization, intense planning and investigation are being undertaken for CAVs concerning innovation, inspections maintenance and manufacture, bringing changes to achieve the objectives of an advanced Intelligent Transportation System (ITS). Given the exponential rise of interest in the automation of vehicles, experts have called for a major research on numerous perspectives of the connected ITS ecosystem. One of the major concerns is the efficient and secure computation of vehicular data to deliver an optimal, safe and reliable transportation service.

One such initiative aiming to contribute towards ITS in the UK is the Cloud Assisted Real-Time Methods for Autonomy (CARMA), the general idea of which is depicted in Figure 1 [2]. The aim of the project is to integrate connected technologies such as cloud infrastructure and Edge Cloud with Vehicular On-board Units (OBU), electronic and computational resources through a communication technology (such as 5G communication, Dedicated Short Range Communication (DSRC), Vehicular Ad-hoc Networks) to establish a connected ecosystem.
There have been a variety of interpretations of connected and autonomous vehicles throughout industry and academia [1], [3].

Whilst often used as a single term, CAV, it is important that there exist a number of autonomous vehicles that are not connected and similarly a number of connected vehicles that have no autonomy. Those vehicles that are both connected and autonomous may or may not be cooperative. A connected vehicle is equipped with the capability of accessing the connected infrastructure and communicating with the world around. Autonomous vehicles have the capability to manoeuvre themselves with little or no human intervention.

Cooperative vehicles, on the other hand have the capability to interact with each other, regularly updating each other with vehicle status information including velocity, latitude and longitude. This is because the changes must be continuously sensed, computed, monitored and acted accordingly. Sensors such as RADAR, LIDAR, Infrared and Cameras would detect and perceive a large amount of data which would need to be co-related and computed with integrated sensors and computer vision to enhance the cognitive capabilities of the vehicles [4].

II. MOTIVATION

The convergence of detected vehicular data requires optimised and efficient utilisation of on-board resources. To achieve an optimal computation of various vehicular applications, offloading data could be considered, as it provides a means of migration of computationally data intensive tasks from OBU to edge or core cloud. This requires planning, prioritisation and interacting with the environment similar to the functioning of robotics and autonomous systems. To achieve this, Machine Learning

algorithms and Artificial Intelligence are often adopted [5]. However, data detection, processing and computation post sensing can be a computational costly process and therefore, offloading data can prove to be an efficient strategy. To ease the on-board vehicular computation, the CARMA project is investigating strategies for offboarding computation.

One way of performing remote execution is to offload data to the cloud, undertake computation and then return to the vehicle the result of the computation. However, it is also possible to undertake this computation in the edge cloud or fog, using local infrastructure and neighbouring vehicles' computational resources. It should be noted though that offloading is not necessarily the optimum solution in all cases. Authors in [6] have proposed a framework utilising cloud computation for offloading computation of data intensive vehicular applications to the cloud. The strategy they propose requires that data should be offloaded to the cloud if the computation time on the vehicle is greater than the sum of the computation time in the cloud and the time to transfer data to the cloud and back.

We argue that this is an oversimplified strategy and that for effective decision-making concerning computational offloading parameters such as the criticality of the operation, the cyber security risks involved [7], [8], [9], [10] and the accuracy of computation should also be factors to consider in computational offloading. This results in a multi-objective problem that requires solving for the decision to be made.

III. METODOLOGY

Unlike the work that is shown in [6], where only execution and transmission time have been considered in the decision, this work aims to propose a new decision module with a set of new parameters, which include risk, r; error, e; and the total time consumption, T. We can define a function $C(T, r, e)$ that considers the "cost" incurred in the computation of a vehicular function. For different vehicular functions, the relative importance of the time taken for computation, the risk of cyber security

compromise and the accuracy of computation vary. For a real-time function that is not safety-critical and contains no sensitive data, the importance of risk and error may be lower than the importance of time. Conversely, for long-distance route planning time may be of less importance than cyber security risk or accuracy. Optimally, of course, we would want to have the quickest computation, at the lowest risk with the highest accuracy. We can think of this as minimising the time, risk and error (the inverse of accuracy). We define the cost of computation onboard as C_o, of offboarding to the cloud as C_c, and offboarding to the edge cloud as C_E as follows:

$$_oC = T_o + a' r_o + b' e_o; \quad C_c = T_c + a' r_c + b' e_c; \quad C_E = T_E + a' r_E + b' e_E;$$

The detailed explanation of parameters is shown below: T_c, T_E and T_o are the total time consumptions of data computation in cloud, edge cloud and OBU, where

$$T_c = t_c + d_{in}/S_{c\_in} + d_{out}/S_{c\_out},$$
$$T_E = t_E + d_{in}/S_{E\_in} + d_{out}/S_{E\_out} \text{ and}$$
$$T_o = t_o. \ t_{c/E/o}$$

is the time consumption for computation in the cloud, edge cloud or OBU. $d_{in/out}$ represents the input or output data size. S_{c_in/c_out} represents the speed of uplink to the cloud or downlink from the cloud. S_{E_in/E_out} represents the speed of uplink to the edge cloud or downlink from the edge cloud. $e_{c/E/o}$ is the difference between calculated function values and true values in cloud, edge cloud or OBU.

For example, two cars C_1 and C_2 travelling at an instantaneous velocity at time t. The cars are 10 meters away from each other and C_2 has observed C_1. Considering the on-board calculated velocity is V_i by C_1 and the observed velocity is V_o by C_2. Let us assume C_2 requires the velocity of a C_1 to utilise the values in a control algorithm. C_2 has options of its own, it can either use its observed value V_o or the value V_i obtained through transmission of messages through different channels such as cloud and edge cloud. Through this way, the error of the cloud or edge cloud-based velocity as $e_{c/E} = |V - V_i|$

and on-board velocity as $e_o = |V - V_o|$. α represents the relative importance of risk, β represents the relative importance of error. $r_{c/E}$ is the potential risks in the data transmission process and also the computation process in the cloud or edge cloud. r_o is the potential risks when the data is processed in OBU. Therefore, if $C_o \leq C_c$ and $C_o \leq C_E$, the computation would take place in the OBU; If $C_c < C_o$ and $C_c < C_E$ then the offloading of data to the cloud can be considered; If $C_E < C_o$ and $C_E < C_c$, the offloading of data to the edge cloud is considered.

I.V. CONCLUSION

This paper introduces the reader to the evolution of connected and autonomous vehicles and explains the constraints in vehicular on-board computation. This limitation can be overcome by exploiting the computational power of remote resources (e.g. edge cloud present in RSU, cloud infrastructure and even the neighbouring vehicles).

Moreover, a new computational offloading decision is proposed for cloud-assistant autonomous vehicle system to make a more-advised decision in computation offloading. We consider this decision maker is more effective where the potential cyber security risks in transmission and computation processes and the accuracy of computation have been considered in the decision process. This decision can be activated when the application release.

The work which in process is includes theoretical analysis, such as formulating the multi-objective optimization problem, quantifying the parameters (α, β, r), and producing simulation results based on different applications. Particular interest may be found in optimizing potential risks to minimize the total cost.

REFERENCES

1. J. B. John McCarthy, David Williams, eta, "Connected&Autonomous Vehicles," 2016.
2. K. Katsaros, A. Stevens, M. Dianati, C. Han, McCullough, A. Mouzakitis, et al., Cooperative automation through the cloud: The CARMA project, 2017.
3. L. Guvenc, B. A. Guvenc, and M. T. Emirler, "Connected and autonomous vehicles," Internet of
4. Things and Data Analytics Handbook, pp. 581-595, 2017.
5. R. Rasshofer and K. Gresser, "Automotive radar and lidar systems for next generation driver assistance functions," Advances in Radio Science, vol. 3, pp. 205-209, 2005.
6. D. A. Pomerleau, "Efficient training of artificial neural networks for autonomous navigation," Neural Computation, vol. 3, pp. 88-97, 1991.
7. A, Ashok, P. Steenkiste, and F. Bai, "Enabling vehicular applications using cloud services through adaptive computation offloading," in Proceedings of the 6th International Workshop on Mobile Cloud Computing and Services, 2015, pp. 1-7.
8. M. Raya, P. Papadimitratos, and J.-P. Hubaux, "Securing vehicular communications," IEEE Wireless
9. Communications, vol. 13, 2006.
10. J. T. Isaac, S. Zeadally, and J. S. Camara, "Security attacks and solutions for vehicular ad hoc networks," IET Communications, vol. 4, pp. 894-903, 2010.
11. M. S. Al-Kahtani, "Survey on security attacks in Vehicular Ad hoc Networks (VANETs)," in Signal Processing and Communication Systems (ICSPCS), 2012 6th International Conference on, 2012, pp. 1-9.
12. E. B. Hamida, H. Noura, and W. Znaidi, "Security of cooperative intelligent transport systems: Standards, threats analysis and cryptographic countermeasures," Electronics, vol. 4, pp. 380-423, 2015.

An Optimised Deep Neural Network Approach for Forest Trail Navigation for UAV Operation within the Forest Canopy

B. G. Maciel-Pearson, Pratrice Carbonneu and T.P. Breckon {b.g.maciel-pearson, patrice.carbonneu and toby.breckon}@durham.ac.uk Department of Computer Science, Durham University, UK

ABSTRACT

Autonomous flight within a forest canopy represents a key challenge for generalised scene understanding on-board a future Unmanned Aerial Vehicle (UAV) platform. Here we present an approach for automatic trail navigation within such an environment that successfully generalises across differing image resolutions - allowing UAV with varying sensor payload capabilities to operate equally in such challenging environmental conditions. Specifically, this work presents an optimised deep neural network architecture, capable of state- of-the-art performance across varying resolution aerial UAV imagery, that improves forest trail detection for UAV guidance even when using significantly low resolution images that are representative of low-cost search and rescue capable UAV platforms.

I. INTRODUCTION

Scene understanding within unstructured environments with varying illumination conditions are critical for autonomous flight within the forest canopy. Growing interest in solving this challenge has motivated researchers to investigate the use of Deep Neural Networks (DNN) to identify trail images for UAV navigation. However, in order to train such a DNN, a large volume of labeled data is required, which is challenging to obtain due to the target task in hand (i.e. sub canopy UAV operation).

T he work of [3] gathered data by using a head-mounted rig with three cameras worn by a human trail walker, allowing their proposed DNN architecture to identify the direction of the trail in a given view - *left, right, forward* . A similar approach is followed by [7] whereby a wide-baseline rig is used, also with three cameras mounted to gather data which they used to augment the dataset of [3] (IDSIA dataset). As a result, the approach presented by [7] is capable of estimating both lateral offset and trail direction. In both cases [3, 7], the authors, follow the common practice of dataset augmentation, via affine image transformations, which adds extra computation without any performance guarantees.

Alternatively, synthetic data, from virtual environment models, could potentially replace or at least supplement hard-won real environment data [5, 6, 9]. However, the significant discrepancy between synthetic data and real-world data often results in models that are trained only on synthetic environment examples not being able to directly transfer this knowledge to real-world operating tasks [2, 8, 5, 1].

Even when training a DNN using only real-world data, it is important to observe that models trained on a limited domain-specific dataset often fail to generalise successfully. In addition, since common DNN architectures require the dataset to be formed from fixed resolution images [4], models commonly fail to generalize across domains.

Our work here is closely related to [3, 7, 2] and demonstrates that the same trail direction required for automous UAV navigation can be acquired by using imagery gathered by a single forward-facing camera (Figure 1).

This is due the fact that the center of the forward-facing camera usually shows the trail ahead. Additionally, we demonstrate that a trail can be identified in unseen parts of a

forest by training the model with data gathered across varying devices and camera resolutions. This not only facilitates more general data gathering but also eliminates the need for synthetic data and augmentation. As result, the same model can be used by UAV with different sensor payload capabilities.

Figure 1: Comparison of three way image cropping performed on varied camera view

3. METHOD

Here we were motivated by the three class problem presented by [3] in which an estimation of the trail direction, {left, right, forward,} is achieved by processing an image triplet of left/right/forward camera views via a DNN. In contrast to [3, 7], our approach uses only a single forward facing camera view which more representative of an operational UAV case. This image view is then itself cropped into {left, right, forward} which can be labeled for trail presence/absence (Figure 1).
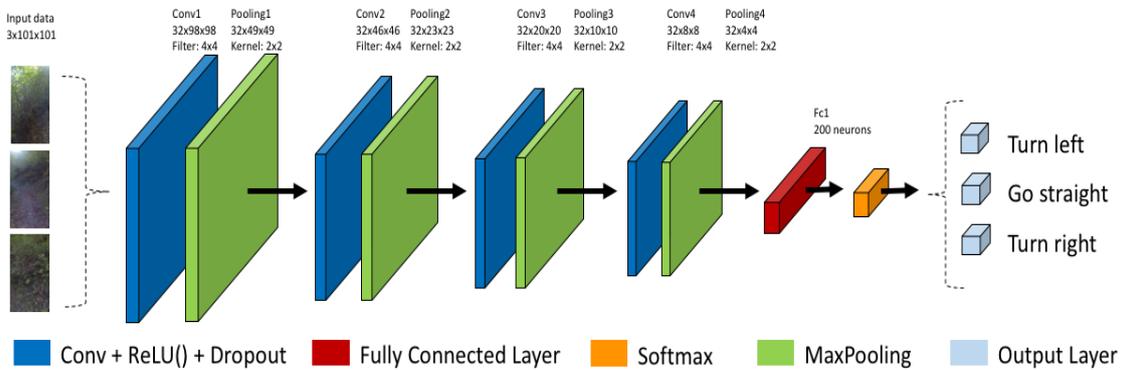
Figure 2: An outline of our DNN architecture - based on [3]

Using the architecture of [3] (illustrated in Figure 2), we evaluate varying image resolution, the use of additional data augmentation (DA) and activation function *(tanh() / ReLU())*. DNN training uses a gradient descent optimiser, random weight initialisation with zero node biases and is performed over 90 epochs with a 0.05 reduction in learning rate per epoch (decay rate: 0.95). For both training and testing we use the high-resolution (752 x 480) IDSIA dataset (from [3]) and a low-resolution (106 x 240) Urpeth Burn (UB) dataset, gathered locally. For training 45,097 high-resolution and 32,017 low-resolution image were used, while for testing 12,251 high-resolution and 5,152 low-resolutions images were used. Further data augmemtation (mirror, translation & rotation) was performed on a copy of this original dataset. For simplicity of reporting, we define NA as non-augmented data obtained results and DA as data augmented obtained results (Table 1).

III. RESULTS

Our experimental results are divided into three sets:- (1) image triplet approach of [3] with differing activation functions *(tanh()/ReLU())* - Table 1 upper 2 sets), (2) our proposed approach (single forward view image, split into three views - Table 1 middle sets in bold) and (3) the impact of high/low/varied image resolutions on performance (Table 1 lower sets). Overall we see what the use of the ReLU() activation outperforms tanh() and our approach gives high levels of accuracy without the need for data augmentation outperforming the prior reported results in [3] (in fact no significant improvement was achieved by data augmentation). Although our approach fails to generalise when trained with high-resolution images on to low-resolution images, it achieves 82% accuracy when low-resolution images are added to the training dataset and achieves 78% accuracy for training and testing on low-resolution images only.

Method	Activation Function	Training Dataset	Testing Dataset	Training Loss	Training Accuracy	Test Loss	Test Accuracy
Giusti *et al.* [3] [DA]	*tanh()*	High	High	1.04	0.46	1.07	0.47
Giusti *et al.* [3] [NA]	*tanh()*	High	High	1.01	0.41	1.02	0.48
Giusti *et al.* [3] [DA]	*ReLU()*	High	High	0.02	1.00	2.97	0.59
Giusti *et al.* [3] [NA]	*ReLU()*	High	High	0.00	1.00	2.56	0.72
Our Approach [DA]	***ReLU()***	**High**	**High**	**0.18**	**0.92**	**0.26**	**0.89**
Our Approach [NA]	***ReLU()***	**High**	**High**	**0.07**	**0.97**	**0.31**	**0.89**
High Resolution[NA]	*ReLU()*	High	Low	0.17	0.94	1.00	0.44
Low Resolution [NA]	*ReLU()*	Low	Low	0.40	0.86	0.58	0.78
Varied Resolutions [NA]	***ReLU()***	**High+Low**	**Low**	**0.24**	**0.93**	**0.51**	**0.82**
Varied Resolutions [NA]	***ReLU()***	**High+Low**	**High**	**0.40**	**0.83**	**0.64**	**0.76**

Table 1: Results showing varying performance across High and Low image dataset combinations.

I.V. CONCLUSION

In this paper, we present an alternative method to gather and process UAV imagery that improves the level of accuracy for trail navigation under forest canopy by training the network using only the data from a single forward facing camera view instead of the triplet view training approach of [3].

Our approach also performs well across varying image resolutions and increases the capability of low-cost UAV platforms with limited payload capacity. Future work will include additional aspects of UAV perception and control targeting end-to-end autonomy across this and other challenging operating environments.

REFERENCES

1. Paul Christiano, Zain Shah, Igor Mordatch, Jonas Schneider, Trevor Blackwell, Joshua Tobin, Pieter Abbeel, and Wojciech Zaremba. Transfer from simulation to real world through learning deep inverse dynamics model. CoRR, abs/1610.03518, 2016.

2. Dhiraj Gandhi, Lerrel Pinto, and Abhinav Gupta. Learning to fly by crashing. CoRR, abs/1704.05588, 2017.

3. Alessandro Giusti, Jerome Guzzi, Dan C. Ciresan, Fang-Lin He, Juan Pablo Rodriguez, Flavio Fontana, Matthias Faessler, Christian Forster, Jurgen Schmidhuber, Gianni Di Caro, Davide Scaramuzza, and Luca L. Gambardella. A machine learning approach to visual perception of forest trails for mobile robots. 1:1–1, 01 2015.

4. Kaiming He, Xiangyu Zhang, Shaoqing Ren, and Jian Sun. Spatial pyramid pooling in deep convolutional networks for visual recognition. CoRR, abs/1406.4729, 2014.

5. Klaas Kelchtermans and Tinne Tuytelaars. How hard is it to cross the room? - training (recurrent) neural networks to steer a UAV. CoRR, abs/1702.07600, 2017.

6. Matthias Mueller, Vincent Casser, Neil Smith, Dominik L. Michels, and Bernard Ghanem. Teaching uavs to race using ue4sim. CoRR, abs/1708.05884, 2017.

7. Nikolai Smolyanskiy, Alexey Kamenev, Jeffrey Smith, and Stan Birchfield. Toward low-flying autonomous MAV trail navigation using deep neural networks for environmental awareness. CoRR, abs/1705.02550, 2017.

8. Lei Tai and Ming Liu. Deep-learning in mobile robotics - from perception to control systems: A survey on why and why not. CoRR, abs/1612.07139, 2016.

9. Tianhao Zhang, Gregory Kahn, Sergey Levine, and Pieter Abbeel. Learning deep control policies for au- tonomous aerial vehicles with mpc-guided policy search. CoRR, abs/1509.06791, 2015.

Conversational human-swarm interaction using IBM Cloud

Alan G. Millard and James R. Williams
alan.millard@york.ac.uk, james.williams@uk.ibm.com

I. INTRODUCTION

Swarm robotics is an approach to the coordination of large numbers of robots that has become an increasingly popular field of research in recent years [1], not least because properly engineered robot swarms are scalable, flexible, and robust, making them an attractive alternative to single-robot systems in many application domains [2]. Since its inception, the field of swarm robotics has grown beyond its roots in purely decentralised control inspired by social insect behaviour [3], now often utilising hybrid centralised/decentralised control architectures that incorporate human operators who guide swarm actions during tasks such as firefighting [4], or the localisation of radiation sources [5].

This kind of human-swarm interaction has attracted significant interest from the research com- munity, spawning an entire sub-field of its own that investigates how human operators, supervisors, and team-mates can interact with robot swarms and receive feedback from them [6]. To date, human- swarm control methods such as the use of graphical user interfaces [5][7] and spatial gestures [8][9][10] have received much attention, but there has been little investigation into the potential of controlling swarm robotic systems with an operator's voice. The few studies that have explored this idea [11][12] are restricted to the use of specific predefined phrases that the human operator is required to learn, resulting in interactions that are unnatural in comparison to the way a human would normally express themselves in speech. In this paper, we present a novel architecture for conversational human-swarm interaction that addresses these issues, allowing swarm robotic systems to be engineered in such a way that a human operator can guide a swarm using spoken dialogue in a more natural manner.

II. ARCHITECTURE FOR CONVERSATIONAL HUMAN-SWARM INTERACTION

IBM Cloud [13] is a cloud platform-as-a-service (free to use for educators and students via the Academic Initiative for Cloud offer [14]) that provides a catalogue of services which developers can use to build applications. As part of this catalogue, IBM offer a number of machine-learning-based services such as language translation, image recognition, and sentiment analysis. We employ the Watson Conversation service [15], which allows developers to define a dialogue tree for a virtual agent/chatbot that can engage with users on a particular topic. The developer defines a set of intents (goals the user may want to achieve), a set of entities (classes of objects relevant to the user's intents), and a set of rules that define how the chatbot should respond based on the entities and intents recognised in the user's input. In addition, the developer provides a set of example phrases for each intent, as well as synonyms for each entity, which are used to train the natural language classifier. The Watson Conversation service can also be configured to ask the user for further information if their intent is unclear, thus making the system robust to the flexibility of natural dialogue.

To conversationally interact with a swarm of robots, we can define the human-swarm interaction as a dialogue using the Watson Conversation service. A human operator's goals can be encoded as intents (e.g. "select robots with at least 50% battery", "add robots to swarm three", "swarm three perform flocking"), and domain objects can be defined as entities (e.g. "robot", "battery",

"swarm three"). The dialogue tree provided by the developer links these intents and entities to operator feedback via natural language responses (like a traditional chatbot), as well as domain-specific responses that can be used to guide the robotic system.

III. CORE ARCHITECTURE

The core architecture for the proposed conversational interaction is shown in Figure 1 (left). The Human-Swarm Interaction Controller (HSIC) is the interface to the human operator commanding the swarm, which streams voice recordings to the Watson Speech to Text service [16] running in the IBM Cloud. This service analyses the audio and converts it into text, then passes it to the Watson Conversation service running the domain-specific dialogue tree, which interprets the human operator's intent and responds accordingly. The HSIC then either requests further information from the operator (if required by the dialogue tree), or dispatches complete commands to the Swarm Manager — a target-specific piece of software written by the developer (e.g. a ROS master [17]) that interprets these swarm-level commands and decomposes them into instructions that are sent to the individual robots, triggering decentralised autonomous swarm behaviours.
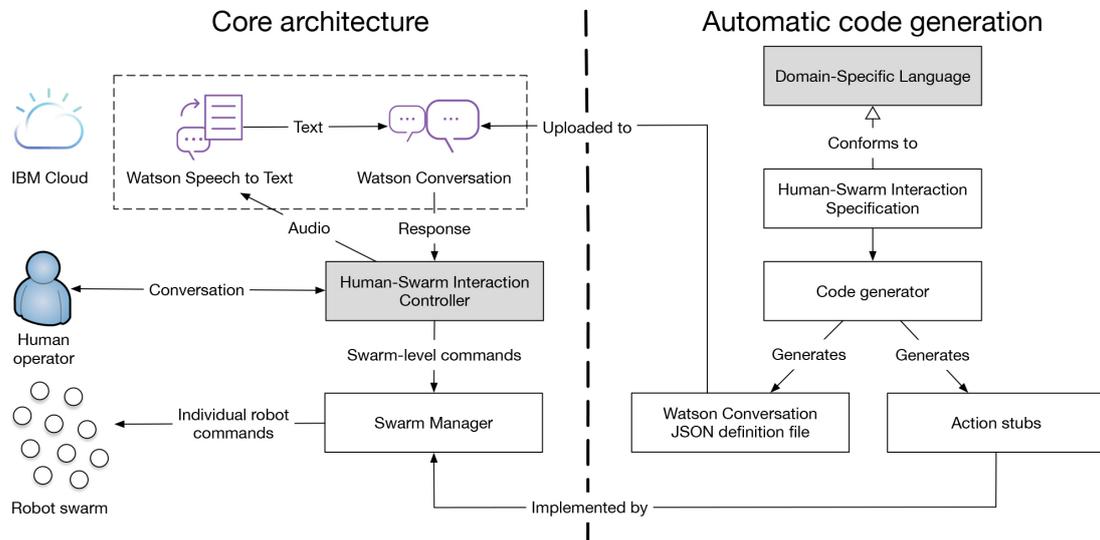
Figure 1: System architecture. *Left:* Core architecture, *Right:* Automatic code generation.

III.AUTOMATIC CODE GENERATION

Developing code for the Watson Conversation definition and the Swarm Manager independently may lead to inconsistencies between the two that are only discovered at run-time. To address this, we propose the use of a Domain-Specific Language (DSL) and a code generator that allows swarm engi- neers to develop both of these artefacts from a single specification (see Figure 1, right), thus ensuring consistency whilst reducing development effort. The code generator produces a JSON file that can be uploaded to the Watson Conversation service running in the IBM Cloud, and corresponding Swarm Manager code stubs for each of the swarm actions defined in the dialogue. The developer then com- pletes the implementation of these stubs to define how the swarm-level commands are decomposed into messages that are sent to the individual robots. When the Swarm Manager receives a command from the HSIC, it invokes the corresponding auto-generated action stub, and the swarm is instructed accordingly. To minimise development effort, a library of common, composable actions can be used in the DSL. These actions might include the ability to select specific robots, assign a name to a selection of robots for later reference, and common swarm behaviours such as flocking and aggregation.

IV. CONCLUSION

In this paper, we have presented an extensible architecture for defining a conversational human-swarm interaction model, which is sufficiently generic to be applied in many target domains. Using a DSL, developers can easily define how a human operator's intents are mapped to swarm-level commands, enabling rapid development of conversational communication. The flexibility of the resulting human-swarm interaction facilitates the use of natural spoken dialogue, which is particularly advantageous in high-pressure situations where human operators may struggle to recall specific predefined commands, and can instead interact with a robot swarm quickly and conversationally to achieve their goals.

REFERENCES

1. M. Brambilla, E. Ferrante, M. Birattari, and M. Dorigo, "Swarm robotics: a review from the swarm engineering perspective," *Swarm Intelligence*, vol. 7, no. 1, pp. 1–41, 2013.
2. E. Şahin, "Swarm robotics: From sources of inspiration to domains of application," in *International work- shop on swarm robotics*. Springer, 2004, pp. 10–20.
3. E. Bonabeau, M. Dorigo, and G. Theraulaz, *Swarm intelligence: from natural to artificial systems*. Oxford University Press, 1999.
4. A. M. Naghsh, J. Gancet, A. Tanoto, and C. Roast, "Analysis and design of human-robot swarm interaction in firefighting," in *17th IEEE International Symposium on Robot and Human Interactive Communication (RO-MAN)*, 2008, pp. 255–260.
5. S. Bashyal and G. K. Venayagamoorthy, "Human swarm interaction for radiation source search and local- ization," in *Swarm Intelligence Symposium (SIS)*. IEEE, 2008, pp. 1–8.
6. A. Kolling, P. Walker, N. Chakraborty, K. Sycara, and M. Lewis, "Human interaction with robot swarms: A survey," *IEEE Transactions on Human-Machine Systems*, vol. 46, no. 1, pp. 9–26, 2016.
7. J. McLurkin, J. Smith, J. Frankel, D. Sotkowitz, D. Blau, and B. Schmidt, "Speaking swarmish: Human- robot interface design for large swarms of autonomous mobile robots." in *AAAI Spring Symposium 2006: To Boldly Go Where No Human-Robot Team Has Gone Before*, 2006, pp. 72–75.
8. J. Nagi, A. Giusti, L. M. Gambardella, and G. A. Di Caro, "Human-swarm interaction using spatial gestures," in *IEEE/RSJ International Conference on Intelligent Robots and Systems (IROS)*, 2014, pp. 3834–3841.
9. G. Podevijn, R. O'Grady, Y. S. Nashed, and M. Dorigo, "Gesturing at subswarms: Towards direct human control of robot swarms," in *Conference Towards Autonomous Robotic Systems*. Springer, 2013, pp. 390–403.
10. S. Nagavalli, M. Chandarana, M. Lewis, and K. Sycara, "Multi-operator gesture control of robotic swarms using wearable devices," in *Tenth International Conference on Advances in Computer-Human Interactions (ACHI)*, March 2017.
11. S. Pourmehr, V. M. Monajjemi, R. Vaughan, and G. Mori, ""You two! Take off!": Creating, modifying and commanding groups of robots using face engagement and indirect speech in voice commands," in *IEEE/RSJ International Conference on Intelligent Robots and Systems (IROS)*, 2013, pp. 137–142.
12. G. Kapellmann-Zafra, J. Chen, and R. Groß, "Using Google Glass in Human–Robot Swarm Interaction," in *Conference Towards Autonomous Robotic Systems*. Springer, 2016, pp. 196–201.
13. IBM Cloud. [Online]. Available: https://www.ibm.com/cloud/
14. Academic Initiative for Cloud offer. [Online]. Available: https://developer.ibm.com/academic/resources/ cloud-offer/
15. IBM Watson Conversation service. [Online]. Available: https://www.ibm.com/watson/services/ conversation/
16. IBM Watson Speech to Text service. [Online]. Available: https://www.ibm.com/watson/services/ speech-to-text/
17. M. Quigley, K. Conley, B. Gerkey, J. Faust, T. Foote, J. Leibs, R. Wheeler, and A. Y. Ng, "ROS: an open-source Robot Operating System," in *ICRA Workshop on Open Source Software*, vol. 3, no. 3.2, 2009, p. 5.

Modelling and Predicting Rhythmic Flow Patterns in Dynamic Environments

Sergi Molina[1], Grzegorz Cielniak[1], Tomáš Krajník[2], qnd Tom Duckett[1]
smolinamellado, gcielniak, tduckett @lincoln.ac.uk,
Lincoln Center for Autonomous Systems, University of Lincoln, United Kingdom
[2] tomas.krajnik@fel.cvut.cz, FEE, Czech Technical University, Prague, Czechia

ABSTRACT

In this paper, we introduce a time-dependent probabilistic map able to model and predict future flow patterns of people in indoor environments. The proposed representation models the likelihood of motion direction by a set of harmonic functions, which efficiently capture long-term (hours to months) variations of crowd movements over time, so from a robotics perspective, this model could be useful to add the predicted human behavior into the control loop to influence the actions of the robot. Our approach is evaluated with data collected from a real environment and initial qualitative results are presented.

I. INTRODUCTION

Representation of the environment dynamics is seen as one of the key challenges to enable autonomous navigation in real-world scenarios, since this representation will help to define how and where the robot should move. This is especially important when deployed in a human-populated context, where significant variations are often observed. Some authors have proposed representations to model the typical (average) motion patterns of dynamic objects1. However, human activities tend to change over time, meaning that static models usually do not capture the real behavior of the environment, leading to inaccuracies over time.

Thus, our method includes the temporal dimension on top of the spatial structure, but unlike previous approaches using an occupancy grid map2, we assume that the observed activities follow some underlying patterns due to the periodic nature of human activities, such as leaving home and returning after work at approximately the same time, or, as in the experiments presented here, people going in one direction or another in a shopping centre depending on the time of day. In the proposed approach, we model the temporal dimension of activities using periodic functions, going from hours to weeks, allowing prediction of future environment states with a compact representation, even during long-term operation.

II. SPATIO-TEMPORAL MODEL

The geometric space is defined using a grid-based representation, where each cell in the grid has 8 associated transitions to the neighbouring cells, and because we are only interested in the state changes, the case of remaining in the same cell is not considered. So in total, we model the likelihood of 8 ncells transitions over time. We consider that a cell is occupied if a person can be found within its boundaries, and the transitions are performed exclusively to neighbouring cells in one time step. To achieve that we have discretized the space and time according to the well-known Nyquist-Shannon theorem and knowing the average walking speed of people in the dataset used for experimentation, giving cells of one metre squared and a sampling frequency of 2 Hz.

In order to handle the temporal dynamics we use the FreMEn framework3. FreMEn is a mathematical tool based on the Fourier Transform, which considers the probability of a given state or event as a function of time and represents it by a combination of

harmonic components. Such a model not only allows representation of environment dynamics over arbitrary timescales with constant memory requirements, but also prediction of future environment states or events. Assuming the transitions follow some periodic patterns over time as a consequence of the natural human activities, we can apply the FreMEn model over each transition, obtaining a probabilistic prediction of each transition happening at any instant of time. Similarly to earlier work4, our approach counts the number of transitions happening in each direction during an interval of time, and normalises these counts so that the most frequent transition is assigned the value of 100. If some periodic patterns can be found, after some training we should observe that some transitions have higher probabilities than others during certain periods of time.

III. EXPERIMENTS

To evaluate the model, we used a pedestrian tracking dataset recorded from the ATC shopping center in Osaka, Japan5. The perception system consists of multiple 3D range sensors, covering an area of approximately 900 m2, so we can follow the same person around the place in every instant of time. The data was recorded every Wednesday and Sunday during a timespan of one year. From all these data, we employed the first 20 consecutive Wednesdays as our training set to learn the model, using the 21st Wednesday as the evaluation day. The recording of each day provides people trajectories starting from approximately 9 a.m. to 9 p.m., so for the rest of day we have set all transitions to 0 simulating the shopping center being closed.

After comparing the predicted model for the evaluation day with the ground truth, we found that the best model was obtained using one FreMEn component, corresponding to a period of one day. In Fig. 1, for better visualization, only a subset of the whole map is plotted, where for each cell the transition with the highest probability for that time is shown.

Within this region, the upper and lower zones remain stable throughout the day, but the middle area presents a noticeable change in the flow direction. In the morning the number of people entering the mall tends to be higher than those leaving, hence the arrows to the left (red), but in the afternoon (Fig.1c and 1d) there are more people leaving so the transition to the right neighboring cell (cyan) tends to have higher probability. Thus the model learned that most of the cells in the centre present a daily change, and is able to predict future states with good generalization of the dynamics.

I.V. DISCUSSION

We have proposed an approach to model the dynamics of human motion, which is able to generate predictions of future crowd movement at a given time. From a robotics perspective, this representation could be very useful for automated task planned or decision-making, adding the predicted human behavior into the control loop to influence the actions taken by the robot, for example, to navigate and plan robot paths with a more natural and harmonious movement with respect to the crowd, moving with the flow and obtaining fewer face-to-face encounters. The model could be also used for semantic clustering of map regions with similar dynamics or studying motion patterns.

For the experiments presented in this paper, we assumed that the environment is fully observable. However, we know this is unlikely to be feasible in a real-world scenario using only the onboard sensors of a mobile robot. So using the capability of FreMEn to work with sparse data3, allowing us to update only the transitions actually observed by the robot, we are planning to study robot exploration strategies to actively keep the spatio-temporal representations up-to-date. These strategies need to take into account not only the spatial domain, but also the temporal dimension, as we need to know if new rhythmic patterns appear in some areas of the map, and the most important ones when they do. Future work will also include testing the model in other scenarios such as warehouse operations to check the method's generalization capabilities.
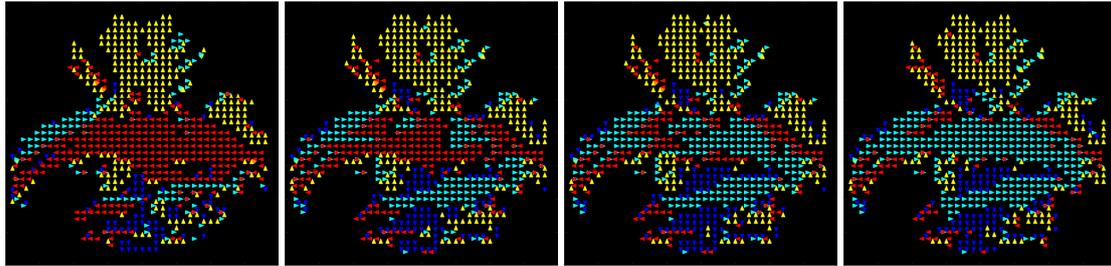
| (a) 10 a.m. | (b) 2 p.m. | (c) 6 p.m. | (d) 9 p.m. |

Figure 1. Model predicted at 4 different times during the evaluation day. Each colour (yellow, green, cyan, blue, dark blue, dark red, red and orange) represents one of the eight possible transition orientations.

ACKNOWLEDGMENT

REFERENCES

1. Kucner, T., J. Saarinen, J., M. Magnusson, M. & Lilienthal, A. J. Conditional transition maps learning motion patterns in dynamics environments. Control. Autom. 1–8 (2007).

2. Mitsou, N. C. & Tzafestas, C. S. Temporal occupancy grid for mobile robot dynamic environment mapping. IEEE Intell. Robots Syst. (2013).

3. Krajnik, T., Fentanes, J. P., Santos, J. & Duckett, T. Fremen: Frequency map enhancement for long-term mobile robot autonomy in changing environments. IEEE Transactions on Robotics (2015).

4. Jovan, F. et al. A poisson-spectral model for modelling temporal patterns in human data observed by a robot. In 2016 IEEE/RSJ International Conference on Intelligent Robots and Systems (IROS), 4013–4018 (2016). DOI 10.1109/IROS.2016.7759591.

5. Brscic, D., Kanda, T., Ikeda, T. & T. Miyashita, T. Person position and body direction tracking in large public spaces using 3d range sensors. IEEE Transactions on Human-Machine Syst. 43, 522–534 (2013).

A Modified Computed Torque Control Approach for a Teleoperation Master-Slave Robot Manipulator System

Ololade O. Obadina, Julius Bernth, Kaspar Althoefer and M. Hasan Shaheed
School of Engineering and Materials Science, Queen Mary University of London.

ABSTRACT

A modified computed torque controller (CTC) is presented in this paper. The proposed approach is demonstrated on one joint of a 4-degree of freedom (DOF) master-slave (MS) robot manipulator and the CTC gain parameters are optimized using the particle swarm optimisation (PSO) algorithm. The feasibility of the proposed controller is tested and compared with the conventional / traditional computed torque control. Results show that the proposed controller performs impressively.

I. INTRODUCTION

Considerable progress in research has been made in developing master-slave (MS) robotic systems for various applications. Some of these areas of application include minimally invasive surgeries [1] and rehabilitation [2]. Limitations imposed by the majority of the existing MS robotic surgical systems include a high cost of equipment and maintenance, steep learning curve for the surgeon and the large physical dimension of the equipment [3], [4]. Thus, the need for smaller sized yet affordable MS robotic systems is growing rapidly.

A major challenge introduced with robotic systems in general involves developing robust controllers that are capable of handling uncertainties and disturbances in the robot's environment. The nonlinearities present in robot manipulator dynamics' make linear feedback control techniques unsuitable for controlling the system efficiently. For instance, the traditional proportional-integral-and-derivative (PID) controller that is widely accepted and simple to implement [5] performs poorly in high speed operations.

Several non-linear control methods [5], [6], [7], [8] have been investigated to meet high speed operation and accurate control requirements in industry, e.g. Computed Torque Control. Computed torque control (CTC) involves feeding back a signal to eliminate the effects of disturbances and nonlinearities, and introduces desired torques that will ensure the error dynamics converges to zero. Some of these nonlinear terms include gravity and friction, and Coriolis and centrifugal torques.

Optimisation algorithms are often used to enhance the performance of controllers, by tuning the controller parameters for optimal control. For example, the PSO algorithm, in comparison to other optimization methods, is valued mostly due to its ease of implementation and a few adjustment parameters [9]. Particle swarm optimisation was first developed by Eberhart and Kennedy [10], and has evolved since it was introduced over two decades ago. The PSO algorithm can be seen to minimize the cost function of an H∞ PID controller for a flexible link manipulator in [11]. Soltanpour [12] also uses the PSO algorithm to adjust the membership functions of fuzzy sliding mode controller for a robot manipulator. These cited examples highlight the versatility of using the PSO algorithm for various types of nonlinear control.

II. MAIN WORK

The master-slave robotic system is a laboratory prototype that consists of the master and slave manipulators. The hand movements of the user holding the master are relayed as measured position signals to the control system, which then sends, scaled and transformed signals to the slave manipulator.

Both master and slave manipulators are dynamically similar where each manipulator has 4 degrees of freedom (DOF) each plus one for grasping at the end effector. The main difference between these manipulators is the presence of position sensors in the master, and actuators in the slave joints respectively. Hence, only the dynamics of the slave manipulator is considered in this work.

The rigid body dynamic equations of the slave manipulator is derived from the Euler-Lagrange [13] method, and the equation for an N-DOF robot manipulator, written in vector form, is described as:

$$\tau = M(\theta)\ddot{\theta} + C(\theta, \dot{\theta}) + G(\theta) \tag{1}$$

Where:- $G(\theta)$, $C(\theta, \dot{\theta})$, τ and $\ddot{\theta}$ are Nx1 vectors of gravitational, Coriolis and centrifugal, driving torque and of robot's acceleration components, respectively. $M(\theta)$ is a NxN positive definite matrix of rigid body inertia.

In general control systems, the overall goal of a controller is to ensure a closed loop system is stable, minimize tracking errors, and ensure robustness against uncertainties and perturbations in closed loop systems.

The general equation of the traditional CTC is described as:

$$\tau = M(\theta)V + D(\theta, \dot{\theta}) \tag{2}$$

where the auxiliary control input, $\underline{V}$ is given:
$$V = \ddot{\theta}_d + 2\zeta\omega_n\dot{e} + \omega_n^2 e \tag{3}$$
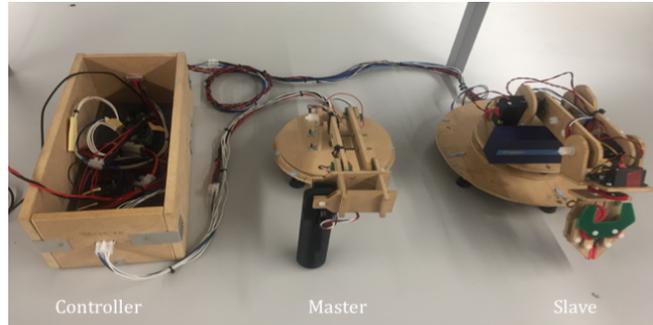
Figure 1: 4-DOF Master-Slave Robot Manipulator System

The modified CTC, however, uses a similar structure as the traditional CTC but incorporates the use of an integral error and omits the desired joint acceleration. The modified auxiliary control law is, thus, expressed as:
$$V = \omega_n^2 e + K_i\varepsilon + 2\zeta\omega_n\dot{e} \tag{4}$$
Therefore, the desired computed joint torques to be inputted into the system can be described mathematically, as:
$$\tau = M(\theta)[\omega_n^2 e + K_i\varepsilon + 2\zeta\omega_n\dot{e}] + D(\theta, \dot{\theta}) \tag{5}$$

where: θ_d is the desired angular position, θ is the actual angular position, e is the tracking error, ε is the integral of the tracking error, e is the derivative of the tracking error, $D(\theta, \theta)$ is the sum of nonlinear Coriolis/centrifugal and gravity terms, and ω_n, ζ, K_i are gains to be tuned for each joint. It can be inferred that the structure of the modified CTC appears very much like a standard PID controller. The gain parameters of the modified CTC are tuned offline using PSO algorithm and an objective cost

The obtained optimal controller is then implemented on the real MS robot system, and its performance is compared with the traditional CTC, as shown in Figure 2a and Fig. 2b:

Figure 2a: Standard CTC on MS Robot - Joint 2   *Figure 2b: Modified CTC on MS Robot - Joint 2*
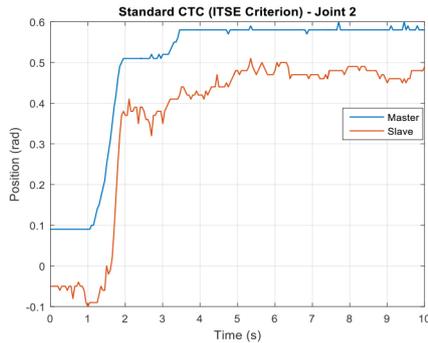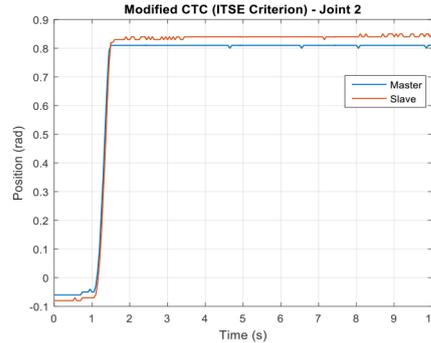
It is noticeable that the standard CTC in Joint 2 causes the slave manipulator to oscillate haphazardly about its steady state (see Fig.2a) while the modified CTC (in Fig. 2b) gives a smoother response. An offset seen in the standard CTC response, caused by the jittery behaviour, induces a steady state error between the master and slave. The modified CTC, however, attempts to get rid of this offset, and the slave manipulator is seen to track the master manipulator remarkably well with a steady state error of approximately 0.05 rad. Obtained result shows that the proposed modified CTC approach is feasible, and in fact performs better than the traditional CTC.

REFERENCES

1. D. B. Camarillo, T. M. Krummel, and J. K. Salisbury, 'Robotic Technology in Surgery: Past, Present, and Future.', *Am. J. Surg.*, vol. 188, no. 4A Suppl, p. 2S–15S, 2004.
2. M. Cortese, M. Cempini, P. Rog, D. A. Ribeiro, and S. R. Soekadar, 'A Mechatronic System for Robot-Mediated Hand Telerehabilitation', *IEEE/ASME Trans. Mechatronics*, vol. PP, no. 99, pp. 1– 12, 2014.
3. V. Vitiello, 'Emerging Robotic Platforms for Minimally Invasive Surgery', *Biomed. Eng. IEEE Rev.*, vol. 6, pp. 111–126, 2013.
4. H. Sang, S. Wang, L. Zhang, C. He, L. Zhang, and X. Wang, 'Control design and implementation of a novel master – slave surgery robot system , MicroHand A', *Int. J. Med. Robot. Comput. Assist. Surg.*, no. 7, pp. 334–347, 2011.
5. Z. Song, J. Yi, D. Zhao, and X. Li, 'A computed torque controller for uncertain robotic manipulator systems: Fuzzy approach', *Fuzzy Sets Syst.*, vol. 154, no. 2, pp. 208–226, 2005.
6. M. . Zhihong and M. Palaniswami, 'Robust tracking control for rigid robotic manipulators', *IEEE Trans. Automat. Contr.*, vol. 39, no. 1, pp. 154–159, 1994.
7. L. Bascetta and P. Rocco, 'Revising the robust-control design for rigid robot manipulators', *IEEE Trans. Robot.*, vol. 26

no. April, pp. 180–187, 2010.
8. H. F. Ho, Y. K. Wong, and A. B. Rad, 'Robust fuzzy tracking control for robotic manipulators',
   a. *Simul. Model. Pract. Theory*, vol. 15, no. 7, pp. 801–816, 2007.
9. M. Geetha, K. . Balajee, and J. Jerome, 'Optimal Tuning of Virtual Feedback PID Controller for a Continuous Stirred Tank Reactor (CSTR) using Particle Swarm Optimization (PSO) Algorithm', in *IEEE-International Conference On Advances In Engineering, Science And Management*, 2012, pp. 94–99.
10. R. Eberhart and J. Kennedy, 'A new optimizer using particle swarm theory', *Proc. Sixth Int. Symp. Micro Mach. Hum. Sci.*, pp. 39–43, 1995.
11. M. Zamani, N. Sadati, and M. K. Ghartemani, 'Design of an H∞ PID controller using particle swarm optimization', *Int. J. Control. Autom. Syst.*, vol. 7, no. 2, pp. 273–280, 2009.
12. M. Soltanpour and M. Khooban, 'A particle swarm optimization approach for fuzzy sliding mode control for tracking the robot manipulator', *Nonlinear Dyn.*, pp. 1–12, 2013.
13. J. J. Craig, *Introduction to Robotics: Mechanics and Control 3rd*, vol. 1, no. 3. 2004.

Bio-Inspired Path Planning for UAVs in Urban Environments

J. Williamson[1], A. Spelt[1], E. L. C. Shepard[2], S. P. Windsor[1] University of Bristol, 2. University of Swansea

I. INTRODUCTION

Small Unmanned Aerial Vehicles or drones are increasingly featured in the media. They have potential as a quick to launch, low cost platform suitable for low altitude flight within the urban environment. However, there are two technology hurdles to overcome before we see a skyline permeated with flying vehicles.

Cityscapes are rife with complex wind flows, potentially destabilising autonomous air vehicles, creating a public safety risk as well as compromising the functionality of the platform. The second technological pitfall is the current battery technology which limits the range and endurance achievable by small flying platforms.

This research looks for engineering solutions inspired from biology. Birds of comparable size and weight are not only able to manage complex wind flow, but also exploit the environment as a locomotive energy source. Urban gull populations have rapidly increased in recent decades and new research indicates that gulls spend almost a third of flight time in soaring [1]. We consider that our city architecture creates wind highways that the gulls navigate for significant energy savings in flight.

Is it then possible, that urban gulls can teach us viable flight strategies for unmanned aerial vehicles in the urban environment?

Solving this question required an excursion Swansea; a seaside city with plenty of gulls that appear to commute along the bay using orographic lift. A row of seafront hotels act as an artificial cliff forcing the on-shore wind to take on a vertical component. A combination of simplified Computation Fluid Dynamics models and empirical bird flight trajectories were used to identify an adaptive flight strategy that improves flight performance by increasing control in gusts and reducing energetic costs [2].
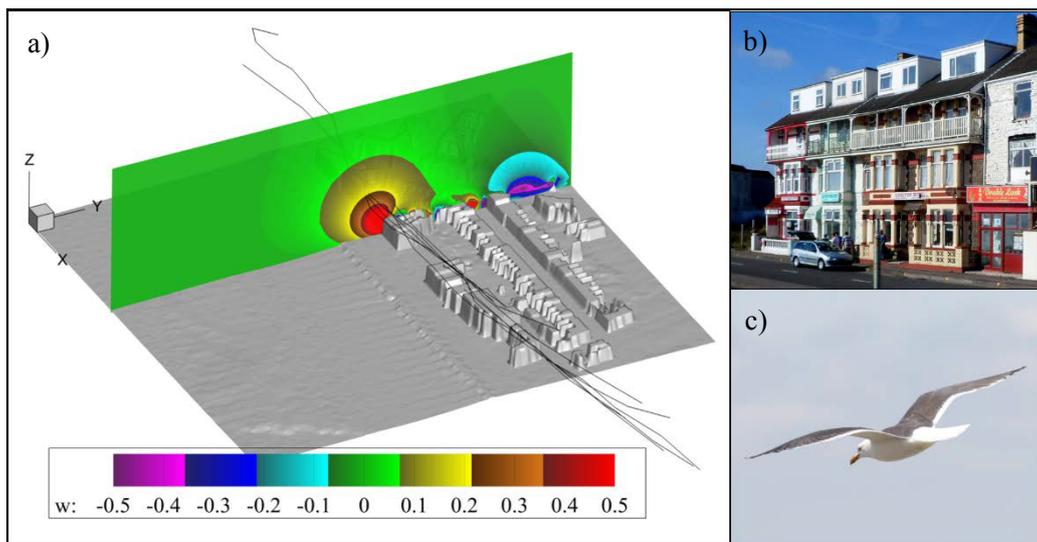

Figure 1: a) The CFD model output in relation to the digital profile of the observation site with the buildings, where the strength of the vertical wind vector component (w, in ms-1) is indicated in colour. The bird flight paths associated with these wind conditions are indicated by black lines. b) The hotels the gulls soar in front of. c) Lesser Black-backed gull in glide.

However, improving city drones will depend on multiple flight strategies. For example, gliding, making use of thermals and orographic soaring. Extending the investigation, ten urban nesting Lesser Black-backed gulls (Larus fuscus) have been tagged with state-of-the-art tracking units [3]. The tags contain GPS and accelerometers which have been used to record the flight paths and behaviours over two breeding seasons.

Figure 2: Lesser Black-backed gull, 5309, wearing a GPS backpack. The backpack records a position using GPS up to every three seconds. Three-axis accelerometers are used to record the behaviours of the gulls, periods of flapping and gliding can be identified due to the difference in forces acting on the body.

Initial data analysis has identified the foraging hotspot which have repeated visits, the gulls alter their flight path depending on the weather conditions. Comparing the variations in these trajectories with the fluctuations in atmospheric conditions could provide insight into the path planning choices of gulls. In addition, understanding the energetic cost function that gulls optimise for would allow tuning of a traditional path planner leading to more efficient routes through the city environment, optimised for the contemporary weather conditions.
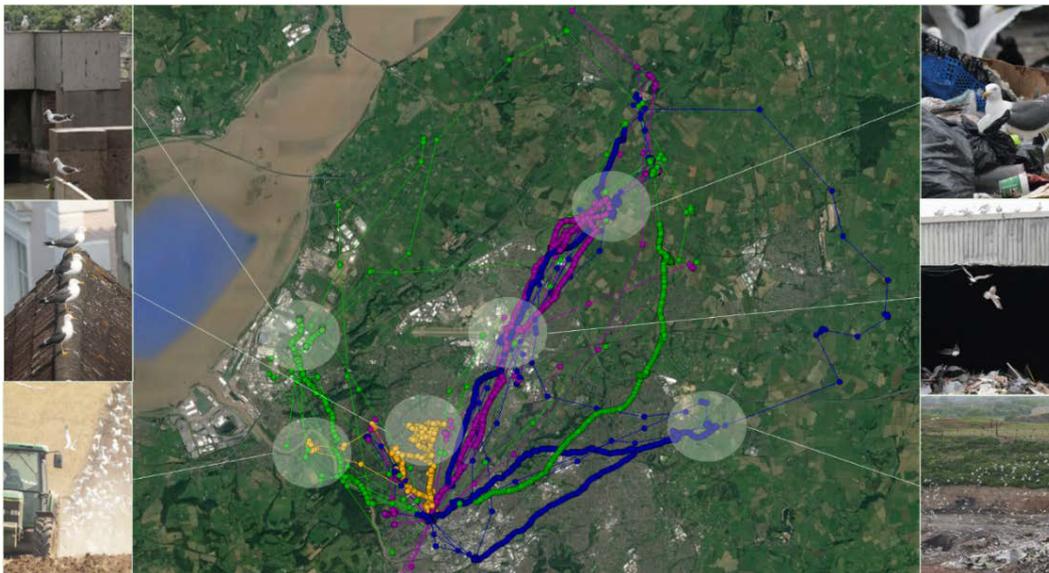
Figure 3: Six foraging hotspots in Bristol are highlighted. The flights of three gulls to these hotspots over two days are shown, each circle indicates a GPS fix. The high-resolution paths indicate a fix at every three to five seconds, the lower resolution flight paths have fixes every twenty minutes. The resolution of the flights is determined by the battery voltage of the GPS unit.

Bio-inspired path planning has significant energy saving and turbulence avoidance implications for small autonomous flying platforms, meaning the futuristic city skyline full of aerial robots is a very real possibility.

REFERENCES

1. Shamoun-Baranes, J., Bouten, W., van Loon, E.E., Meijer, C. and Camphuysen, C.J., 2016.Flap, or soar? How a flight generalist responds to its aerial environment. *Phil. Trans. R. Soc. B*, *371*(1704), p.20150395.

2. Shepard, E.L., Williamson, C. and Windsor, S.P., 2016. Fine-scale flight strategies of gulls in urban airflows indicate risk and reward in city living. *Phil. Trans. R. Soc. B*, *371*(1704), p.20150394.

3. Bouten, W., Baaij, E.W., Shamoun-Baranes, J. and Camphuysen, K.C., 2013. A flexible GPS tracking system for studying bird behaviour at multiple scales. *Journal of Ornithology*, *154*(2), pp.571-580.

Utilising humanoid robots to assist children with autism learn about Visual Perspective Taking

Luke Jai Wood, Ben Robins, Gabriella Lakatos, Dag Sverre Syrdal, Abolfazl Zaraki and Kerstin Dautenhahn
Adaptive Systems Research Group, School of Computer Science, University of Hertfordshire, United Kingdom
{l.wood, b.robins, g.lakatos, d.s.syrdal, a.zaraki, k.dautenhahn}@herts.ac.uk

I. INTRODUCTION

In this paper we provide an overview of the study we have recently conducted investigating the possibility of using humanoid robots to teach children with Autism Spectrum Condition (ASC) about Visual Perspective Taking (VPT). VPT is the ability to see the world from another person's perspective, something that children with ASC often find difficult. Using a humanoid has a distinct advantage in this situation because the robots Field Of View (FOV) can be shown directly to the children using a screen to display what the robot can see from the camera in its eye. Our study working with 12 children in a local special needs secondary school indicates that using this approach to teach children with ASC about VPT has some potential.

II. BACKGROUND

Since the late 90's a vast amount of research has been carried out investigating how robots can be used to encourage communication, social interaction and collaborative play amongst children with ASC [1-5]. However, to date very little research has been conducted into investigating the possibility of using robots to assist develop the VPT skills of children with ASC. VPT is the ability to see the world from another person's perspective, taking into account what they see and how they see it, drawing upon both spatial and social information [6].
setup with additional equipment being used.

Games devised

In attempting to devise an approach teaching children with ASC about VPT, we developed 9 games that started out very basic and incrementally become more difficult, but are all focused on the concepts of VPT. Some of these games included elements of well-

According to Flavell there are two levels of VPT: VPT1, the ability to understand that other people have a different line of sight to ourselves and VPT2, the understanding that two people viewing the same item from different points in space may see different things [6]. The research outlined in this paper provides a brief overview of the games we developed and tested with 12 children aged between 11 and 14 that had been diagnosed with ASC or similar condition in a local special needs school.

III. METHOD

Equipment setup

The standard equipment layout can be seen in Figure 1. The cameras used to record the sessions had wide angled lenses to ensure that the child was always in view and the Kinect sensor was also used to record data for future analysis and testing of activity recognition algorithms. The screen was placed next to the robot in order for the child to see what the robot could see. There were some small variations on this
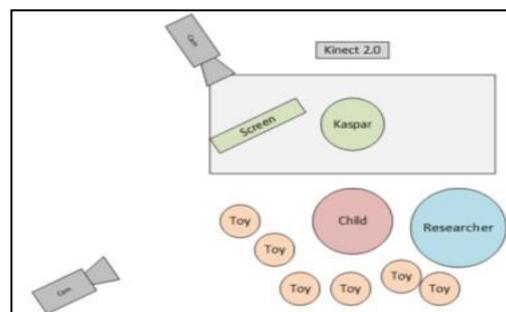

Figure 1. Generic equipment layout

known games such as "I Spy" and "Hide and Seek" that the children could play with the Kaspar robot [7, 8]. The games involved a number of different combinations of actions, starting with moving objects into and out of the robots FOV, and then physically

controlling the robot's line of sight. The key to these games is giving the children the ability to see the world from the robot's perspective and to assist them in learning about VPT. Details of the individual games are as follows:

Game 1: Show me an animal and I'll make the sound: This is a VPT1 game as the children learn that Kaspar has a different line of sight from their own. This game involves the child freely showing Kaspar animal toys of the child's choice while Kaspar looks straight ahead not moving its head or eyes.

Game 2: I'll ask for the animal, you find me the animal: Building on game 1 in this game the children perform the same task but have to follow the robots instructions on what toy to show it.

Game 3: Make me look and I'll tell you what it is: This is again a VPT1 game but in this game the children will physically manipulate the orientation of the robots head to view toys placed around the room. Similar to game 1, the children have the freedom to show Kaspar any toy without limitation.

Game 4: I'll tell you what I want to see and you need to show me: Combining aspects from both games 2 and 3, in this game the child controls where Kaspar looks by physical manipulation of the head, but must follow the robots instructions on what toy it wants to see.

Game 5: What you see is not the same as what I see: This game is a VPT2 exercise the children are given a cube with different pictures on each side. The child must follow Kaspars' instructions and show the robot the requested toy, see Figure 2 (B).

Game 6: I spy with my little eye…: This game is based on the well-known game I spy. The toys are placed around the room and the child needs to work out and pick up the toy that Kaspar is referring to and show the toy to Kaspar.

Game 7: What can we see?: In this game a turntable with a divider is placed on the table and a child places a toy on the turntable. The researcher then moves the turntable into different positions and asks the child questions about the visibility of the object in relation to the robot, this is therefore a VPT2 exercise.

Game 8: Who can see what?: Similar to game 7, the child will answer questions on the visibility of toys placed in a holder, however in this game the child will place three toys into the holder and the holder has 3 different positions in terms of the toys visibility to the robot.

Game 9: Where will I look?: This game is inspired by the well-established Sally-Anne test [9] that is a psychological test, used in developmental psychology to measure a person's social cognitive ability to attribute false beliefs to others. In this game there are two boxes, a blue box and a red box, both have lids. The child has one toy and Kaspar asks the child to put it one of the boxes then place the lid on it whist Kaspar watches. The robot then goes to sleep and closes its eyes.

Whilst Kaspar's eyes are closed and the robot is "sleeping", the researcher encourages the child to move the toy into the opposite container and place the lid on it. The researcher then asks the child to wake Kaspar up to continue playing. When the robot wakes up, the researcher asks the child to point where the robot would look for the toy to establish if the child has a Theory of Mind.

Figure 2. Children interacting with robot during study

I.V. DISCUSSION

The 12 children that took part in this study all possessed different levels of ability and as a result took part in a different number of sessions. In total 69 sessions were run at the school and the games that we devised flowed well and were playable for the children. All of the children managed to complete the most basic games successfully, see Figure 2 (A). Some of the more complex games such as the VPT2 task some children struggled with but most eventually managed this successfully, see Figure 2 (B). The final game that was a Theory of Mind exercise many of the children still struggled with, however some children did make some progress in learning about this, see Figure 2 (C). Generally the games worked as anticipated and the lessons learned from this first pilot-study will be taken into account when conducting our next study in the field.

REFERENCES

1. P. Pennisi, T. Alessandro, T. Gennaro, B. Lucia, R. Liliana, G. Sebastiano, and P. Giovanni, "Autism and social robotics: A systematic review" Autism Research, 2015. C
2. .Robins, K. Dautenhahn, L. Wood, and A. Zaraki, "Developing Interaction Scenarios with a Humanoid Robot to Encourage Visual Perspective Taking Skills in Children with Autism– Preliminary Proof of Concept Tests," in International Conference on Social Robotics, 2017, pp. 147-155: Springer.
3. L. J. Wood, A. Zaraki, M. L. Walters, O. Novanda, B. Robins, and K. Dautenhahn, "The Iterative Development of the Humanoid Robot Kaspar: An Assistive Robot for Children with Autism," in International Conference on Social Robotics, 2017, pp. 53-63: Springer.
4. L. J. Wood, H. Lehmann, K. Dautenhahn, B. Robins, A. Rainer, and

V. FUTURE WORK

Because this research is part of the EU Horizon 2020 BabyRobot project, a project which aims to develop semi-autonomous robotic systems that can work in real world settings and assist with real world problems, a semi-autonomous implementation of the games will be implemented and tested in a school [10].

Prior to developing the games for this work there were some technological considerations take into account and all of the games devised had the potential to apply a level of automation to them which is what we will focus on in the near future.

D. S. Syrdal, "Robot- Mediated Interviews with Children: What do potential users think?," Interaction Studies, vol. Vol. 17:3, pp. pp. 439–461, 2016.
5. L. J. Wood, K. Dautenhahn, H. Lehmann, B. Robins, A. Rainer, and D. S. Syrdal, "Robot- Mediated Interviews: Do robots possess advantages over human interviewers when talking to children with special needs?," presented at the International Conference on Social Robotics, Bristol, UK, 27th - 29th October, 2013.
6. J. H. Flavell, "The development of knowledge about visual perception," in Nebraska symposium on motivation, 1977: University of Nebraska Press.
7. K. Dautenhahn, C. L. Nehaniv, M. L. Walters, B. Robins, H. Kose-Bagci, N. Assif Mirza, and M. Blow, "KASPAR: A minimally expressive humanoid robot for human–robot interaction research," Applied Bionics and Biomechanics, vol. 6, pp. 369-397, 2009.
8. L. Wood, K. Dautenhahn, B. Robins, and A. Zaraki, "Developing child-robot interaction scenarios with a humanoid robot to assist children with autism in developing visual perspective taking skills," in Proceedings of the 26th IEEE

International Symposium on Robots and Human Interactive Communication (Ro-Man), 2017, pp. 1-6.

9. S. Baron-Cohen, A. M. Leslie, and U. Frith, "Does the autistic child have a "theory of mind"?,"

10. Cognition, vol. 21, no. 1, pp. 37-46, 1985.

11. A.Zaraki, K. Dautenhahn, L. Wood, O. Novanda, and B. Robins, "Toward Autonomous Child- Robot Interaction: Development of an Interactive Architecture for the Humanoid Kaspar Robot," presented at the 3rd Workshop on Child-Robot Interaction (CRI2017) in International Conference on Human Robot Interaction (ACM/IEEE HRI 2017), Vienna, Austria, 6-9 March 2017.

Table of Contents

Poster Papers

A practical mSVG interaction method for patrol, search, and rescue aerobots

Ayodeji O. Abioye[1], Stephen D. Prior[1], Glyn T. Thomas[1], Peter Saddington[2], & Sarvapali D. Ramchurn[1] [1]Fac. of Eng. & the Env., University of Southampton, UK. [2]Tekever Ltd, Southampton, UK

ABSTRACT

This paper briefly presents the multimodal speech and visual gesture (mSVG) control for aerobots at higher nCA autonomy levels, using a patrol, search, and rescue application example. The developed mSVG control architecture was presented and briefly discussed. This was successfully tested using both MATLAB simulation and python based ROS Gazebo UAV simulations. Some limitations were identified, which formed the basis for the further works presented. KEYWORDS: mSVG, aerobot, HCI, visual gesture, speech

I. INTRODUCTION

This paper is interested in how the increasing leagues of human operators interact with small multi-rotor UAVs. According to Green *et al.* (2007), "It is clear that people use speech, gesture, gaze and non-verbal cues to communicate in the clearest possible fashion." Abioye *et al.* (2016, 2017) identified the need for smart and intuitive control interaction methods for aerobots (aerial robots) on higher nCA autonomy levels. Such aerobots could include a patrol, search, and rescue robot in the Alps, Southcentral Europe. If a UAV could be developed to patrol dangerous regions of the Alps, providing signposting to climbers, alerting search and rescue teams of any incident, and supporting search and rescue team operations; and if the patrol UAV is meant to interact with climbers when needed, perhaps an intangible HHI-like multimodal speech and visual gesture (mSVG) interaction method could proof very useful in such climber aerobotic interaction.

II. LITERATURE REVIEW MULTIMODAL INTERFACES

Cacace, Finzi, and Lippiello (2016) investigated multimodal speech and gesture communication with multiple UAVs in a search and rescue mission, using the Julius framework (Lee, Kawahara and Shikano, 2001) and Myo device for speech and gesture respectively. Fernandez *et al.* (2016) investigated the use of natural user interfaces (NUIs) in the control of small UAVs using the Aerostack software framework. Harris and Barber (2014) and Barber et al. (2016) investigated the performance of a speech and gesture multimodal interface for soldier-robot team communication during an ISR mission, even considering complex semantic navigation commands such as "*perch over there* (speech + pointing gesture), *on the tank to the right of the stone monument* (speech)" (Borkowski and Siemiatkowska, 2010; Barber, Howard and Walter, 2016). Related research by Hill, Barber, and Evans (2015), suggested that multimodal speech and gesture communication was a means to achieving an enhanced naturalistic communication, reducing workload and improving human-robot communication experience. Kattoju *et al.* (2016) also investigated the effectiveness of speech and gesture communication in a soldier-robot interaction. Cauchard *et al.* (2015) and Obaid *et al.* (2016) conducted elicitation study to determine intuitive gestures for controlling UAVs.

Research - Multimodal Speech and Visual Gesture (mSVG)
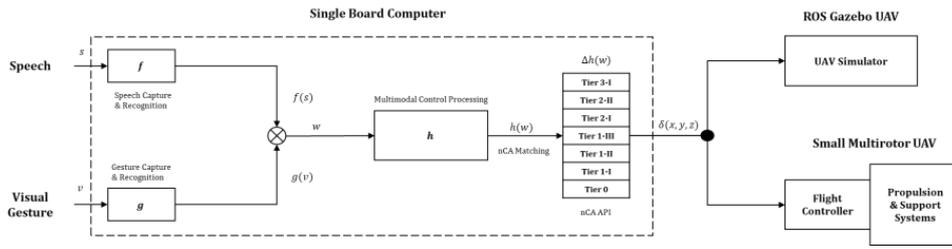
Figure 1: mSVG design architecture – control capture, processing, and execution.

The mSVG technique is basically the multimodal combination of speech and visual gesture, a method that leverages familiar human-human type interaction, in human aerobotic interaction. This combination could be sequential or complementary. The underlying architecture of how this technique is designed to work is as described in Figure 1. Speech is captured via a microphone, processed and recognised using the CMU Sphinx ASR with custom-defined phonetic dictionary containing only the set of command vocabulary, in order to increase recognition speed and accuracy. The speech input, u_{spe} $h = [\ _1,\ _2,\ _3, \dots,\ _n]$, is processed into the control symbol $f(\ )$. Visual gesture is captured via a camera connected to the aerobot SBC computer. In the preliminary work, a simple finger-coded visual gesture control commands set was developed to be recognised through a combination of two OpenCV algorithms – Haar cascade for hand tracking and convex hull for finger counting. The visual gesture control command, $_g$

$=[\ _1,\ _2,\ _3, \dots,\ _m]$, is also being processed into control symbols (v).

These are then combined into a standardized control symbol, $w = (\ ) + (\ )$, which is then passed into the multimodal control processing (MCP) framework. $h(\ )$ is the resultant control output generated after the multimodal combination of both the speech and the visual gesture input. $\delta(x,\ y,\ z) = \Delta h(\ )$

Where Δ is a function generated by the nCA API to modify the MCP output, $h(\ )$, to enable compatibility with multiple nCA navigational control autonomy levels. $(\ ,\ ,\ )$ is the increment/decrement change in 3-dimensional position of the UAV with respect to its previous position. A mathematical set model was developed and used to describe the computational algorithm mapping speech and visual gestures control symbols to UAV control operations to be executed.

I.V. RESULTS - MATALAB AND ROS GAZEBO SIMULATION

Based on the mathematical set model, the mSVG control navigation was simulated in MATLAB, which was then implemented in python for easy integration of algorithm on a single board computer (in this case, Odroid XU4 SBC), and simulated on a rotors gazebo firefly UAV simulator in an open world environment. In each case, a series of command such as 'go forward', 'go up half metre', 'go right one metre', 'hover at three metre', 'and', 'hover', 'go forward backward two half metre', 'patrol', etc. were successfully tested.
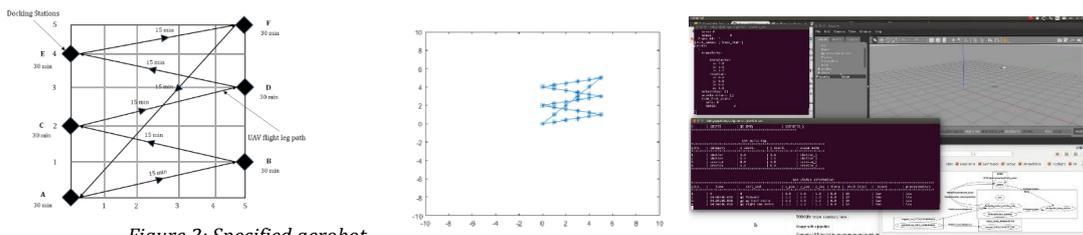
Figure 2: Specified aerobot patrol grid, MATLAB simulation, and ROS Gazebo Simulation

The main limitations of the proposed system is 1) its susceptibility to speech corruption during capture, due to the noise generated by the multirotor propulsion systems and other loud ambient noise such as in stormy weathers, 2) the effect of poor visibility level on visual gesture capture, as could be the case at night, or in cloudy or misty weather. The next phase of this research is already underway to determine the range of effectiveness of the mSVG method under varying noise and visibility levels. This could inform the possibility of working around this or developing techniques that may extend this range, thereby extending the usefulness of the propose mSVG technique over a much wider application area. Also, a comparison of the mSVG and RC joystick in terms of training time, same nCA Tier task completion rate, and cognitive workload requirement, is currently being conducted.

REFERENCES

1. Abioye, A. O., Prior, S. D., Thomas, G. T. and Saddington, P. (2016) 'The Multimodal Edge of Human Aerobotic Interaction', in Blashki, K. and Xiao, Y. (eds) *International Conferences Interfaces and Human Computer Interaction*. Madeira, Portugal: IADIS Press, pp. 243–248.

2. Abioye, A. O., Prior, S. D., Thomas, G. T., Saddington, P. and Ramchurn, S. D. (2017) 'Multimodal Human Aerobotic Interaction', in Isaías, P. (ed.) *Smart Technology Applications in Business Environments*. IGI Global, pp. 39–62.

3. Barber, D. J., Howard, T. M. and Walter, M. R. (2016) 'A multimodal interface for real-time soldier- robot teaming', 9837, p. 98370M. doi: 10.1117/12.2224401.

4. Borkowski, A. and Siemiatkowska, B. (2010) 'Towards semantic navigation in mobile robotics',

5. *Graph Transformations and Model-Driven Engineering*, pp. 719–748.

6. Cacace, J., Finzi, A. and Lippiello, V. (2016) 'Multimodal Interaction with Multiple Co-located Drones in Search and Rescue Missions', *CoRR*, abs/1605.0, pp. 1–6.

7. Cauchard, J. R., Jane, L. E., Zhai, K. Y. and Landay, J. A. (2015) 'Drone & me: an exploration into natural human-drone interaction', *Proceedings of the 2015 ACM International Joint Conference on Pervasive and Ubiquitous Computing*, pp. 361–365. doi: 10.1145/2750858.2805823.

8. Fernandez, R. A. S., Sanchez-lopez, J. L., Sampedro, C., Bavle, H., Molina, M. and Campoy, P. (2016) 'Natural User Interfaces for Human-Drone Multi-Modal Interaction', in *2016 International Conference on Unmanned Aircraft Systems (ICUAS)*. Arlington, VA USA: IEEE, pp. 1013–1022.

9. Green, S., Chen, X., Billinnghurst, M. and Chase, J. G. (2007) 'Human Robot Collaboration: an Augmented Reality Approach a Literature Review and Analysis', *Mechatronics*, 5(1), pp. 1–10. doi: 10.1115/DETC2007-34227.

10. Harris, J. and Barber, D. (2014) 'Speech and Gesture Interfaces for Squad Level Human Robot Teaming', in Karlsen, R. E., Gage, D. W., Shoemaker, C. M., and Gerhart, G. R. (eds) *Unmanned Systems Technology Xvi*. SPIE. doi: 10.1117/12.2052961.

11. Hill, S. G., Barber, D. and Evans, A. W. (2015) 'Achieving the Vision of Effective Soldier-Robot Teaming: Recent Work in Multimodal Communication', *Proceedings of the Tenth Annual ACM/IEEE International Conference on Human-Robot Interaction Extended Abstracts*, pp. 177–178. doi: 10.1145/2701973.2702026.

12. Kattoju, R. K., Barber, D. J., Abich, J. and Harris, J. (2016) 'Technological evaluation of gesture and speech interfaces for enabling dismounted soldier-robot dialogue', 9837, p. 98370N. doi: 10.1117/12.2223894.

13. Lee, a., Kawahara, T. and Shikano, K. (2001) 'Julius — an Open Source Real-Time Large Vocabulary Recognition Engine', *Eurospeech*, pp. 1691–1694.

14. Obaid, M., Kistler, F., Kasparaviciute, G., Yantaç, A. E. and Fjeld, M. (2016) 'HowWould You Gesture Navigate a Drone? A User-Centered Approach to Control a Drone', in *Proceedings of the 20th International Academic Mindtrek Conference*. Tampere, Finland: ACM New York, NY, USA, pp. 113– 121. doi: 10.1145/2994310.2994348.

Variable series elastic link: Advancing stiffness controllability in robot manipulators

A. Ali,[1] A. Calanca,[2] J. Konstantinova,[1] P. Fiorini,[2] K. Althoefer[1] [1]Advanced Robotics @ Queen Mary, Queen Mary University of London, UK [2]Robotics Lab ALTAIR, Department of Computer Science, University of Verona, Italy

ABSTRACT

Research into robot compliance has received world-wide interest for many decades. With the proposal of the series elastic actuator (SEA) by Gill Pratt and Matt Williamson 20 years ago, the research in this area has sky-rocketed with many roboticists aiming to create robotic structures that lend themselves to operate safely in the vicinity of humans. The approach proposed by Pratt and Williamson to create inherently compliant actuators has recently found its way into commercially-available products, the Baxter and Sawyer robots – robotic devices that are certified to operate nearby humans, e.g., for use in shared autonomy factory environments. Taking inspiration from the SEA concept and amalgamating new advancements in the area of soft material robotics, we propose the fundamentally new concept of variable series elastic links (VSEL) as a novel component to create manipulation devices that can alter their stiffness to accommodate their dynamic response depending on environmental situations. The proposed VSEL is a link structure made of an inner inflatable chamber and an outer, inextensible fabric sheath that depending on its chamber's air pressure changes its stiffness. Similar to the SEA concept, the VSEL introduces an element of compliance to robotic structures – however, extending from the standard SEA, the VSEL has a number of advantages: it is low-cost, can be easily integrated into robot arm designs replacing the standard rigid link, can sense interaction forces across the link structure and, most importantly, allows to adjust its stiffness and hence the robot's compliance over a wide range. Exploiting the modeling and control advancements in the area of SEA, this paper explores novel analytical models to improve the understanding of the dynamic behavior of the proposed VSEL with future work focusing on creating a control architecture for VSEL based robot arms. This paper introduces a number of models; future work will investigate their suitability to model the dynamic behavior of VSEL links.

I. INTRODUCTION

Series elastic actuators (SEAs) are a widespread actuation technology to implement stable interaction control while providing high transparency [1]–[3]. SEAs are composed of a traditional motor (usually an electric motor) in series with a compliant element (typically a spring) that is, in turn, connected to the robotic link. Series elastic actuators have been said to enable excellent force control using inexpensive components [4]. In reality, however, numerous expensive spring designs have been proposed in the literature to realize compact series elastic actuators [5], [6].

In this paper we promote a novel design concept: the variable series elastic link (VSEL). The VSEL is the response to a natural question: why adding expensive compliance in series with a joint-located actuator, when the link represents itself as a very suitable place to achieve a compliant robot structure? Extending the SEL concept, an affordable solution is achieved by substituting two high-cost components (the series compliance and the rigid link) with a single inexpensive component: an inflatable, stiffness-controllable link made from low-cost components.

Moreover, sensing the force at the link level has significant advantages over the force sensing capability in an SEA which is at actuation level. Furthermore, by neglecting the link inertia and representing it as a pure elastic element (air is lightweight and compliant) it is possible to prove that the VSEL retains the established control advantages of SEAs, i.e. force sensor collocation and improved force control robustness [1]–[3].

II. SERIES COMPLIANCE ARRANGEMENT AND MODELING

Series compliance, realized by SEAs, comes at the cost of inferior position controllability and additional mechanical complexity. A widely used model for SEAs is the one represented in Figure 1a where θ is the motor position, q is the link position, J_m is the motor inertia, k and d are the in-between compliance stiffness and damping, respectively, and τ_m and τ_s are the motor input torque and the spring torque, respectively. Interestingly, most of the advantages and properties of SEAs has been explained using such a simple model. When considering a robotic application, this model can only represents the actuator subsystem and a more meaningful model should at least account for the robotic link as in Figure 1b where J represents the link inertia. Here, more realistically, the robot is in contact with the environment through the link. This representation highlights that by feeding back the spring displacement only the motor dynamics can be shaped [1] or controlled and not the whole robot dynamics which includes the link. This SEA-link model also highlights some of the disadvantages of SEAs. In particular, it can be shown that, depending on the link mass [2], the position controllability can worsen and the impact safety may degrade.

Within the VSEL concept the compliance [3] is arranged between the link and the environment instead of at motor level. Thus we realistically come back to the model in Figure 1a. Indeed, the VSEL is filled with air which is inherently lightweight and compliant, thus, its inertia can be neglected and the link can be modelled as a pure

Figure 1. (a) A widely used, oversimplified SEA model. The same model can be used for VSEL. (b) An extended SEA model including the robot link.

elastic element. With respect to the model in Figure 1b, the model in Figure 1a leads to the following advantages:

1. The link deflection directly measures the robot-environment interaction that is the physical quantity we desire to shape in interaction control (and not the motor-link interaction as in the case of the SEA).

2. Avoiding the spring between the motor and the link, the link position becomes collocated leading to enhanced position controllability.

3. The impact safety is augmented because the compliant interface is located between the robot and the environment allowing to decouple not only the motor inertia but also the link inertia.

It is noted that the compliance arrangement in Figure 1.a) retains the established control advantages of SEAs, i.e. force sensor collocation and improved force control robustness.

III. CONCLUSIONS

By arranging the compliance along the link we gain improved control and safety with respect to using the compliance between the motor and the link when compared to SEAs. Thus, we want to propose here the concept of Variable Series Elastic Links (VSELs) to overcome the main limitations of SEAs.

In particular, we consider fabric-based, inflatable links, which can be implemented using low-cost components. Future work will consider the challenges imposed by using light elastic links, including position control in the presence of soft elements and the practicalities of dealing with inflatable links.

REFERENCES

1. R.C.Goertz,"FundamentalsofGeneralPurpose RemoteManipulators," *Nucleonics*, vol. 10, pp. 36–42, 1952.

2. Whitney, "Force Feedback Control of Manipulator Fine Motions," *Transactions of the ASME Journal of Dynamical Systems Measurement Control*, vol. 99, no. 2, pp. 91–97, 1977.

3. S. Eppinger and W. Seering, "On dynamic models of robot force control," *Proceedings. 1986 IEEE International Conference on Robotics and Automation*, vol. 3, pp. 29–34, 1986. [Online]. Available: http://ieeexplore.ieee.org/lpdocs/epic03/wrapper.htm?arnumber=1087723

4. ——, "Understanding bandwidth limitations in robot force control," *Proceedings. 1987 IEEE International Conference on Robotics and Automation*, vol. 4, pp. 904–909, 1987. [Online]. Available: http://ieeexplore.ieee.org/xpls/abs_all.jsp?arnumber=1087932

5. J. E. Colgate and G. G. Schenkel, "Passivity of a class of sampled-data systems: Application   to haptic interfaces," *Journal of Robotic Systems*, vol. 14, no. 1, pp. 37–47, jan 1997. [Online]. Available: http://doi.wiley.com/10.1002/%28SICI%291097-4563%28199701%2914%3A1%3C37%3A%3AAID- ROB4%3E3.0.CO%3B2-V

6. J. E. Colgate and J. M. Brown, "Factors affecting the Z-Width of a haptic display," *Proceedings of the 1994 IEEE International Conference on Robotics and Automation*, pp. 3205– 3210, 1994.

Depth-Map Improvement Via Architectural Priors

Paul Amayo, Pedro Piniés, Lina M. Paz, Paul Newman, Oxford Robotics Institute, Oxford University

ABSTRACT

The deployment and safe use of robots in large scale environments is intrinsically tied to their ability to create on demand accurate representations of the environments they are operating in. Depth-maps from visual sensors offer a solution to this problem however current depth-map estimation techniques from cameras often struggle to accurately estimate the depth of large texture-less regions. In urban scenes these texture-less regions are largely by construction planar. In this work we present two vision-only methods, one implicit and one explicit, to incorporate architectural planar priors into depth-map extraction together with their subsequent reconstructions of the environment.

I. INTRODUCTION

With the recent strides in autonomous driving and deployment of robots in large-scale urban environments the ability of robots to create better maps of these environments over large scales have become increasingly important. Laser scanners remain the sensor suite of choice however their cost, especially of 3D lasers, creates a barrier to their widespread use. Dense depth-maps created from monocular/stereo cameras offer a low-cost solution that can naturally deal with both the scale and lighting conditions of outdoor environments but do not have the accuracy of RGB-D cameras which are in turn restricted to small-scale and low-light indoor scenes.

Current state-of-the-art methods for creating dense depth-maps with cameras are based on powerful variational optimisation algorithms [1], [2]. These in general have two terms that are minimised as shown in Equation 1.

Firstly a data term that measures the photoconsistency (over a set of consecutive images in the case of a monocular camera or a stereo pair of images) of the depth estimation. Followed by a regularisation term that enforces depth smoothness for homogeneous surfaces while simultaneously attempting to preserve sharp discontinuities between different objects in the scene. The minimisation process involves the application of a primal-dual optimisation scheme [3].

The natural challenge in these techniques is dealing with large, plain and planar structures where the data term is of little use, with the lack of texture in these areas restricting the use of photo-consistency. Planar priors can be incorporated implicitly into the original variational problem by reaching for a Total Generalized Variation (TGV) regularization term that favours planar surfaces by allowing the depth to change at a constant rate shown in Equation 2.

EQUATION 1:

$$\min_{\zeta} E_{data}(\zeta) + E_{reg}(\zeta).$$

EQUATION 2:

$$E_{reg}(d) = \min_{w \in \mathbb{R}^2} \alpha_1 \int_{\Omega} |d - \mathbf{w}| \mathrm{d}x\mathrm{d}y + \alpha_2 \int_{\Omega} |\mathbf{w}| \mathrm{d}x\mathrm{d}y$$

46

Fig. 1. A qualitative perspective of this paper. A dense depth-map (left) of a planar wall surface created by a state-of-the-art Total Generalised Variation algorithm is displayed. As expected the algorithm results in a noisy output on the largely textureless wall and road. Explicitly discovering planar regions and from there invoking a planar prior to restricted areas results in an improved depth-map (right), showing a marked improvement in the depth estimation along the wall and road.

As demonstrated in Figure 1, the implicit TGV approach still struggles to estimate the depth of the textureless walls and roads creating a noisy depth map. To improve on this we reach for an explicit incorporation of planar priors using a fast per-pixel labelling, as shown in Figure 1 this results in a marked improvement in the depth-map. The planar priors are extracted through a vision-only two view homography segmentation that makes no assumptions about the layout of the scene [4]. Once the planar priors are retrieved, we propose a labelling of the image pixels to the corresponding underlying planes. This per-pixel labelling is driven by a fast, parallel, global energy minimisation algorithm, this brings real-time capabilities into the depth-map improvement. The energy is formulated as follows:

$$\sum_{l=1}^{L} \sum_{i=1}^{n} l\rho(\mathbf{u})l\varphi_l(\mathbf{u}) + \lambda \sum_{i=1}^{n} \omega_N l \quad _N\varphi_l(\mathbf{u})\mathbf{S}Z_p \qquad (3)$$

$$\underbrace{\hspace{3cm}}_{\text{Data Term}} \qquad \underbrace{\hspace{3cm}}_{\text{Smoothness Term}}$$

Where L is the number of planar priors hypotheses with an addition of the non-planar label ⬜ that is provided by the TGV depth-map, with the nodes $\mathbf{u} \, D$ the image pixels. With $\varphi(\mathbf{u})$ being the indicator function and $\rho(\mathbf{u})$ is the photo-consistency measured between images. The photo-consistency is determined using the depths provided through the planar priors and the variational depth-map and then projecting and comparing this to the subsequent images used in the two-view homography segmentation. The smoothness term penalises depth discontinuities between neighbouring pixels based on their plane labels.

The depth-maps from these two approaches can be fused to create a dense reconstruction of the environment. In this work we opt for the approach of Tanner at al. [5]. This was then deployed on regions of the KITTI dataset [6] as shown in Figure 2. From this Figure it can be seen that the introduction of the planar priors results in more complete reconstructions (bottom row) over the evaluated sections than the raw TGV depth-maps (top row). Holes in the reconstruction created as a result of the noisy depth maps in textureless regions are filled as resulting in a smoother and more complete reconstruction.

Fig. 2. Sample results of dense reconstructions from the fusion of depth maps in the two evaluated sections are shown in this figure. The top row of images corresponds to the reconstructions produced using the TGV depth maps. It can be seen that the noise on the depth maps results in some gaps in the reconstruction. By improving these depth maps with planar priors in our approach the results can be improved on significantly as shown in the bottom row. Resulting in a more accurate map of the world.

II. CONCLUSION

In this work efforts to improve the depth-map estimation through architectural priors are presented. We demonstrate that by explicitly including planar priors through a fast labelling more accurate depth- maps of urban scenes can be created. These depth-maps when fused show a more accurate picture of the environment available to robots even over large-scale environments. This allows for the addition of higher- level functionality into robots especially in applications where complex interaction with the environment is needed without the need for expensive sensor suites.

REFERENCES

1. J. Stühmer, S. Gumhold, and D. Cremers, "Real-time dense geometry from a handheld camera," in *Joint Pattern Recognition Symposium*. Springer, 2010, pp. 11–20.
2. G. Graber, T. Pock, and H. Bischof, "Online 3d reconstruction using convex optimization," in *Computer Vision Workshops (ICCV Workshops), 2011 IEEE International Conference on*. IEEE, 2011, pp. 708–711.
3. A. Chambolle and T. Pock, "A first-order primal-dual algorithm for convex problems with applications to imaging," *Journal of Mathematical Imaging and Vision*, vol. 40, no. 1, pp. 120–145, 2011.
4. C. Raposo and J. P. Barreto, "Theory and practice of structure-from-motion using affine correspondences," in *Proceedings of the IEEE Conference on Computer Vision and Pattern Recognition*, 2016, pp. 5470–5478.
5. M. Tanner, P. Piniés, L. M. Paz, and P. Newman, "Keep geometry in context: Using contextual priors for very-large-scale 3d dense reconstructions," in *Robotics: Science and Systems, Workshop on Geometry and Beyond: Representations, Physics, and Scene Understanding for Robotics*, June 2016.
6. A. Geiger, P. Lenz, and R. Urtasun, "Are we ready for autonomous driving? the kitti vision benchmark suite," in *Conference on Computer Vision and Pattern Recognition (CVPR)*, 2012.

Mona: an Affordable Mobile Robot for Swarm Robotic Applications

F. Arvin, J. Espinosa, B. Bird, A. West, S. Watson, and B. Lennox
School of Electrical and Electronic Engineering, The University of Manchester

ABSTRACT

Mobile robots are playing a significant role in multi and swarm robotic research studies. The high cost of commercial mobile robots is a significant challenge that limits the number of swarm based research studies that implement real robotic platforms. On the other hand, the observed results from simulated robots using simulation software are not representative of results that would be obtained using real robots. There are therefore considerable benefits in the development of an affordable open-source and flexible platform that allows students and researchers to implement experiments using real robot systems. *Mona* is an open-source and open-hardware mobile robot that has been developed at the University of Manchester for this purpose. Mona provides a robotic solution that can be programmed and operated using a user-friendly interface, Arduino, with relative ease. The low cost of the platform means that it is feasible for a large number of these robots to be used in swarm robotic scenarios.

I. INTRODUCTION

Swarm robotics is a relatively new concept in multi-robotic collective behaviour research studies that has emerged from studies using robots with limited abilities that are assigned to following simple tasks [1]. Swarm robotic scenarios are mostly inspired form social behaviour of insects and other animals and there have been many successful implementations of swarm behaviours which have been directly inspired from nature (e.g. honeybees [2], cockroaches [3], ants [4], and birds [5]). As highlighted in [6], one of the main criteria of swarm robotics is operating experiments with a "large number of robots", typically at least 10 - 20. Recently, the number of robots used in swarm robotics has increased dramatically with swarm sizes of up to 1000 robots being reported [7]. To implement such large sizes of swarms with commercial robots can therefore be very costly. To tackle this issue, affordable open-source and open-hardware robotic platforms are playing an important role in research and education.

Several mobile robots have been developed and successfully deployed in swarm robotic research studies, such as Khepera [8], Alice [9], Jasmine [10], E-puck [11], Colias [12], SwarmBot [13], Kilobot [14], and S-bot [15]. In these studies bio-inspired collective behaviour has been imitated, however, despite this work only a limited number of low-cost, open-source, and open-hardware mobile robots are available for use in swarm robotic research studies. For example, 'Colias' is an open-source, low-cost mobile robot that was developed for application to swarm scenarios. A large group of Colias robots played the role of young honeybees role to mimic BEECLUST aggregation [16]. Colias has also been utilised to study bio-inspired vision mechanism [17] and artificial pheromone communication system [18]. Recently, Mona has been developed as a low-cost mobile robot for research and education purposes. The first version of Mona was utilised in a study on the feasibility of creating a Perpetual Robot

Swarm system, where the robot was able to recharge itself whilst in motion [19]. The Mona robot has been developed, in collaboration with a commercial partner, as a low-cost platform (£100) for robotic education and swarm/collaborative

research. It has been successfully used for teaching on an undergraduate unit and MSc projects in University of Manchester. The rest of this paper provides briefly on its design and capabilities.

II. MONA ROBOT

Mona (Fig. 1) uses a circular PCB board with the diameter of 8 cm accommodates its modules including main processor, motors and drivers, infra-red proximity sensors, power management, and 3.7 V Li-Po battery. Mona is a modular robot hence any module that uses the serial communication standards (i.e. RS232, I^2C, and SPI) can be easily attached to the robot. Due to open-source criterion of the Mona, Arduino [20] that is one of the

most successful open- source platforms was used to program the Mona. The important reasons to use Arduino were:
i) it is relatively easy platform in comparison to other open-source platforms, ii) the rich set of online forums and available libraries with free access, and iii) variety of Arduino compatible programming environments especially for young age students.
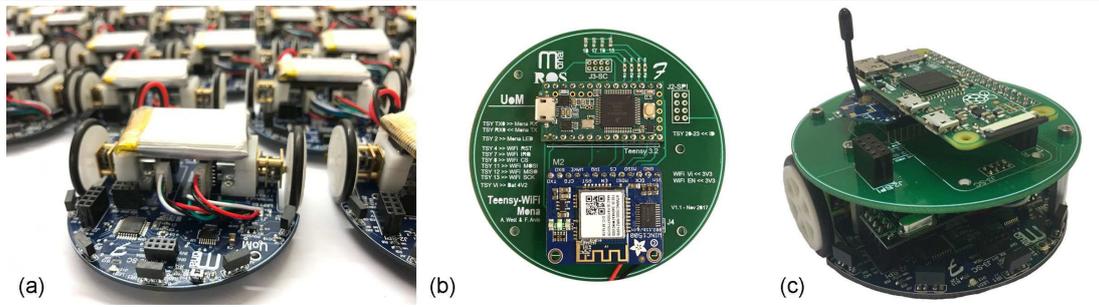
Figure 1: (a) Mona robot, (b) ROS module (breakout board for Teensy 3.2 and WiFi), and (c) an expansion board for the off-the-shelf modules: Raspberry Pi Zero, RF transceiver, and XBee.

An AVR 8-bit microcontroller (Atmega-328, with 32 KB in-system self-programmable flash memory and 2 KB internal SRAM) was utilised as the main processor. The main clock source is an external 16 MHz crystal oscillator. Two micro DC gearhead motors (with a high gear ratio of 280:1) and two wheels with diameter of 28 mm move Mona with a maximum speed of 10 cm/s. The rotational speed for each motor is controlled individually using a pulse-width modulation (PWM) technique. Each motor is controlled separately with a macroscopic model of the utilized motors [21].

In addition, the utilised motors have magnetic encoders attached to the back side of the motors. Each encoder generates two pulses per rev (before gear), which provides enough precision in terms of wheels' displacement. The output of the

encoders can be used as an input to a proportional-integral-derivative (PID) controller for closed-loop motion control.
The main sensory system which is used in Mona is the short-range infra-red (IR) proximity sensors. Five sensors in front half of the robot, which were located in 35° angular distance estimate the distance of an obstacle by translating the received reflected IR to an analogue voltage [22]. Mona also monitors its battery level using an ADC (analog-to-digital converter) channel of the main processor by sampling its battery level by a voltage divider including two resistors.

To study on possibility of controlling Mona using ROS (Robot Operating System), a breakout board has been made that supports a Teensy 3.2 module and a WiFi module, as shown in Fig. 1(b). The board was attached on top of Mona

and communicates via UART (universal asynchronous receiver-transmitter). In this configuration, an ID was assigned to each Mona and the base-station (ROS server) receives sensory readings from each Mona and also sends commands to Mona's motors and LEDs via WiFi module. In addition, a breakout board as shown in Fig. 1(c) has been developed which supports: i) Raspberry Pi Zero, ii) XBee module, and iii) NRF24L01 RF transceiver. The board is mounted on top of the main platform and is able to communicate with the main platform using RS232 serial port.

Mona has been developed based on an AVR RISC micro-controller (ATMega328P). The architecture of the robot allows connecting the robot to Arduino-based platforms via a USB cable. However, it is possible to use any programming language which was developed for AVR micro-controllers including C, C++, Java, Pascal, Basic, and Assembly. Mona's design library and codes are available at [23].

REFERENCES

1. L. Bayındır, "A review of swarm robotics tasks," *Neurocomputing*, vol. 172, pp. 292–321, 2016.

2. T. Schmickl, R. Thenius, C. Moeslinger, G. Radspieler, S. Kernbach, M. Szymanski, and K. Crailsheim, "Get in touch: cooperative decision making based on robot-to-robot collisions," *Autonomous Agents and Multi-Agent Systems*, vol. 18, no. 1, pp. 133–155, 2009.

3. S. Garnier, J. Gautrais, M. Asadpour, C. Jost, and G. Theraulaz, "Self-Organized Aggregation Triggers Collective Decision Making in a Group of Cockroach-Like Robots," *Adaptive Behavior*, vol. 17, no. 2, pp. 109– 133, 2009.

4. E. Ferrante, A. E. Turgut, E. Duéñez-Guzmán, M. Dorigo, and T. Wenseleers, "Evolution of self-organized task specialization in robot swarms," *PLoS Comput Biol*, vol. 11, no. 8, p. e1004273, 2015.

5. A. E. Turgut, H. Çelikkanat, F. Gokçe, and E. Şahin, "Self-organized Flocking in Mobile Robot Swarms," *Swarm Intelligence*, vol. 2, no. 2, pp. 97– 120, 2008.

6. E. Şahin, "Swarm robotics: From sources of inspiration to domains of application," in *International workshop on swarm robotics*, pp. 10–20, Springer, 2004.

7. G. Valentini, E. Ferrante, H. Hamann, and M. Dorigo, "Collective decision with 100 kilobots: speed versus accuracy in binary discrimination problems," *Autonomous Agents and Multi-Agent Systems*, vol. 30, no. 3, pp. 553–580, 2016.

8. F. Mondada, E. Franzi, and P. Ienne, "Mobile robot miniaturisation: A tool for investigation in control algorithms," in *Experimental robotics III*, pp. 501–513, Springer, 1994.

9. G. Caprari, T. Estier, and R. Siegwart, "Fascination of down scaling - alice the sugar cube robot," *Journal of Micro-Mechatronics*, vol. 1, no. 3, pp. 177– 189, 2002.

10. S. Kernbach, R. Thenius, O. Kernbach, and T. Schmickl, "Re-embodiment of Honeybee Aggregation Behavior in an Artificial Micro-Robotic System," *Adaptive Behavior*, vol. 17, no. 3, pp. 237–259, 2009.

11. F. Mondada, M. Bonani, X. Raemy, J. Pugh, C. Cianci, A. Klaptocz, S. Magnenat, J.-C. Zufferey, C. Floreano, and A. Martinoli, "The e-puck, a robot designed for education in engineering," in *9th conference on autonomous robot systems and competitions*, 2009.

12. F. Arvin, J. Murray, C. Zhang, and S. Yue, "Colias: An Autonomous Micro Robot for Swarm Robotic Applications," *International Journal of Advanced Robotic Systems*, vol. 11, no. 113, pp. 1– 10, 2014.

13. J. McLurkin, J. Smith, J. Frankel, D. Sotkowitz, D. Blau, and B. Schmidt, "Speaking swarmish: Human- robot interface design for large swarms of autonomous mobile robots," in *AAAI spring symposium*, 2006.

14. M. Rubenstein, C. Ahler, N. Hoff, A. Cabrera, and R. Nagpal, "Kilobot: A low cost robot with scalable operations designed for collective behaviors," *Robotics and Autonomous Systems*, vol. 62, no. 7, pp. 966–975, 2014.

15. F. Mondada, G. C. Pettinaro, A. Guignard, I. W. Kwee, D. Floreano, J.-L.

Deneubourg, S. Nolfi, L. M. Gambardella, and M. Dorigo, "Swarm-bot: A new distributed robotic concept," *Autonomous robots*, vol. 17, no. 2-3, pp. 193–221, 2004.

16. F. Arvin, A. E. Turgut, T. Krajník, and S. Yue, "Investigation of cue-based aggregation in static and dynamic environments with a mobile robot swarm," *Adaptive Behavior*, vol. 24, no. 2, pp. 102–118, 2016.

17. C. Hu, F. Arvin, C. Xiong, and S. Yue, "A Bio-inspired Embedded Vision System for Autonomous Micro- robots: the LGMD Case," *IEEE Transactions on Cognitive and Developmental Systems*, vol. 9, no. 3, pp. 241 – 254, 2017.

18. F. Arvin, T. KrajnÃk, A. E. Turgut, and S. Yue, "COSΦ: Artificial pheromone system for robotic swarms research," in *IEEE/RSJ International Conference on Intelligent Robots and Systems (IROS)*, pp. 407–412, Sept 2015.

19. F. Arvin, S. Watson, A. E. Turgut, J. Espinosa, T. Krajník, and B. Lennox, "Perpetual Robot Swarm: Long- term Autonomy of Mobile Robots Using On-the-fly Inductive Charging," *Journal of Intelligent & Robotic Systems*, 2017.

20. M. Banzi and M. Shiloh, *Getting Started with Arduino: The Open Source Electronics Prototyping Platform*. Maker Media, Inc., 2014.

21. F. Arvin and M. Bekravi, "Encoderless Position Estimation and Error Correction Techniques for Miniature Mobile Robots," *Turkish Journal of Electrical Engineering & Computer Sciences*, vol. 21, pp. 1631–1645, 2013.

22. F. Arvin, K. Samsudin, and A. R. Ramli, "Development of IR-Based Short-Range Communication Techniques for Swarm Robot Applications," *Advances in Electrical and Computer Engineering*, vol. 10, no. 4, pp. 61–68, 2010.

23. Mona library. https://github.com/MonaRobot.

Reactive Magnetic-field-inspired Algorithm for Robot Navigation in Unknown Environments: Preliminary Results (Extended Abstract)

*Ahmad Ataka[1], Hak-Keung Lam[1], and Kaspar Althoefer[2] *†*

II. INTRODUCTION

The field of robot navigation, path planning, and obstacle avoidance have been extensively studied in the robotics community over the past thirty years [1], [2]. Classical geometrical planning, such as the visibility graph, cell decomposition, and Voronoi diagram [1], and a more recent sampling-based planning [3], [4], [5] have been able to solve a wide range of problems such as computer animation, assembly planning, and com- putational structural biology [2]. However, achieving collision-free navigation becomes more challenging as the robot applications move from well-defined environments (as common in industrial applications) towards unknown environments (such as those where the robot has to cope with the presence of moving humans). Therefore, the ability of the robot to reach the desired target whilst avoiding obstacles on-line with limited information of the environment becomes important.

In this paper, we present preliminary results of the magnetic-field-inspired algorithm for reactive robot navigation. The algorithm is reactive in the sense that it uses only the local most-updated sensory data to pro- duce the motion, and hence, does not rely on prior knowledge of the obstacle's position and geometry. Our algorithm goes beyond the standard electric-field-based artificial potential field (APF) being able to generate paths in environments with convex obstacle without experiencing local minima. It also outperforms previ- ous magnetic-field-inspired navigation methods [6], [7], [8] since it does not rely on prior knowledge of the obstacles' geometrical properties.

II. MAGNETIC FIELD-INSPIRED NAVIGATION

From the classical law of electromagnetism, a wire segment carrying electrical current i_o will produce a mag- netic field $\mathbf{B}$. A particle with positive charge q moving close to the current-carrying wire will be affected by the presence of the magnetic field with a force $\mathbf{F}$ whose direction is perpendicular to both particle's velocity $\mathbf{v}$ and magnetic field $\mathbf{B}$. Due to this phenomena, the produced force will result to deviation rather than repulsion (as is the case for electric field) in the particle's course of movement. Inspired by this physical phenomenon, we can think of a robot as a charged particle with velocity $\mathbf{v}$ and the obstacle surface as a current-carrying wire. The artificial current $\mathbf{l}_o$ flowing on the obstacle surface located at position $\mathbf{r}_o$ with respect to the robot is designed in such a way that the generated force $\mathbf{F}$ will guide the robot to follow obstacle boundary instead.

To make the robot located at $\mathbf{p}$ to follow the direction of $\mathbf{l}_o$, the force applied to the robot can be written as follows:

$$\mathbf{F}(\mathbf{r}_o) = c \; \mathbf{l}_a \times (\mathbf{l}_o \times \mathbf{l}_a) \; f(|\mathbf{r}_o|, |\dot{\mathbf{p}}|), \qquad (1)$$

where $c > 0$ is a scalar constant, $\mathbf{l}_a$ stands for the robot's velocity direction defined as $\mathbf{l}_a = \frac{\dot{\mathbf{p}}}{|\dot{\mathbf{p}}|}$. To minimize the change of the velocity direction, and thus minimizing unwanted oscillation, the proposed induced current direction $\mathbf{l}_o$ is designed to be the projection of the robot's velocity direction $\mathbf{l}_a$ on to the obstacle surface, as illustrated in Fig. 1a. We assume that obstacle surface at every closest point will always have a normal vector

---

[1]A. Ataka and H.K. Lam are with The Centre for Robotics Research (CoRe), Department of Informatics, Kings College London, London WC2R 2LS, United Kingdom. Corresponding author e-mail: ahmad.ataka@kcl.ac.uk

†[2]K. Althoefer is with the School of Engineering and Material Science, Queen Mary University of London, London E1 4NS.

(a)   (b)
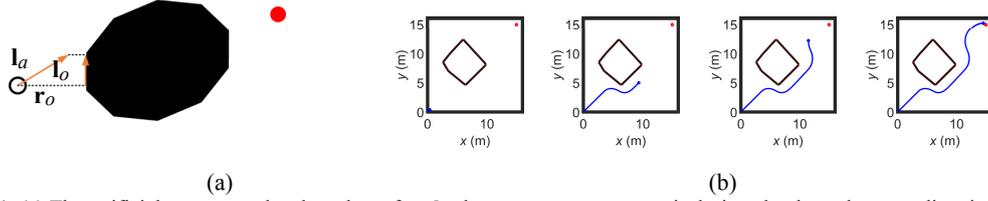
Figure 1: (a) The artificial current on the obstacle surface $\mathbf{l}_o$, drawn as orange arrows, is designed to have the same direction as the projection of the robot's velocity $\mathbf{l}_a$ on to obstacle surface. (b) The magnetic-field-inspired navigation is applied to a point-like robot moving in R^2.

(a)   (b)   (c)   (d)

(e)   (f)
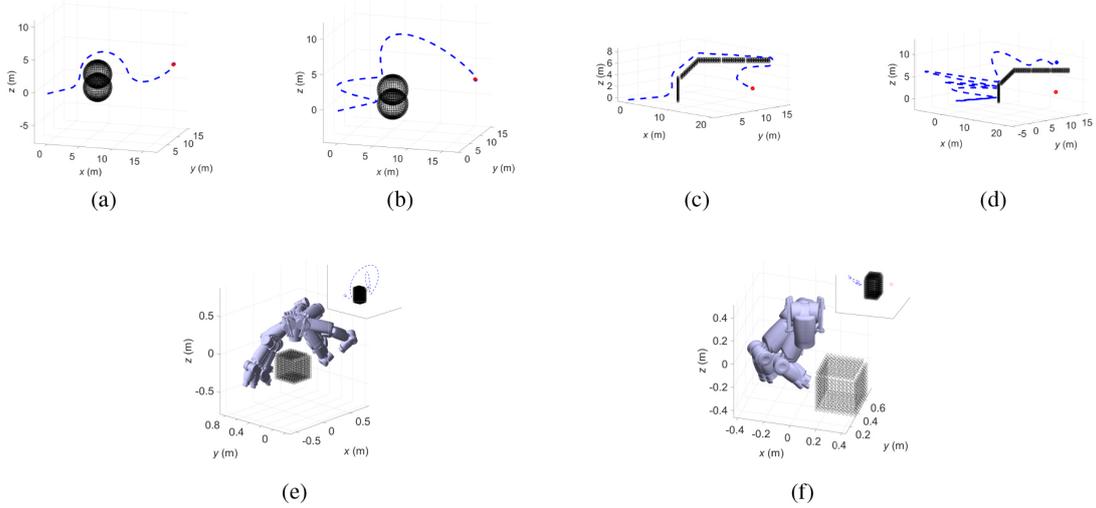
Figure 2: A point-like robot is guided using (a) the proposed algorithm and (b) standard APF for environment consisting of double spheres and using (c) the proposed algorithm and (d) standard APF in environment consisting of roof-like building. (e) The proposed algorithm and (f) standard APF are applied to the model of 7 DOFs Baxter arm moving in environment consisting of cube obstacle. The inset plot shows the tip's trajectory drawn in blue line, its starting point drawn as a blue dot, and the target position drawn as a red dot.

$\mathbf{n}$ in the opposite direction of $\mathbf{r}_o$ such that the current direction $\mathbf{l}_o$ can then be written as $\mathbf{l}_o = \mathbf{l}_a - \frac{(\mathbf{l}_a^T \mathbf{r}_o)\mathbf{r}_o}{|\mathbf{r}_o|^2}$. To complete the description of the algorithm, we choose the function $f(|\mathbf{r}_o|, |\dot{\mathbf{p}}|)$ to be $f(|\mathbf{r}_o|, |\dot{\mathbf{p}}|) = \frac{|\dot{\mathbf{p}}|}{|\mathbf{r}_o|}$.

III. RESULTS AND DISCUSSION

A point-like robot with the dynamics of double integrator and a 7 degrees of freedom (DOF) Baxter arm are used as models in our simulation. The control law which will govern the robot towards the goal and avoiding obstacle is represented as combination of a PD controller towards the goal and the magnetic-field-inspired obstacle avoidance terms as expressed in (1) which will be activated once the distance between robot and obstacle closer than a limit distance r_l. The robot is assumed to be able to sense the surrounding environments as far as some distance $r_s \gtrsim r_l$ in all directions.

In Fig. 1b, we can see the performance of the algorithm in planar environment. Fig. 2 shows the results for 3D case, in which the environment consists of spherical objects (Fig. 2a-Fig. 2b) or roof-like objects (Fig. 2c-Fig. 2d). We see how the proposed algorithm (Fig. 2a and Fig. 2c) outperforms the standard APF (Fig. 2b and Fig. 2d) for both cases. The algorithm is also used to guide the tip of the Baxter arm in avoiding unknown obstacle in the form of a cube as shown in Fig. 2e, while the standard APF fails to guide the tip towards the target (Fig. 2f). Hence, we conclude that the proposed magnetic-field-inspired algorithm is a promising candidate to be used to navigate various robotics platforms.

REFERENCES

1. J.-C. Latombe, *Robot Motion Planning*. Norwell, MA, USA: Kluwer Academic Publishers, 1991.

2. H. Choset, K. M. Lynch, S. Hutchinson, G. A. Kantor, W. Burgard, L. E. Kavraki, and S. Thrun, *Principles of Robot Motion: Theory, Algorithms, and Implementations*.

3. L. E. Kavraki, P. vestka, J.-C. Latombe, and M. H. Overmars, "Probabilistic roadmaps for path planning in high-dimensional configuration spaces," *IEEE Trans. Robot. Autom.*, vol. 12, no. 4, pp. 566–580, 1996.

4. S. M. LaValle, "Rapidly-exploring random trees: A new tool for path planning," Dept. Comput. Sci., Iowa State Univ., Ames, IA, USA, Tech. Rep. TR 98-11, 1998.

5. M. Elbanhawi and M. Simic, "Sampling-based robot motion planning: A Review," *IEEE Access*, vol. 2, pp. 56–77, 2014.

6. S. Haddadin, R. Belder, and A. Albu-Schffer, "Dynamic motion planning for robots in partially unknown environments," in *IFAC World Congr.*, vol. 18, 2005. Cambridge, MA: MIT Press, Jun. 2005.

7. L. Singh, H. Stephanou, and J. Wen, "Real-time robot motion control with circulatory fields," in *Proc. IEEE Int. Conf. Robot. Autom.*, vol. 3, Apr. 1996, pp. 2737–2742 vol.3.

8. L. Singh, J. Wen, and H. Stephanou, "Motion planning and dynamic control of a linked manipulator using modified magnetic fields," in *Proc. IEEE Int. Conf. Control Applicat.*, Oct. 1997, pp. 9–15.

FURO: Pipe Inspection Robot for Radiological Characterisation

Liam Brown1,2, Joaquin Carrasco1, Simon Watson1, and Barry Lennox1

I. INTRODUCTION

In the 1930s nuclear fission was discovered, this led to many countries including the United Kingdom, to begin research into nuclear materials [1]. At the time, the major interest in fission was weaponising it, leading to projects such as the Manhattan Project in the early 1940s [1]. After World War II the race for nuclear arms continued, leading into the cold war [2].

Nuclear facilities required for research were constructed quickly to keep up with the arms race. Due to the speed and limited knowledge of the dangers of exposure to nuclear material, fewer precautions and exact records were taken at the time. Once these nuclear facilities had been fully utilised they were retired and sealed off. 70 years after the race began there is a need to decommission the facilities as the structures are starting to age and if they are left it could lead to further contamination of the surrounding environment.

All of these facilities contain pipework, meaning there is miles of uncharacterised pipes within them. If it is uncharacterised it must be disposed of as contaminated waste which is a costly procedure. Workers currently check the pipework manually by entering the hazardous zones to dismantle and scan it for radiation. This is not only difficult and unconformable work but it is a risk to the workers health. The processes of dismantling the pipework also generates a large amount of secondary waste in the form of hazmat suits and tools, which all need to be disposed of.

If a low-cost robotic system existed that could autonomously scan the miles of pipework and characterise (both radiologically and geometrically) sections of pipe, it could significantly reduce the cost of decommissioning without the risk of

exposure to the workers.

The aim of this research is to produce a low-cost, disposable robotic system that can navigate through an unknown pipe network with a minimum diameter of 50 mm, whilst radiologically characterising and mapping the pipework.

Fig. 1. Photo of pipework from an exemplar facility

There has been a large drive in the utility industry for the development of pipe inspection vehicles, these predominantly operate within pipework with diameters of 160   600 mm [3], [4]. Robots that are able to travel within smaller pipes exist [5], [6] but these are unable to safely navigate junctions or too complex in their design. A bespoke pipe inspection robot has therefore been developed.

The development of a 50 mm pipe inspection robot is very challenging due to issues relating to miniaturisation. For theevaluation stage of the research, a 150 mm prototype (named FURO) has been developed, which later will be miniaturised.

FURO has three radial tracked drive units each capable of producing 4 Nm of torque, which is sufficient to allow the robot   to climb with a 1 kg payload. The tracks aid in grip within the potentially low friction pipework. FURO is shown in Fig.2.
A fourth motor drives a central lead screw

mechanism that is able to vary the diameter of the robot between 126   175 mm.   The lead screw is also used for active wall pressing to allow the robot to climb. Due to the sacrificial nature of the robot, it   is designed using low-cost 3D printed parts. This not only aids with the cost but allows bespoke small parts to be made.

FURO operates on the ROS framework [7]. The current prototype uses a PC base station with a joystick for manual control. The manual control is used to verify the robot is mechanically able to navigate different scenarios. FURO is able to reliably overcome horizontal, vertical and corner sections of pipe with the manual control.

The first major challenge associated with navigating within pipes are junctions; the simplest of these is the 90◦ bend. As discussed FURO is able to navigate corners with manual control. The user manual set the corner direction (in relation to the robot) and radius, the robot uses that to calculate the required velocities for the drive unit. To make this system autonomous,   the robot must be able to detect the parameters of the corner so it can determine the path lengths for the velocities.

Current sensing solutions are either too large, expensive or computationally heavy to be deployed on FURO. A mechanical feeler sensor has been developed to detect the pipe features ahead. These feelers are depicted on the FURO prototype in Fig. 2.

The feelers consist of a potentiometer, spring, arm and encoder which are not only mechanically simple but also makes the sensor computationally light to sample. The voltage change over the potentiometer relates to the angle of the feelers this is passed to the prediction algorithm to determine the pipe parameters.

Fig. 3 shows the raw data from the feeler sensors as they enter the corner. The red feeler entered the corner in line with the inside of the bend, whist the other feelers were at   120◦. It can be seen that the red feeler changes with the largest magnitude to the other feelers, this is expected as the greatest change over the entrance distance is experienced here. The blue and green feelers are expected to change by a similar magnitude to each other but less than, and in the opposite direction to, the red   feeler which is exactly what is observed.

Fig. 2. FURO prototype
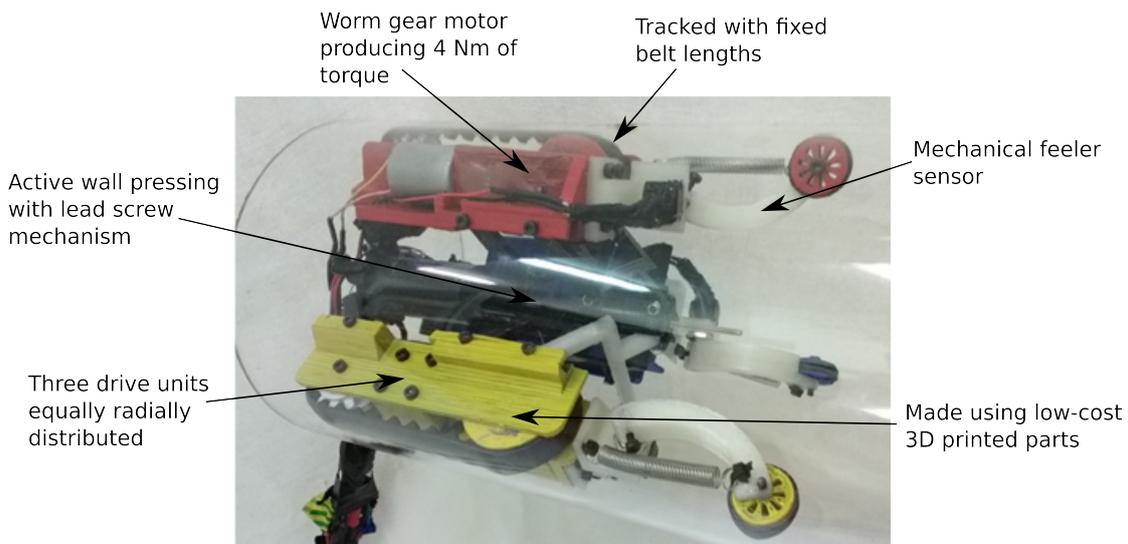
[1] Dept of Control, School of Electrical and Electronic Engineering, Engineering and Physical Sciences, The University of Manchester
[2] Corresponding Author: liam.brown-5@postgrad.manchester.ac.uk (Liam Brown)
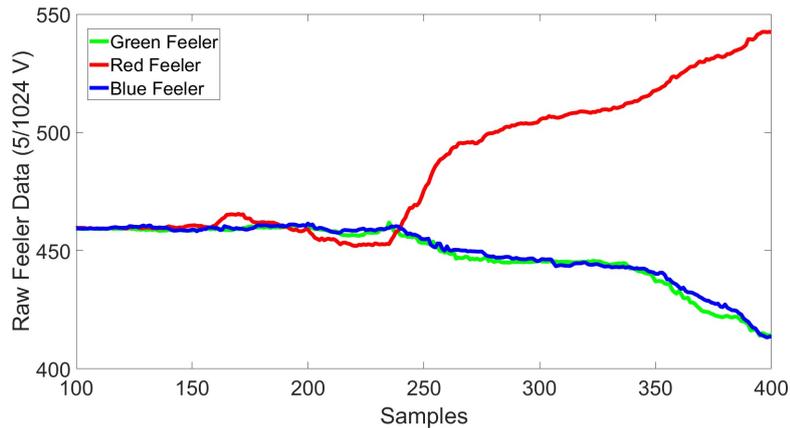
Fig. 3. Raw data from feeler sensors entering a corner

Once the raw data from the feelers is gathered, a method of detecting the corner parameters from this information is determined. The raw data is converted to angles and is used with a kinematic model to determine the location of all three feelers. A prediction is made on the direction (in relation to the robot) and radius of the corner. Once the parameters of the corner have been estimated they can be used to determine the required velocities from the drive units to allow FURO to pass through a corner.

To summarise, using three mechanical feeler sensors, the proposed sensor will detect the paraters of the corner to allow the FURO prototype to autonomously navigate around any corner with a minimum radius of 150 mm (short elbow) up to 90◦ in any direction. Further work for FURO includes characterising the performance of the feelers, extending the feeler detection to varying radii and angle corners and miniaturising the system to a 50 mm pipe.

ACKNOWLEDGEMENTS

REFERENCES
1. Wagemans, The nuclear fission process. CRC press, 1991

2. Kaysen, R. McNamara, and G. Rathjens, "Nuclear weapons after the cold war," Foreign Affairs, vol. 70, no. 4, pp. 95–110, 1991.

3. S. Ryew, S. Baik, S. Ryu, K. M. Jung, S. Roh, and H. R. Choi, "In-pipe inspection robot system with active steering mechanism," in Proceedings, 2000 IEEE/RSJ International Conference on Intelligent Robots and Systems, 2000.(IROS 2000)., vol. 3. IEEE, 2000, pp. 1652–1657.

4. J. Okamoto, J. C. Adamowski, M. S. Tsuzuki, F. Buiochi, and C. S. Camerini, "Autonomous system for oil pipelines inspection," Mechatronics, vol. 9, no. 7, pp. 731–743, 1999.

5. A. Kakogawa, T. Nishimura, and S. Ma, "Development of a screw drive in-pipe robot for passing through bent and branch pipes," in Robotics (ISR), 2013 44th International Symposium on. IEEE, 2013, pp. 1–6.

6. S.-g. Roh and H. R. Choi, "Differential-drive in-pipe robot for moving inside urban gas pipelines," Robotics, IEEE Transactions on, vol. 21, no. 1, pp. 1–17, 2005.

7. "ROS - Kinetic Kame," 2017, Open Source Robotics Foundation.

Hypertonic Saline Solution for Signal Transmission and Steering in MRI-guided Intravascular Catheterisation

Alberto Caenazzo, Kaspar Althoefer Centre for Advanced Robotics @ Queen Mary (ARQ)
Email: A.Caenazzo@qmul.ac.uk, K.Althoefer@qmul.ac.uk

ABSTRACT

Use of traditional low-impedance sensor leads is highly undesirable in intravascular catheters to be used with MRI guidance; thermal safety and quality of imaging are particularly impacted by these components. In this paper, we are showing that hypertonic saline solution, a high-impedance body-like fluid, could be a compatible and effective signal transmission medium when used in MRI-compatible catheters. We also propose a simple type of catheter design that can be steered hydraulically using the same saline solution. Integration of hydraulic steering is not required for MRI-compatibility; however efficient design can bring advantages in terms of structural simplicity and miniaturisation. Manufacturing of proof-of-concept prototypes using 3D printing is underway.

I. INTRODUCTION

Intravascular catheterization is nowadays a standard technique for many types of minimally invasive diagnostic and surgical procedures. Catheters are typically guided using fluoroscopy – however, this imaging technique uses ionizing radiation and is associated with an increase in risk of cancer and other side effects for patients and attending medical staff. Real-time Magnetic Resonance Imaging (MRI) has been recently developed as a safer, more effective alternative to fluoroscopy; however, practical implementation of MRI is not proving easy. Some intravascular procedures (e.g. interventional electrophysiology studies) require electrical signals to be transmitted outside the body – this is almost universally achieved with thin metal or otherwise low-impedance wires.
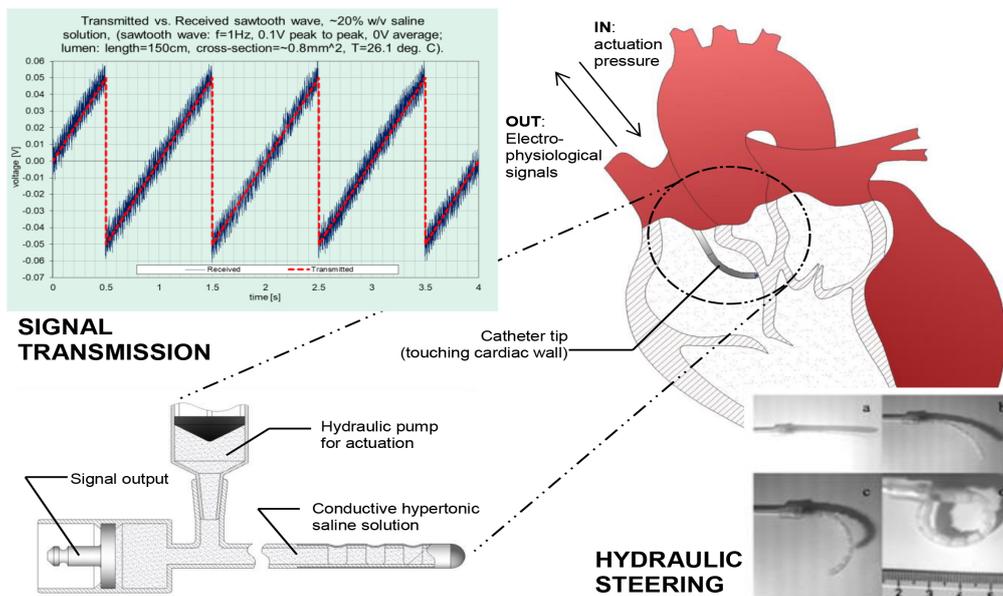
Fig. 1. Summary of our vision. A catheter using the same hypertonic saline solution for signal transmission and steering is used to collect electrophysiological signals from inside the heart.

Unfortunately, such components are particularly undesirable in an MRI environment as they have the potential of heating to dangerous levels; imaging artefacts may also arise, making guidance and positioning of catheters particularly difficult. While methods have been devised to increase MRI-compatibility of such systems, difficulties have been reported.

II. METHODOLOGY

Our approach takes inspiration from non-invasive examinations of the electrical signals generated by the heart, e.g. electro-cardiography. With some rough approximation, these signals are collected after passing bodily tissues; these, in turn, can be roughly approximated as normal saline solution (0.9% weight/volume), which is itself a rather poor conductor. Performance of such systems is, however, very well established. Stemming from this, we determined that hypertonic concentrations (i.e. well above normal concentration) offer good signal transmission properties when tested in narrow catheter-like lumens (1mm internal diameter, 100+ cm in length) at similar voltages and frequencies as cardiac electrophysiological signals collected directly. An example is shown in the chart on top left corner of fig. 1, where the signal received through a catheter-like lumen follows very closely the transmitted signal (net of the 50Hz mains noise captured by the unshielded test-rig). Being similar in composition to human tissues and only marginally more conductive, hypertonic

saline solution appears feasible as a MRI-compatible substitute of traditional low-impedance wires. The safety profile of hypertonic saline solution in case of accidental spillage into the bloodstream is also very good, with 20% and 7% reported as safe concentrations for adult and paediatric patients respectively.

We also investigated the integration of hydraulic steering using the same conductive fluid. MRI-compatible steering mechanisms can be devised without the need of an hydraulic system, e.g. using tendons or push-rods made of MRI-compatible polymers. However, it can make sense to re-use components that are already available in the body of the catheter. Our proof-of-concept design uses a very simple 1-DOF mechanism that is steered by removing a small volume of fluid, and re-straightened by pumping in back the same volume (see the insert in the bottom right corner of fig. 1). Variances in the conductive cross-section (thus in resistivity) in the steering tip are limited, thus not affecting the overall signal transmission properties of the whole catheter. We are currently in the manufacturing stages of a functional prototype, while at the same time testing designs, materials and assembly techniques that can be useful in future production. Use of 3D printing has enabled to significantly reduce the time and costs involved to test ideas, with results that are more than satisfactory considering the minuscule size of the components being printed (e.g. fig. 2).
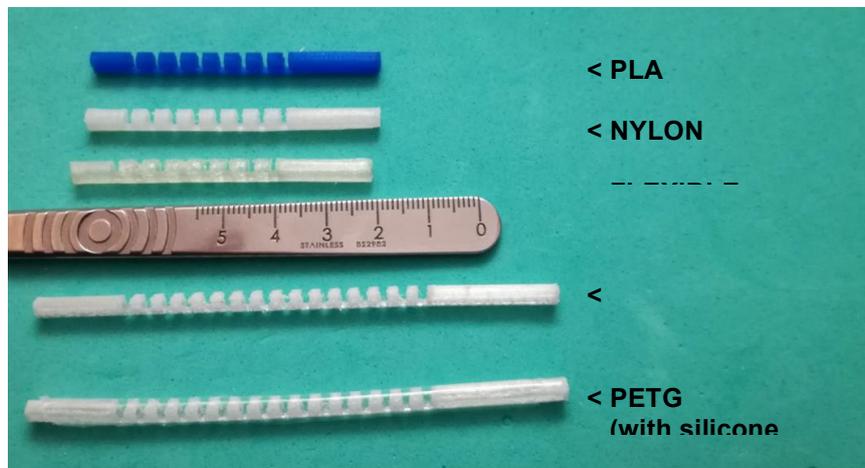
Fig. 2. Examples of 3D printed hydraulic catheter structures ready to be assembled. 3D printing has enabled time- and cost-efficient testing of various designs and materials.

III. CONCLUSION

Stemming from our positive results, we believe that the problem of signal transmission in MRI-guided intravascular catheterisation can be solved, or at least greatly simplified, through the use of hypertonic saline solution instead of traditional metal wires. The integration of signal transmission and hydraulic steering can be an added bonus to achieve better performance and effectiveness in actual manufacturing.

REFERENCES

1. K. Koning et al., Catheters and guidewires in interventional MRI: problems and solutions, 2001, Medica Mundi 45/1, 31-39.
2. Bhagirat et al., Interventional Cardiac Magnetic Resonance Imaging in Electrophysiology, 2014
3. Radiometer Analytical, Conductivity, Theory and Practice. Villerurbanne, France, 2004.
4. S. Liu, J. Kruse, Biopotential Electrode Sensors in ECG/EEG/EMG Systems. Analog Devices Inc., 2008.
5. Haga Y. et al., Small diameter hydraulic active bending catheter using laser processed super elastic alloy and silicone rubber tube, Proceedings of the 3rd Annual International IEEE EMBS Special Topic Conference on Microtechnologies in Medicine and Biology 2005;245-248
6. Caenazzo, H. Liu, K. Althoefer, Integrated Signal Transmission And Hydraulic Steering Using Hypertonic Saline Solution In MRI-Compatible Intravascular Catheters, Abstract book of the 24th Congress of EAES, 2016
7. Ataollahi, R. Karim, A. S. Fallah, K. Rhode, R. Razavi, L. D. Seneviratne, T. Schaeffter, K. Althoefer, Three-Degree-of-Freedom MR-Compatible Multisegment Cardiac Catheter Steering Mechanism, IEEE Transactions on Biomedical Engineering 63 (11), 2425-2435, 2013.

Embodying risk assessment and situational awareness for safe HRI from physical and cognitive control architectures.

Antonella Camilleri, Dr.Sanya Dogramadzi and Dr.Praminda Caleb-Solly at Bristol Robotic Laboratory, UWE.

I. CONTEXT

The Human Robot Interaction (HRI) activities currently reported in the scientific literature are mostly simple Human-Robot activities of passing objects or completing collaborative assembly tasks. Physical and cognitive multimodal sensory input for supporting HRI have been researched to allow sharing space and tasks with a human. So far it has been shown that explicit knowledge management both in symbolic and geometric (surrounding environment and object label) provide more natural human-robot interaction (Lemaignan, Warnier, Sisbot, et al., 2017). This perception and interpretation of the surrounding environment provide the robot with the ability of knowing, reasoning, risk assessing and eventually cooperating. This is of vital importance when it comes to cooperating with robots which go beyond cooperation around a structured environment of an assembly table. Having collaborative robots that are build up to the standards are not enough unless they are able to reason safely especially when having humans in the loop that have less control over their actions and the surrounding environment, for example assistive robots for older adults. Many researchers focused on acquiring humans' senses and building perception of the environment either by using direct physical interaction or through cognitive architectures. Nevertheless, the embodied intelligence in a robotic system can contribute to safety since reasoning about the environment based on the objective task can lead to a safer approach to HRI.

For a safe interaction, situational awareness and a risk assessment based on feedback from physical and cognitive models of user in the robot workspace are fundamental. Therefore, the aim of this project is to propose a safe HRI framework embedded in a decision making layer based on the combination of physical and cognitive robot interactions with its environment and the users. The physical and cognitive interaction input to an HRI control architecture are important for non-expert users. Interaction with non-expert users requires cognitive awareness input to predict and anticipate user actions trough the typical human-like input modalities (gaze, voice feedback, movement of arms, emotion detection etc.) which can significantly differ for non-expert users. For instance, elderly people with impairments can have limited functional capability of some modalities (for example cannot move hands for a dressing task; cannot give voice feedback or cannot enhance predication trough gaze due to a stroke) and force feedback from the end effector can provide significant amount of situational awareness of the task being carried out (Erickson, Clegg, Yu, et al., 2017).

II. BACKGROUND LITERATURE REVIEW

In HRI risk assessment and situational awareness are not always evaluated before robot actions are executed and such HRI application are rarely put in the context of non-expert robot user such as in assisting physically or cognitively impaired adults in their daily activities. Close physical HRI needs to rely on decision making processes based on the risks and situational awareness in a current context. Question that are still valid are: How can the situational awareness be achieved? Which approach is better? - creating cognitive intelligence or by using traditional physical HRI methods? When it comes to safety, a combination of these HRI approaches could be the answer. We will take inspiration in how humans make decisions based on combined multimodal sensory

information in safety critical situations. Based on this approach cognitive architectures that build situational awareness based on the cues from the surrounding environment are reviewed.

III. COGNITIVE ARCHITECTURES AND HRI

Cognitive robotics can perhaps be defined as a study of understanding how and why people act the way they do. This approach is driven by the hypothesis that for robots and autonomous systems to be more capable and intelligent than human-like representations, strategies and knowledge will eventually result in a higher level of collaboration and interaction between robots and humans. A question that researchers are still striving to understand is how people organize knowledge and produce intelligent behaviour. (Kurup & Lebiere, 2012) present the relevant architectural concepts and principles and illustrate them using nine cognitive architectures that are under active development – Soar, ACT-R, CLARION, GMU-BICA, Polyscheme, Co-JACK, ADAPT, ACT-R/E, and SS-RIC. (Kurup & Lebiere, 2012) argued that "the current robotics approach to solving problems, referred to as the algorithmic approach, is inadequate for the kinds of problems that need to be solved for general intelligence tasks. Instead, the cognitive architecture approach, with the separation of architecture and content, an emphasis on memory over computation, performance bounded by environmental and task constraints and automatic life-long learning" are a better approach.

(Baxter, Lemaignan & Trafton, 2016) state that cognitive architectures are constructs that pursue to account for cognition used as a set of domain-general structures, mechanisms and processes which are often inspired by human cognition. Cognitive HRI is sometimes seen as a safer way of sharing the same perspective of an activity. In (Huang & Mutlu, 2016) a gaze tracker and speech recognition are used to create an intent predictor and an anticipatory motion planner. This method shows that effectiveness of the robot in responding to the user requests is improved. The anticipatory action here results in a significantly improved human-robot collaboration while the intention prediction based on gaze tracking incorrectly inferred 18.75%. (Tan & Kawamura, 2015) present an approach to develop a cognitive social robot model in which imitation learning, intention recognition and cognitive behaviour control were integrated. The proposed framework is built from a human gesture estimation agent, an intent recognition agent, a cognitive control agent and a behaviour generalization agent. This framework imitates the learning and human intention recognition. (Malheiro, Bicho, Machado, et al., 2017) In this work, a cognitive control architecture that attributes crucial cognitive and social capabilities is proposed through a software framework that facilitates the implementation of Cognitive Dynamic Neural Field (DNF). All of the above mentioned cognitive architectures embody a robotic platform with abilities for human-like thinking to predict intentions, adapt to situations from previously targeted goal or to give social capabilities. However, risk assessment and situational awareness are not evaluated before actions are executed and no framework has the capabilities to learn update action selection based on past experience by rewarding or discarding cues.

I.V. CHALLENGES IN COGNITIVE AND ROBOTIC AREAS

The grand challenges faced in robotics and more specifically in assistive robotics are mass-personalization, that is, the ability of having a solution with one person that would work equally and efficiently for someone else (Khatib & Siciliano, n.d.). Another grand challenge is that of having robotic autonomy which is increased when having reduced communication, physical, and/or cognitive abilities. By addressing these challenges, one would gain advantage of having an HRI framework which is modular and presents efficient and effective solution. (Rajan & Saffiotti, 2017) suggest that AI is now more than ever ready to be applied to robotics and brings together the developing field of integrated AI and Robotics. (Rajan & Saffiotti, 2017) emphasise that research still needs to answer intersections between robotics and cognitive challenges. Research for assistive robots has progressed in areas of

manipulation and rehabilitation aids, and cognitive aids in forms of small pet-like to engage the patient to promote personal health, growth and interaction but very few has been done in daily assisting elderly adults in close proximity like for example helping them to get dressed. As a recapitulation, we have three main goals for this project:

To investigate which appropriate cognitive architecture can incorporate situational awareness based on the cues and physical interaction gathered from the surrounding environment in order to ensure a safe decision making framework for a robotic systems.

To implement the integrated cognitive architecture on a robotic platform and ensure that adaptation and correct action selection is based on the knowledge and past experience gathered. To provide guidelines for achieving safe HRI in the context of older adults care environments.

V. CONTRIBUTION AND IMPORTANCE TO HRI AS A RESEARCH FIELD

This study contributes to research in human-robot interaction since it tries to fill a part of the gap in research where close proximity interaction is based on a safety framework where physical and cognitive interaction work concurrently to achieve one same goal. In close-proximity, physical feedback is requirement for achieving safe HRI. On the other hand being able to make the correct decision and having robots with embodied intelligence that can make safe decisions based on the surrounding risks and contextual situations is important and still not achieved.

REFERENCES

1. Baxter, P.E., De Greeff, J. & Belpaeme, T. (2013) Cognitive architecture for human-robot interaction: Towards behavioural alignment. Biologically Inspired Cognitive Architectures. [Online] 630–39. Available from: doi:10.1016/j.bica.2013.07.002.
2. Erickson, Z., Clegg, A., Yu, W., Turk, G., et al. (2017) What Does the Person Feel? Learning to Infer Applied Forces During Robot-Assisted Dressing. 2017 IEEE International Conference on Robotics and Automation (ICRA). [Online] 6058–6065. Available from: doi:10.1109/ICRA.2017.7989718.
3. Huang, C.M. & Mutlu, B. (2016) Anticipatory robot control for efficient human-robot collaboration.
4. ACM/IEEE International Conference on Human-Robot Interaction. [Online] 2016–April (Section V), 83– 90. Available from: doi:10.1109/HRI.2016.7451737.
5. Kurup, U. & Lebiere, C. (2012) What can cognitive architectures do for robotics? Biologically Inspired Cognitive Architectures. [Online] 288–99. Available from: doi:10.1016/j.bica.2012.07.004.
6. Lemaignan, S., Warnier, M., Sisbot, E.A., Clodic, A., et al. (2017) Artificial cognition for social human–robot interaction: An implementation. Artificial Intelligence. [Online] 24745–69. Available from: doi:10.1016/j.artint.2016.07.002 [Accessed: 30 August 2017].
7. Malheiro, T., Bicho, E., Machado, T., Louro, L., et al. (2017) A software framework for the implementation of dynamic neural field control architectures for human-robot interaction. 146–152.
8. Rajan, K. & Saffiotti, A. (2017) Towards a science of integrated AI and Robotics. Artificial Intelligence. [Online] 2471–9. Available from: doi:10.1016/j.artint.2017.03.003.
9. Tan, H. & Kawamura, K. (2015) Generation of acceptable actions using imitation learning, intention recognition, and cognitive control. Proceedings - IEEE International Workshop on Robot and Human Interactive Communication. [Online] 2015–Novem389–393. Available from: doi:10.1109/ROMAN.2015.7333662.

People's Perceptions of Task Criticality and Preferences for Robot Autonomy

Adeline Chanseau, Kerstin Dautenhahn, Michael Walters, Gabriella Lakatos, Kheng Lee Koay and Maha Salem, School of Computer Science, University of Hertfordshire

ABSTRACT

The concept of criticality is relatively new to the Human-Robot Interaction (HRI) community. Now that robots are becoming more routinely available to the public, it is important to understand what makes a task critical, and how this is linked to people's preferences for different levels of autonomy for domestic robot companions. To do so, we first conducted a live study to see how much autonomy people would give to a robot to perform a simple task. We then conducted a questionnaire study to investigate how people classify task criticality, which builds up to our future study that will explore how task criticality affects the way people want to have control their robot - performing the task.

I. BACKGROUND AND MOTIVATION

As more companion robots become commercially available to the public, it is important to understand how much in control of their robots people want to be [1], [2]. In our previous study [1] we showed that the more controlling and anxious about robots people were, the more autonomous they wanted the robot to be. As we hypothesised that people's perceived level of control depends on the criticality of the task the robot performs, we chose to investigate how people rate the criticality of a task. In order for people to evaluate a task criticality, we provided Yanco and Drury's definition of criticality applied Human-Robot Interaction [3], which is "the importance of getting the task done correctly in terms of its negative effects should problems occur". Ezer et   al. [4], who performed a study to see whether the criticality of a task has any effect on users delegating tasks   to a home robot companion, found that people were less willing to have a robot performing a low critical task   if it requires a large amount of interaction with the robot. However,   the researchers admitted they were unsure of the results since there were no clear findings regarding the different levels of criticality perceived   for   the   tasks.   According   to Tzafestas [5], there are three levels of criticality: low, medium and high. However,

he did not explain how to differentiate these levels of criticality. According to Beer et al. [6], [7] and Mitzer et al. [8], the level of the criticality of the task depends on how preferable it is for the user to have a human performing   a critical task such as giving medication. We chose to investigate what factors people consider when rating task criticality to attempt to give a guideline. As task criticality is difficult to disentangle from other concepts, we narrow our focus on domestic robot companions.

II. METHODS AND RESEARCH QUESTIONS

To investigate the user's perception of control and task criticality, two studies were conducted. The aim of the first study was to answer how people's perception of control (i.e. how much control over the robot's autonomy people want to have) can affect the level of autonomy they give to a robot, while the second study aimed to uncover what type of criteria people considered to rate the criticality of a task.

A. First study: live study in the domestic environment

This study [1] was conducted in a smart house environment with two different robots: an autonomous mobile companion robot, Sunflower [9], and a vacuum cleaning robot, Roomba [10]. Three conditions were set: in the first condition, the companion robot mentioned to the participants that the

bathroom needed to be vacuumed and the participant had to manually turn on the Roomba robot. In the second condition, the companion robot made the same statement as in the first condition, but offered the option for the user to remotely turn on the Roomba robot. In the third condition, the companion robot made the same statement as in the first condition, and turned on the Roomba robot without any confirmation needed from the participant. The robot companion mentioned to the participant that cleaning was ongoing. Twenty-five people (11 females and 14 males) participated in the study (M_{age} = 36.16, SD_{age} = 13.04). Each participants experienced each conditions in a randomised order. After each condition, participants had to complete a short questionnaire which measured the user's perception of who was in control of the interaction. Participants' level of desired control were evaluated before their interaction with the robots started, with the

desirability control scale (DCS) [11], which is a validated standardised test [12].

B. Second study: Questionnaire study on attribution of criticality

This questionnaire study contained an open-ended questions section and a ranking section. Two pictures of robots were shown: a robot companion robot, Sunflower [9], and a vacuum cleaning robot Roomba [10] to provide context. In the open-ended questions section, participants were asked what they considered a high critical task and a low critical task were for a robot companion. The ranking section provided a list of 12 different tasks people had to rank, from the most critical task to the least. 101 participants were recruited from the University of Hertfordshire (50 females and 51 males with M_{age} = 25.70, SD_{age} = 9.59) for this study.

III. RESULTS AND DISCUSSION

A. First study: type of control over the robot preferred by the user

Results (see Fig.1) suggest there is a shift in the perceived level of control of the robot companion. It seems to increase as participants felt they could delegate more control to the robot, so they do not need to perform any physical action for the cleaning to happen. However the perception of control of the situation slightly decreases as the participant becomes more passive (see Fig.1). Although these results suggest a

perception of decreased control, 60% of the participants preferred the third condition. This suggests that there is a tendency for people to accept to relinquish control of the action, if they believed to still possess some indirect control through the robot companion. The Pearson's chi square test shows there is an association between participant's level of desired control and their perceived level of control in each conditions.

$(\chi^2 (12) = 33.777, p_{C1} < 0.001 \chi^2_{C2}$ (12) $= 33.014, p_{C2} < 0.001$, and χ^2_{C3} (12) $= 29.565, p_{C3} < 0.03)$.
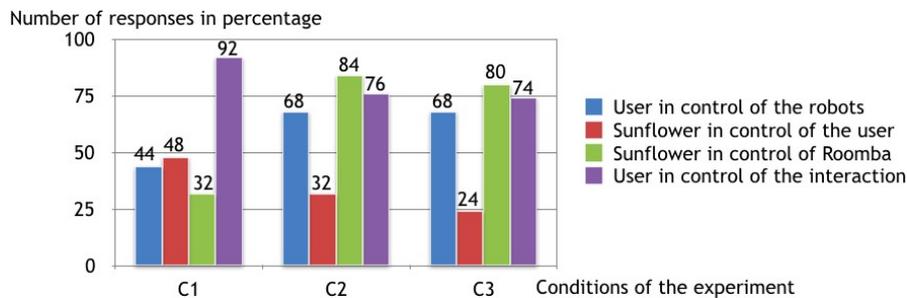

Fig. 1: User's perception of control of the robots

B. Second study: classification of tasks depending on criticality

The results of the questionnaire study show that among the 12 tasks given to rank, tasks related to safety   and time constraint were consistently ranked as high critical ("There is some smoke in the kitchen. The robot   is calling the fire service.", "You have   just remembered that you need to see the doctor this week for a blood   test. The robot is booking the appointment for you.", "You have lost your car keys and need to pick up your friend in an hour.

The robot is looking for your car keys"). Tasks linked to entertainment were always rated as low critical ("You are sitting on the sofa, relaxed. The robot is performing a dance for entertainment.", "You are home and want to be entertained. The robot is telling you a joke." and "You are bored.

The robot reads some poems to please you."). Over 75% of the participants considered safety orientated tasks as the most critical and over 80% of the participants rated entertainment-orientated tasks as the least critical.

V. CONCLUSION AND FUTURE WORK

To conclude, this work suggests that people accept to relinquish some control of the desired action if their perception of control of their robot companion was sufficiently high. It also showed that the most important factors that people take into consideration when rating the criticality of a task for high or low seemed to be   safety and entertainment. Therefore, in our future study we will investigate if people are still ready to relinquish some control of the desired action for high critical tasks, and if the task itself affects the perception of the robot.

REFERENCES

1. Chanseau, K. Dautenhahn, K. L. Koay, and M. Salem, "Who is in charge? sense of control and robot anxiety in human-robot interaction," in *Robot and Human Interactive Communication (RO-MAN), 2016 25th IEEE International Symposium on*, 2016.

2. Schiffhauer, J. Bernotat, F. Eyssel, R. Bröhl, and J. Adriaans, "Let the user decide! user preferences regarding functions, apps, and interfaces of a smart home and a service robot," in *International Conference on Social Robotics*. Springer, 2016, pp. 971–981.

3. H. A. Yanco and J. L. Drury, "A taxonomy for human-robot interaction," in *Proceedings of the AAAI Fall Symposium on Human- Robot Interaction*, 2002, pp. 111–119.

4. Ezer, A. D. Fisk, and W. A. Rogers, "More than a servant: Self- reported willingness of younger and older adults to having a robot perform interactive and critical tasks in the home," in *Proceedings of the Human Factors and Ergonomics Society Annual Meeting*, vol. 53, no. 2. SAGE Publications Sage CA: Los Angeles, CA, 2009, pp. 136–140.

5. S. G. Tzafestas, "Human-robot social interaction," in *Sociorobot World*. Springer, 2016, ch. 4, pp. 53–69.

6. J. M. Beer, A. D. Fisk, and W. A. Rogers, "Toward a psychological framework for levels of robot autonomy in human-robot interaction," Georgia Institute of Technology, Tech. Rep., 2012.

7. J. Beer, A. D. Fisk, and W. A. Rogers, "Toward a framework for levels of robot autonomy in human-robot interaction," *Journal   of Human-Robot Interaction*, vol. 3, no. 2, p. 74, 2014.

8. T. L. Mitzner, C.-A. Smarr, J. M. Beer, T. L. Chen, J. M. Springman, A. Prakash, C. C. Kemp, and W. A. Rogers, "Older adults' acceptance of assistive robots for the home," Technical Report HFA-TR-1105 Atlanta, GA: Georgia Institute of Technology School of Psychology–Human Factors and Aging Laboratory, Tech. Rep., 2011.

9. K. L. Koay, G. Lakatos, D. S. Syrdal, M. Gácsi, B. Bereczky, K. Dautenhahn, A. Miklósi, and M. L. Walters, "Hey! there is someone at your door. a hearing robot using visual communication signals of hearing dogs to communicate intent," in *Artificial Life (ALIFE), 2013 IEEE Symposium on*. IEEE, 2013, pp. 90–97.

10. J.-Y. Sung, L. Guo, R. E. Grinter, and H. I. Christensen, *"My Roomba Is Rambo": Intimate Home Appliances*. Springer, 2007.

11. J. M. Burger and H. M. Cooper, "The desirability of control," *Motivation and emotion*, vol. 3, no. 4, pp. 381–393, 1979.

12. L. E. McCutcheon, "The desirability of control scale: Still reliable and valid twenty years later," *Current research in social psychology*, vol. 5, no. 15, pp. 225–235, 2000.

Multi-plane Motion Planning for Multi-Legged Robots

Wei Cheah[1,2], Peter Green[1], Simon Watson[1], Barry Lennox[1] and Farshad Arvin[1]

ABSTRACT

Hexapods are desirable due to its statically stable motions and redundant configuration. Studies on motion planning for these robots are in environments that are wide and contacts are typically made on the plane they are travelling on. Large obstacles or narrow pathway are avoided by planning another route. This limits areas that the robot is able to access such as in confined areas or discontinuous path. This paper presents the concept of multi-plane motion planning for multi-legged robots, specifically for hexapods to address limitations of their inherent design and on existing motion planners. A conceptual hexapod for multi-plane motion is also detailed.

I. INTRODUCTION

Mobile robots are increasingly used and researched to meet the demands in improving efficiency and carrying out operations dangerous for humans [1]. Legged robots have better capabilities in surpassing uneven environments compared to wheeled or tracked robots [2]. This is partly attributed to legged robots' capabilities in traversing on discontinuous path [3]. Among the different classes of legged robots (bipeds, quadrupeds, hexapods, octopods) [4], hexapods are well suited to applications that require statically stable motions and redundant configuration, such as in search and rescue or demining operations whereby in the event of an explosion results in a damaged leg, the robot will still be able to continue its mission [5]. Current research on hexapods has largely employed irregular terrains as their experimental environment such as rocks [6], snow [7], blocks [8] and steep terrains [9]. The commonalities in these motions are that the environment in wide areas and contacts are typically made on the plane they are travelling on. The motion planners employed plans route that avoids large obstacles or narrow pathways. This limits areas that the robot is able to access such as in confined areas or discontinuous path, as shown in Fig. 1. Such scenarios occur in urban environments following a disaster [10]. This paper presents the concept of multi-plane motion planning for multi-legged robots, specifically for hexapods to address limitations of their inherent design, and on existing motion planners. A conceptual hexapod for multi-plane motion is also detailed.
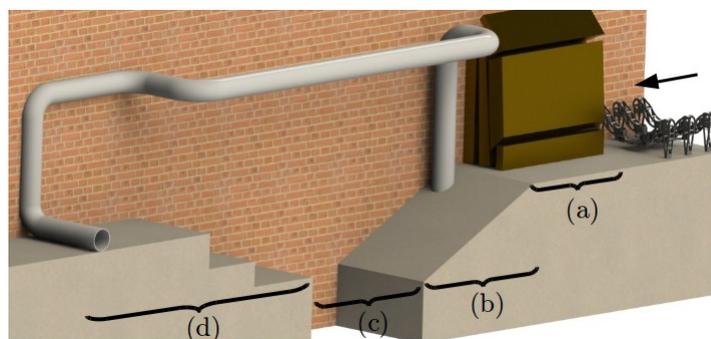
Fig. 1. Confined environment scenarios (a) narrow pathway (b) gradient slope (c) pit (d) steps and large obstacles

[1] School of Electrical and Electronic Engineering, The University of Manchester, UK
[2] Corresponding Author: wei.cheah@manchester.ac.uk (Wei Cheah)

II. MULTI-PLANE MOTION PLANNING

As mentioned earlier, most experiments for hexapods have been conducted on wide areas. For irregular terrains, this can often be approximated as a single plane and possibly with height data (2.5D map) [11].   The same is done on walls, gradient slopes and varying sizes of obstacles where they are flatten down onto   a single plane [12]. This simplifies the motion planning involved where the robot's path and contacts are subsequently planned along this plane with no contact on walls and large obstacles. This constrains the robot's motion and contacts to the plane it is on. Thus for any type of motion or gait used, the footprint of   the robot remains largely the same and the robot's weight is supported by the plane.

Using existing motion planners would not work for the scenario shown in Fig. 1 as

motions. For narrow pathway, different gaits have been proposed for reducing the robot's footprint but remains limited to the robot's body width [13]; the use of a semi- ellipsoid attached to the back of a RHeX type robot for running through flexible beams has been proposed but is only applicable to this particular type of robot [14]. The HyQ quadruped showed chimney walking in simulation (experiments were limited due to joint torque limitations) [15]. However, the robot started and ended within the chimney itself. The motion planner for executing the motions in Fig. 2 would need to plan the motion for moving into the respective stances (sideways, chimney) before moving forwards based on those stances. Recovery from those stances will also be needed on exit i.e. going from sideways to flat.
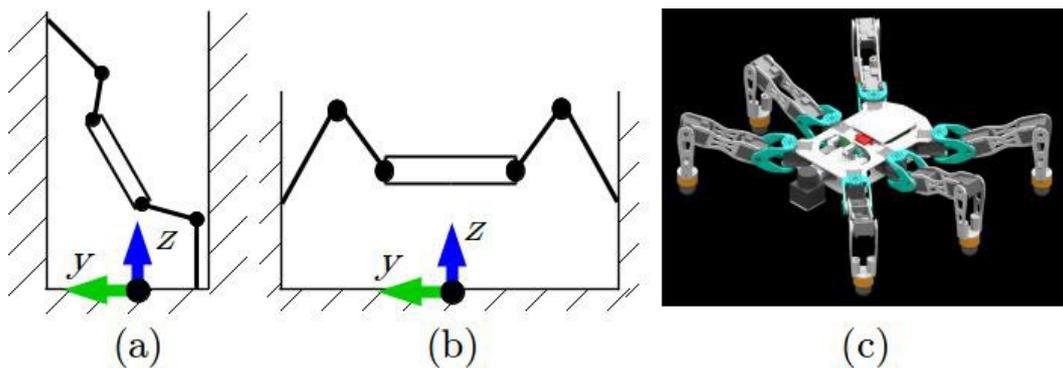
Fig. 2. (a) Sideways walking (b) Chimney walking (c) Conceptual hexapod

contacts are constrained to the plane it is travelling on. Segment *a* and *c* are impassable as the large footprint of the robot prevents it from passing through *a* while the pit in *c* is too large and deep for the robot to step in or over. To pass through, motions that reduces the footprint and does not require its weight to be supported by the plane it is traversing on is required. Two examples of such motion is sideways (Fig. 2a) and chimney (Fig. 2b) walking. In the first instance, the robot starts by rearing up sideways and then walk along in this manner (Fig 2a). This reduces its footprint enabling it to pass through pathways even narrower than its body width. In the next instance, using the walls for contact would enable the robot to chimney walk across the pit.
There have only been few studies on such

The requirements for a hexapod executing such motions are on their joint requirements. A number of methodology for designing legged robots have been reviewed in [16]. Current state-of-art hexapods employ the characteristic motion approach, subjecting the robot to motions such as the tripod gait [5], standing on two legs [17] or walking up stairs [18], to identify link and joint parameters. This approach will needs to be extended for the motions shown in Fig. 2. By designing the robot to be symmetrical about its body sagittal plane, there is no need for complex self-righting hardware or motions required on exit [19] or falling over [20]. Fig. 2c shows the CAD design based on these concepts for a hexapod that is adaptable to operate in confined environments, capable of the reach required for these motions. A

simple self-righting technique is employed by mounting the sensors that are required on the top side of the body to be rotated about the body axis by an actuator.

REFERENCES

1. Kroll, "A survey on mobile robots for industrial inspection," in Proceedings of the Int. Conf. on Intelligent Autonomous Systems IAS10, Baden-Baden, Germany, pp. 406–414, 2008.
2. K. J. Waldron, V. J. Vohnout, A. Pery, and R. B. McGhee, "Configuration design of the adaptive suspension vehicle," The International Journal of Robotics Research, vol. 3, no. 2, pp. 37–48, 1984.
3. P. Gonzalez, E. Garcia, and J. Estremera, Quadrupedal locomotion: an introduction to the control of four-legged robots. Springer Science & Business Media, 2007.
4. S. Kajita and B. Espiau, "Legged robots," in Springer handbook of robotics, pp. 361–389, Springer, 2008.
5. P. G. De Santos, J. Cobano, E. Garcia, J. Estremera, and M. Armada, "A six-legged robot-based system for humanitarian demining missions," Mechatronics, vol. 17, no. 8, pp. 417–430, 2007.
6. Bjelonic, N. Kottege, and P. Beckerle, "Proprioceptive control of an over-actuated hexapod robot in unstructured terrain," in Intelligent Robots and Systems (IROS), 2016 IEEE/RSJ International Conference on, pp. 2042–2049, IEEE, 2016.
7. X. Xiong, F. Wörgötter, and P. Manoonpong, "Neuromechanical control for hexapedal robot walking on challenging surfaces and surface classification," Robotics and Autonomous Systems, vol. 62, no. 12, pp. 1777–1789, 2014.
8. Y. Xu, F. Gao, Y. Pan, and X. Chai, "Hexapod adaptive gait inspired by human behavior for six-legged robot without force sensor," Journal of Intelligent & Robotic Systems, pp. 1–17, 2017.
9. K. Hauser, T. Bretl, J.-C. Latombe, K. Harada, and B. Wilcox, "Motion planning for legged robots on varied terrain," The International Journal of Robotics Research, vol. 27, no. 11-12, pp. 1325–1349, 2008.
10. R. R. Murphy, S. Tadokoro, D. Nardi, A. Jacoff, P. Fiorini, H. Choset, and A. M. Erkmen, "Search and rescue robotics," in
11. Springer Handbook of Robotics, pp. 1151–1173, Springer, 2008.
12. S. Bartoszyk, P. Kasprzak, and D. Belter, "Terrain-aware motion planning for a walking robot," in Robot Motion and Control (RoMoCo), 2017 11th International

Workshop on, pp. 29–34, IEEE, 2017.
13. Stelzer, H. Hirschmüller, and M. Görner, "Stereo-vision-based navigation of a six-legged walking robot in unknown rough terrain," The International Journal of Robotics Research, vol. 31, no. 4, pp. 381–402, 2012.
14. Z.-Y. Wang, X.-L. Ding, and A. Rovetta, "Analysis of typical locomotion of a symmetric hexapod robot," Robotica, vol. 28, no. 6, pp. 893–907, 2010.
15. Li, A. O. Pullin, D. W. Haldane, H. K. Lam, R. S. Fearing, and R. J. Full, "Terradynamically streamlined shapes in animals and robots enhance traversability through densely cluttered terrain," Bioinspiration & biomimetics, vol. 10, no. 4, p. 046003, 2015.
16. Focchi, A. Del Prete, I. Havoutis, R. Featherstone, D. G. Caldwell, and C. Semini, "High-slope terrain locomotion for torque-controlled quadruped robots," Autonomous Robots, vol. 41, no. 1, pp. 259–272, 2017.
17. Semini, V. Barasuol, J. Goldsmith, M. Frigerio, M. Focchi, Y. Gao, and D. G. Caldwell, "Design of the hydraulically actuated, torque-controlled quadruped robot hyq2max," IEEE/ASME Transactions on Mechatronics, vol. 22, no. 2, pp. 635–646, 2017.
18. J.-Y. Kim and B.-H. Jun, "Design of six-legged walking robot, little crabster for underwater walking and operation," Advanced Robotics, vol. 28, no. 2, pp. 77–89, 2014.
19. Belter and K. Walas, "A compact walking robot–flexible research and development platform," in Recent Advances in Automation, Robotics and Measuring Techniques, pp. 343–352, Springer, 2014.
20. Li, C. C. Kessens, A. Young, R. S. Fearing, and R. J. Full, "Cockroach-inspired winged robot reveals principles of ground-based dynamic self-righting," in Intelligent Robots and Systems (IROS), 2016 IEEE/RSJ International Conference on, pp. 2128–2134, IEEE, 2016.
21. S. Peng, X. Ding, F. Yang, and K. Xu, "Motion planning and implementation for the self-recovery of an overturned multi-legged robot," Robotica, vol. 35, no. 5, pp. 1107–1120, 2017.

Wireless Communications in Nuclear Decommissioning Environments

A. Di Buono$^{a, b}$, N. Cockbain^a, P.R. Green^b, B. Lennox^b

ABSTRACT

The use of Wireless Sensor Networks (WSN) is now widespread, with well-documented deployments across a diverse range of sectors including aerospace, agri-science and consumer electronics. In the nuclear industry there have been successful deployments of the WSN technologies for instrumentation and control, however, there are significant challenges that need to be addressed before wireless sensing can be used in nuclear decommissioning environments. These challenges include: limited sources of power; the radiation tolerance of the sensor and communication system components; the severe attenuation of wireless signals through reinforced wall structures; and the need to deliver secure, interoperable and reliable communication.

I. INTRODUCTION

Robotics and Automation applications within the nuclear decommissioning industry are rapidly increasing to reduce the cost, time and dose exposure of workers [1]. In addition, there is the need to store nuclear waste and monitoring the condition of the packages in the stores [2]. The design, prototype and evaluation of Wireless Sensor Network with the capability to deliver remote sensing and control can result in reduction of the cost and time to install robotics application and improve the performance, collecting data from hard to reach places not designed to be decommissioned. As a result a successful application can lead to an increase of robotics and automation in the nuclear Industry.

II. BENEFITS AND CHALLENGES

Wireless Sensor Networks are extensively employed in agriculture, classic examples are application to monitor soil and crop properties [3] [4]. Similarly in the aerospace industry it is possible to find useful example of Wireless Sensors Networks in harsh environments, to monitor gas turbine engines [5].

In the nuclear industry there have been initiatives to deploy Commercial Off The Shelf (COTS) wireless instrumentation and control systems [6]. One such initiative resulted in Sellafield's first application of this technology [7], with reported time saving of 16 weeks and a cost saving of £185k. However, there remain a number of significant challenges to address if Wireless Sensor Networks are to be deployed in nuclear decommissioning environments. One key challenge is the damaged to COTS integrated circuits caused by the high radiation levels and elevated temperatures. There are also fundamental communication challenges resulting from the very high signal attenuation experienced by Radio Frequency (RF) signals propagating through reinforced concrete wall and floor structures. In addition, many legacy buildings in nuclear facilities were not designed to be decommissioning, and limited access and unknown conditions are a further problem. In these situations the wireless sensing systems will need to be battery-powered, with the possibility of power harvesting.

III. WIRELESS SENSOR NETWORK FOR NUCLEAR DECOMMISSIONING INDUSTRY

A research project, sponsored by the Centre for Innovative Nuclear Decommissioning (CINDe) and the University of Manchester, has been tasked with designing, prototyping and experimentally evaluating a Wireless Sensor Network with the capability to communicate
through reinforced concrete wall and floor structures in nuclear decommissioning

environments. Figure 1 shows the block diagram of the proposed Wireless Sensors Network system.

The system is composed of two main parts: a set of wireless sensing nodes in the nuclear decommissioning environment and a base station node in the operator environment. The sensor nodes and the base station node are separated by reinforced concrete wall / floor structures. Each sensor node comprises: a number of sensors; a wireless transceiver with the capability to transmit sensor data and to receive control and configuration commands from the base station node; a memory device to store sensor measurements; and a control system to coordinate the function of the node. The sensor node will be powered using power scavenging and storage techniques.

The base station node comprises a wireless transceiver and a control system. The wireless transceiver receives sensor measurement data from the wireless sensing nodes and is able to control the function of the sensing nodes by transmitting control and configuration information. Whilst only one base station node is shown in Figure 1, it will be possible to incorporate multiple base station nodes to support operation over larger areas.

The communication system will be asymmetric, in that in the nuclear

decommissioning environment we will deploy a device designed using simple electronic COTS components to limit the effect of radiation and to minimise power consumption. Conversely, the base station node will need to compensate for the imperfections, such us the frequency drift, in the transmitted signal resulting from the use of low- complexity COTS components. The control systems will play a fundamental role in the design of the Wireless Sensor Networks; in fact they will be designed with the capability of error detection and forward correction. Another key point of the Wireless Sensor Network will be to ensure an adequate and predictable operational life span, which guarantee benefits in terms of system costs and the dose exposure of workers. The operational life span will be dictated by the power consumption profiles of the sensor nodes (assuming that they are purely battery operated), and by the effect of radiation on the COTS electronics components. The second aspect will be investigated using the Dalton Cumbrian Facility irradiation capability [8], where the electronic components will be tested using the Cobalt 60 Irradiator and measuring the effect of total ionization dose on component characteristics.

The Wireless Sensor networks will ensure the security of sensitive nuclear information, by encrypting all transmitted data and by actively controlling the range of the wireless transmissions
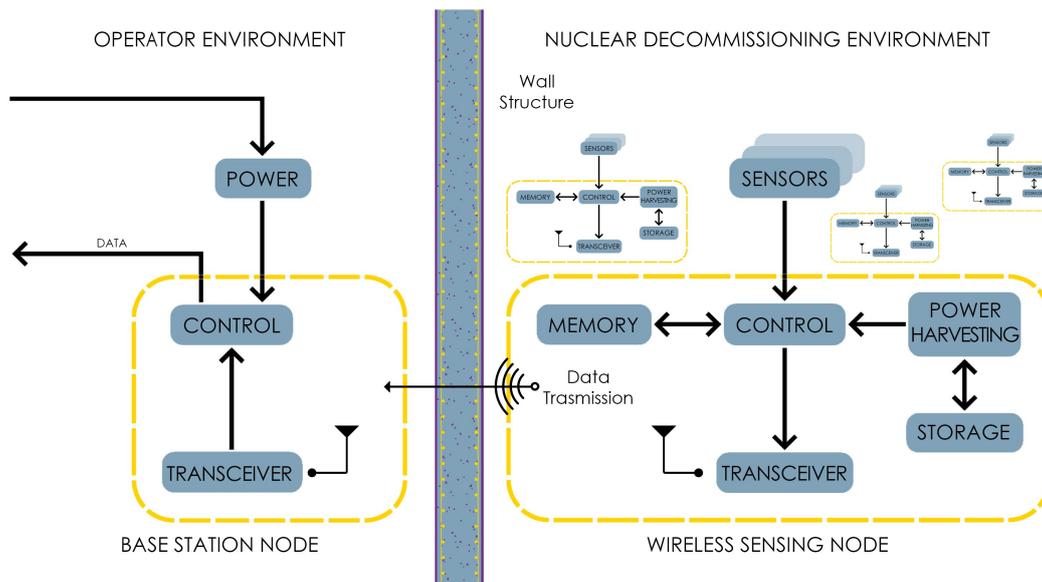
Figure 1 - Block diagram of Wireless Sensor Network System

V. CONCLUSION

This paper has shown the concept design of a Wireless Sensor Network System for application in nuclear decommissioning environments. A successful prototype will give the opportunity to increase the use of WSN technologies and hence support the deployment of robotic and autonomous systems in the Nuclear Industry. This will deliver the benefits of reduced installation costs and reduced completion times for decommissioning activities.

REFERENCES

1. Derek W. Seward, Mohamed J. Bakari, "The Use of Robotics and Automation in Nuclear Decommissioning", 22nd International Symposium on Automation and Robotics in Construction 1 ISARC 2005, September 2005.
2. Nuclear Decommissioning Authority, "WPS/640: Guidance on the Monitoring of Waste Packages during Storage", March 2008.
3. Chuan Wang, "Development of Plough-able RFID Sensor Network Systems for Precision Agriculture,
4. PhD thesis University of Manchester, 2016.
5. Peter Michael Green, "A wireless sensor network for in-crop sensing", PhD Thesis University of Manchester, 2013.
6. Hassan H. Khalili, Peter R. Green, Danielle George, Graham Watson, Werner Schiffers, "Wireless sensor networks for monitoring gas turbine engines during development", 2017 IEEE Symposium on Computers and Communications, pp.1325-1331, July 2017.
7. Tom S Nobes, Chris Murphy, "Deciding to Use Wireless Control and Instruments in the UK Nuclear Industry", Measurement and Control, vol. 47, 2: pp. 58-64, First Published February 28, 2014.
8. Tom S Nobes and Chris Murphy, "UK Nuclear Industry First Wireless Applications", IET Conference Proceedings, 2014.
9. L. Leay, W. Bower, G. Horne, P. Wady, A. Baidak, M. Pottinger, M. Nancekievill, A. Smith, S. Watson,
10. P. Green, B. Lennox, J. LaVerne, and S. Pimblott, "Development of irradiation capabilities to address the challenges of the nuclear industry", Nuclear Instruments and Methods in Physics Research B, vol. 343, pp. 62–69, 2015.

Dry versus Wet EEG electrode systems in Motor Imagery Classification

Inês Domingos [1], Fani Deligianni [1] and Guang-Zhong Yang [1]
[1] The Hamlyn Centre for Robotic Surgery, Imperial College London, UK

ABSTRACT

Motor imagery (MI) classification performance is important in developing robust brain computer interface environments for neuro-rehabilitation of patients and robotic prosthesis control. To bring this technology to everyday use, compact, wireless new EEG acquisition systems have been developed. These systems are highly portable, wireless and they are based on dry, active electrodes, which does not require the use of conductive gel. As a result they are more prone to interference via noise sources that are commonly around and their signal-to-noise ratio may be low. Here, we device a number of motor imagery tasks along with actual movements of the limbs and compare the classification performance of a dry 16-channel and a wet, 32- channel, wireless EEG system. Our results demonstrate the feasibility of home use of dry electrode systems with a small number of sensors.

I. INTRODUCTION

The motor imagery in Brain Computer Interface (BCI) is defined as the activity of mentally simulating a given action without the actual execution of the movement. Several studies have shown that performing a motor imagery session activates partially the same brain regions as the performance of the real task and it can increase motor performance [1] [2]. Therefore, it is widely used in rehabilitation, for example, for persons with Parkinson disease, stroke or any other motor deficit [3]. The first studies regarding motor imagery focused mainly in hand and arms movements [3]. Recently, those studies started to embrace also the leg and feet movements, in order to study the neurophysiology of human gait. In 2007, Baker et al. demonstrated a high temporal correlation in EEG signal between imagined and actual walking patterns, which confirmed that MI uses similar cerebral resources as the ones used during actual gait [4]. Several studies, have showed that MI practice improves walking in patients with hemiparesis and stroke [5], [6]. This means that the motor imagery promotes learning by reinforcing processes at the cortical level [6]. Research teams are also trying to combine BCI with exoskeleton robots. Recently, Zhouyang Wang et al. proposed a lower limb

exoskeleton robot controlled with MI to walk forward, sit down, and stand up [7].

There are several challenges associated with detecting motor intention in imagery movement tasks of the legs/hands even for just two classes [8] [9]. These challenges result in long training sessions and large inter- subject variability in the performance. The number, placement and type of EEG channels/electrodes play a critical role. The use of fewer channels helps to decrease the computational complexity and develop methods that allow real-time feedback to the user, which can substantially increase the learning rate. Electrodes can be either wet or dry. Wet electrodes require the application of conductive gel that improves the signal quality. However, they require long preparation times and impede the use of the technology at everyday scenarios. Dry electrodes may overcome this problem, reducing montage times and subject discomfort but the signal quality is poorer.

In this study, we contrast several two-classes experiments that include MI of the hands, legs and actual movements of the legs based on a graz-BCI stimulation paradigm. We have acquired data from both a dry 16-

channel and a 32-channels wet system and compare their offline classification performance.

II. METHODS

Experimental Setup: EEG data was recorded from six healthy participants (3 males and 3 females, 25.5 ± 6.7453 years). None of the participants had previous motor imagery experience. We used two g.tec Nautilus, EEG wireless acquisition systems with active-electrodes: i) a 16-channels dry, g.Sahara electrodes, cap and a 32-channels, wet g.ladybird cap. The EEG caps were placed accordingly to the 10-20 system. Note that out of the six participants only two repeated the experiments with the wet system.

The study comprised of:
i) a two-class MI task that involved imaginary movements of the left and right arms, ii) a two-class MI task that involved imaginary movements of the right and left legs and iii) a task with actual movements of the left and right leg while the subject was sited.

We followed a Graz-BCI stimulus paradigm to collect data for offline classification (30 randomised trials per class) [10]. The cues were displayed with Psychtoolbox-3 (Matlab R2017b) and the EEG acquisition/analyss was performed with OpenVibe 1.3 [11] [12] [13] [14].

Feature extraction and classification: The signal was temporally filtered in the alpha (8-12Hz) and beta bands (12-30 Hz). For the feature extraction, we selected four seconds of the signal, half a second after the cue (stimulation based epoching). Then, the signal was also splitted in blocks of one second, every 16th second (time based epoching), and the logarithmic band power was calculated. Features were also extracted

based on a Common Spatial Pattern (CSP) filter, which increases the signal variance for one condition while minimizing the variance for the other condition. For classification, we used Linear Discriminant Analysis (LDA) which exploits hyperplanes to separate the data representing different classes, assuming a normal distribution, with equal covariance matrix for both classes. The LDA classifier was trained to detect left/right movements based on a seven-fold cross-validation procedure. Both of the classifiers used are linear classifiers, since nonlinear classifiers are not as widespread as the first ones in BCI applications.

III. RESULTS

In table 1-2, we show results obtained from the dry and wet cap, respectively. Feature extraction is based on five scenarios: LDA and CSP are based on the standard motor imagery tasks implemented with Openvibe, whereas LDA (Alpha), LDA (Beta) and CSP (Beta) have been modified to bandpass the signal in alpha or beta bands, respectively. The combination of a beta bandpass filter with a CSP filter has shown the best classification rate. This method shows a better performance, since it relies on a decomposition of the raw EEG signal into spatial patterns, which are extracted from two distinct populations (left and right).

Firstly, we re-reference all the channels to the reference channel and subsequently we selected channels based on their location with respect to the motor cortex. For the dry cap, the reference channel selected was the Cz and the channels were F3, Fz, F4, T7, C3, C4, T8, P3, Pz, P4, Figure 1. For the wet cap, it was used the same electrode configuration as the dry cap and a different configuration according to [15], where we selected the channels F3,F4,FC5,FC6,C3,C4 with Fz as the reference, Figure 2.

Figure 1 - Channels locations for the dry cap with channels represented in red and reference represented in

Figure 2 - Channels locations for the wet cap. Configuration 1 (in red and yellow) and configuration 2 (in green and blue)

V. CONCLUSION

Our results show that careful selection of electrode location is more important than having a dense map of electrodes. Dry systems are more sensitive to interference and their signal-to-noise quality is low. Nevertheless, with an appropriate sensor selection process and feature extraction, their classification performance can increase. This would make EEG systems user-friendly and more reliable. Future work should focus on how to dynamically select the optimum EEG sensor configuration.

REFERENCES

1. Jeannerod, "The representing brain: neural correlates of motor intention and imagery," Behavioral and Brain Sciences , vol. 17, pp. 187-245, 1994.
2. T. Hanakawa, I. Immisch, K. Toma, M. Dimyan, P. Van Gelderen and M. Hallett, "Functional Properties of Brain Areas Associated With Motor Execution and Imagery," Journal of Neurophysiology, vol. 89, pp. 989-1002, 2003.
3. S. Page, P. Levine, S. Sisto and M. Johnston, "A randomized efficacy and feasibility study of imagery in acute stroke," Clinical Rehabilitation, vol. 15, p. 233–240, 2001.
4. Bakker, J. Stevens, I. Toni and B. Bloem, "Motor imagery of gait: a quantitative approach," Experimental Brain Research, vol. 179, pp. 497-504, 2007.
5. R. Dickstein, E. Marcovitz and A. Dunsky, "Motor Imagery for Gait Rehabilitation in Post-Stroke Hemiparesis," Physical Therapy, vol. 84, p. 1167–1177, 2004.
6. K. Oostra, G. Vanderstraeten and G. Vingerhoets, "nfluence of motor imagery training on gait rehabilitation in sub-acute stroke: A randomized controlled trial," J Rehabil Med, vol. 47, pp. 204-209, 2015.
7. Z. Wang, C. Wang, G. Wu, Y. Luo and X. Wu, "A Control System of Lower Limb Exoskeleton Robots Based on Motor Imagery," in International Conference on Information and Automation (ICIA), Macau, China, 2017.
8. Navarro, B. Hubais and F. Sepulveda, "A Comparison of Time, Frequency and ICA Based Features and Five Classifiers for Wrist Movement Classification in EEG Signals," in Engineering in Medicine and Biology Society, Shanghai, China, 2005.
9. F. Ghani, H. Sultan, D. Anwar, O. Farooq and Y. Khan, "Classification of Wrist Movements Using EEG Signals," Journal of Next Generation Information Technology (JNIT), vol. 4, pp. 29-39, 2013.
10. G. Pfurtscheller, C. Neuper, G. R. Müller, B. Obermaier, G. Krausz, A. Schlögl, R. Scherer, B. Graimann, C. Keinrath, D. Skliris, M. Wörtz, . G. Supp and C. Schrank, "Graz-BCI: state of the art and clinical applications," IEEE Transactions on Neural Systems and Rehabilitation Engineering, vol. 11, no. 2, pp. 1- 4, 2003.
11. D. H. Brainard, "The Psychophysics Toolbox," Spatial Vision, vol. 10, pp. 433-436, 1997.
12. D. G. Pelli, "The VideoToolbox software for visual psychophysics: transforming numbers into movies.," Spatial Vision, vol. 10, pp. 437- 442, 1997.
13. Kleiner, D. Brainard, D. Pelli, A. Ingling, R. Murray and C. Broussard, "What's new in psychtoolbox- 3," Perception, vol. 36, pp. 1-16, 2007.
14. Y. Renard, F. Lotte, G. Gibert, Congedo M., E. Maby, V. Delannoy, O. Bertrand and A. Lécuyer, "OpenViBE: An Open-Source Software Platform to Design, Test and Use Brain-Computer Interfaces in Real and Virtual Environments," Presence : teleoperators and virtual environments, vol. 19, 2010.
15. J. Andreu-Perez, F. Cao, H. Hagras and G. Yang, "A Self-Adaptive Online Brain Machine Interface of a Humanoid Robot through a General Type-2 Fuzzy Inference System," IEEE Transactions on Fuzzy Systems, no. 99, p. 1, 2016.

Autonomous robot navigation using GPU enhanced neural networks

Norbert Domcsek, James Knight, Thomas Nowotny
School of Engineering and Informatics, University of Sussex, Brighton, UK, nd234@sussex.ac.uk,
J.C.Knight@sussex.ac.uk, T.Nowotny@sussex.ac.uk

ABSTRACT

One of the many potential applications of autonomous robotics is to explore hazardous environment, or example in the wake of a natural disaster. Existing systems have to be controlled remotely which restricts their range and makes them vulnerable to signal latency and loss. Here, we present an autonomous wheeled robot controlled by a spiking neuron network that implements a visual obstacle avoidance behavior. We simulate this network using our GeNN simulator running on an NVIDIA Jetson Tx1 device, which enables thousands of neurons to be simulated in real time at very low power. We demonstrate the robot's performance in a range of experiments.

I. INTRODUCTION

One of the most researched areas of robotics is the autonomous exploration of unknown or dangerous places like in deep-sea and extra-terrestrial planet exploration. Navigation is a difficult problem in these applications because GPS data may be inaccurate or not available, the locations of the objects in the environment are unknown and remote control may not be available due to extreme delays or no signal at all. Therefore, there is a need for robots, which can act and explore the environment autonomously. Existing implementations for navigation include SLAM methods [1], which exploit sensor fusion using a probabilistic approach. Obstacle detection also has been achieved using optical flow [2], lasers [3], stereo cameras [4], and IR sensors [5]. Here we present a method for obstacle avoidance based on a spiking neural network. Spiking neural networks (SNN) represent a special class of artificial neural networks in which the neurons communicate with discrete spike events. Their similarity to biological neural circuits enable both, the analysis of certain, peripheral brain circuits and to equip robots with similar brain-like controllers. There are a number of advantages to this approach. Information is processed asynchronously in an event driven way, which can greatly simplify simulating large networks [7] in real-time.

We can also harness the power of massively parallel systems and SNN are not fragile in the presence of sensory noise. Cope et al. [6] already developed a flying drone controlled by a spiking neural network, but the computations were performed on a separate workstation, which limits mobility and usability outside the laboratory. Here, we designed a 2-wheeled robot (Figure 1.), equipped with sensors of different modalities and on-board GPU acceleration, which allows to simulate the SNN in real-time, making the robot completely self-contained.

II. METHODS

A. Hardware

Our robot was designed to allow modularity and extra sensors to be added. We equipped the robot with a Jetson Tx1 board (NVIDIA) which is a credit-card sized computer with integrated GPU accelerator. The GPU of this computer has 256 cores, which is powerful enough to run large neural networks and heavy image processing in real time with low power requirements. The robot uses a web-camera for visual input and is controlled with an Arduino Uno. A prototyping board on the Arduino allows extra sensors to be added. The Jetson Tx1 and the Arduino Uno are connected with an I2C bus, which provides about 100kbps data transfers.

B. Visual obstacle avoidance

The robot receives its input from the webcamera in the form of a stream of RGB images. These images are then pre-processed and input into the neural network. Based on the spike frequency in the output neurons, we steer the robot into left, right or forward directions. The pre-processing stage aims to convert the input images to intensity values which can be used as inputs to the neural network. These steps produce a low-resolution image of the outline of an object, with the static background removed (Figure 1. B). The pre-processing using the following steps. We convert images to gray-scale and perform histogram equalization. After Gaussian- smoothing and downscaling to 32x32 pixels we eventually perform a frame subtraction of temporally adjacent frames to extract the outlines of an object.

C. Neural network structure

For this research, we have used the Leaky Integrate-and-Fire neuron (LIF) model as it is a simple and fast neuron computation model. The neurons connect to each other with synapses that transmit discrete spike events. Excitatory inputs increase the membrane voltage while inhibitory inputs decrease it. If the incoming signal increases the membrane voltage above the threshold, the neuron will fire and its membrane voltage will be reset. The simulation was implemented in the GeNN (GPU Enhanced Neural Network) simulator [8, 9] which allows neural network simulation with different neuron parameters on the GPU. We simulated 1024 LIF neurons in the visual input layer using pre-processed images where we mapped the pixel intensity values to the individual neurons, 8 LIF neurons in the middle filtering layer which aimed to reduce high frequency spatial noise, and finally 2 LIF neurons in the motor control layer. The input neurons connected to the filter neurons with excitatory synapses. The weights of the synapses were set stronger in the middle of the images and weaker at the edges to ensure faster turning if the obstacle is in front of the robot. The morphology of the network is illustrated in Figure 1. C. The network aims to recognize vertical and horizontal line shapes in the input image. Given enough neuron activations in one or more of these regions, the filter layer activates the motor neurons, which decide the direction to steer.
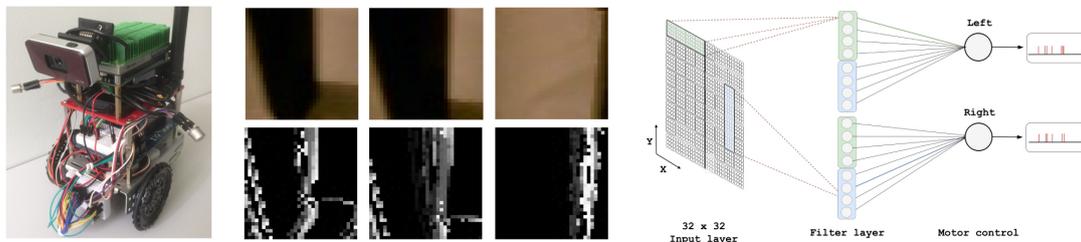

Figure 1. (A) The robot. (B) Obstacle from the view of the robot before (upper row) and after pre-processing (lower row). The pre-processed image is input to the neural network (C). The network recognizes vertical and horizontal shapes and activates the motor control neurons to steer away from obstacles.

III. RESULTS

To test the obstacle avoidance feature, we created an obstacle course and ran experiments. 4 tests were done each for 10 minutes using a different network setup and different kind of obstacles. The obstacles were either tall with a long vertical edge, or low with a long horizontal edge. In the tests, we examined the performance of the network when disabling its horizontal feature detector and when enabling it. In trial 1, we disabled horizontal feautres and used low obstacles. In trial 2, we enabled horizontal connections with low obstacles. In trial 3 and 4 we used high obstacles with vertical, then with vertical and horizontal features respectively. Based on the results, we concluded that the robot can avoid obstacles with long vertical edges using a network with only vertical feature detectors, but in order to avoid a wider range of obstacles, both horizontal and vertical features should be enabled. The trials are shown on Figure 2 where we draw the robot's trajectory and indicate whether the robot collided.

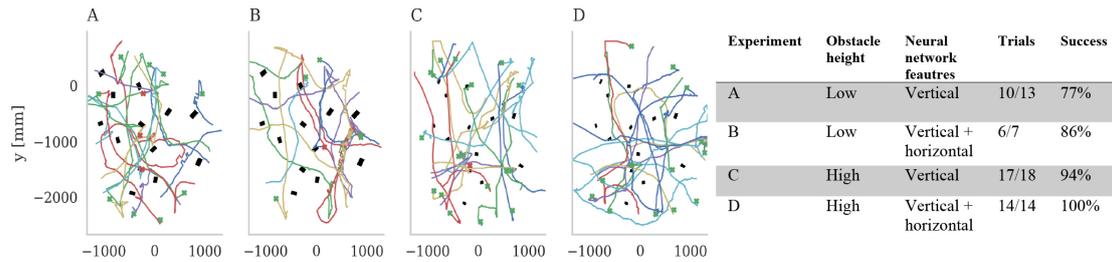| Experiment	Obstacle height	Neural network feautres	Trials	Success
A	Low	Vertical	10/13	77%
B	Low	Vertical + horizontal	6/7	86%
C	High	Vertical	17/18	94%
D	High	Vertical + horizontal	14/14	100%

Figure 2. Obstacle avoidance in an arena. The green crosses indicate a success and red crosses indicate where the experiment was terminated due to collision with an obstacle. The coloured lines are the trajectories of the robot. The rectangle shaped black markers indicate the position and the orientation of an obstacle. Wider black markers (A,B) represent lower obstacles and smaller markers (C, D) high, vertical obstacles. The table on the right shows the performance of the experiments with different parameters.

ACKNOWLEDGMENTS

REFERENCES

1. Leonard, J.J. and Durrant-Whyte, H.F., 1991, November. Simultaneous map building and localization for an autonomous mobile robot. In *Intelligent Robots and Systems' 91.'Intelligence for Mechanical Systems, Proceedings IROS'91. IEEE/RSJ International Workshop on* (pp. 1442-1447). Ieee.

2. Souhila, K., & Karim, A. (n.d.). Optical Flow Based Robot Obstacle Avoidance. International Journal of Advanced Robotic Systems, 4(1), International Journal of Advanced Robotic Systems, 2007, Vol.4(1).

3. Martinez, J., Pozo-Ruz, A., Pedraza, S., & Fernandez, R. (1998). Object following and obstacle avoidance using a laser scanner in the outdoor mobile robot Auriga-/spl alpha/. *Intelligent Robots and Systems, 1998. Proceedings., 1998 IEEE/RSJ International Conference on, 1*, 204-209.

4. Lagisetty, Philip, Padhi, & Bhat. (2013). Object detection and obstacle avoidance for mobile robot using stereo camera. Control Applications (CCA), 2013 IEEE International Conference on, 605-610.

5. Gacsadi, V. Tiponut, I. Gavrilut, & L. Tepelea. (2008). Obstacles Avoidance Method for an Autonomous Mobile Robot using Two IR Sensors. Journal of Electrical and Electronics Engineering, 1(1), 194-197.

6. Cope, A., Sabo, C., Gurney, K., Vasilaki, E., Marshall, J., & Ayers, J. (2016). A Model for an Angular Velocity- Tuned Motion Detector Accounting for Deviations in the Corridor-Centering Response of the Bee. *PLoS Computational Biology, 12*(5), PLoS Computational Biology, 2016, Vol.12(5).

7. Watts, L., 1994. Event-driven simulation of networks of spiking neurons. In *Advances in neural information processing systems* (pp. 927-934).

8. Yavuz, J. Turner and T. Nowotny (2016). GeNN: a code generation framework for accelerated brain simulations. Scientific Reports 6:18854. doi: 10.1038/srep18854 2.

9. GeNN, http://genn-team.github.io/genn/, accessed 2016-05-04

Wireless Power Transfer for Gas Pipe Inspection Robots

Viktor Doychinov∗, Bilal Kaddouh∗, George Mills∗, Bilal Malik∗, Nutapong Somjit∗, Ian D Robertson ∗Robotics at Leeds, University of Leeds, Leeds, United Kingdom

ABSTRACT

Wireless power transfer in metal pipes is a promising alternative to tethered exploration robots, with strong potential to enable longer operating times. Here we present experimental results, including rectification efficiency, for a prototype gas pipe inspection robot with wireless power receiver functionality.

Index Terms
Wireless Power Transfer, Gas Pipe, Remote Inspection, Autonomous Systems, Robotics

I. INTRODUCTION

The use of high-power electromagnetic (EM) waves for Wireless Power Transmission (WPT) has been studied since the late 19th century [1], with arguably one of the most famous demonstrators being the "Microwave Powered Helicopter" by W. C. Brown [2]. The two main modalities investigated by the research community are near-field non-radiative power transfer, such as magnetic, inductive, and capacitive coupling; and far-field power transfer through highly directional antennas [3], [4].

The near-field methods have successfully been adopted in commercial products for efficient charging of consumer electronics. With the increased popularity of Electric Vehicles (EV) concepts have been proposed for their continuous charging via capacitive coupling systems [5]. The main disadvantage of the near-field method of power transfer is the short maximum operating distance, which is on the order just a few centimetres [6]. On the other hand, far-field systems suffer from large propagation losses through atmospheric attenuation and absorption, limiting the amount of power that can be delivered to a receiver [7]. Furthermore, regulations on transmitted power in the Industrial, Scientific, and Medical (ISM) bands further limit the potential deployments of such systems to low-powered Internet-of-Things sensors [8]–[10].

Recently, another mode of WPT has been proposed, and that is WPT in shielded metal pipes, which can potentially deliver higher power, on the order of several Watts, at distances up to tens of metres [11]. This is enabled by considering the pipes as circular waveguides, which support low-loss EM propagation [12]. This in turn opens up exciting opportunities for remote powering and charging of pipe inspection robots, eliminating the need for a tethered power connection.

In this paper, we present experimental results of WPT to a small robot, designed to fit in and inspect 25.4 mm diameter gas pipes. Details of the robot prototype are given, as well as measurements of the electromagnetic propagation environment within the pipe used for these tests. Finally, a short discussion on the WPT module performance is included.

II. SCENARIO DESCRIPTION AND ROBOT PROTOTYPE

A photograph showing the experimental setup is given in Fig. 1a. The pipe used is a decommissioned 2 metre long cast iron pipe. A Keysight E8267D Vector Signal Generator is used to provide the EM signal, which can then be coupled to the pipe through a standard gain horn antenna, as shown in Fig. 1d.
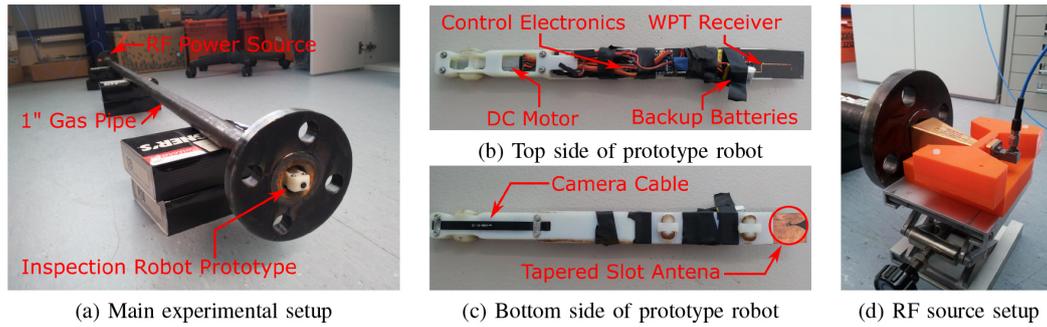
(a) Main experimental setup   (c) Bottom side of prototype robot   (d) RF source setup

(b) Top side of prototype robot

Fig. 1: Pipe measurement setup, including prototype robot and method of supplying RF power.

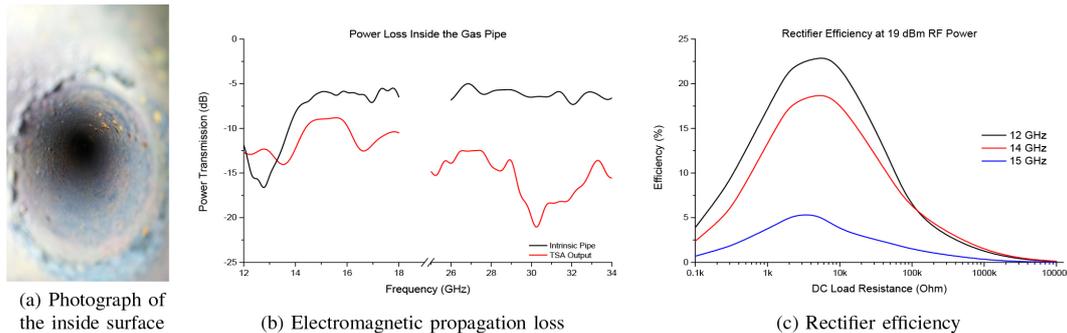(a) Photograph of the inside surface   (b) Electromagnetic propagation loss   (c) Rectifier efficiency

Fig. 2: Overview of the electromagnetic performance of the measurement setup.

In this scenario, the aim is to deliver as much power as possible when the robot is at the far end of the pipe, with input RF power limited by the capabilities of the E8267D.

The details of the robot prototype are presented in Fig. 1b and Fig. 1c. The body of the robot is 3D printed as a whole using a Stratasys Objet1000 Multi-Material 3D printer, and houses the MCU (Pololu Baby Orangutan), a single brushed DC motor, backup batteries (2 x 3.7 V 100 mAh LiPo), as well as a night-vision camera. The robot also includes the WPT module, which is discussed in Section III.

III. PIPE PROPAGATION MEASUREMENTS AND WPT MODULE

As mentioned earlier, metal pipes act as circular waveguides from an EM propagation point of view. The lowest cut-off frequency, i.e. the frequency below which propagation in the waveguide cannot occur, is an important parameter of any waveguide, and is dependent on its diameter. For the pipe used in this experiment, this was found to be 6.922 GHz [13].

Furthermore, the assumption for low loss is dependent on the surface roughness of the inside of the pipe being low [14]. In the case of the cast iron pipe used in this paper, this was found to not be the case, as illustrated by Fig. 2a. The propagation loss inside the pipe was then measured using a Keysight N5247 PNA-X, resulting in Fig. 2b. Loss results are shown both for the pipe on its own, as well as a composite loss when a Tapered Slot Antenna (TSA) [15] is used at the receiver end. The frequency ranges for which data is presented correspond to those for which horn antennas were available at the time of the experiments. Once the total propagation losses are known, and the RF input power level can be calculated, an RF- to-DC rectifier can be designed. It has been shown that the efficiency of a rectifier is a function of input power level, frequency, input impedance, and DC load resistance [16]. It is also dependent on the type of semiconductor element used, i.e. a diode or a transistor, as well as overall circuit topology [7], [16]. For the WPT receiver used with the prototype robot, an 8-stage voltage doubler topology was thus selected, using commercially available low-barrier Schottky diodes (Avago HSMS-286C). The circuit was implemented on a low-loss PTFE substrate (Duroid 5880), with a TSA used to couple the incoming EM energy to the rectifier. The output of the rectifier can then be connected to a voltage regulator and a battery charging circuit,

although physical space might become an issue. Details of the rectifier circuit are included in Fig. 1b and Fig. 1c.

The rectifier, as well as the TSA, were designed with dual-band operation in mind, with the bands being Ku-band (12 GHz − 18 GHz) and Ka-band (26.5 GHz − 40 GHz). Rectification efficiency, defined as $\eta = P_{DC}/P_{RF}$, was found to be better for lower frequencies, with best performance (23%, 18 mW P_{DC}) obtained at a frequency of 12 GHz and 19 dBm of RF power at the input of the rectifier. A comparison between several frequencies in the Ku-band for different DC load resistances is presented in Fig. 2c.

I.V. CONCLUSION

Experimental results on EM propagation in a metal pipe, as well as WPT for powering and charginG of a prototype robot have been presented and discussed. We have successfully demonstrated RF-to-DC rectification with up to 23% efficiency at the end of a 2 metre long gas pipe, which can be used to extend the operating lifetime of an autonomous inspection robot.

REFERENCES

1. Shinohara, *Wireless power transfer via radiowaves*. Wiley, 2013.
2. W. C. Brown, "The Microwave Powered Helicopter," *The Journal of Microwave Power & Electromagnetic Energy*, vol. 1, no. 1, 1966.
3. Borges Carvalho, A. Georgiadis, A. Costanzo, H. Rogier, A. Collado, J. A. Garcia, S. Lucyszyn, P. Mezzanotte,
4. J. Kracek, D. Masotti, A. J. S. Boaventura, M. de las Nieves Ruiz Lavin, M. Pinuela, D. C. Yates, P. D. Mitcheson, M. Mazanek, and V. Pankrac, "Wireless Power Transmission: R&D Activities Within Europe," *IEEE Transactions on Microwave Theory and Techniques*, vol. 62, no. 4, pp. 1031–1045, 4 2014. [Online]. Available: http://ieeexplore.ieee.org/document/6734736/
5. Cost Action IC1301 Team, "Europe and the Future for WPT : European Contributions to Wireless Power Transfer Technology,"
6. *IEEE Microwave Magazine*, vol. 18, no. 4, pp. 56–87, 6 2017. [Online]. Available: http://ieeexplore.ieee.org/document/7920430/
7. H. Zhang, F. Lu, H. Hofmann, W. Liu, and C. C. Mi, "A Four-Plate Compact Capacitive Coupler Design and LCL-Compensated Topology for Capacitive Power Transfer in Electric Vehicle Charging Application," *IEEE Transactions on Power Electronics*, vol. 31, no. 12, pp. 8541–8551, 2016.
8. J. Dai and D. C. Ludois, "A Survey of Wireless Power Transfer and a Critical Comparison of Inductive and Capacitive Coupling for Small Gap Applications,"
IEEE Transactions on Power Electronics, vol. 30, no. 11, pp. 6017–6029, 2015.
9. Z. Popovic, "Cut the Cord: Low-Power Far-Field Wireless Powering," *IEEE Microwave Magazine*, vol. 14, no. 2, pp. 55–62, 2013.
10. Ofcom, "UK Interface Requirement 2005," 2006. [Online]. Available: http://stakeholders.ofcom.org.uk/spectrum/technical/ interface-requirements/
11. ——, "UK Interface Requirement 2006," 2006. [Online]. Available: http://stakeholders.ofcom.org.uk/spectrum/technical/ interface-requirements/
12. ——, "UK Interface Requirement 2007," 2007. [Online]. Available: http://stakeholders.ofcom.org.uk/spectrum/technical/ interface-requirements/
13. ITU-R, "SM.2392-0 Applications of wireless power transmission via radio frequency beam," Geneva, Tech. Rep., 2016. [Online]. Available: http://www.itu.int/pub/R-REP-SM.2392-2016
14. M. Pozar, *Microwave engineering*, 4th ed. Wiley, 2012.
15. N. Marcuvitz and Institution of Electrical Engineers. *Waveguide handbook*.
16. K. Chang, *Encyclopedia of RF and microwave engineering*. John Wiley, 2005.
17. J. L. Volakis, *Antenna engineering handbook*, 4th ed. McGraw-Hill, 2007.
18. R. Valenta and G. D. Durgin, "Harvesting Wireless Power: Survey of Energy-Harvester Conversion Efficiency in Far-Field, Wireless Power Transfer Systems," *IEEE Microwave Magazine*, vol. 15, no. 4, pp. 108–120, 2014.

Graphical Signage Decreases Negative Attitudes towards Robots and Robot Anxiety in Human-Robot Co-working

Iveta Eimontaite1, Ian Gwilt3, David Cameron1, Jonathan M. Aitken1, Joe Rolph2, Saeid Mokaram1, James Law11 Sheffield Robotics, The University of Sheffield, UK, 2 Art & Design Research Centre, Sheffield Hallam University, UK, 3 School of Art, Architecture and Design, University of South Australia, Australia

ABSTRACT

To achieve full potential of collaborative robots, human operators need confidence in robotic co-worker technologies and their capacities. We compare the impact of dynamic signage with static signage on the human-robot collaboration task performance. The results provide evidence that dynamic signage resulted in a significant decrease of NARS scores and static signage in a decrease of RAS scores after the interaction with the robot.

Keywords: Human–Robot Collaboration · Static and Dynamic Graphical Signage · Negative Attitudes towards Robots · Robot Anxiety Scale · Manufacturing · Efficiency

I. INTRODUCTION

The UK's manufacturing sector is the 8th largest in the world. It accounts for 44% of UK exports, contributes 10% to GVA, and employs 2.6m people[1], yet the sector is poised to undergo considerable change with Industry 4.0. One of the biggest changes will be to automation, with emergence of collaborative robotics [1], which will transform the way people work with machines. To be successfully integrated, this new technology will have to gain trust and acceptance of the human workforce.

Industrial robots, although not a new phenomenon, can still feel threatening to human workers, which can lead to higher stress levels [2, 3]. This is of particular significance to collaborative robots where workers will be required to work with, and around, active uncaged robots. Acceptance and trust have both been identified by industry partners as major challenges facing deployment of collaborative robots, and the issues are exacerbated if users feel they do not have enough information or training on the technology. Effective information communication can aid human–robot interaction, graphical signage, in particular, has benefits for manufacturing including: not requiring individuals to have prior experience in signage [4, 5], being language invariant [6], not being impeded by noisy environments, and reducing cognitive load [7].

Previous results from the studies conducted by our lab show that the presence of signage can increase efficiency and participant well-being [8, 9]. In this paper we present preliminary results comparing the effects of static and dynamic signage on participants' negative attitudes and anxiety towards robots.

I. METHODS

Participants and graphical signage. The current analysis concerns two groups of participants: The first group of participants (University of Sheffield students and staff (N

_____

= 30)) were presented with static signage developed in accordance to ISO conventions [10]. The signs illustrated human–robot interaction events, such as the force required to manually manipulate the robot, and the robot's speed. The second group contained shop-floor workers with no experience in working with robot from an industrial partner (N = 21).

These participants were presented with screen-based dynamic graphical signage, which had been refined from the static signage during co-creation workshops with a separate group of industry employees. This signage provided real-time information about robot operational processes, i.e. when to manually manipulate the robot and when not to touch it. The work was approved by the University of Sheffield Ethics Committee.

Procedure, task and measures. Static signage trials were conducted in a laboratory setting designed to resemble an industrial work cell, whilst dynamic signage trials were conducted in a factory environment. The procedure and task for both groups were identical.

Prior to the task, participants signed a consent form, and filled in: a questionnaire measuring their demographic information, an experience with robots questionnaire [11], a sub-scale measuring anxiety towards the behavioural characteristics of robots from the Robot Anxiety Scale (RAS, [12]), and a subscale of attitudes towards interaction with robots from the Negative Attitudes towards Robots Scale (NARS, [13]). Participants then interacted with a robot on a collaborative task. The task consisted of 16 narrow tubes positioned vertically on a workbench, with 6 containing M5 bolts. The tubes were too narrow to extract bolts by hand, instead requiring use of the robot (a KUKA LBR iiwa 7 R800) with an attached magnetic probe.

The robot had been pre-programmed with the location of the tubes, but had no means of sensing the locations of the 6 bolts. Therefore, in order to complete the task, participants needed to co-work with the robot by manually positioning the end effector near a tube containing a bolt; the robot would then refine its position, based on the closest tube position, and extract the bolt. Participants were provided with no other verbal information on the robot's operational abilities, and their accuracy (collected bolts/number of trials) was measured during the interaction with the robot. After having completed the task (or after 10 minutes if not) participants once again filled in RAS and NARS scales. The whole experiment lasted around 30 minutes.

III. RESULTS

Both groups of participants did not significantly differ in their experience with robots, $D(50) = 1.29$, $p = .072$ (static M = 17.03, SD = 8.33; dynamic M = 10.48, SD = 4.90). The comparison of accuracy rates between static and dynamic signage participants showed no significant difference, $t(48.9) = -0.34$, $p = .738$, Fig 1A.

Further analysis investigated the effects of the two types of signage on the attitudes (NARS) and anxiety towards robots (RAS). The change in the NARS and RAS scores were calculated by subtracting pre-interaction from post-interaction scores.

Moderated regression with an outcome of NARS Change, predictor of Accuracy, and moderator of Signage (dynamic vs. static) showed that this model was significant in predicting NARS Change ($F(3, 47) = 3.90$, $p = .014$, $R^2 = .20$). Examination of moderators showed a significant effect of interaction NARS Change by Accuracy for dynamic signage ($t = -2.76$, $p = .008$, $b = -7.77$; Fig 1 B). The same interaction with static signage was not significant ($t = -1.71$, $p = .094$, $b = -2.87$). Further analysis with a predictor of Accuracy, outcome RAS Change, and moderator of Signage showed the model was approaching significance ($F(3, 47) = 2.70$, $p = .056$, $R^2 = .15$). Static signage as a moderator showed a significant interaction of RAS Change by Accuracy ($t = -2.69$, $p = .010$, $b = -6.22$; Fig 1 C) while with dynamic signage RAS Change was not affected by the Accuracy ($t = -0.91$, $p = .366$, $b = -3.54$)
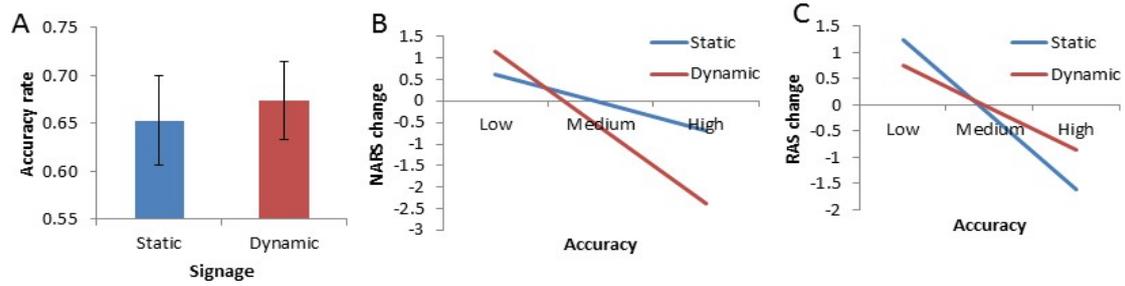
Figure 1: (A) Accuracy rates in static signage and dynamic signage participant groups; (B) Change in Negative Attitudes towards Robots (NARS) scores as a function of Accuracy moderated by the Signage; (C) Change in Robots Anxiety Scale (RAS) scores as a function of Accuracy moderated by the Signage.

I.V. DISCUSSION

This work investigated the differences between static and dynamic graphical signage on participants' negative attitudes and anxiety towards robots in a collaborative task. The findings showed that although groups did not differ in their accuracy, moderated regression analysis suggested that signage can decrease negative attitudes and anxiety towards robots after the interaction as a function of increasing accuracy. Dynamic signage participants showed a significant decrease in NARS scores, and static signage resulted in decrease in RAS scores. As participants did not differ in their experience with robots and analysis used the change between participants' pre- and post-interaction scores, such finding suggests differential signage effect. This is crucially important while working to increase trust and acceptance of robots in manufacturing. While

NARS and RAS scores are known to correlate [14], the differential effects of signage on these scales need to be investigated further.

"Social" aspects of human-robot collaboration in manufacturing are still largely understudied, and, even then, the majority of these studies concentrate on trained robotics users. Our study is contributing to the existing literature by investigating low skilled workforce. Further strength lies in higher ecological validity as work was conducted in factory environment. Taken together, the results indicate that, by involving workforce in the technology development and integration in the workplace, we increase their acceptance of new processes, and by communicating information about robot we have improved robot user's comfort.

REFERENCES

1. Executive Summary World Robotics 2016 Industrial Robots. International Federation of Robotics (IFR) (2016)

2. Mathews, A., Mackintosh, B.: A cognitive model of selective processing in anxiety. Cogn. Ther. Res. 22, 539–560 (1998)

3. Ozer, E.M., Bandura, A.: Mechanisms governing empowerment effects: a self-efficacy analysis. J. Pers. Soc. Psychol. 58, 472 (1990)

4. Tufte, E.R.: The visual display of quantitative information. Graphics Press, Connecticut (1993)

5. Frixione, M., Lombardi, A.: Street Signs and Ikea Instruction Sheets: Pragmatics and Pictorial Communication. Rev. Philos. Psychol. 6, 133–149 (2015).

6. Ben-Bassat, T., Shinar, D.: Ergonomic Guidelines for Traffic Sign Design Increase Sign Comprehension. Hum. Factors J. Hum. Factors Ergon. Soc. 48, 182–195 (2006).

7. Lamont, D., Kenyon, S., Lyons, G.: Dyslexia and mobility-related social exclusion: the role of travel information provision. J. Transp. Geogr. 26, 147–157 (2013).

8. Eimontaite, I., Gwilt, I., Cameron, D., Aitken, J.M., Rolph, J., Mokaram, S., Law, J.: Assessing Graphical Robot Aids for Interactive Co-working. In: Schlick, C. and Trzcieliński, S. (eds.) Advances in Ergonomics of Manufacturing: Managing the Enterprise of the Future. pp. 229–239. Springer International Publishing, Cham (2016)

9. Eimontaite, I., Gwilt, I., Cameron, D., Aitken, J., Rolph, J., Mokaram, S., Law, J.: Dynamic Graphical Signage Improves Response Time and Decreases Negative Attitudes towards Robots in Human-Robot Co-working. In: Proceedings of the 10th International Workshop on Human-Friendly Robotics (2017)

10. ISO 3864-1: Graphical symbols - Safety colours and safety signs -Part 1: Design principles for safety signs and safety markings.

11. MacDorman, K.F., Vasudevan, S.K., Ho, C.-C.: Does Japan really have robot mania? Comparing attitudes by implicit and explicit measures. AI Soc. 23, 485–510 (2009).

12. Nomura, T., Suzuki, T., Kanda, T., Kato, K.: Measurement of anxiety toward robots. In: Robot and Human Interactive Communication, 2006. ROMAN 2006. The 15th IEEE International Symposium on. pp. 372–377. IEEE (2006)

13. Nomura, T., Suzuki, T., Kanda, T., Kato, K.: Measurement of negative attitudes toward robots. Interact. Stud. 7, 437–454 (2006)

14. Nomura, T., Kanda, T., Suzuki, T., Kato, K.: Prediction of Human Behavior in Human--Robot Interaction Using Psychological Scales for Anxiety and Negative Attitudes Toward Robots. IEEE Trans. Robot. 24, 442–451 (2018).

Designed on computers, built by robots

Hatem Fakhruldeen, Anthony Pipe and Farid Dailami

I. INTRODUCTION

The demand in today's manufacturing for small batch production and more customization has raised, due to market and consumer demands [1], raised the need for flexible assembly systems. Additionally, 20%- 50% of the total production time and 20%-30% of the total production cost is typically spent on product assembly [2]. Thus, lots of research has been done to utilize the flexibility and versatility provided by robots to build a flexible robotic assembly (RA) system. Our work tries to build on that and integrate the different components of RA, in order to build a system that combines both assembly can be roughly divided into RA planning methods, and RA execution methods. In e current state of art, many of these methods still need improvement in terms of performance and reliability. Moreover, these publications were focused on very specific RA tasks or only operated in simulation. None of the reviewed works attempted to combine planning and execution in a practical system, therefore this represents the next step in advancing the research.

This research tries to take an initial step towards that by building a system that combines both RA planning and
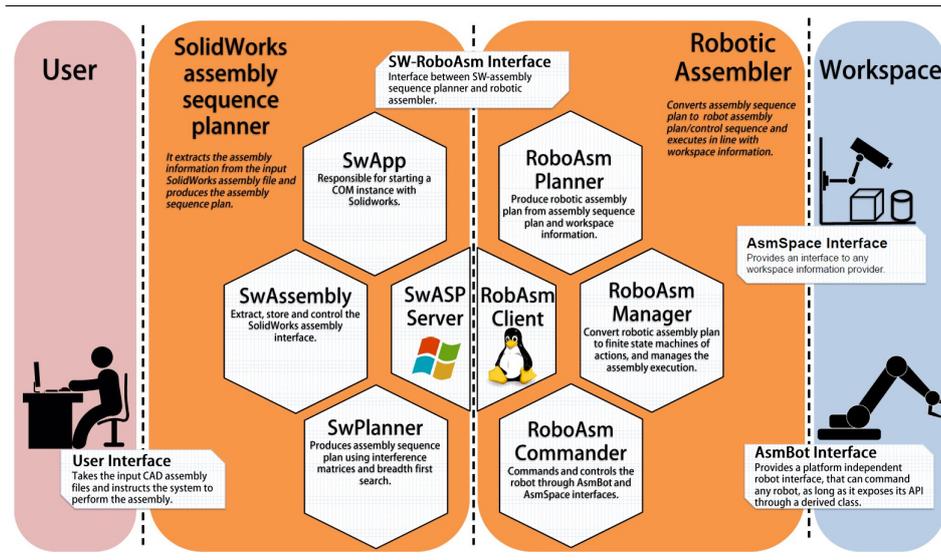

Figure 1: The developed RA system overall architecture.

planning and execution. The system would take assembly CAD information as input, and produce the assembled objects as an output on the other end.

Research in the area of RA is vast and diverse, since it involves many disciplines, considerations and methods. However, it execution in one complete architecture that takes only assembly CAD designs on one end, and produces the assembled objects on the other end, without any human involvement in between. This system takes Solidworks[3] CAD assembly files as input through the provided interface, and on the other end

*Bristol robotics laboratory, university of west of England

pro- duces the assembly by commanding the robotic system and sensors through the 'AsmBot' and 'AsmSpace' modular interfaces respectively. This architecture is illustrated in figure 1.

The first component in our architecture is the Assembly Sequence Planner (ASP) module. It first extracts the assembly information from the input Solidworks assembly file by means of the 'swAssembly' submodule; and then the 'swPlanner' submodule produces the assembly sequence plan, using interference matrices, mating information and col- lision detection[4],[5]. Finally the 'ASP server' submodule starts a server, so that this information can be shared with multiple RA planners running on different platforms. The ASP was developed using Solidworks C++ API.

The robotic assembler module communicates with 'ASP server', to retrieve the assembly sequence plan and other information extracted from the CAD model, with the help of 'ASP client'. Moreover, it can retrieve the assembly workspace information, such as objects' locations, poses, workspace obstacles, etc., from the external sensory systems through the 'AsmSpace' interface. The RA tasks plan is then produced from this information in the 'RA planner' submodule and sent to the 'RA manager' which translates each task into a finite state machine (FSM) composed from skills, which are also FSMs composed from elementary actions. This is similar to the works [6] and [7].

Finally, to give the system the ability to execute with different robots 'AsmBot' interface was developed that translates robot elementary actions to the specifiedrobotAPI commands. This allows changing the assembly robot without the need to modify any of the other modules or worry about programming. Similarly, 'AsmSpace' interface was implemented to allow changing/adding sensors to the system effortlessly. The RA Commander executes the RA plan, monitors its progress, and provides updates to the user through the 'ASP client' interface.

All these modules were completed and the whole system was tested in a series of experiments that involved simple assemblies composed from peg in a hole mates. These experiments illustrated our system functionality and its potential as a complete RA system. The robotic assembler was implemented using C++ and ROS. In addition, the 'AsmBot' and 'AsmSpace' interfaces were used to command a UR5 robotic arm with a Robotiq85 gripper and to retrieve the parts workspace information from Pickit3D vision system respectively. In the current implementation, only position control was used. The next steps involve improving the ASP capabilities to deal with more complex assemblies and equipping it with an optimizer to produce better plans. Finally, once that is completed, the system will be tested in an industrial assembly to illustrate its complete potential as a fully automated flexible assembly system.

REFERENCES

1. N.F. Edmondson and A.H. Redford, "Generic flexible assembly system design," *Assembly Automation*, vol. 22, pp. 139–152, June 2002.

2. L. D. Xu, C. Wang, Z. Bi, and J. Yu, "AutoAssem: An Automated Assembly Planning System for Com- plex Products," *IEEE Transactions on Industrial Informatics*, vol. 8, pp. 669–678, Aug. 2012. General Framework.

3. S. Corporation, *SolidWorks user's manual*, 2015.

4. R. B. Hadj, M. Trigui, and N. Aifaoui, "Toward an integrated CAD assembly sequence planning solu- tion," *Proceedings of the Institution of Mechanical Engineers, Part C: Journal of Mechanical Engineering Science*, p. 0954406214564412, Dec. 2014. reviewed.

5. L.-M. Ou and X. Xu, "Relationship matrix based automatic assembly sequence generation from a CAD model," *Computer-Aided Design*, vol. 45, pp. 1053–1067, July 2013.

6. U. Thomas, G. Hirzinger, B. Rumpe, C. Schulze, and A. Wortmann, "A new skill based robot pro- gramming language using UML/P Statecharts," in *2013 IEEE International Conference on Robotics and Automation (ICRA)*, pp. 461–466, May 2013. Reviewed.

7. Butting, B. Rumpe, C. Schulze, U. Thomas, and A. Wortmann, "Modeling Reusable, Platform- Independent Robot Assembly Processes," *arXiv:1601.02452 [cs]*, Jan. 2016. Reviewed.

Bio-mimetic pneumatic soft prosthetic hand

Jan Fras and Kaspar Althoefer [*†]

ABSTRACT

Traditional prosthetic hand devices are rigid, heavy and expensive. In order to satisfy demanding manipulation tasks they require either sophisticated controlling strategies or complex mechanics. In this work we present a soft pneumatic prosthetic hand, which is not only very cheap in production, but also very simple to control due to its mechanical compliance. It can be very easily reshaped and resized in order to fit a particular patient needs. The aim of this research is to provide children patients with a device that can be frequently exchanged whenever a bigger size is needed or the device is broken. Due to its softness and compliance the device is mechanically safe even for very small children.

I. INTRODUCTION AND OBJECTIVE

As traditional rigid prosthetic hands have a number of draw- backs, soft robotics renders itself as a potential improvement of amputee people manipulation capabilities. Most important is that soft prosthetics can be significantly cheaper than a traditional one as it does not require neither sophisticated mechanical structure nor small and expensive electrical motors.

Thanks to that soft prosthetic can be especially suitable for young patients as their growth makes frequent prosthetic change a must. Other advantage is a soft prosthetic can be very easily controlled due to its compliance and adaptation capabilities. Even one degree of actuation may be sufficient for many grasping tasks.

A number of soft hands have been presented so far and they were also considered to be used as prosthetics [1–3]. They offer a similar morphology to a real human hand, however, their shape and appearance differ a lot from actual human limb. For that reason we propose a new soft prosthetic hand design that provides 6

Figure 1: Soft prosthetic hand

possible degrees of freedom including a motion corresponding with the base joint of the thumb, the carpometacarpal joint. Such a joint is designed to allow the thumb to work in both apposition and opposition modes, see Figure 1.

II. DESIGN

Hand

The hand design is based on a 3D scan of a real human hand in order to make it as bio-mimic as possible. It consists of 6 fluidic actuators, one per finger and two for the thumb, see Figure 2. The actuators are a hollow chambers with circular cross

section that tend to elongate when pressurized. They are constrained by an exoskeleton made of stiff silicone, so the translational expansion is transferred into bending motion of the fingers, see Figure 4. Unlike the real human hand in the presented device the bending motion of the fingers is distributed along their length as they are made of soft material and there are no discrete joints inside.

We shown in previous research that it is possible to achieve finite rotary joints using only soft materials [4], but we found such solution not applicable in that case due to excessive joint size and the need of using separate actuator for each joint. Using such actuators would make the design and the manufacturing unnecessarily too complex.
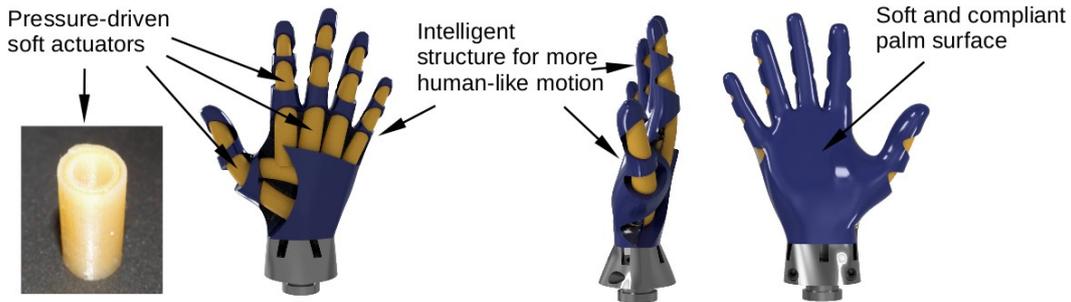
Figure 2: Structure of the hand

Actuator

As mentioned above, the actuators are pneumatic conical chambers that tend to elongate when pressurized. The diameter of each actuator varies depending on its length in order to fit the finger geometry and maximize the torque generated in the base finger joint. In order to constrain the radial expansion of the fingers a helical reinforcement made of a polyester thread is used. Such an actuation strategy has been already successfully embedded for manipulation, locomotion and grasping [4–6]. The bending of fingers in the desired direction has been achieved by combining the longitudinal expansion of the actuators with less flexible material on the internal side of the fingers and the palm surface. Each of the actuators can be controlled independently but due to their flexibility and compliance they can also efficiently work in groups. Such a property makes the dexterous manipulation less control-complex and allows the hand structure to take over part of the controller's effort.

Manufacturing

The manufacturing process is very much similar to the process described in [4–6]. It involves several sil- icone moulding steps and utilizes a set of 3D printed moulds. The materials used are two silicones of different stiffnesses and polyester thread used

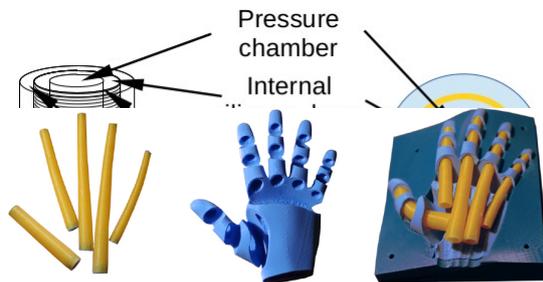for the reinforcement. The process starts with preparing the thread to be embedded

Figure 3: Structure of the actuator

into the fingers structure. The thread is winded tightly onto long conical cores. When wrapped the cores are enclosed within the mould and cast with soft silicone. The mould keeps them centred and creates a thin and uniform layer of silicone that bounds the reinforcing thread.

Figure 4: From the left, actuators, exoskeleton, parts of the hand in the main mould

As the rods diameter decrease with its length, the silicone layer with the thread inside can be easily removed from the rods towards the wider end, Figure 5

In the next stage a thin layer of silicone is added inside the actuators by filling them with silicone and inserting thinner rods.

Such layer protects the rein- forcing thread from detaching the initial structure when pressurized. The pre-prepared actuators and some auxiliary structures made of soft silicone are then arranged in a final mould that shapes the hand.
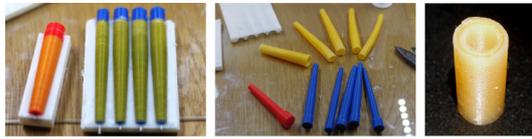

Figure 5: Actuators manufacturing: reinforcement, external layer, cross-section - reinforcement and internal layer visible.

The auxiliary structures help to provide more flexibility into the hand where required (e.g. in between the base - metacarpophalangeal - joint of each finger and the palm surface). When all the above is done, the mold is closed and the stiff silicone is injected into it that as the last manufacturing step.

III. CONCLUSIONS

Presented soft hand is an early prototype and has not been extensively tested yet. Nevertheless it shows high potential in terms of grasping capabilities and receives very positive feedback regarding its appearance and features. As the very next step we aim to conduct experiments to determine how the hand performs in different grasping tasks and how much grasping force it can generate.

We also consider hydraulic and pneumatic actuation. The goal of this research is to create prosthetic, but we will need to solve several issues before, including small and mobile yet powerful pressure source and a proper controlling interface.

REFERENCES

1. Raphael Deimel and Oliver Brock. A novel type of compliant and underactuated robotic hand for dexterous grasping. *The International Journal of Robotics Research*, 35(1-3):161–185, 2016.

2. Huichan Zhao, Kevin O'Brien, Shuo Li, and Robert F Shepherd. Optoelectronically innervated soft prosthetic hand via stretchable optical waveguides. *Sci. Robot.*, 1(1):eaai7529, 2016.

3. Stefan Schulz, Christian Pylatiuk, and Georg Bretthauer. A new ultralight anthropomorphic hand. In *Robotics and Automation, 2001. Proceedings 2001 ICRA. IEEE International Conference on*, volume 3, pages 2437–2441. IEEE, 2001.\

4. J. Fras, Y. Noh, H Wurdemann, and K. Althoefer. Soft fluidic rotary actuator with improved actuation properties. In *International Conference on Intelligent Robots and Systems*. IEEE, 2017.

5. J. Fras, J. Czarnowski, M. Macias, J. Glowka, M. Cianchetti, and A. Menciassi. New stiff-flop module construction idea for improved actuation and sensing. In *International Conference on Robotics and Automation*, pages 2901–2906. IEEE, 2015.

6. J. Fras, M. Macias, F. Czubaczynski, P. Salek, and J. Glowka. Soft flexible gripper design, charac- terization and application. In *International Conference SCIT, Warsaw, Poland*. Springer, 2016.

Preliminary Evaluation of the Workspace for Upper Limb Robotic Rehabilitation with 3-Dimensional Reaching Tasks

Daniel Freer[1], Konrad Leibrandt[1], Piyamate Wisanuvej[1,2], Jindong Liu[1], and Guang-Zhong Yang[1] [1]Hamlyn Centre, Imperial College London, [2]Kasetsart University

I. INTRODUCTION

End effector-based robotic rehabilitation has improved physical therapy of the upper limb substantially by providing patient motivation and instant feedback[1, 2]. The end effector of a rehabilitation robot is typically held by the user, moving with them to retrain functional tasks without restricting intermediary joints of the arm. However, most of these systems only facilitate movement in a 2D planar workspace [2], which begs research into a 3D end effector based upper limb robotic rehabilitation platform.

The design process for a rehabilitative robot requires analysis of the workspaces of both the robotic manipulator and the human limb. Using a system that can access the entire reach of a patient's arm may be useful, but most standard rehabilitation protocols do not utilize this whole space. Upper limb rehabilitation tasks are focused on function, such as reaching for and holding objects. Robotic rehabilitation platforms have often been built around reaching tasks, and motor rehabilitation can be studied with respect to a patient's response to perturbation of the reaching task [3]. For this reason, the human arm workspace used in this study was constrained to the task of reaching in 3D space.

II. METHODS

The workspace of the arm was simulated using 100 reaching tasks. These tasks are defined by 10 angle configurations between 30 and +30 degrees of θ_{SF} and θ_{SA} representing the maximum and minimum shoulder flexion and abduction, respectively, at the end of the reach. Each reaching primitive was subdivided into 30 time steps and was simulated 5 times, with a small random variation added to each joint at each time step. The joint trajectories for simulation of the reaching task were based on start and endpoints of human joint motion[4] (Table 1), and were simulated on MATLAB using a simple 7 degrees-of-freedom (DoF) model of the human arm. This model was designed using anthropometric values for length [5], with 3 DoF at the shoulder, 2 at the elbow, and 2 at the wrist. Equation 1 describes the relationship between joint movement and time.

$$\theta(t) = \theta_{start} + (tan^{-1}(t)/\pi + 1/2)(\theta_{initial} - \theta_{final})$$

in front of the shoulder; ii.) 10 cm in front and 5 cm lateral to the shoulder; and iii.) 0.5 m lateral and 0.5 m in front of the subject's shoulder. For all three placements the robot was rotated, putting its z-direction in the horizontal plane and pointing toward the arm.

At each position of the simulated hand, inverse kinematics of the robot matched this position and orientation. To determine which placement of the robot was optimal a cost function was developed, taking into consideration: i.) unreachable points (UP); and ii.) collisions with the arm. An unreachable point was defined whenever the distance between robot end effector and the desired Cartesian point was greater than 0.1 meters. Collisions occurred when any part of the robot moved into a restricted region, defined by planes parallel to the z-axis and in line with each segment of the arm. Because there are 6 joints of the robot that could cross these planes, this was divided by 6 in the cost function.
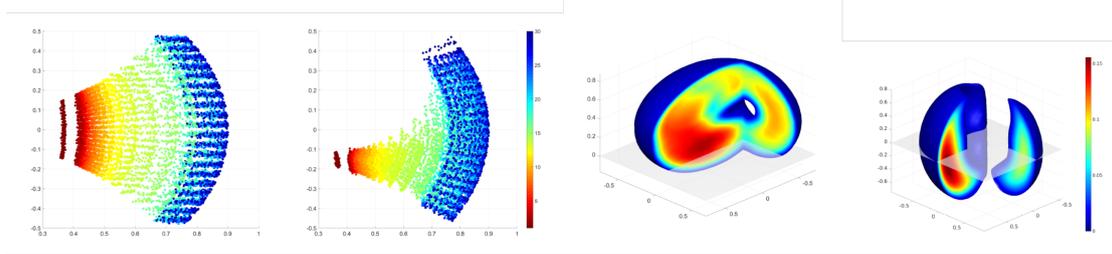
Figure 1: Workspace analysis of (from left to right) arm reaching movements from the top and side, then the full workspaces of the Hamlyn Active Arm and the human arm.

Joint	Motion	Initial	Final
Shoulder	Flex/Ext	-90	θ_{SF}
Shoulder	Abd/Add	$-\theta_{SA}$	θ_{SA}
Shoulder	Rotation	θ_{SA}/π	$-\theta_{SA}/\pi$
Elbow	Flex/Ext	130	0
Wrist	Abd/Add	-40	0

Table 1: Initial and final joint angles while reaching

	Shoulder	In Front	Side
UP	6746	747	3771
Collisions	43387	46994	38401
Cost	13977	8579	10171

Table 2: Cost table for three robot placements.

III. RESULTS

The joint trajectories used in this study resulted in a curved trajectory of the hand when reaching for high or low points, while reaching strictly to the left or right yielded a relatively straight path. Shoulder rotation in the opposite direction of shoulder abduction reduced left/right curvature from previous trials. The calculated workspace for the arm during these reaching tasks is shown in Figure 1. The unreachable points, potential collisions and costs for each configuration are shown in Table 2.

Placing the robot near the shoulder yielded the highest overall cost, with many more unreachable points than either of the other two options. This is likely because of a dead zone near the base of the robot. This dead zone is visualized in 1. However, this is with the robot standing upward as opposed to pointing sideways. The lowest cost was seen when the robot was placed in front of the patient, facing back towards them. This cost was low primarily because only about 5 percent of the simulations were unreachable. Placing the robot to the side had moderately good performance, but could not encompass the movements far away from the base placement.

I.V. DISCUSSION

This paper explored the necessary workspace for a 3-dimensional rehabilitation robot for the upper limb.

Results indicated that for limited reaching tasks, placing the robot in front of the patient and facing back toward them is the optimal configuration. However, none of the three configurations that were investigated covered the entire workspace for the reaching task. This indicates that it is useful to redesign aspects of the robot such as link lengths. In addition, optimal placement of the robot's base for each configuration could be mathematically determined rather than a simple visual estimation.

Furthermore employing a cost function which considers further joint- and task-space constraints might provide a better measure to optimize the design of the robot. Constraints to consider can include dexterity, the orientation of the end effector and the length of each robotic link. In addition a broader evaluation of collision avoidance could be implemented, which would attempt multiple robot configurations in case of collision before choosing the final pose for cost calculation.

Finally, while the reaching task is commonly employed for rehabilitation of patients after a stroke, including only this piece of the workspace in the design of a robotic system severely limits its robustness. More emphasis has to be put into developing systems for other activities of daily living that could

benefit from robotic rehabilitation. The activities targeted for a particular rehabilitation protocol may change which

design and placement of the robot is most appropriate.

REFERENCES

1. M. Babaiasl, S. H. Mahdioun, P. Jaryani, and M. Yazdani, "A review of technological and clinical aspects of robot-aided rehabilitation of upper-extremity after stroke." *Disability and rehabilitation. Assistive technology*, vol. 00, no. 00, pp. 1–18, 2015. [Online]. Available: http://www.ncbi.nlm.nih.gov/pubmed/25600057

2. H. I. Krebs, J. J. Palazzolo, L. Dipietro, M. Ferraro, J. Krol, K. Rannekleiv, B. T. Volpe, and Hogan, "Rehabilitation robotics: Performance-based progressive robot-assisted therapy," *Au- tonomous Robots*, vol. 15, no. 1, pp. 7–20, 2003.

3. R. a. Scheidt, D. J. Reinkensmeyer, M. a. Conditt, W. Z. Rymer, and F. a. Mussa-Ivaldi, "Persis- tence of motor adaptation during constrained, multi-joint, arm movements." *Journal of neurophys- iology*, vol. 84, no. 2, pp. 853–862, 2000.

4. Lacquaniti and J. F. Soechting, "Coordination of arm and wrist motion during a reaching task." *The Journal of neuroscience : the official journal of the Society for Neuroscience*, vol. 2, no. 4, pp. 399–408, 1982.

5. S. Plagenhoef, F. G. Evans, and T. Abdelnour, "Anatomical Data for Analyzing Human Motion,"

6. *Research Quarterly for Exercise and Sport*, vol. 54, no. 2, pp. 169–178, 1983.

7. P. Wisanuvej, K. Leibrandt, J. Liu, and G.-z. Yang, "Hands-on reconfigurable robotic surgical instrument holder arm," pp. 2471–2476, 2016.

3D Convolutional Neural Networks for Tree Detection using Automatically Annotated LiDAR data

Ananya Gupta[1,2], Jonathan Byrne[1], David Moloney[1], Simon Watson[2], Hujun Yin[2]

[1]Intel Corporation [2]The University of Manchester

I. INTRODUCTION

LiDAR data provides a useful means to collect information for a number of tasks such as forest surveying and urban planning (Treepedia, 2015). However, this data needs to be annotated in order for it to be useful. Currently most of this annotation is done manually as is the case in urban green cover surveys, where identifying trees in the cities is a long, laborious process.

This work focuses on making this urban tree annotation process autonomous by the means of using data present in high quality LiDAR scans to automatically label trees. This annotated data can then be used in conjunction with deep learning to identify trees in LiDAR scans without the requisite information.

II. METHODS

In order to identify trees in LiDAR scans, ground points are first identified and filtered using a Progressive Morphological Filter. This filtered scan is then voxelized in a sparse 3D hierarchical data structure, VOLA (Byrne et al., 2017), in order to reduce the input resolution. A 2 bits per voxel approach is used to encode additional information such as colour, intensity and number of returns information.

LiDAR laser pulses can be reflected once (as in the case of a flat surface such as the ground) or multiple times (from edges of buildings, trees etc.). Based on the insight that tree regions have a high number of returns, voxels with a high number of returns are identified and retained, followed by connected component analysis to isolate individual tree canopies.

A horizontal bounding box is fitted around the tree canopies and is extended to ground in

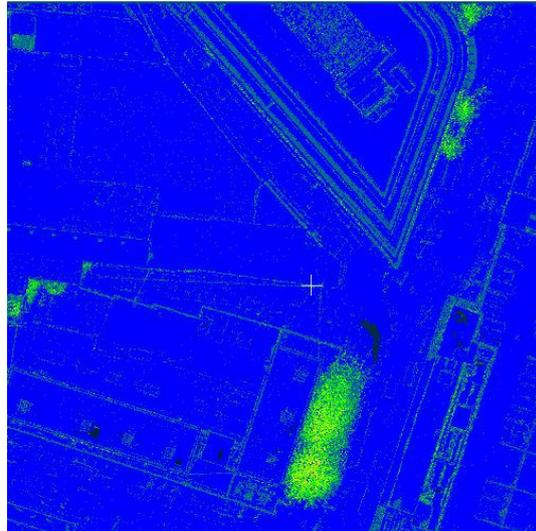the vertical dimension in order to capture the tree trunks.

Figure 1: LiDAR scan showing decreasing number of returns: Green>Blue

The trees identified in this case are used as positive samples to train a 3D convolutional neural network (CNN) (Maturana et al., 2015) for tree detection. The structure of the network can be seen in Figure 2.

A number of non-tree regions are extracted from the LiDAR scans as negative training samples for the network. The training data is augmented by adding noise, rotating the data around the horizontal plane and by jittering it in all 3 dimensions.
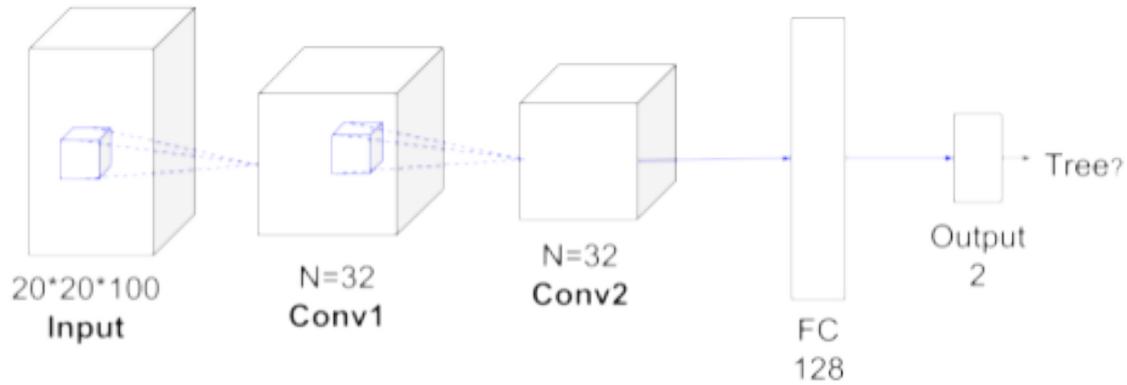
Figure 2: Structure of 3D Convolutional Neural Network

III. RESULTS

The tree annotation method was tested on a dense airborne LiDAR dataset of Dublin city (Laefer et al., 2015). A subset of the scan was manually annotated for 535 trees and the algorithm was able to correctly identify 469 trees. It returned 56 regions incorrectly identified as trees and had a precision of 0.88 with a recall of 0.89 with 0.88 as the overall accuracy.

The 3D CNN was tested on a publicly available ground based LiDAR dataset which contains both rural and urban scenes (Hackel et al., 2017). The results show that the neural network is able to correctly identify most trees in scan with a few false positives. It misses some of the trees right at the edges of the scan, which is possibly due to the missing data in those regions.

I.V. DISCUSSION AND CONCLUSION

The methods described in this work provide a way to annotate LiDAR data for trees using the number of returns information. The results show that the algorithm is able to correctly identify most of the trees in an urban setting. This work also introduces a CNN to detect trees in LiDAR scans which do not contain the number of returns information.

The results in this case show that the network is able to identify trees in ground based LiDAR scans which essentially only have depth information (not complete 3D), while being trained on data which is from an aerial LiDAR scan which has full 3D information.

REFERENCES

1. Byrne, J., Caulfield, S., Xu, X., Pena, D., Baugh, G., & Moloney, D. (2017). Applications of the VOLA Format for 3D Data Knowledge Discovery . In *International Conference on Natural Computation, Fuzzy Systems and Knowledge Discovery* (pp. 1–8).

2. Hackel, T., Savinov, N., Ladicky, L., Wegner, J. D., Schindler, K., & Pollefeys, M. (2017). Semantic3D.net: A new Large-scale Point Cloud Classification Benchmark. http://doi.org/10.5194/isprs-annals-IV-1-W1-91-2017

3. Laefer, D. F., Abuwarda, S., Vo, A.-V., Truong-Hong, L., & Gharibi, H. (2015). 2015 Aerial Laser and Photogrammetry Survey of Dublin City Collection Record. http://doi.org/10.17609/N8MQ0N

4. Maturana, D., & Scherer, S. (2015). VoxNet: A 3D Convolutional Neural Network for real-time object recognition. *Intelligent Robots and Systems (IROS), 2015 IEEE/RSJ International Conference on*, 922–928. http://doi.org/10.1109/IROS.2015.7353481

5. Treepedia. (2015). MIT Senseable City Lab. Retrieved fro http://senseable.mit.edu/treepedia

Active Human Detection with a Mobile Robot

Mohamed Heshmat[&], Manuel Fernandez-Carmona[*], Zhi Yan[*] and Nicola Bellotto[*] * L-CAS, School of Computer Science, University of Lincoln (UK) & Faculty of Science, Sohag University (Egypt), Email: mabdelwahab, mfernandezcarmona, zyan, nbellotto @lincoln.ac.uk*

ABSTRACT

A modified computed torque controller (CTC) is presented in this paper. The proposed approach is demonstrated on one joint of a 4-degree of freedom (DOF) master-slave (MS) robot manipulator and the CTC gain parameters are optimized using the particle swarm optimisation (PSO) algorithm. The feasibility of the proposed controller is tested and compared with the conventional / traditional computed torque control. Results show that the proposed controller performs impressively.

I. INTRODUCTION

Mobile robots are already sharing environments with humans, especially for indoor applications. Providing services to and interacting with people are the most important tasks for such robots. Therefore, research in sensing methods and algorithms for human detection has received considerable attention in the last decades.

Human detectors for autonomous mobile robots encounter several challenges. Humans can assume a variety of poses (standing, sitting, etc.) and be observed from different views [1]. Another challenge is detecting occluded humans, which is one of the most difficult problems, though a few attempts have been proposed to deal with it [2]. Determining whether there is an occlusion or not is a key issue in itself [3]. The authors in [4] proposed a method to find the best robot pose for human observation. First, the robot locates the human using colour segmentation and then it moves around him/her to select the best observation pose. Although their work improved the detection confidence, it's still challenged by occlusions and human motion.

Active Perception (AP) seeks to control and guide the acquisition of sensor data in order to improve the performance of the input process and maximise the information acquisition [5]. The robot has to decide the optimal sensing configuration based on the current situation. AP systems therefore include a dynamic control of the robot behaviour, key for applications in real, changing environments. Recently, AP has been proved useful in many different scenarios [6, 7, 8]. However, to our knowledge, there are no AP systems for human detection with a mobile robot, as proposed in the current work. Active human detection is a particular AP system that seeks to overcome some of the previous challenges. The AP can guide the observation process and move the robot to the best available poses for human detection.

In our system, the best available poses are selected according to the human detection confidence, using a pre-learnt observation model. The latter is a distribution of the detection confidence values for multiple robot- human pose configurations, as shown in Fig. 1. The X and Y axes represent the distance between the robot and the origin (the human). In order to build this model, we collect a set of human confidence measurements and apply a 2D polynomic regression model to obtain the expected confidence for any new human-robot pose. The human detection method used in our system is a real-time RGB-D based upper body detector [9].

In this preliminary work, our system is tested in a ROS simulation environment, shown in Fig. 3. The architecture of the proposed active human detection system is shown in Fig. 2. The system starts with an initial human

detection.

Then, the robot moves to find the best available view for human detection, based on the known confidence model, and taking into account the motion cost. If the human changes his pose, the system adapts by selecting a new robot pose accordingly, at least as long as the human remains in the robot's field of view. In case of occlusion, instead, the robot selects a new pose from the set of available poses and avoids the area of the previous occlusion.
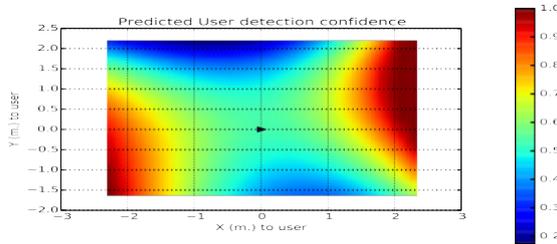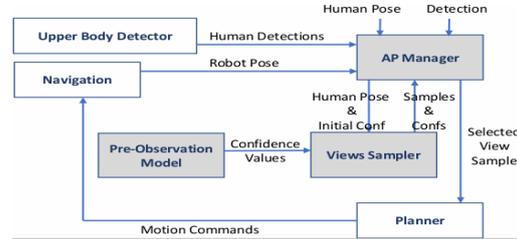

Figure (1) The pre-observation model

Figure (2) System architecture

SYSTEM DESIGN

The system design has a simple and modular structure, compatible with a standard ROS stack, which facilitates future developments and improvements. Fig. 2 shows the full system architecture. The gray modules implement the key contributions of this work.

The system starts with an RGB-D upper body detection, which provides an initial human position and observation confidence. The human orientation is computed from the shoulders using the method proposed in [10]. Combining this information with the pre-observation model of detection confidence, the views-sampler generates several viewpoints randomly distributed around the person.

These viewpoint samples are such that the expected human detection confidence is better than the previous one. Finally, the AP manager selects the next best viewpoint from the available samples that maximizes the expected detection confidence and minimizes the robot's moving cost.

TESTING RESULTS

The active human detection system continuously tries to improve its confidence. If the person moves or is occluded by an obstacle, the robot moves as well to find a more suitable position for high-confidence human detection. We performed some simulations (Fig. 3) to test our method against a typical passive approach in case of occlusion (Fig. 4) along with human motion. For the latter, in particular, it is clear that with a static robot (passive approach) the human detection confidence decreases as the human moves, as shown in Fig. 5.

In contrast, Fig. 6 shows that our active approach can guide the robot towards good observation viewpoints. It is worth noting that the current implementation is not able to cope with a relatively fast-moving person, therefore it can only provide high-confidence detections for very short time intervals.

CONCLUSIONS

In this work, we have presented some preliminary work on active human detection, which has the potential to succeed in many situations where passive detection approaches usually fail. Initial simulation tests, however, highlighted the difficulty of dealing with fast moving humans.

Our future work will focus on new strategies for active human detection that can prevent occlusions and take into account the limitations of a mobile robot platform, such as its limited field of view. We will also validate our approach in new real-world experiments
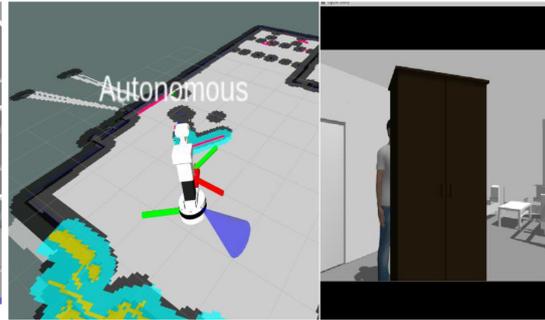
Figure (3) Simulation environment
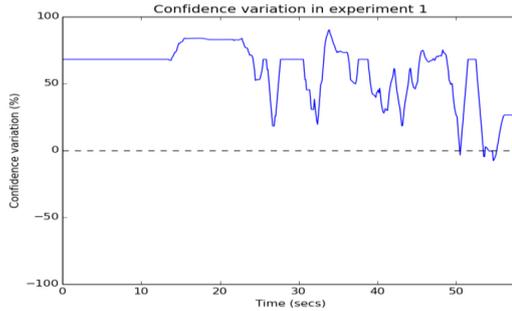

Figure (4) Occlusion example

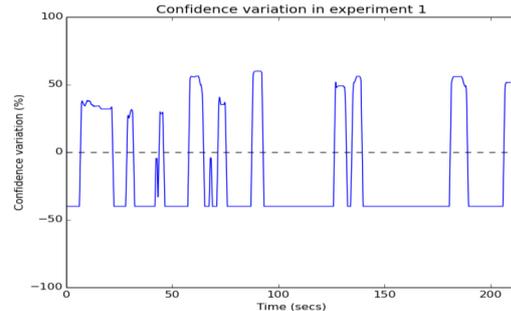Figure (5) Human motion (passive system)

Figure (6) Human motion (active system)

REFERENCES

1. Benjamin Choi, Cetin Meriçli, Joydeep Biswas, and Manuela Veloso. 2013. Fast human detection for indoor mobile robots using depth images. In IEEE International Conference on Robotics and Automation (ICRA). 1108–1113.

2. Duc Thanh Nguyen, Wanqing Li, and Philip O Ogunbona. 2016. Human detection from images and videos: a survey. Pattern Recognition 51, 148–175.

3. Markus Enzweiler, Angela Eigenstetter, Bernt Schiele, and Dariu M Gavrila. 2010. Multi-cue pedestrian classification with partial occlusion handling. In IEEE International Conference on Computer vision and Pattern Recognition (CVPR). 990–997.

4. Jianhao Du and Weihua Sheng. 2013. Active view planning for human observation through a RGB-D camera. In IEEE Workshop on Robot Vision (WORV). 114–119.

5. Ruzena Bajcsy, Yiannis Aloimonos, and John K. Tsotsos. 2017. Revisiting active perception. Autonomous Robots, 1–20.

6. Nathan F Lepora, Uriel Martinez-Hernandez, and Tony J Prescott. 2013. Active Bayesian Perception for Simultaneous Object Localization and Identification. In Robotics: Science and Systems.

7. Timothy Patten, Michael Zillich, Robert Fitch, Markus Vincze, and Salah Sukkarieh. 2016. Viewpoint evaluation for online 3D active object classification. IEEE Robotics and Automation Letters 1, 1, 73–81.

8. Thorsten Gedicke, Martin Günther, and Joachim Hertzberg. 2016. FLAP for CAOS: Forward-Looking Active Perception for Clutter-Aware Object Search. In IFAC Symposium on Intelligent Autonomous Vehicles (IAV). 114–119.

9. Omid Hosseini Jafari, Dennis Mitzel, and Bastian Leibe. 2014. Real-time RGB-D based people detection and tracking for mobile robots and head-worn cameras. In IEEE International Conference on Robotics and Automation (ICRA). 5636–5643.

10. S. Cosar, C. Coppola, and N. Bellotto. 2017. Volume-based Human Re-Identification with RGB-D Cameras. In Proc. of the 12th Int. Joint Conf. on Computer Vision, Imaging and Computer Graphics Theory and Applications (VISIGRAPP). 389–397.

Proof-of-Concept Swarm of Self-Organising Drones Aimed at Fighting Wildfires

Mauro S. Innocente and Paolo Grasso, Smart Vehicles Control Laboratory, Institute for Future Transport and Cities, Coventry University

I. INTRODUCTION

Swarm Intelligence (SI) comprises a relatively novel route to Artificial Intelligence (AI) which stems from decentralised and self-organising behaviour observed in groups of simple social animals in nature such as ant and bee colonies, fish schools, and bird flocks. By way of collaboration, these animals are able to accomplish tasks that are far beyond their individual capabilities, and even beyond the simple aggregation of all of their individual capabilities. That is to say, the whole is more than the sum of its parts. Thus, SI is the branch of AI that deals with the collective behaviour that emerges from decentralised self-organising systems. Self-Organisation occurs with no central control or sense of purpose, as individuals only interact locally with one another and with the environment, inducing the emergence of coherent global patterns. Swarm robotics is a novel approach to the coordination of large numbers of simple and relatively inexpensive robots, which emerged as the application of SI to multi-robot systems. Different from other SI studies, swarm robotics puts emphasis on the physical embodiment of individuals [1].

Swarm robotics and Unmanned Aerial Vehicles (UAVs) technology have progressed at an increasingly fast pace for the past two decades, extending their capabilities and the kinds of problems they can help tackle. UAVs can now be equipped with a range of advanced cameras, thermal imagers and sensors which enable them to operate in remote areas, dangerous environments, and even through solid smoke while still being able to perform tasks such as surveying, mapping or locating people. Some of their current applications include aerial photography and filming, information gathering, provision of essential supplies for disaster management, support of search and rescue operations, mapping inaccessible locations, field surveying, and crop health monitoring. Autonomous UAVs have been used to establish resilient communications networks for emergency response [2] [3]. With regards to fire-fighting, UAV technology has been used to perform tasks such as forest surveillance, building fire risk maps, wildfire detection and monitoring, gathering data for a human decision-maker, assisting search and rescue operations, and situational awareness [4].

Given the hazardous nature of the activity, fighting fires by means of disposable and relatively inexpensive robots in place of humans is of special interest. In addition, the use of fleets of decentralised cooperative and self-organising robots results in a robust and resilient system with distributed decision-making which can cope with uncertainty, errors, and the failure or loss of a few nonessential units without jeopardising the overall mission. However, to the best of our knowledge, the use of self-organising swarms of autonomous UAVs for the actual deed of putting out fires has remained notably unexplored.

This paper comprises a proof-of-concept to demonstrate the feasibility and potential of employing swarm robotics to fight fires autonomously. To this end, an efficient yet realistic physics-based model of the spread of wildfires is developed, which is then coupled with a model of a fleet of self-organising drones whose coordination mechanism is based on a forgetful particle swarm algorithm. The aim is to develop algorithms for swarms of autonomous drones to self-organise to develop the ability to fight the spread of wildfires without human intervention. This research is timely, since Robotics and AI (RAI) as well as Robotics

and Autonomous Systems (RAS) are identified as priority areas by the Engineering and Physical Sciences Research Council (EPSRC), as well as in the Industrial and Digital Strategies [5], [6] [7]. In addition, the UK government identified RAS as one of the Eight Great Technologies that will propel the UK to future growth [8], [9]. This topic is also supported by the UK-RAS Network which predicts that RAS will play an increasingly important role in disaster relief by reducing costs and response times and increasing capabilities [10].

II. FIRE-SPREAD MODEL

A physics-based fire-spread model was designed and implemented as a two-dimensional reaction-diffusion equation that describes the combustion of a mono-phase medium composed of pre-mixed gas of fuel and air.

This comprises a simplified version of the model in [11]. It is also assumed that there is no atmospheric wind and the transport equations can therefore be neglected.

In order to compensate for this, the diffusion coefficient is increased and two pseudo-3D terms are added into the energy balance equation to account for the energy losses due to convection and radiation in the third dimension.

Radiation in the horizontal directions is modelled to affect only the neighbour cells. The heat capacity at constant pressure is assumed to be constant for each chemical species within the considered temperature range. The fire-spread model can be represented by a system of five partial differential equations, one for the enthalpy balance and four for the chemical species formation (CO_2 and H_2O) or consumption (Fuel and O_2):

$$\begin{cases} \rho c_p \frac{\partial T}{\partial t} = -\rho h_c \frac{M}{M_{fuel}} r + k \frac{\partial}{\partial x}\left(\frac{1}{c_p}\frac{\partial c_p T}{\partial x}\right) + k \frac{\partial}{\partial y}\left(\frac{1}{c_p}\frac{\partial c_p T}{\partial y}\right) + \dots \\[2mm] + k \frac{\partial}{\partial x}\left(\frac{1}{c_p}\frac{\partial h_c}{\partial x}\right) + k \frac{\partial}{\partial y}\left(\frac{1}{c_p}\frac{\partial h_c}{\partial y}\right) + C_a(T_0 - T) + \sigma\varepsilon\left[4dx\frac{\partial}{\partial x}\left(T^3\frac{\partial T}{\partial x}\right) + 4dy\frac{\partial}{\partial y}\left(T^3\frac{\partial T}{\partial y}\right) + \frac{T_0^4 - T^4}{dz}\right] \\[2mm] \frac{\partial X_\alpha}{\partial t} = -\frac{\theta_\alpha}{\theta_{fuel}} \cdot \frac{M}{M_{fuel}} \cdot r \quad \text{with} \quad \alpha = 1,\dots,4 \end{cases} \qquad (1)$$
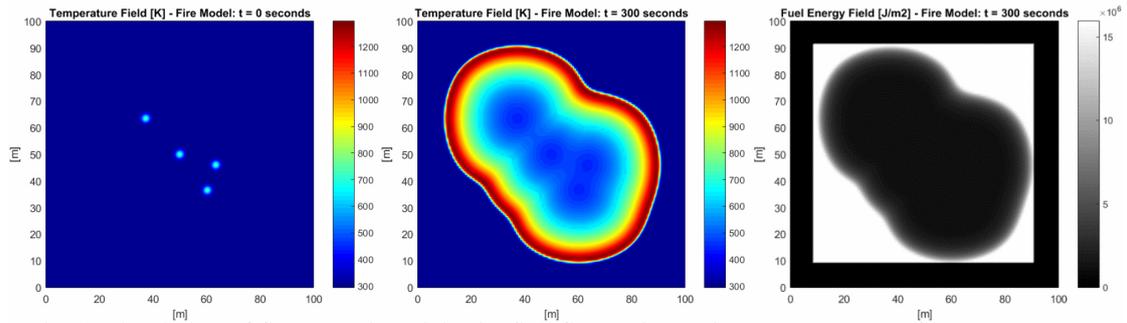

Fig. 1: Simulation of fire-spread model. The first figure shows the temperature profile once 4 sparks have occurred, the second one shows the temperature profile after 5 minutes, and the last one shows fuel energy density after 5 minutes (black: no fuel).

The system is closed with the equations for the molar mass of the mixture, the heat capacity of the mixture, the combustion rate (Arrhenius equation), and the combustion enthalpy. Fig. 1 shows an example of this model being used for the prediction of the temperature profile and fuel energy density five minutes after four sparks have occurred. While very efficient, the simulation of this model using Matlab and a standard PC still

runs about five times slower than real-time (without visualisation).

III. SELF-ORGANISATION MODEL

At this early stage of the research, the swarm of drones has been modelled as 2D massless particles whose self-organisation is based on the particle swarm algorithm. Modifications were introduced to handle particles' memories in a dynamic environment, and to
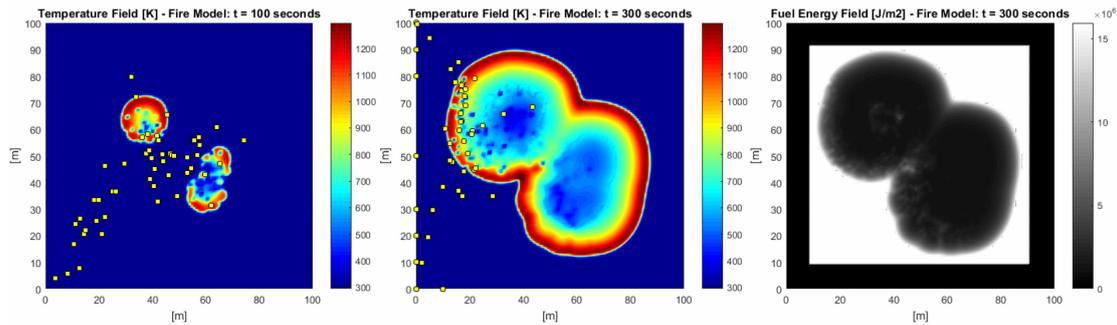
103

Fig. 2: Simulation of self-organising drones fighting the spread of a wildfire. The first figure shows temperature 100 seconds after 4 sparks have occurred, the second one shows the same after 5 minutes, and the last one shows fuel energy density after 5 minutes.

control the level of stochasticity so as to smoothen the erratic behavior. While the fire model is updated every quarter of a second, sensor measurements and drones' memories are updated every second. Maximum speed permitted is set to 10 m/s.

I.V. FUTURE WORK

Future work includes the incorporation of collision avoidance algorithms, and the modelling of the actual drones to include flight dynamics and local controllers. We have also developed a more advanced fire- spread model which accounts for transport phenomena due to varying pressure and temperature inspired by [12] and [13], though atmospheric wind is yet to be included.

However, this model is too demanding to be used extensively. We are also exploring the use of the Fire Dynamics Simulator (FDS) [14], the FIRESITE wildfire growth simulator [15], and of models based on cellular automata and Lattice Boltzmann.

REFERENCES

1. Şahin, S. Girgin, L. Bayindir and A. E. Turgut, "Swarm Robotics," in *Swarm Intelligence. Natural*
2. *Computing Series*, C. Blum and D. Merkle, Eds., Springer, Berlin, Heidelberg, 2008, pp. 87-100.
3. S. Hauert, S. Leven, J.-C. Zufferey and D. Floreano, "The swarming micro air vehicle network (SMAVNET) project," [Online]. Available: http://lis2.epfl.ch/CompletedResearchProjects/SwarmingMAVs/index.php. [Accessed 12 01 2018].
4. J. Ueyama, H. Freitas, B. S. Faiçal, G. P. Filho, P. Fini, G. Pessin, P. H. Gomes and L. A. Villas, "Exploiting the use of unmanned aerial vehicles to provide resilience in wireless sensor networks," *IEEE Communications Magazine,* pp. 81-87, 2014.
5. J. C. Jones, "SMART fire fighting: the use of unmanned aircraft systems in the fire service," *NFPA 2015 Responder Forum,* 2015.
6. "Building our Industrial Strategy," HM government green paper, 2017.
7. "Industrial strategy. Building a Britain fit for the future," HM government white paper, 2017.
8. "The Digital Strategy," HM government policy paper, 2017
9. Willets, "Eight Great Technologies," Policy Exchange, London, 2013.
10. "Robotics and Artificial Intelligence, Fifth Report of Session 2016-17," House of Commons Science and Technology Committee, 2016.
11. "Extreme Environments Robotics: Robotics for Emergency Response, Disaster Relief and Resilience," UK-RAS white papers, 2017.
12. L. Ferragut, M. I. Asensio and S. Monedero, "A numerical method for solving convection–reaction– diffusion multivalued equations in fire spread modelling," *Advances in Engineering Software,* vol. 38, pp. 366-371, 2007.
13. Séro-Guillaume and J. Margerit, "Modelling forest fires. Part I: a complete set of equations derived by extended irreversible

thermodynamics," *International Journal of Heat and Mass Transfer,* vol. 45, pp. 1705-1722, 2002.

14. J. Margerit and O. Séro-Guillaume, "Modelling forest fires. Part II: reduction to two-dimensional models and simulation of propagation," *International Journal of Heat and Mass Transfer,* vol. 45, p. 1723–1737, 2002.

15. K. McGrattan, S. Hostikka, R. McDermott, J. Floyd, C. Weinschenk and K. Overholt, "Fire Dynamics Simulator Technical Reference Guide. Volume 1: Mathematical Model," VTT Technical Research Centre of Finland, 2013.

16. A. Finney, "FARSITE: Fire area simulator-model development and evaluation," U.S. Department of Agriculture, Forest Service, Rocky Mountain Research Station, 2004.

An innovative elbow exoskeleton for stages of post-stroke rehabilitation

Soumya K. Manna[1], Venketesh N. Dubey [1, 2] Faculty of Science and Technology, Bournemouth University

ABSTRACT

Post-stroke rehabilitation can be mainly categorized into three phases. In the acute phase, mostly an external support is required because the patient has no power left to move their arm whereas at the mid recovery level patients require a more assistive support to continue with the rehabilitation training. In the final recovery stage patients are given rigorous training to work-out against variable levels of resistance to increase the arm resilience and their weight lifting capacity. The mechanical requirements for these three stages of rehabilitations are different, whether offered manually or through exoskeletons. To achieve the above requirements, an innovative mechanism has been developed for integrating the three phases of rehabilitation in a single exoskeleton. To evaluate the rate of recovery, three joint parameters have been identified and incorporated into the framework for planning the rehabilitation strategy.

I. INTRODUCTION

There have been a growing number of stroke patients which has over-burdened the support available for manual therapy hence exoskeletons were developed to carry out stroke rehabilitation [1]. Over the two decades of research in this area it has yet not been established what standard therapy could be provided or what kind of exercises are required after stroke [2]. The common rehabilitation strategy consists of three types of exercises [3], fully supported, partially assistive and in resistive mode; still most of the existing exoskeletons can provide only a particular type of training either in assistive or resistive mode and they seldom provide support as per the requirements of rehabilitation. Many adaptive exoskeletons can generate a variety of exercises [4], however, the functionality of those systems is reliant on the sensors employed [5] and the antagonistic impact of its controlling features [6]. To overcome this shortfall an innovative elbow exoskeleton has been designed in such a way that it offers three modes of rehabilitation in a single structure over the full operating range of the exoskeleton.

II. MECHANISM DESIGN OF THE EXOSKELETON

The schematic diagram and the exoskeleton mechanisms are shown in Fig. 1. For most of the existing exoskeletons electric motors are used where the required joint torque is controlled by the motor depending on the dynamics of the model, however, in this design the same functionality has been achieved at mechanical level so that the device can be fine-tuned to the user's requirement. In the designed elbow exoskeleton (Fig. 1), the mode of exercise is separated by the region of operation which is decided by the position (x) of the nut slider driven by the motor via leadscrew. The three rehabilitation regions are defined as; the electric motor based joint control, spring (S_2) based assistive force and spring (S_3 and S_4) based resistive force to provide full range of rehabilitation exercises. The exoskeleton consists of a series of springs, compression (S_1, S_5, S_6), extension (S_2, S_3, S_4) and torsional (S_7 and S_8) for producing different levels of exercises and switching between different rehabilitation regimes. With this strategy, the energy source is only used in the first region to power to the motor whereas the other two regions operate on the stiffness of the springs. The springs used in the exoskeleton allow switching between different regions using their stiffness property, as a result, no extra energy source is required to move from one training regime to another making it an energy efficient mechanism. The aim of the designed exoskeleton is to use as fewer actuators as possible for the whole operation making it a

portable device for the patient. In the First region ($0 \leq x < x_1$), a fixed number of motor rotations restrict the position of the nut slider in a specific frame where the nut slider and the concentric slider are attached by a lock thus allowing the elbow joint to be fully controlled by the motor. In the Second region ($x_1 \leq x < x_2$) both sliders are unlocked due to the difference in stiffness between S_5 and S_6 causing the elbow joint to be fully supported by the spring (S_2). The mechanical arrangement of the slider along with the two torsional springs (S_7 and S_8) change the span of displacement of S_2 (due to the movement of the nut slider towards the baseplate) which generates a variable spring force; S_1 restores the whole arrangement to its original position at the end of the movement range. In the Third region ($x_2 \leq x < x_3$) both S_3 and S_4 are stretched by the nut slider bringing a variable contact force around the elbow joint and a different resistive force for elbow movement. All these features have been achieved using a single motor. A prototype developed to validate the operational integrity uses ABS (Acrylonitrile butadiene styrene) as the structural material due to its high fracture toughness and light weight, shown worn by the user (Fig. 1). The overall weight of the system is 1.8 kg.
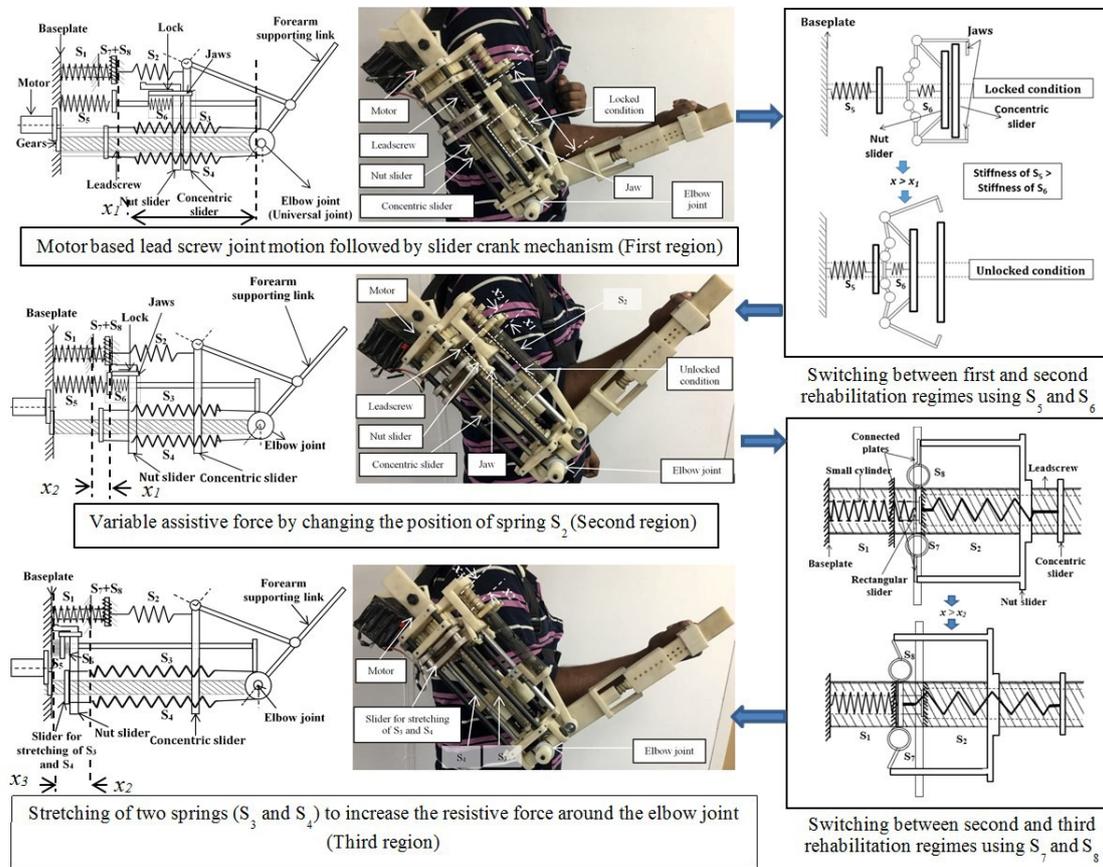

Figure 1. Structural framework of the elbow exoskeleton

III. WORKING PRINCIPLE

Based on the joint parameters (range, frequency and weight lifting capacity) of the user, the recovery stage can be defined as prescribed by the physiotherapist. The control algorithm will automatically put the nut slider in a specific position required for the exercise. The advantage of the system is that in case of any malfunction due to sensory data, it is still possible to alter the region manually. Fig. 2 shows the rehabilitation strategy for this device.
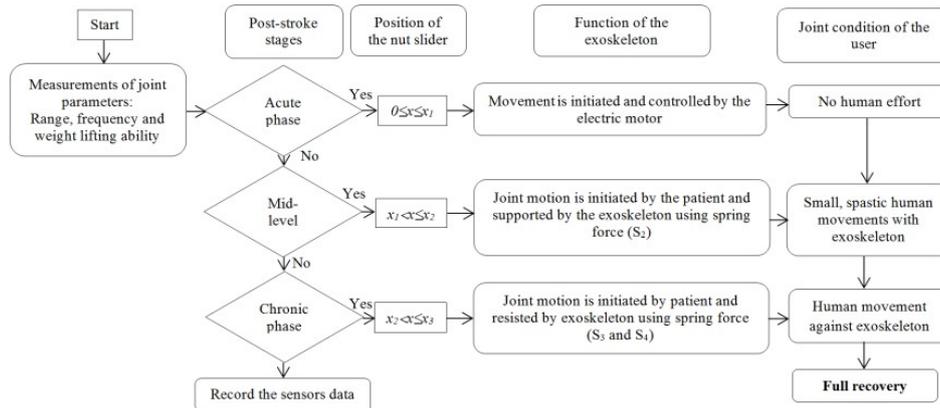
Figure 2. Exoskeleton based rehabilitation strategy

I. V. CONCLUSION

In this design the energy source is only utilised in the first region to provide power to the motor whereas in other two regions, the exoskeleton can work as energy-free system supported by springs. Although the hardware based approach appears to be complex yet it may be more user-friendly for human interaction.

REFERENCES

1. H. S. Lo and S. Q. Xie. 2012. Exoskeleton robots for upper-limb rehabilitation: State of the art and future prospects. Medical Engineering & Physics. 34(3), 261-268. DOI: http://dx.doi.org/10.1016/j.medengphy.2011.10.004.

2. S. K. Manna and V. N. Dubey. 2017. Upper Arm Exoskeletons-What specifications will meet users' acceptability? 1st ed.: Robotics: New Research, Nova Science Publisher, 123-169, ISBN: 978-1- 63485-986-8.

3. W. Chonnaparamutt and W. Supsi. 2016. SEFRE: Semiexoskeleton Rehabilitation System. Applied Bionics and Biomechanics. (2016), 1-12. DOI: http://dx.doi.org/10.1155/2016/8306765.

4. L. Peternel, T. Noda, T. Petrič, A. Ude, J. Morimoto and J. Babič. 2016. Adaptive Control of Exoskeleton Robots for Periodic Assistive Behaviours Based on EMG Feedback Minimisation. PLOS ONE. (2016), 1-26. DOI: 10.1371/journal.pone.0148942.

5. N. Nazmi, M. A. A. Rahman, S. I. Yamamoto, S. A. Ahmad, H. Zamzuri and S. A. Mazlan. 2016. A Review of Classification Techniques of EMG Signals during Isotonic and Isometric Contractions. Sensors. 16(8), 1304. DOI: 10.3390/s16081304.

6. E. T. Wolbrecht, V. Chan, V. Le, S. C. Cramer, D. J. Reinkensmeyer and J. E. Bobrow. 2007. Real- time computer modeling of weakness following stroke optimizes robotic assistance for movement therapy. In 3rd International IEEE/EMBS Conference on Neural Engineering. HI, USA, 152-158. DOI: 10.1109/CNE.2007.369635.

Durable Robotic Control Systems for Humans and Challenging Environments

Guy Burroughes[1] and Ronan Kelly[1] [1] RACE, UK Atomic Energy Authority

ABSTRACT

In an ageing population the need for assistive robotics has a great potential to address issues around the increasing demand for nursing and caregiving. Areas that robots may play a role are in helping with the activities of daily living (ADL) and dressing is the focus of this paper. Successful integration of these robots into society will require careful consideration of factors such as safety and interaction. We believe that these systems should be able to predict the user's intention for maximum safety and task efficiency. Using data collected from human-human interaction (HHI) experiments, features were prepared and assessed for importance and models were trained to classify the dressing task segment and which end effector to move; left, right or both simultaneously. Long short term-memory networks (LSTM) were explored to predict these outcomes one time-step ahead. The networks were assessed against a variety of hyper-parameters including the depth of the hidden layers. The models show promise for correctly classifying task segment based on user pose, with the best test accuracy >95%.

I. INTRODUCTION

The European Spallation Source (ESS) is a multi-disciplinary research facility, which will be the world's most powerful pulsed neutron source. A critical component of ESS will be a facility for handling radioactive waste and preparing it for safe disposal; this facility must operate for at least 40 years. Safe disposal of ESS waste requires the dexterous robotic manipulation of large, highly activated payloads in a shielded chamber: a hot cell.

The ESS ACF will contain equipment for dividing large activated components and storing them in shielded containers. Due to the high levels of radiation being emitted by the components, it is not safe for a human to do this from within the cell. It is therefore necessary to remotely handle the components and operate size reduction equipment, requiring robotic manipulators to be operated by humans in a control room outside the cell. This human-in-the-loop control requires advanced control systems, intuitive interfaces and precision haptics.

II. BACKGROUND

JET has been remotely maintained since the mid 1990's, accumulating a legacy of over 35,000 person-hours of operations time. Routine remote maintenance work is undertaken by a dexterous, force-reflecting master-slave servo-manipulator called MASCOTT. The MASCOTT slave unit is transported on the end of a 12-metre-long articulated robot: a Boom. Meanwhile the MASCOTT master station is driven by a team of experienced operators situated in the Remote Handling Control Room. A second articulated Boom works in parallel with the first to transfer components and tools between storage facilities outside the torus and the workplace within the torus. Commitment to a human-in-the-loop philosophy has allowed the jet remote handling capability to increase in step with the number of applications. this philosophy has resulted in a flexible remote handling system, whereby expensive and difficult to procure elements such as the articulated boom and mascot are not required to change with the application. However due to decades of contract extensions and short-term engineering adaptations, the plant has become tightly coupled, meaning that small engineering changes in one area can have knock-on effects on the rest of the system. One example is the case whereby the control cubicle for camera units was adapted to also control the remote welding rig, as there was spare capacity. This in turn meant that the camera system could no longer be safely

accessed during welding operations, delaying necessary upgrades. Repeated adaptations of this kind are harmful to the maintainability of a long-lived plant, and hence a key focus for the ESS ACF control system design is maximising Reliability, Availability and Maintainability (RAM).

III. A DISTRIBUTED CONTROL ARCHITECTURE

The overarching requirement for the ESS ACF Control System is to bind together a kaleidoscope of devices into a single coherent system, allowing control of all aspects of the facility from a single control room. This integration of dozens of third-party functional units must be implemented at varying levels, ranging from closed-loop control of individual motor drives or command-and-response style PLC control up to high-level inverse kinematics solving and logical interlocks. The long lifespan and complexity of the facility precludes a monolithic architecture like that of the JET remote handling system. Aside from the obvious maintainability issues it would cause, the constrained size of the control room would not allow dedicated Human-Machine Interface (HMI) stations for each piece of controlled equipment. Instead, a distributed design providing flexible software-based HMIs has been chosen.
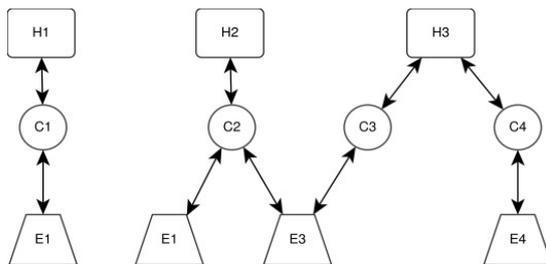

Figure 1: Example Control System Configuration. Hn is a software HMI, Cn is a remote Controller device and En is a unit of equipment such as a robot.

The ESS ACF will require advanced control systems that will need to be maintainable and upgradable for decades, whilst also meeting stringent safety and functional requirements. For this purpose, it has been determined that the RACE's CorteX control systems framework will be used. CorteX is a robust decentralised systems-of-systems framework, which enables pieces of complex equipment to communicate. The framework utilises extensive layers of abstraction combined with standardised self-describing communications to make the ESS ACF control system maintainable, upgradable, and avoid needless vendor lock-in. The ESS ACF control system will be comprised of reusable modules that can be proven and verified. The system will implement logical interlocks between devices to maximise equipment lifespan, but will not provide Functional or Radiological safety. This design decision has been made to limit undue burden on the control system and allow for more conventional and proven safety solutions to exist in parallel, allowing rapid development and integration with third party systems.

The unusually extensive level of control systems integration will optimise Human-Machine interactions, as a single unified HMI for controlling all aspects of the plant will be presented to operators. This will help reduce training costs and the number of incidents caused by human error. The data-driven Graphical User Interface will allow rapid reconfiguration as operational needs evolve over the lifespan of the facility. Finally, the deep level of integration allows all sensor data to be accessible from a single unified data structure. The primary advantage of this in the short-term is the provision of condition monitoring analysis, which allows anomalies in hardware to be identified and quickly corrected as part of an ongoing preventative maintenance scheme. More importantly, it lays the foundations for autonomous control strategies to be developed, by providing a single interface for monitoring and controlling the facility.

I.V. CONCLUSION

The ESS ACF will use a state-of-the-art distributed control system, built using the CorteX framework. This system will provide a unified interface between human operators and robotic equipment, optimising process workflows with a focus on long-term reliability, availability and maintainability.

Flexibility for future upgrades such as autonomy is built into the system architecture, allowing the system to be used for the projected 40-year lifespan of the European Spallation Source and beyond.

Synthetic Viewing for Robotic Handling Facilities

Ronan Kelly[1] and Guy Burroughes[1] [1] RACE, UK Atomic Energy Authority

ABSTRACT

RACE is developing a synthetic viewing system for use by operators of robots in the ESS Active Cells Facility. The system uses 3D visualisations to provide operators with clear and intuitive means of understanding their remote environment. This paper presents the proposed design of the system and proposes future extensions for enhancing human-robot interaction for remote applications.

I. INTRODUCTION

The European Spallation Source (ESS) is a multi-disciplinary research facility which will be the world's most powerful pulsed neutron source. A critical component of ESS will be a facility for handling radioactive waste and preparing it for safe disposal. Safe disposal of ESS waste requires the dexterous tele-manipulation of large, highly activated payloads in a shielded chamber: a hot cell. Traditionally hot cells are built with lead glass windows to allow direct observation by operators. However, as the complexity and scale of required handling operations increases, the restrictions imposed by such windows become problematic, motivating the development of hot cells without any windows. RACE is building on its experience operating the Joint European Torus (JET) remote handling system to develop a windowless hot cell for the ESS Active Cells Facility (ACF), featuring a fully integrated remote handling system and a state-of-the-art synthetic viewing system.

II. BACKGROUND

A synthetic vision system (SVS) is a computer-mediated reality system for remote operation, that uses 3D to provide operators with clear and intuitive means of understanding their remote environment. For the JET remote handling system, operators utilise synthetic views created by a virtual reality system, which is constantly updated in real-time with position data relating to the robotic systems. This supplements a comprehensive, low-latency CCTV viewing system.

The virtual reality system incorporates a 3D model of the current environment, consisting of all robotic systems and serviceable components, as well as all the specialised tools which can be deployed. This model is continuously updated throughout operations to represent the precise configuration of JET and the RH systems as in Figure 1. The positions of remote handling robots are automatically displayed based on the position sensor data from their respective control systems, while any planned automatic moves are illustrated as semi-transparent green indicator "ghosts" of the target pose.

The VR display is central to the JET remote handling control room, and allows the

Figure 1: JET remote handling control room with SVS on central display.

operators to clearly see the state of the robotic systems and the JET machine itself, providing views that cannot be obtained by cameras (1). In addition to supporting live operations in real-time, the virtual reality tools can be used in combination with simulated robotic control systems to allow operation planners to design and trial-run remote handling tasks offline in their own office, without access to the real systems. Motion path plans can be generated in this offline environment, and used to conduct validation mock-ups in virtual reality, which are independently reviewed prior to approval for live operations.

with entering the maintenance cell and carrying out operations involving the whole system. A system like this would allow a complete Technical Design Review to include a full operation demonstration with simulated cell.

This can include visually indicating the state of brakes or torques on robot joints, or illustrating the currently measured radiation map (3) or physical point cloud. Similarly, mixed reality can be employed, such that real camera views can be superimposed into the VR scene to provide greater fidelity.
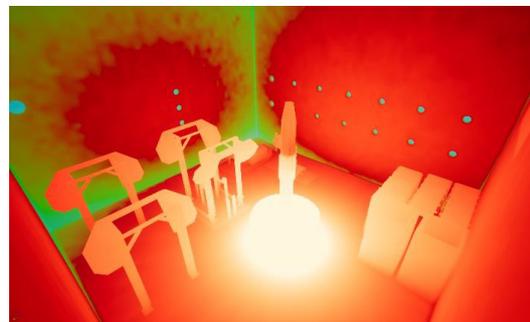
III. SYNTHETIC VIEWING

Figure 2: Control room for a simulated ESS windowless hot cell.

The ESS ACF contains an environment similar to JET, but with additional constraints due to the higher radiation doses that will be present. For a windowless hot-cell with limited sensors that are prone to failure, a synthetic viewing system will be critical. The system will provide an outlook to the probable state of the hot cell, allowing for more effective operations to be performed. For example, the elbows of a tele-manipulator can be monitored in three dimensions (with no camera views) for possible collision.

However, a Virtual Reality (VR) simulation has many more useful properties and functions, such as in JET, where the simulator is used for training and operations testing (2). A control room can be populated with simulated camera views, and operational constraints can be tested, such as reachability, lighting conditions, and radiation dose. With the use of immersive VR hardware, human elements in the Remote Maintenance system can also be tested, such as operators tasked

Figure 3: Radiation dose map visualisation in an ESS hot cell.

I.V. CONCLUSION

The recent advance in simulation and VR technologies has opened many opportunities to rapidly improve the current state of the art of Remote Handling. Mixed reality technologies can extend the current Synthetic Viewing system to include advanced simulation data, sensed data, and operations data conveyed in an effective, intuitive, and contextual fashion. This Synthetic Viewing solution could be used to improve all parts of the operation: from development to execution and review.

REFERENCES

1. Operational experience feedback in JET Remote Handling. O. David, A.B. Loving, J.D. Palmer,
   S. Ciattaglia, J.P. Friconneau. s.l. : Fusion Engineering and Design, 2005, Vols. Volumes 75–79. ISSN 0920-3796.
2. The use of virtual reality for preparation and implementation of JET remote handling operations.
   S. Sanders, A.C. Rolfe. ISSN 0920-379, s.l. : Fusion Engineering and Design, 2003, Vol. Volume 69.
3. Minimising operator dose during JET shutdown using virtual reality. Jonathan Naish, Alex Burns. ISSN 0920-3796, s.l. : Fusion Engineering and Design, 2017, Vol. Volume 124.

Designing a novel bipedal Silent Agile Robust Autonomous Host (S.A.R.A.H.)

Christos Kouppas[1] *◆, Michalis Rodosthenous[2], Nurdaulet Sagyndyk[2], Qinggang Meng[1], Mark King[1], and Dennis Majoe[2]

[1] Loughborough University, Loughborough, United Kingdom. C.Kouppas@lboro.ac.uk

[2] Motion Robotics LTD, Southampton, United Kingdom.

ABSTRACT

S.A.R.A.H. (Silent Agile Robust Autonomous Host) is a project that is co-funded from Innovate UK's scheme "Emerging and Enabling Technologies". The project's aim is to develop a novel design of a bipedal robot which uses patent pending actuators that rely on bare electromagnets and not on DC motors. The locomotion of the bipedal will be based on flightless birds, combining pattern generated locomotions with neural network predictions for the next movement to optimize the walk. The neural network will have the ability to evolve in to deep learning to learn online and exchange knowledge with other robots. Finally, as a host it has the ability to carry an external module on its' upper body, e.g. arm manipulators.

I. INTRODUCTION

Humans as animals, despite the flexibility and dexterity that their legs provide, do not walk as efficiently as other animals. In comparison, to flightless birds, humans can consume double the amount of oxygen. Struthionidae Struthio (Ostrich) is one of the most efficient animals (comparing the oxygen consumption divided by its weight) and up to 40% more efficient than humans [8]. S.A.R.A.H. (Silent Agile Robust Autonomous Host) is inspired by the flightless birds' locomotion to reduce its power consumption and as a result increase its operational time.

Mechanically, S.A.R.A.H. is combining the patent pending "bang-bang" actuators from Motion Robotics LTD [1] in conjunction with hydraulics. The actuators use the power of electromagnets to generate the required torque in order to rotate the joints. The hydraulics, on the other hand, are used for damping and breaking. For control, 5 Atmel microchips [6] and 2 Raspberry Pi 3 (RPi3) [7] are used in a hierarchy. One of the RPi3 is responsible for the control of the motion (written in C) and the other is responsible for learning and executing neural network classifications (written in Python).

II. FIRST PROTOTYPE DESIGN

The robot has 6 controllable joints (3 in each leg) and 2 semi-controllable joints (one in each foot). The controllable (Fig.1a, Green Dots) joints are controlled by 2 actuators that operate antagonistically; when one is ON the other is OFF. The joints also include one hydraulic mechanism which provides damping, spring and breaking. The mechanism is locked when the actuators are not powered, thus, the robot has the ability to maintain its posture without consuming energy. The

(a) DoFs and skeleton of S.A.R.A.H.

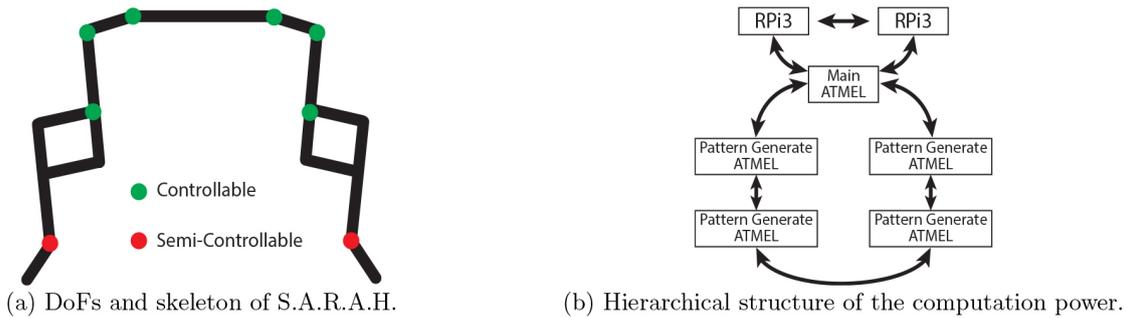(b) Hierarchical structure of the computation power.

Fig. 1: DoFs and Hierarchy

semi-controllable (Fig.1a, Red Dots) joints do not utilize an actuator but an additional hydraulic mechanism is attached. The controllability that the two hydraulic mechanisms can achieve is based on the combination of leg's trajectory, gravity and timing of the power down. The use of hydraulic mechanism reduces the power consumption, especially in the standby mode as only the "brain" remains operational. The configuration is inspired from ostriches and is a big part of the novelty of the robot. The electromechanical parts are powered by three $12V$, $14Ah$ Lithium Iron Batteries that provide up to $36V$ and $30A$

The "brain" of S.A.R.A.H. is based on low-cost hardware, in order to reduce the future production costs and utilizes multiple chips to distribute the tasks more efficiently. The computational power comes from 2 RPi3 (low-cost board, less than £30) and 5 Atmel SAMC21 boards (low-cost microchip, less than £5), which are connected in a hierarchical order (Figure 1b). The RPi3s have the top position in the hierarchy and they communicate with the main Atmel.

The main Atmel is then responsible in communicating with the other Atmels (2 each side). One Atmel in each leg is responsible for data collection and actuation for the abduction/adduction and flexion/extension of the hip joint. The other is responsible for the data collection and the control of the "knee" and foot joints. One of the two RPi3 is executing a neural network to predict the possible falling region in order to suggest counter-

moves to the other RPi3. Then, that RPi3 will calculate the input variables for the Atmel boards. Those variables are mainly, the required voltage to each actuator, the time of activation and the release time of the hydraulics. The order of activation cannot change, which means if the left/right leg starts moving it has to execute a series of moves until it is finished. The "brain" is powered by a separate battery, similar to the one that was described previously.

The locomotion of the robot is different in comparison to typical humanoids, that is to increase the efficiency at the cost of dexterity. S.A.R.A.H. has 12 Degrees of Freedom (DoFs) from which 6 are controllable and 6 are semi-controlled. The locomotion is simple and begins with (see Fig.2a): (i) the "knee" shortening, (ii) moving the leg in front by flexion of the hip, (iii) extending the "knee" to hit the floor and (iv) moving the leg backwards by extension of the hip.

The stability of the bipedal robot, is based on an unstable system. The robot will be stabilized by making steps, not by controlling its upward position. Finally, the upper body is reserved for external modules which can be designed in the future. The aim is to provide a generic host, flexible to meet the users needs, but that is able to stand, walk and recover from pushes. This will provide a platform third-party organisations, that have expertise in providing services to consumers, an opportunity to design their own external modules.
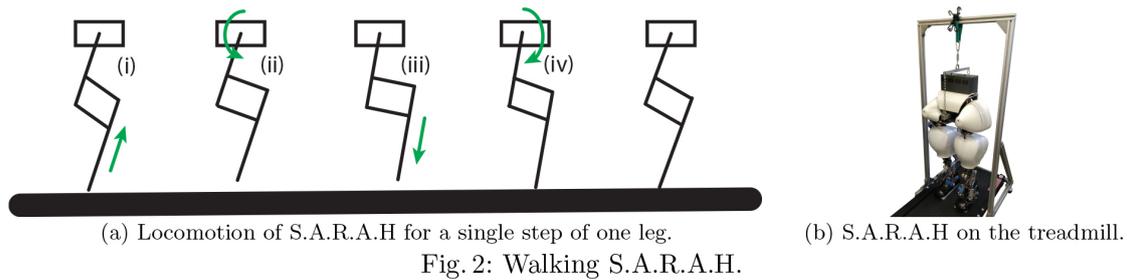
(a) Locomotion of S.A.R.A.H for a single step of one leg.

(b) S.A.R.A.H on the treadmill.

Fig. 2: Walking S.A.R.A.H.

III. S.A.R.A.H.'S PRELIMINARY PERFORMANCE

The first prototype does not include the abduction/adduction actuators and in its' current state, the hydraulics are disabled. For that reason, all the experiments were undertaken with S.A.R.A.H. hanging from an external structure from a substantially stabilising elastic support, as can be seen in Fig.2b.

The prototype weighs $45kg$ (50% actuators/batteries/hydraulics, 25% skeleton, 25% shell) and is able to make steps with a maximum stride length of $5cm$ and stride rate of 140 *steps/minute*. The stride rate is comparable to humans' running [5], however the step is still too small. Its operational time is up to 1 hour of continuous walk.

The neural network is able to predict the region in which the robot may fall and generate a countermove in order to keep the main body stable. The algorithm is run on a RPi3 and has a decision time of $50ms$ ($20Hz$) and is quicker than the human reflex time ($2 - 5Hz$) [2, 3, 4].

I.V. DISCUSSION

Thus far, the combination of the novel actuators (provide high speed limb's motion) with Neural Networks (provide the correct timing and choice of limb) had positive results. The Neural Network offers a novel alternative to classical control theory and suits the quasi on/off activation control of the pattern generators. The skeletal design reduces DoFs and number of actuators required to implement leg shortening during locomotion. The gait is bioinspired, with quick limb movements interspaced with time delays during which, the hydraulics are bracing the actuators offering high energy savings.

V. FUTURE WORK

In the short-term, the first aim is to add the missing actuators and, in turn, perform tests in sideways motion. The second aim, is to enable the hydraulics and perform the tests without the weight supports. In the long-term, when the second prototype is developed, the weight of the structured will be reduced and the hydraulics system will be redesigned to allow greater rotation in each joint.

REFERENCES

1. Motion Robotics LTD, https://www.motion-robotics.co.uk/

2. Abbasi-Kesbi, R., Memarzadeh-Tehran, H., Deen, M.J.: Technique to estimate human reac- tion time based on visual perception. Healthcare Technology Letters 4(2), 73–77 (2017), http: //digital-library.theiet.org/content/journals/10.1049/htl.2016.0106

3. Birren, J.E., Botwinick, J.: Age Differences in finger, jaw, and foot reaction time to auditory stimuli. Journal of Gerontology 10(4), 429–432 (1955)

4. Grice, G.R., Nullmeyer, R., Spiker, V.A.: Human reaction time: toward a general theory. Journal of Experimental Psychology: General 111(1), 135–153 (1982)

5. Latt, M.D., Menz, H.B., Fung, V.S., Lord, S.R.: Walking speed, cadence and step length are selected to optimize the stability of head and pelvis accelerations. Experimental Brain Research 184(2), 201–209 (2008)

6. Microchip, A.: SAM C21 Xplained Pro Evaluation Kit (2017), http://www.atmel.com/tools/ATSAMC21-XPRO.aspx

7. RaspberryPi: Raspberry Pi 3 Model B (2017), https://www.raspberrypi.org/products/raspberry-pi-3-model-b/

8. Taylor, C.R., Heglund, N.C., Maloiy, G.M.: Energetics and mechanics of terrestrial locomotion. I. Metabolic energy consumption as a function of speed and body size in birds and mammals. The Journal of experimental biology 97(1), 1–21 (1982)

Will robots suffer from road rage?

Chris Lamb[1] and Gary Staunton[1]
1. RACE (UKAEA), Culham Science Centre, Abingdon, OX14 3DB, UK

I. THE PRIZE

The first advanced robot many we experience may well be an autonomous vehicle (or driverless car). Autonomous Vehicle (AV) technology has made huge strides in recent years moving from a mainstay of science fiction to the first forays on public roads. Indeed, AV are almost unique in technology development in so far as estimates of when they will reach market are being brought forward – industry predictions now talk of the majority of new car sales in 2030 being of vehicles with high levels of autonomy. This optimism on early uptake is based on a combination of developments in sensing, data processing, data compression, data storage and machine learning.

The promise in AV stems from a wide range of potential and perceived benefits, the biggest of these is increased road safety through a reduction in the number of driver error-induced accidents – where research shows that around 90% of all motor vehicle crashes are caused, at least in part, by human on the UK economy will be £51 billion in 2030 based on AV creating 320,000 additional jobs, avoiding 25,000 serious accidents and saving 2,500 lives between now and 2030 (KPMG, 2015).

II. THE CHALLENGES

The progression to where cars require no human input is a complex and multi-dimensional one, and to aid understanding of this, the Society of Automotive Engineers published a classification system and supporting definitions that are widely used across the automotive sector. This approach is summarised in Figure 1. Today we see cars such as the Tesla operating at Level 3, but an increasing number of Level 4 cars are being tested. The final step from Level 4 to 5, which will see vehicles being able to undertake any end-to- end journeys without any supervision from a driver, will be transformative, but also hugely challenging with technological, social, cultural, political, commercial and legal implications. Not least
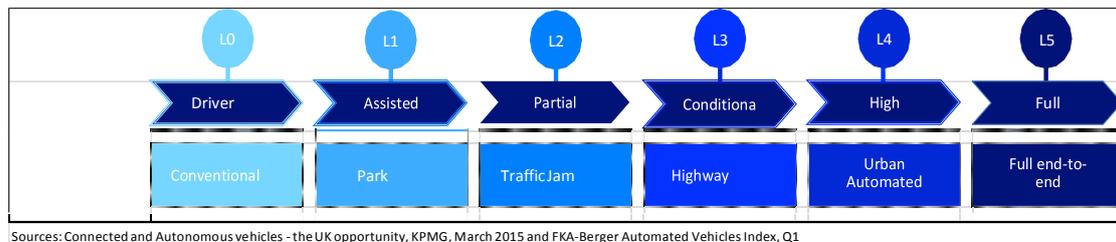

Figure 1: SAE Levels for Automated Driving Systems

error (US National Department of Transportation , 2008). There are however, numerous other benefits including: improved mobility for the disabled and elderly; reduced road congestion via reactive traffic flow control; productive travel time; higher utilisation of individual vehicles reducing the number of vehicles required per capita; and a reduced need for parking, freeing-up space in urban areas. The associated economic impact of the technology is also considerable - with KPMG reporting that the total impact of AV in terms of how human drivers will interpret the AI-driven decisions of an AV.

The challenges facing the AV community as they attempt to transform the way humans interact with our cars are numerous – and not all technical. Along the way we will have to address questions such as: How do you fully prepare AVs for use on open roads without fully characterising their interactions with driven vehicles in all conditions? How do you characterise these interactions without

exposing the public to AV technology before it is mature enough for it to be safe? How will road users behave towards autonomous vehicles? Will people give them a wide berth out of fear of them doing something unexpected? Or will the public test the limits of the technology under the assumption that the technology should be smart enough to cope with anything they throw at them? How do you start introducing AVs into the roads? How will an AV be insured for use? How will the public react to the first AVs incidents?

Part of the challenge lies in how we transition from roads where all the vehicles are controlled by a human driver to one where all vehicles are computer controlled with predictable behaviour and responses. While the end scenario of pervasive, connected, fully-integrated autonomous vehicles is relatively easy to imagine, the journey to get there during which driven and driverless cars interact heavily, can look long, treacherous and chaotic. And it is in this mixed-mode that questions such as 'will robots suffer from road rage?' will need to be answered – where the opening hypothesis is that the robot will not be the bully, but may well be bullied by other (human) road users.

I.V. PUBLIC AND STAKEHOLDER PERCEPTION

A feasibility study funded by Innovate UK and CCAV (Centre for Connected Autonomous Vehicles), (Westbourne Engagement, 2016), tried to answer some of the earlier posed questions. It concluded that stakeholders were significantly more positive towards the concept of driverless cars on UK roads (81%) than members of the public (54%) indicating that there is much to do in order to bridge the gap in public perception of the technology.

Regarding safety, it was largely accepted (59% of respondents) that the roads would be safer with driverless car technologies, for example they would reduce speeding and dangerous manoeuvres, however, there were concerns about security, standards and whether any technology could be truly prepared for all eventualities. But again, members of the public were found to feel

significantly less positive (49%) here than stakeholder groups (80%) reinforcing the work required to give the public the same level of confidence as those connected to the field. Stakeholders are aware of this and described how they believe "public perception of safety concerns to be a major barrier to the acceptance of fully automated vehicles, and how new technologies would need to be gradually introduced to navigate this." As important as it is to understand public perceptions towards AV and how they differ to stakeholder perceptions, it is possible that the differing views of these groups on how AV should react in complex real-world situations could trigger hostile responses on the part of the human driver. In such cases AV could well become the victims of road rage.

V. THE RESPONSE

The need to meet this challenge means that the emerging AV industry is continually testing and developing its vehicles. Indeed, the Department for Transport code of practice for driverless car testing states (Department for Transport, 2015):

"*Manufacturers have a responsibility to ensure that highly and fully automated vehicle technologies undergo thorough testing and development before being brought to market. Much of this development can be done in test laboratories or on dedicated test tracks and proving grounds. However, to help ensure that these technologies are capable of safely handling the many varied situations that they may encounter throughout their service life, it is expected that controlled 'real-world' testing will also be necessary*".
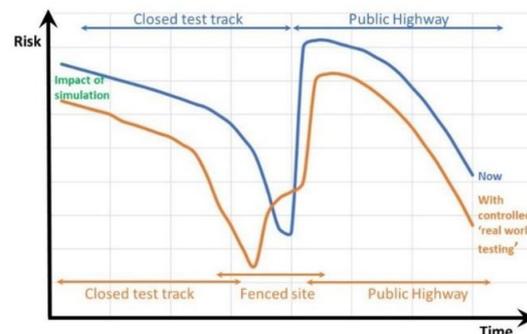

Figure 2: De-risking AV introduction

The transition from closed to open road testing is crucial and as such the lessons learnt from "controlled real-world testing" will have huge relevance to the safe emergence and acceptability of AV. Without "controlled real-world testing" on a substantive, mixed road network where other vehicles, pedestrians, cyclists etc. have free (and random) access within a suitably monitored and supportive environment, there is a risk that the process of gaining 'authority to operate' from the general public could become even more problematic.

Another output of the CCAV-Innovate UK feasibility study, was a transport plan that took the learnings from the stakeholder consultation, combining a gradual introduction of AVs on to roads via a novel intermediate step referred to as 'fenced site testing'. Figure 2 shows how a combination of simulation and the intermediate 'Fenced Site' step can de-risk the transition from closed to open road testing by feeding back learnings from early interactions into development activities.

The plan outlined the three phases of use. 'Phase 1' is defined as the use of autonomous vehicles in a controlled environment around an AV hub on a closed site. 'Phase 2' is the use of a whole access-controlled or 'fenced' site, as a validation area, and involves the use of vehicles by workers on site to introduce real word aspects in a controlled manner. 'Phase 3' involves the transport of persons over short and pre-defined journeys on public roads. Culham Science Centre was identified as an ideal location and has since seen Phases 1 and 2 initiated, with planning underway to connect the Science Centre to Culham Train station and other locations in Oxfordshire for Phase 3.

The interaction between human and robot (AV) through this period, could prove critical in the safe and controlled introduction of driverless cars on to our roads and a measure of our success in achieving this will be the extent to which human drivers do not try to take advantage of the fact that AV are 'hard wired' to obey the rules of the road through hostile and intimidating behaviours.

REFERENCES

1. Department for Transport. (2015). A Pathway to Driverless Cars: A Code of Practise for Testing.
2. KPMG. (2015). Connected and Autonomous Vehicles - the UK Opportunity.
3. US National Department of Transportation . (2008). National Motor Vehicle Crash Causation Survey. *Report to Congress*.
4. Westbourne Engagement. (2016). PAVE Public Consultation Findings Report.

Using Robots to Model Mental Disorders∗

Matthew Lewis and Lola Canamero Embodied Emotion, Cognition and (Inter-)Action Lab, University of Hertfordshire, UK {M.Lewis4|L.Canamero}@herts.ac.uk

ABSTRACT

We are currently at a point where the use of robots to model human mental disorders is possible, and this capability will only increase. By considering the lessons learned from animal models, we argue that robot models of human mental disorders can complement existing approaches in mental health research.

I. INTRODUCTION

We are currently at a point where the use of robots to model human mental disorders is possible, and this capability will only increase. It is true that current robots are a long way from re- producing the capabilities of human beings, and it might be seen as insulting that complex human disorders could be modeled with such distant approximations. However, for many years, animal models of mental disorders have been used for human mental disorders. We therefore take stock, and examine how we should progress in the use of robot models.

II. MODELS OF MENTAL DISORDERS

In his section, we define and briefly discuss four types of models for mental disorders.

A *conceptual model of a mental disorder* is a theoretical construct that links underlying causes (etiology), either proposed or observed, with observed symptoms and correlates. A conceptual model serves as a framework for understanding, and should have explanatory and predictive power with respect to the condition being modeled. For example, Shafran [2] gives five models for Obsessive-Compulsive Disorder based variously on: a faulty appraisal of normal intrusive thoughts, an excessive emphasis on control of one's own thoughts, and a self-perpetuating mechanism of checking behaviour. There is not necessarily a need for one "true" model, and different models may be complementary, having different emphases, levels of abstraction or uses

An *animal model of a mental disorder* is a non- human animal used to study brain–

behaviour relations with the goal of gaining insight into, and to enable predictions about, these relations in humans [3]. Animal models may be induced by genetic manipulation, drugs, or by environmental manipulation. Alternatively, they may be naturally occurring. They have the advantage that they model a complete system (organism and environment), and they use a real animal, hence a real nervous system. However, there are limits to how closely a non-human animal can be used to model human mental disorders. There are also ethical issues associated with animal experimentation.

A *computational model of a mental disorder* is a realisation, or partial realisation, of a theoretical model in a computer. The emerging field of computational psychiatry includes within its scope the development of computational models of psychiatric disorders [4]. These models have the advantage that, by their nature, they are highly specified and so any results should be replicable and can be analysed in detail. However, due to the complexity of implementing such a model, they are typically only partial implementations (e.g. of a neurological subsystem) or they work at a relatively high level of abstraction. In addition, they do not necessarily include any behavioural element, a true closed-loop interaction with the environment, or the effects of contextual and environmental elements.

A *robot model of a mental disorder* include an embedded realisation of a conceptual model in an embodied, interacting robot and its environment. This introduces elements that are present in animal models, but which purely computational models lack. Thus far, there have been relatively few explicit robot models of mental disorders, with work Yamashita and Tani [5] being one of the rare examples. However, work in biologically-inspired autonomous robots is linked, since models of behaviour can also potentially serve as models of pathological behaviour. For example, our previous work on pleasure and behaviour [6] has links to addiction.

III. LEARNING FROM ANIMAL MODELS

In order to maximise the potential of robot models, it is instructive to learn from what has been learned from many years of using animal models. Animal models can be evaluated and validated along four criteria [7]: *face validity* (phenomenological similarity), *construct validity* (validity of the underlying mechanism), *predictive validity* (whether, for example, the model can predict effective interventions) and *reliability* (whether results are robust and reproducible).

Thinking about how these criteria relate to robot models, we make the following observations. Face validity can be easy to achieve in robot models: a robot can simply be programmed to behave in a pathological fashion. However, with- out construct validity, in this case face validity becomes meaningless. Therefore, we should not work from the direction of face validity, but use it as a validation criterion.

If robot models are based on theoretical models, then construct validity either comes from this development process, or, if the model is hypothetical, then the robot model serves are a test of the model itself. Predictive validity is important in the context of developing clinical interventions, it is there- fore something that should be targeted by robot models in order to maximise their contribution to translational research.

Reliability is something that to some extent comes naturally from using robot models: it is possible to replicate experiments. However, since it may be the theoretical model that is of interest, not the specific implementation, efforts should also be made to produce alternative implementations of the same theoretical model, to demonstrate that the behaviour of a model is not due to a detail of implementation (you may then ask if that implementation detail should be included in the theoretical model).

Finally, with robot models we can easily "look inside" our model to examine cognitive processes as they happen. While this can be done to some extent with animals, it is limited, and the techniques may be invasive. By doing this we may gain insights into how mental illness is experienced from the inside (symptoms such as con- fusion, alienation from one's own actions, paranoia), going beyond the behavioural aspects that are the most readily examined in animal models.

I.V. ADVANTAGES OF ROBOT MODELS

One significant advantage of computational models, including robot models, over animal models is that it allows precise operationalisation and explicit implementation of an underlying theoretical model. While models may be implemented in animals, experimenters may not always have enough control over the biology to implement it a theoretical model as precisely as desired.

In addition to this, robot models have vastly reduced ethical issues compared to animal models. It is also easier to control environmental con- founding factors that are not part of the model with robots than with animals. For example, experimental results in animals have been unexpectedly affected by experimenter smells [8]. Such effects can be limited in robots since we have more knowledge of, and control over, their sensory systems.

Bearing in mind the criterion of predictive validity, above, robot models

may also allow us to test interventions. For example, they may test simulated drugs that have a targeted effect on one element of the model, such as a receptor, when no such chemical is yet known, or when known chemicals have undesirable side effects. However, in or- der to do this, potential targets (pharmaceutical or otherwise) needs to be part of the underlying model.

Robot models can also take advantage of their embodied aspect. Mental disorders frequently have embodied aspects, such as a distorted sense of the body, and some therapeutic interventions are also embodied (e.g. exercise, art therapy). Symptoms of mental disorders may also be partly due to dysfunctions in the perception- action loop. By taking this into account, robot models can be used as tools where purely computational models are not suitable.

Robot models for mental disorders are a promising direction for research, to be used in conjunction with existing animal and purely computational models. However, in order to achieve their potential thought needs to be given to how they are used. Implementation of existing theoretical models has promise, but these models need to be assessed in terms of face validity (of both phenotypes and "hidden" endphenotypes), predictive validity and reliability. With predictive power, robot models can then contribute to translational research of treatments.

REFERENCES

1. M. Lewis and L. Cañamero, "Robot models of mental disorders," in *Proc. 7th International Conference on Affective Computing and In- telligent Interaction, Workshops and Demos (ACIIW 2017)*, (San Antonio, TX), pp. 193– 200, IEEE, 2017.

2. R. Shafran, "Cognitive-behavioral models of OCD," in *Concepts and Controversies in Obsessive-Compulsive Disorder* (J. S. Abramowitz and A. C. Houts, eds.), pp. 229– 260, Boston, MA: Springer, 2005.

3. F. J. van der Staay, "Animal models of behav- ioral dysfunctions: Basic concepts and classi- fications, and an evaluation strategy," *Brain Research Reviews*, vol. 52, no. 1, pp. 131–159, 2006.

4. Q. J. M. Huys, T. V. Maia, and M. J. Frank, "Computational psychiatry as a bridge from neuroscience to clinical applications," *Nature Neuroscience*, vol. 19, no. 3, pp. 404–413, 2016.

5. Y. Yamashita and J. Tani, "Spontaneous prediction error generation in schizophrenia," *PLoS ONE*, vol. 7, no. 5, pp. 1–8, 2012.

6. M. Lewis and L. Cañamero, "Hedonic qual- ity or reward? A study of basic pleasure in homeostasis and decision making of a moti- vated autonomous robot," *Adaptive Behavior*, vol. 24, pp. 267–291, 2016.

7. P. Willner, "Validation criteria for animal models of human mental disorders: Learned helplessness as a paradigm case," *Progress in Neuro-Psychopharmacology and Biological Psychiatry*, vol. 10, no. 6, pp. 677–690, 1986.

8. R. E. Sorge, L. J. Martin, K. A. Isbester, S. G. Sotocinal, S. Rosen, A. H. Tuttle, J. S. Wieskopf, E. L. Acland, A. Dokova, A. Kadoura, P. Leger, J. C. S. Mapplebeck, McPhail, A. Delaney, G. Wigerblad, A. P. Schumann, T. Quinn, J. Frasnelli, C. I. Svens- son, W. F. Sternberg, and J. S. Mogil, "Olfac- tory exposure to males, including men, causes stress and related analgesia in rodents," *Na- ture Methods*, vol. 11, no. 6, pp. 629–632, 2014.

Camera-based Flexible Force and Tactile Sensor

Wanlin Li[1], Jelizaveta Konstantinova[1], Yohan Noh[2], Akram Alomainy[3] and Kaspar Althoefer[1]

[1] Advanced Robotics @ Queen Mary (ARQ), Queen Mary University of London, London, UK
[2] Department of Informatics, King's College London, [3] School of Electonic Engineering and Computer Science, Queen Mary University of London

ABSTRACT

Tactile and force perception for robotic application is an important feature required to detect and measure physical interaction with the environment. Grasping, object recognition and detection are examples of a field that can largely benefit from multi-modal tactile and force feedback. We present a camera-based flexible sensor that can measure both tactile and force information. In this work design and measurement principle of the device are discussed. The sensor working principle is based on the deformation of elastomers using LEDs to illuminate the contact area, and a camera to capture the resultant deformation of a soft part that is in contact with the environment.

I. INTRODUCTION

The principle goal of the proposed research is to investigate the design and application of a hybrid, optical- based three-axis force sensor and tactile sensor, for the purpose of improvement of capability for robot touch sensors [1-6]. It is desirable for tactile sensors [7-12] to measure both the external contacted forces and moments and observe the patterns of the contact surface. For instance, it is important for a robot hand to perform manipulation tasks [13-15], such as grasping and exploration, using tactile sensors mounted on the fingertip to provide sensory information. With the rapid development of miniature cameras and image processing techniques, optical-based tactile sensor have been popular in the past ten years [2][3][13]. For example, TACTIP sensor [2] is a biologically-inspired sensing device with a dome structure, composed of a silicone outer skin with inward facing nodule pins. The sensor is capable of sensing pressure, shear force, surface strain for detecting edges, and texture, but disadvantageously its resolution is relatively low and the captured image warps due to the hemispherical surface. The Optical Three-axis tactile sensor [3] is a domelike robotic finger that is capable of sensing normal and shearing force. However, since there are 41 rubber sensing elements attached to the dome, the data processing is computationally expensive. Thus, we present a flat-surface sensor with eight force sensing elements and tactile information capture component located in the center. We use a high- definition webcam for the acquisition of deformation due to applied forces. In this research we present a novel device comprised of elastomer that measures both force and tactile information (Figure 1).
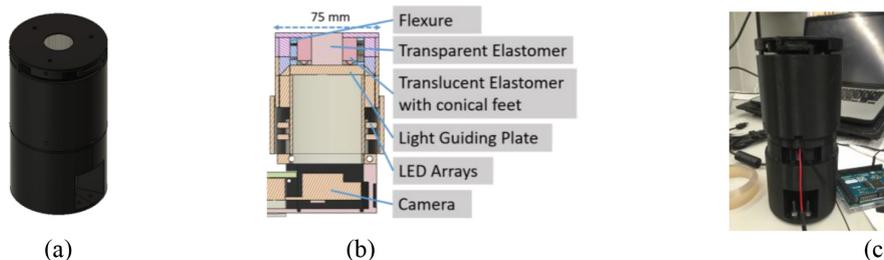

Figure 1. Force and tactile sensor design. (a) Model of force and tactile sensor. (b) Schematic design (c) Prototype of force and tactile sensor.

II. SENSOR DESIGN

We introduce a novel sensor that can be miniaturised and integrated with a robotic finger, Figure 1. The proposed sensor can be used to measure three force and moment components and contact pattern. The sensor consists of the following parts: elastomer part, force sensitive structure, LED arrays and CCD camera.

The interface of the device that is in contact with the environment is the elastomer part together with a flexible force sensitive structure. The elastomer part is composed of two elastomers coated with a hollow membrane on top (a transparent elastomer is wrapped in a translucent elastomer with eight conical leg-like sensing elements underneath). The force sensitive structure resembles a flexible cantilever structure. In addition, there is a rigid structure that

sensor allows high-resolution sensing with a spatial resolution of 2 microns.

To give a better understanding of the working principle of the tactile sensor, simulation and real case are presented when applying an external force (Figure 2). The deformations of the elastomer part can be segmented in two sections. The first section is the centre area and the second corresponds to the outer area showing the conical legs. Initially when there is no contact with the sensor, the centre area shows the natural environment scene. The camera captures each conical leg as a circle with a point in the centre where the circle is the contour of the feet cap attached to the translucent elastomer and the point is the tip contacting the supporting plate. Figure 2(c) shows the image capture resulting from a lateral force being applied, and the deformations of the eight conical feet are captured at the outer area.

(a) (b) (c)
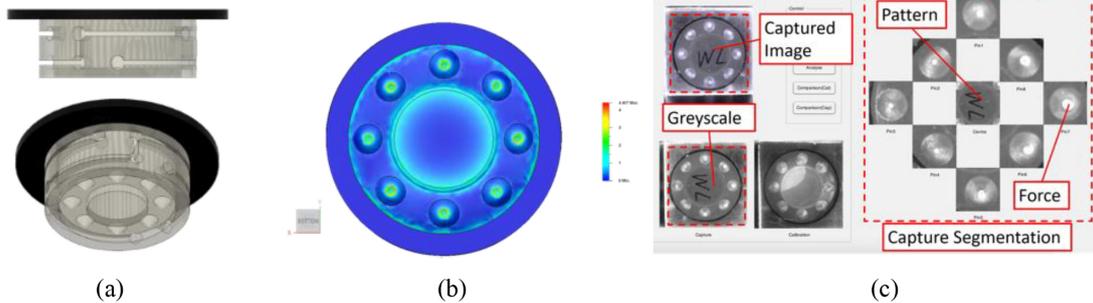
Figure 2. Force sensitive structure and elastomer part. (a) CAD design of the force sensitive structure; (b) FEA simulation shows the strain behaviour under normal load of the combination of the force sensitive structure and the elastomer part; (c) User Interface of the sensor when lateral load is applied on the sensor.

stabilizes the soft elastomer part, Figure 2 a. The elastomer part and flexure are fixed on a hard transparent acrylic sheet. The elastomer part is illuminated with white light through the LED array placed inside the device. 3D-printed dark covers outside the device are used to block the external light from disturbing the illumination inside. The camera captures deformations in both elastomers to measure the applied force based on the deformations of eight individual legs circularly located on the bottom side of the outside elastomer. The tactile information will be measured based on the pattern presented by the transparent inner elastomer with black marks on its surface. However, the current sensor has not attached the marks so marks cannot be seen in Figure 2(c). The

III. CONCLUSIONS AND FUTURE WORK

In this work, we introduce the design of a novel hybrid, optical-based tactile sensor that can sense both force information and tactile information. The device is based on a combination of a force sensitive structure and an elastomer part. A calibration will be performed to obtain the calibration matrix based on two cases (normal force and normal force combined with two lateral moments). Based on an initial experimental evaluation, the measurement range of the proposed sensor can sustain 12 N axial load and 2N lateral load. The camera can capture the image of the contact surface and estimate the applied force by regression method. Marks will be added on the transparent elastomer

surface and tactile information can be measured by finding the shift vector in optical flow method. The number of the conical legs can be reduced to three instead of eight to measure the three axis force components and this could also reduce the computation during the real-time processing. Smaller camera (Logitech C270 for example) can be used to for the sensor miniaturisation.

REFERENCES

1. R. Lazzarini, R. Magni and P. Dario, "A tactile array sensor layered in an artificial skin", in Proceed- ings of the IEEE/RSJ International Conference on Intelligent Robots and Systems, Human Robot In- teraction and Cooperative Robots, vol. 3, pp. 114-119, 1995.
2. Winstone, G. Griffiths, T. Pipe and J. Rossiter, "TACTIP—Tactile fingertip device texture analysis through optical tracking of skin features", in Biomimetic Biohybrid Systems, pp. 323-334, 2013.
3. Ohka, Y. Mitsuya, I. Higashioka and H. Kabeshita, "An experimental optical three-axis tactile sensor for micro-robots", in Robotica 23, 457–465, 2005.
4. P. Polygerinos, L.D. Seneviratne, R. Razavi, T. Schaeffter and K. Althoefer, "Triaxial catheter-tip force sensor for MRI-guided cardiac procedures", in IEEE/ASME Transactions on mechatronics, 18, pp. 386-396, 2013.
5. S. Denei, P. Maiolino, E. Baglini and G. Cannata, "Development of an integrated tactile sensor system for clothes manipulation and classification using industrial grippers", in IEEE Sensors Journal, pp. 99, 2017.
6. J. Rossiter, T. Mukai, "An LED-based tactile sensor for multi-sensing over large areas", in IEEE 5th International Conference on Sensors (IEEE-Sensors), pp. 835–838, 2006.
7. E.S. Hwang, J.H. Seo and Y.J. Kim, "A polymer-based flexible tactile sensor for both normal and shear load detections and its application for robotics", in IEEE/ASME Journal of Microelectromechan- ical Systems, vol. 16, no. 3, pp. 556-563, 2007.
8. W. Yuan, R. Li, M.A. Srinivasan and E.H. Adelson, "Measurement of shear and slip with a GelSight tactile sensor", in 2015 IEEE International Conference on Robotics and Automation (ICRA), pp. 304- 311, 2015.
9. Lowe, A. King, E. Lovett and T. Papakostas, "Flexible tactile sensor technology: bringing haptics to life", in Sensor review, 24(1): 33-36, 2004.
10. M.K. Johnson, E.H. Adelson, "Retrographic sensing for the measurement of surface texture and shape", in Computer Vision and Pattern Recognition, 2009. CVPR 2009. IEEE Conference on. IEEE, pp. 1070-1077, 2009.
11. Y. Yamada, M. Morizono, U. Umetani and T. Takahashi, "Highly soft viscoelastic robot skin with a contact object-location-sensing capability", in IEEE Transactions on Industrial Electronics, 52(4):960–968, 2005.
12. M.Y. Cheng, C.M. Tsao, Y.T. Lai, Y. Yang, "A novel highly-twistable tactile sensing array using extendable spiral electrodes", in IEEE 22nd International Conference on Micro Electro Mechanical Systems (MEMS), pp. 92–95, 2009.
13. W. Yuan, M.A. Srinivasan and E.H. Adelson, "Estimating object hardness with a gelsight touch sensor", in 2016 IEEE/RSJ International Conference on Intelligent Robots and Systems (IROS), IEEE, pp. 208-215, 2016.
14. M. Ohka, N. Morisawa and H. Yussof, "Trajectory generation of robotic fingers based on tri-axial tac- tile data for cap screwing task", in IEEE International Conference on Robotics and Automation, ICRA'09, IEEE, pp. 883-888, 2009.
15. H. Yousef, M. Boukallel and K. Althoefer, "Tactile sensing for dexterous in-hand manipulation in ro- botics—A review", in Sensors and Actuators A: physical, 167(2): 171-187, 2011.
16. Y. Noh, S. Sareh, J. Back and K. Althoefer, "A three-axial body force sensor for flexible manipula- tors", in 2014 IEEE International Conference on Robotics and Automation (ICRA), IEEE, pp. 6388- 6393, 2014.

A proposed structure to capture the operational and technical capabilities of different robots

Manal Linjawi and Prof Roger Moore, Department of computer science, University of Sheffield, Sheffield, UK {malinjawi1,r.moore}@sheffield.ac.uk

I. INTRODUCTION

Every day a new robot is developed with advanced characteristics and sophisticated qualities. With this expansion in robot technology comes a need for a classification scheme that allows us to talk about what any robot (current or future) can and cannot do, regardless of the domain it operates in. However, most robot classification systems (e.g., domain [14], field [13], size [4], ontology [11]) do not cover all aspects of the robot's capabilities and are not able to define the difference between robots in different fields, or even in the same field. There is therefore a need to develop a classification system for robot characteristics and capabilities that would describe robots in abstract dimensions to allow direct comparisons and easier documentation and avoid misrepresentation. Here we propose such a conceptual structure that allows us to represent the features and conceivable ability of any robot in any field. The conceptual structure would enable designers to optimize robot capabilities against application requirements and also help the application developers to select the most appropriate robot.

II. THE STRUCTURE

The proposed structure divides robot characteristics into three layers [9], as presented in the Fig.1. *The robot features layer,* presented in Fig.1 in layer(1), covers the robot's hardware and software. The hardware features capture all the sensors, actuators, kinetics, kinematics, embodiment, morphology, locomotion, etc. The software features capture the operating systems (e.g., ROS, or YARP), architectures and any programmable modules installed within the robot (e.g.,visual or tactile processing) [14]. This layer also covers networking and memory concepts such as Wi-Fi and iCloud. The hardware and software determine the robot's capabilities and type of interactions [8][2].

A. *The robot technical capabilities layer,* presented in Fig.1 in layer(2), is divided into three parts:
  1. The first part of the technical capabilities layer presents the robot's capabilities and categorizes them into the following areas, as shown in Fig.1 in layer (2) section(A):

(a) The perception and interpretive capabilities, presented in (A-1), categorize the robot's perception capabilities into social perception, cognitive perception, and physical perception. This also includes the robot's modes of perception, known as the interaction mode, which represents the data-collection method, e.g., visual, auditory, and physical (mechanical, magnetic, chemical, signal, haptic). This data is translated in order to perform any of the perception capability types[14].

(b) The robot's task abilities, presented in (A-2), categorize the tasks that the robot can perform into physical tasks (e.g., mobility and manipulation), social tasks (e.g., emotions, social structure, relationships and behaviours [3][5]), and cognitive tasks (e.g., learning, reasoning, skill gathering, and problem-solving) [14].

(c) The robot's actions and envisioning ability, presented in (A-3), categorizes the actions performed by the robot as physical, cognitive, or social. The action

performed by the robot is considered as one of the listed task abilities mentioned above in (A-2) [14].

The technical layer also covers the robot's general abilities. These are not included in any of the categorized capabilities above but are considered to be a higher level of ability, such as task complexity ability level, adaptability, and dependability. This layer also includes the robot's level of autonomy [14].

2. The second part of the technical capabilities covers the interaction capabilities of the robot, presented in Fig.1 in layer(2) section(B). This illustrates the type of interactions towards humans, other robots, or the environment [17]. The interaction is performed according to the robot's capabilities and represents the interaction cycle, also known as 'the robot-world feedback loop' [15]. The interaction cycle is categorized as cognitive, social or physical [14]. The dynamic interaction cycle presents the robot's behaviour or action for a specific skill within a defined intelligence (presented in the next section). This part also includes various interaction classifications such as paradigms, roles [2], and social models of interactions [3][1], etc.

3. The third part of the technical capabilities clarifies the 'intelligence' that the robot acquires, presented in Fig.1 in layer(2) section(C). It outlines the purpose of the robot's performance and describes the external perception of its actions [12]. This intelligence is obtained through a specific

behaviour or a set of actions. [6]. There are several types of intelligence/skill that might be acquired by the robot [16][10][7]: physical-morphological intelligence, such as bodily-kinaesthetic skills or visual-spatial skills; cognitive intelligence, such as learning logical-mathematical skills, exchanging information; social intelligence, such as capturing musical or verbal-linguistic skills; and collective intelligence, which captures emerging skills in combining either heterogeneous or homogeneous robots, such as collaboration or cooperative skills.

B. *The robot operational capabilities layer,* presented in Fig.1 in layer(3), defines the robot's operational profile in terms of cost, duration, safety, testing, training, acceptance, and usability. This also covers the operational environment capabilities of the robot (e.g., ground, aerial, or underwater [13]).

III. CONCLUSION

The proposed structure provides a straightforward method for distinguishing robot characteristics across any domain and capability profile. It also delivers a schematic model to support all robots in the robotic domain with a comprehensive description. The structure also enriches the robotic field and its literature with a new classification system for better robot deployment. In particular, the proposed scheme provides an important extension to the 'Robotic 2020, Multi-Annual Roadmap'(MAR) [14].

REFERENCES

1. Breazeal, C.: Toward sociable robots. Robotics and autonomous systems 42(3), 167–175 (2003)
2. Breazeal, C.: Social interactions in HRI: the robot view. IEEE Transactions on Systems, Man, and Cybernetics, Part C (Applications and Reviews) 34(2), 181–186 (2004)
3. Dautenhahn, K.: Socially intelligent robots: dimensions of human–robot interaction. Philosophical Transactions of the Royal Society of London B: Biological Sciences 362(1480), 679–704 (2007)
4. Dobra, A.: General classification of robots. size criteria. In: Proc. of Robotics in Alpe-

Adria-Danube Region (RAAD). pp. 1–6. IEEE (2014)
5. Fong, T., Nourbakhsh, I., Dautenhahn, K.: A survey of socially interactive robots. Robotics and autonomous systems 42(3), 143– 166 (2003)
6. Kihlstrom, J.F., Cantor, N.: Social intelligence. Handbook of intelligence 2, 359–379 (2000)
7. ManagementMania: Thorndike's intelligence theory. Retrieve from https://managementmania.com/en/thorndikes -intelligence- theory (2016)
8. McGrenere, J., Ho, W.: Affordances: Clarifying and evolving a concept. In: Graphics interface. vol. 2000, pp. 179–186 (2000)

9. Moore, R.K.: The future of speech-based services: bringing in the benefit. COST249 workshop on Voice Operated Telecom Services (2000)

10. Pal, H. R., P.A..T.P.: Theories of intelligence. Everymans Science 39(3), 181–192 (2004)

11. Prestes, E., Carbonera, J.L., Fiorini, S.R., Jorge, V.A., Abel, M., Madhavan, R., Locoro, A., Goncalves, P., Barreto, M.E., Habib, M., et al.: Towards a core ontology for robotics and automation. Robotics and Autonomous Systems 61(11), 1193–1204 (2013)

12. Schaefer, K.E., Billings, D.R., Hancock, P.A.: Robots vs. machines: Identifying user perceptions and classifications. In: Proc. of Cognitive Methods in Situation Awareness and Decision Support (CogSIMA). pp. 138–141. IEEE (2012)

13. Siciliano, B., Khatib, O.: Springer handbook of robotics. Springer (2016)

14. SPARC Robotics, eu-Robotics AISBL, Brussels, Belgium: Robotics Multi-Annual Roadmap for Robotics in Europe, Horizon 2020 (2016)

15. Winfield, A.: Robotics: A very short introduction. Oxford University Press (2012)

16. Winfield, A.F.T.: How intelligent is your intelligent robot?. arXiv preprint arXiv:1712.08878 (2017)

17. Yanco, H.A., Drury, J.L.: A taxonomy for human-robot interaction. In: Proc. of AAAI Fall Symposium on Human-Robot Interaction. pp. 111–119 (2002)

An Optimised Deep Neural Network Approach for Forest Trail Navigation for UAV Operation within the Forest Canopy

B. G. Maciel-Pearson, Pratrice Carbonneu and T.P. Breckon, {b.g.maciel-pearson, patrice.carbonneu and toby.breckon}@durham.ac.uk Department of Computer Science, Durham University, UK

ABSTRACT

Autonomous flight within a forest canopy represents a key challenge for generalised scene understanding on-board a future Unmanned Aerial Vehicle (UAV) platform. Here we present an approach for automatic trail navigation within such an environment that successfully generalises across differing image resolutions - allowing UAV with varying sensor payload capabilities to operate equally in such challenging environmental conditions. Specifically, this work presents an optimised deep neural network architecture, capable of state- of-the-art performance across varying resolution aerial UAV imagery, that improves forest trail detection for UAV guidance even when using significantly low resolution images that are representative of low-cost search and rescue capable UAV platforms.

I. INTRODUCTION

Scene understanding within unstructured environments with varying illumination conditions are critical for autonomous flight within the forest canopy. Growing interest in solving this challenge has motivated researchers to investigate the use of Deep Neural Networks (DNN) to identify trail images for UAV navigation. However, in order to train such a DNN, a large volume of labeled data is required, which is challenging to obtain due to the target task in hand (i.e. sub canopy UAV operation).

The work of [3] gathered data by using a head-mounted rig with three cameras worn by a human trail walker, allowing their proposed DNN architecture to identify the direction of the trail in a given view - *lef t, right, f orward* . A similar approach is followed by [7] whereby a wide-baseline rig is used, also with three cameras mounted to gather data, which they used to augment the dataset of [3] (IDSIA dataset). As a result, the approach presented by [7] is capable of estimating both lateral offset and trail direction. In both cases [3, 7],

the authors, follow the common practice of dataset augmentation, via affine image transformations, which adds extra computation without any performance guarantees.

Alternatively, synthetic data, from virtual environment models, could potentially replace or at least supplement hard-won real environment data [5, 6, 9]. However, the significant discrepancy between synthetic data and real-world data often results in models that are trained only on synthetic environment examples not being able to directly transfer this knowledge to real-world operating tasks [2, 8, 5, 1].

Even when training a DNN using only real-world data, it is important to observe that models trained on a limited domain-specific dataset often fail to generalise successfully. In addition, since common DNN architectures require the dataset to be formed from fixed resolution images [4], modS.A.R.A.Hels commonly fail to generalize across domains.

Our work here is closely related to [3, 7, 2] and demonstrates that the same trail direction required for autonomous UAV navigation can be acquired by using imagery gathered by a single forward-facing camera (Figure 1). This is due the fact that the center of the forward-facing camera usually shows the trail ahead. Additionally, we demonstrate that a trail can be identified in unseen parts of a forest by training the model with data gathered across varying devices and camera resolutions. This not only facilitates more general data gathering but also eliminates the need for synthetic

In contrast to [3, 7], our approach uses only a single forward facing camera view which more representative of an operational UAV case. This image view is then itself cropped into *{left; right; forward}* which can be labeled for trail presence/absence (Figure 1).

Using the architecture of [3] (illustrated in Figure 2), we evaluate varying image resolution, the use of additional data augmentation (DA) and activation function (*tanh() / ReLU()*). DNN training uses a gradient descent optimiser, random weight initialisation with zero node biases and is performed over 90 epochs with
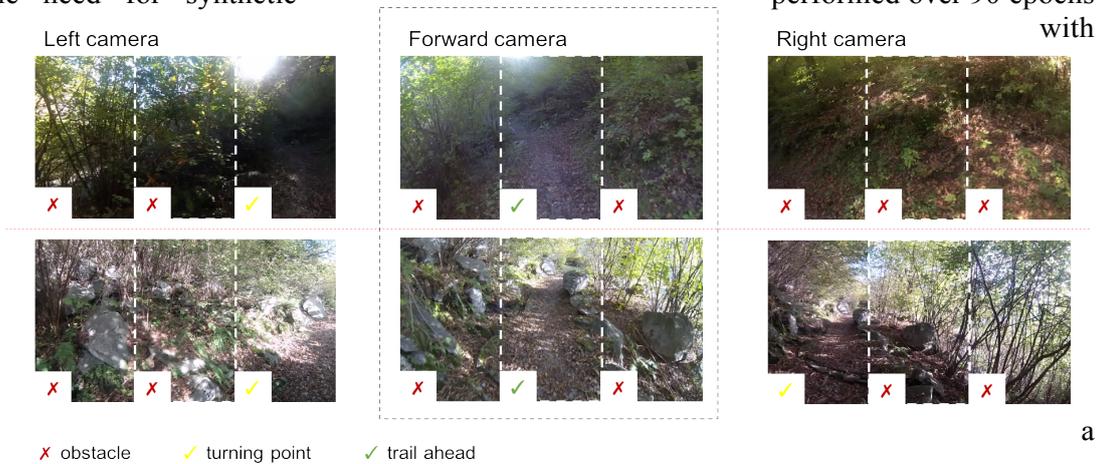
Figure 1: Comparison of three way image cropping performed on varied camera
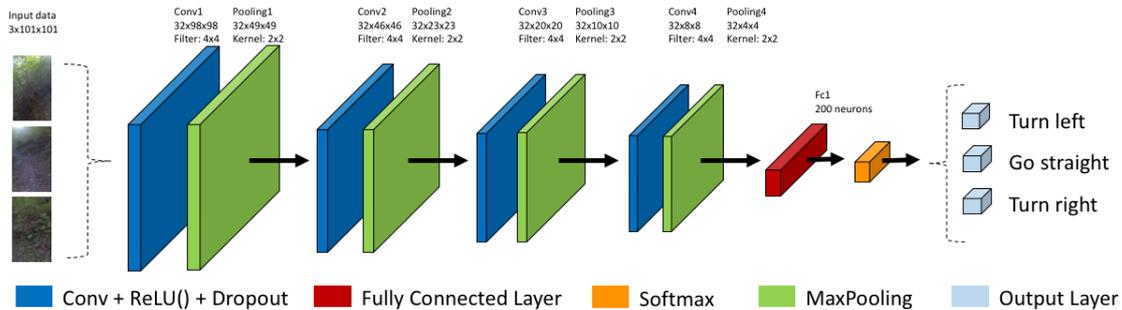
Figure 2: An outline of our DNN architecture - based on [3]

data and augmentation. As result, the same model can be used by UAV with different sensor payload capabilities.

II. METHOD

Here we were motivated by the three class problem presented by [3] in which an estimation of the trail direction, *{left; right; forward}* is achieved by processing an image triplet of left/right/forward camera views via a DNN.

0.05 reduction in learning rate per epoch (decay rate: 0.95). For both training and testing we use the high-resolution (752 480) IDSIA dataset (from [3]) and a low-resolution (106 240) Urpeth Burn (UB) dataset, gathered locally. For training 45,097 high-resolution and 32,017 low-resolution image were used, while for testing 12,251 high-resolution and 5,152 low-resolutions images were used. Further data augmemtation (mirror, translation &

rotation) was performed on a copy of this original dataset. For simplicity of reporting, we define *NA* as non augmented data obtained results and *DA* as data augmented obtained results (Table 1).

III. RESULTS

Our experimental results are divided into three sets:- (1) image triplet approach of [3] with differing activation functions (*tanh()/ReLU()* - Table 1 upper 2 sets), (2) our proposed approach (single forward view image, split into three views - Table 1 middle sets in bold) and (3) the impact of high/low/varied image resolutions on performance (Table 1 lower sets).

Overall we see what the use of the ReLU() activation outperforms tanh() and our approach gives high levels of accuracy without the need for data augmentation outperforming the prior reported results in [3] (*in fact no significant improvement was achieved by data augmentation*). Although our approach fails to generalise when trained with high-resolution images on to low resolution images, it achieves 82% accuracy when low-resolution images are added to the training dataset and achieves 78% accuracy for training and testing on low-resolution images only.

Method	Activation Function	Training Dataset	Testing Dataset	Training Loss	Training Accuracy	Test Loss	Test Accuracy
Giusti *et al.* [3] [DA]	*tanh()*	High	High	1.04	0.46	1.07	0.47
Giusti *et al.* [3] [NA]	*tanh()*	High	High	1.01	0.41	1.02	0.48
Giusti *et al.* [3] [DA]	*ReLU()*	High	High	0.02	1.00	2.97	0.59
Giusti *et al.* [3] [NA]	*ReLU()*	High	High	0.00	1.00	2.56	0.72
Our Approach [DA]	***ReLU()***	**High**	**High**	**0.18**	**0.92**	**0.26**	**0.89**
Our Approach [NA]	***ReLU()***	**High**	**High**	**0.07**	**0.97**	**0.31**	**0.89**
High Resolution[NA]	*ReLU()*	High	Low	0.17	0.94	1.00	0.44
Low Resolution [NA]	*ReLU()*	Low	Low	0.40	0.86	0.58	0.78
Varied Resolutions [NA]	***ReLU()***	**High+Low**	**Low**	**0.24**	**0.93**	**0.51**	**0.82**
Varied Resolutions [NA]	***ReLU()***	**High+Low**	**High**	**0.40**	**0.83**	**0.64**	**0.76**

Table 1: Results showing varying performance across High and Low image dataset combinations.

I.V. CONCLUSION

In this paper, we present an alternative method to gather and process UAV imagery that improves the level of accuracy for trail navigation under forest canopy by training the network using only the data from a single forward facing camera view instead of the triplet view training approach of [3]. Our approach also performs well across varying image resolutions and increases the capability of low-cost UAV platforms with limited payload capacity. Future work will include additional aspects of UAV perception and control targeting end-to-end autonomy across this and other challenging operating environments.

REFERENCES

1. Paul Christiano, Zain Shah, Igor Mordatch, Jonas Schneider, Trevor Blackwell, Joshua Tobin, Pieter Abbeel, and Wojciech Zaremba. Transfer from simulation to real world through learning deep inverse dynamics model. *CoRR*, abs/1610.03518, 2016.

2. Dhiraj Gandhi, Lerrel Pinto, and Abhinav Gupta. Learning to fly by crashing. *CoRR*, abs/1704.05588, 2017.

3. Alessandro Giusti, Jerome Guzzi, Dan C. Ciresan, Fang-Lin He, Juan Pablo Rodriguez, Flavio Fontana, Matthias Faessler, Christian Forster, Jurgen Schmidhuber, Gianni Di Caro, Davide Scaramuzza, and Luca

4. Gambardella. A machine learning approach to visual perception of forest trails for mobile robots. 1:1–1, 01 2015.

5. Kaiming He, Xiangyu Zhang, Shaoqing Ren, and Jian Sun. Spatial pyramid pooling in deep convolutional networks for visual recognition. *CoRR*, abs/1406.4729, 2014.

6. Klaas Kelchtermans and Tinne Tuytelaars. How hard is it to cross the room? - training (recurrent) neural networks to steer a UAV. *CoRR*, abs/1702.07600, 2017.

7. Matthias Mueller, Vincent Casser, Neil

Smith, Dominik L. Michels, and Bernard Ghanem. Teaching uavs to race using ue4sim. *CoRR*, abs/1708.05884, 2017.

8. Nikolai Smolyanskiy, Alexey Kamenev, Jeffrey Smith, and Stan Birchfield. Toward low-flying autonomous MAV trail navigation using deep neural networks for environmental awareness. *CoRR*, abs/1705.02550, 2017.

9. Lei Tai and Ming Liu. Deep-learning in mobile robotics - from perception to control systems: A survey on why and why not. *CoRR*, abs/1612.07139, 2016.

10. Tianhao Zhang, Gregory Kahn, Sergey Levine, and Pieter Abbeel. Learning deep control policies for au- tonomous aerial vehicles with mpc-guided policy search. *CoRR*, abs/1509.06791, 201

Swarm Robots For Picking Litter In Urban Environments

Simon Obute Obute[1†], Jordan Boyle[2], Mehmet Dogar[1], Robert Richardson[2]

[1] School of Computing, [2] Department of Mechanical Engineering, University of Leeds, Leeds

I. INTRODUCTION

Litter is any rubbish that has not been properly disposed. Examples include plastic bags, cans and cigarette butts, which are probabilistically distributed in the environment [1]. These substances, especially non- biodegradable litter, have harmful effects on both land and marine ecosystem, thus causing several countries to incur large financial expenditure regarding the handling of litter in the environment. For instance, the annual running cost for clearing litter in the United Kingdom is at least £800 million [2]. Moreover, handling litter is not a desirable job for humans [3]. In addition to preventive measures being taken by societies in addressing the problem of litter, this research is focused on the development of swarm robotics foraging technology for picking litter in urban environments, which represent a major source of litter [1]. This proposed technology is deemed effective because of the nature of litter distribution in the environment which is suitable for the operational procedure of swarm robots' foraging task of searching, exploiting and transporting targets to designated deposit site(s) [4].

Swarm robotics research is a branch of multi-robot system that is made up of autonomous robots which make use of local sensing of their surrounding and communication with neighbouring robots to achieve collective group behaviour without the need for centralised control. The original motivation for swarm robot foraging is from biological swarms like ants that are able to forage for food located hundreds of metres away from their nest – a task that is impossible for a single ant to accomplish without cooperation with other ants [5], [6]. Extensive reviews on swarm robotics have been conducted in [6] and [7], while [4] and [8] provide thorough investigation of swarm robot foraging algorithms.

II. PROBLEM DESCRIPTION AND OBJECTIVES

Robots performing the task of foraging litter in an environment continuously switch from searching, exploiting and homing states. This is a challenging task that integrates studies in swarm algorithms, robot vision, object manipulation, locomotion on various terrains, obstacle avoidance and communication in the presence of sensing noise. The swarm also needs to overcome hardware constraints such as limitations in energy/power and litter-carrying capacity of the robot. The primary focus of this research is the searching and homing phases (the green highlights in Figure 1).
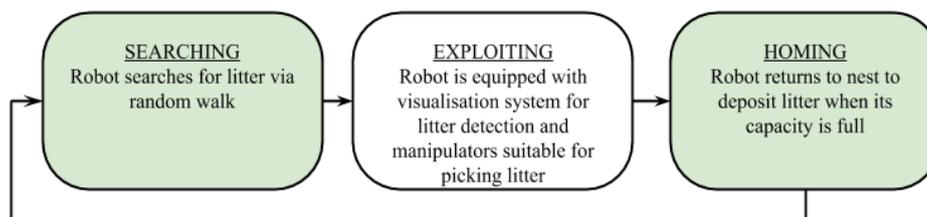
Figure 1 The foraging operational process of swarm robots.

Some studies in swarm robotics foraging have used unrealistic assumptions such as grid world model in [9] and pheromone trails

---

[†] Email contact scsoo@leeds.ac.uk

communication in [10]. These particular types of approaches do not effectively assess the nature of challenges that robot swarms encounter in real world environments. In the present research, the primary goal is to develop a swarm foraging algorithm that takes into consideration realistic constraints and uncertainties during simulation experiments. This will bridge the gap between simulations and the actual robotic demonstration of the performance of foraging algorithm. To realise this target, Gazebo – a multi-robot simulator managed by the Open-Source Robotics Foundation – has been chosen for conducting simulation experiments during the development of the algorithm. The simulator has native support for Robot Operating System, and as well as multiple physics engines such as ODE, Simbody and Bullet to provide realistic environment modelling [11].

III. SWARM DEVELOPMENT APPROACH

To successfully accomplish the litter picking task, each robot in the swarm needs to be equipped with: on- board vision processing for identifying litter, manipulation mechanism for physically handling litter, locomotion ability on varying terrains, means of communication with other robots to achieve cooperation among swarm members and obstacle avoidance among other desirable qualities.

the various features needed for picking litter. In the current simulation, 20 robots are used to forage litter that are uniformly distributed in a $100m2$ space at a density of 1 litter per 2. Each robot is equipped with a 60° field of view camera and maximum collection capacity of 3 litter objects. Figure 3 shows images of a robot and its corresponding camera view in the bottom section as it detects (Figure 3(a)), approaches (Figure 3(b)) and picks up a red box litter (Figure 3(c)). The litter is removed from the simulated environment when it makes contact with the gripper. This simplification of the litter picking procedure is necessary in order to concentrate on the development of the swarm algorithm for achieving collective swarm behaviour when solving the litter problem.

The simulation result shown in Figure 4 represents the uniform random walk swarm robot algorithm used as a default comparison for foraging algorithms like those in [12] and [13]. The central nest for depositing litter is represented as the brown circle. Figure 4(a) is the initial state of the simulation environment, while Figures 4(b) and 4(c) represent 30 and 300 seconds simulation time steps, respectively.

A complete simulation video is available at https://goo.gl/CFwSqG. Whenever a robot encounters an obstacle, it avoids this barrier by turning away in a
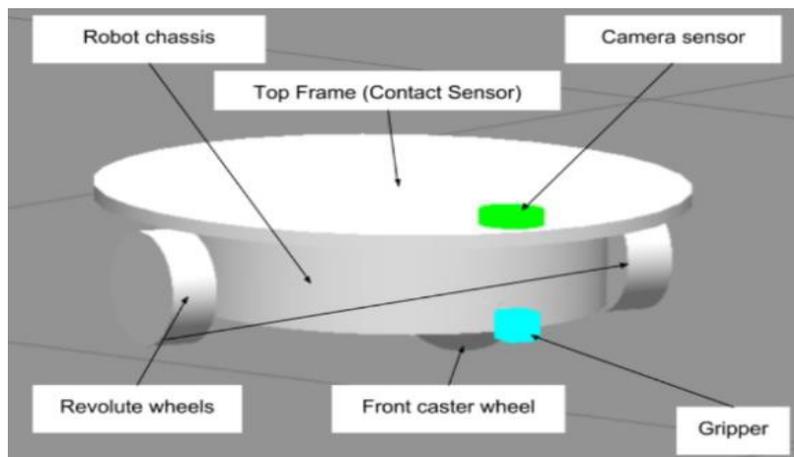
Figure 2 Simplified robot model for picking litter

Figure 2 illustrates a simplified representation of the robot model and shows

different direction from it. Furthermore, when a robot's capacity is full, it goes to the

deposition site and drops all of its collected litter before resuming the search for new litter.
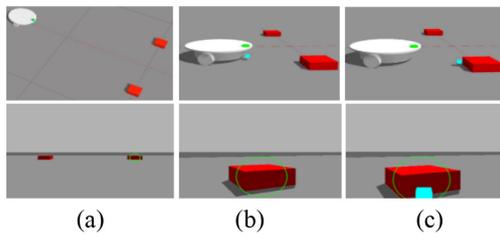

(a)   (b)   (c)

Figure 3 Representation of the litter picking process by a robot.
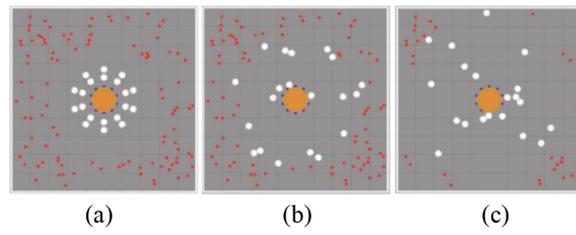

(a)   (b)   (c)

Figure 4 Simulation result of a swarm of 20 litter foraging robots.

I.V. CONCLUSION

The principle of swarm robotic foraging is well suited to address the problem of litter in urban environments. In this work, the development of a swarm algorithm that takes into consideration the hardware constraints for robots performing litter foraging in real world environment has been proposed. This is unlike the unrealistic assumptions presented in some previous studies when developing swarm robotics foraging algorithms.

With regard to further work, we intend to develop a swarm cooperation strategy to aid collective swarm behaviour when performing the search and retrieval of litter. In addition, heterogeneity will be included in the swarm development in order to provide a simplified robot design and specialization.

For example, the swarm can be made up of both small and large sized robots, where large robots serve as transport, charging station and litter deposit sites for the small robots that perform the search and collection of litter.

Moreover, the small robots can be designed to perform specialized functions in order to cater for different terrain and litter types. Following the development of the swarm algorithm, it will be incorporated into other works on vision and litter manipulation to provide a hardware platform for evaluating the performance of the robot swarm in handling the litter.

REFERENCES

1. T. Barnes, "What's Littering Britain? A Survey of British Litter," Heroes, 2010. [Online]. Available: www.litterheroes.co.uk.
2. Betts et al., "Litter and fly-tipping in England Seventh Report of Session 2014–15 Communities and Local Government Committee," 2015.
3. Cavallo et al., "Development of a Socially Believable Multi-Robot Solution from Town to Home," Cognit. Comput., vol. 6, no. 4, pp. 954–967, 2014.
4. F. Winfield, "Foraging Robots," Encyclopedia of Complexity and Systems Science. New York: Springer, pp. 3682–3700, 2009.
5. L. Lach, C. L. Parr, and K. L. Abbott, Ant Ecology. Oxford University Press, 2010.
6. L. Bayindir, "A review of swarm robotics tasks," Neurocomputing, vol. 172, pp. 292–321, 2016.
7. Brambilla, E. Ferrante, M. Birattari, and M. Dorigo, "Swarm robotics: A review from the swarm engineering perspective," Swarm Intell., vol. 7, no. 1, pp. 1–41, 2013.
8. Zedadra, N. Jouandeau, H. Seridi, and G. Fortino, "Multi-Agent Foraging: state-of-the-art and research challenges," Complex Adapt. Syst. Model., vol. 5, no. 3, 2017.
9. Zedadra, H. Seridi, N. Jouandeau, and G. Fortino, "A distributed foraging algorithm based on artificial potential field," in 2015 12th International Symposium on Programming and Systems (ISPS), 2015, pp. 1–6.
10. A. Lima and G. M. B. Oliveira, "A cellular automata ant memory model of foraging in a swarm of robots," Appl. Math. Model., vol. 47, pp. 551–572, Jul. 2017.
11. S. Ivaldi, V. Padois, and F. Nori, "Tools for dynamics simulation of robots: a survey based on user feedback," CoRR, 2014.
12. Hoff, "Multi-Robot Foraging for Swarms of Simple Robots," Harvard University, 2011.
13. Fioriti, F. Fratichini, S. Chiesa, and C. Moriconi, "Levy Foraging in a Dynamic Environment – Extending the Levy Search," Int. J. Adv. Robot. Syst., vol. 12, no. 7, p. 98, Jul. 2015.

Robot for Bridge Bearing Inspection – Extended Abstract

H. Peel*, S. Luo, A. G. Cohn R. Fuentes
*School of Civil Engineering, University of Leeds

I. INTRODUCTION

Bridge bearings transfer the loads from the superstructure of bridges (e.g., the deck) to the abutments or intermediate supports, which then transfer the loads to the bridge foundations. Bearings are an integral part of bridge structures and their failure can have considerable impact on the bridge life [1, 2], leading to the overall failure of the entire bridge [3]. The inspection requirements for structural bridge bearings are detailed in the relevant European Standard [4] as: "close visual inspection without measurements, spaced at equal, reasonably frequent, intervals", with inspections occurring at least as often as the bridge structure is assessed. However, the bridge bearing space is often limited in size and not accessible or hazardous for human access.

Robotic platforms mounted with sensors have been deployed for bridge inspection, usually with a focus on structural condition or material degradation [5, 6, 7] of the bridge. However, there has been no development of a robotic platform specifically for bridge bearing inspection, where close access to the bearings is required to obtain sufficient detail. In order to achieve autonomy when performing robotic inspections, a robust localisation approach is essential, especially since errors in the limited bearing space could lead to catastrophic failures such as the robot falling from height.

The aim of the project is to create a robotic solution to make bridge bearing inspections safer and more repeatable. In this work, existing algorithms are considered to develop autonomous navigation in the bridge bearing space. Data collection was performed at the Millennium Bridge, Leeds. Full details of this work can be found in [8].

II. ROBOTIC PLATFORM AND SENSORS

The robotic platform used in this work is a commercial product called a DiddyBorg (a six-wheeled robot with a Perspex chassis, that is built around the Raspberry Pi single-board computer), which has been modified to accommodate additional sensors. A 2D LiDAR called the RPLIDAR was used for mapping and navigation. A Raspberry Pi 5MP RGB camera was also used for navigation, but the data from the camera can also be used for inspection applications. The Robot Operating System (ROS) was to send messages from sensors and between the robot and laptop used for computation. Data collection was performed by tele-operating the robot in the bearing enclosure.

III. SLAM AND LOCALISATION METHODS

Simultaneous Localisation and Mapping (SLAM) is one particular area of research in robotics where the robot uses on-board sensors to build a map and find its position in the map at the same time. Two types of SLAM are considered in this work: Hector SLAM and Orientated Rotated Brief (ORB) SLAM. A localisation only method named Adaptive Monte-Carlo Localisation (AMCL) is also considered. AMCL requires an existing map, and the position of the robot is determined within this map.

I.V. ORB-SLAM

ORB-SLAM is a form of Visual SLAM with both monocular and stereo implementations [9]. Features are extracted from the input monocular images using Oriented Fast and Rotated Brief (ORB) descriptors, chosen for fast extraction and matching. A 3D map of the environment is then created. ORB-SLAM was chosen as a candidate for localisation because it has been shown to work in urban implementations [9] and has also been implemented using the Raspberry Pi camera in an indoor office environment [10].

V.HECTOR SLAM

Hector SLAM [11] is primarily a 2D SLAM approach that incorporates 2D LiDAR scans into a planar map. In Hector SLAM, a fast scan-matching approach is used, which takes advantage of the ldistance measurement noise and high scan rates of modern LiDAR [11]. In this work, the maps created using Hector SLAM are saved and used as an input to AMCL for localisation only.

V.I. ADAPTIVE MONTE-CARLO LOCALISATION (AMCL)

For inspection applications it is useful to have a known map to highlight targets for inspection or areas of interest in advance, which is possible using AMCL. In AMCL, the knowledge that the robot holds about its environment is represented by a set of particles, where each particle represents a potential position and orientation of the robot. A known starting location can be given as an input, around which the particles spread. In AMCL, the number of particle are adapted over time (a detailed description of the approach is given in [13]), allowing better computational efficiency. Sensor data for localisation is provided by the 2D LiDAR.

V.I.I. DISCUSSION OF INITIAL FINDINGS

Adequate image features were present in the environment to use ORB SLAM in the bridge bearing enclosure, with added texture being provided by dirt and cracks on planar surfaces. However, changes in the lighting conditions caused a tracking failure and tracking was also lost due to abrupt or fast motions of the robot. When the tracking was lost, the robot had to return to a previous key frame and localisation in the map was performed globally. Until a known location can be found, the robot is lost in the environment.

When using Hector SLAM, some discrepancies were recorded in the map due to uneven terrain in the bearing enclosure, causing the 2D LIDAR to tilt, creating inconsistencies in the mapped area. In addition, a low wall in the enclosure is not visible in the since the 2D LIDAR was higher than the wall when mounted on the robot, and

hence the wall not detected by the sensor. This error may cause problems as the robot could potentially be navigated out of the enclosure. Discrepancies in the map are also caused by reflections off water (the bridge crosses a river), which causes large range values in certain areas of the map.

To compare the results from ORB-SLAM and Hector SLAM, the trajectory outputted by both methods was recorded simultaneously. The overall trajectories are very similar in shape, however, the trajectory for ORB-SLAM is less accurate and has greater variation than Hector SLAM and gaps appear when the trajectory crosses itself. These differences are caused by ORB-SLAM recording the location of key- frames and not every image frame. As a result, the robot position is given as the nearest key-frame location.

Localisation of the robot using AMCL was successful in the bridge bearing environment. However, the following challenges were evident: when using pre-existing maps is if the environment changes, the map may no longer be representative. For example, localisation was temporarily lost, when the wall is not a known landmark and some particles are placed outside of the map. In addition, a known start position can be difficult to provide accurately in the bridge bearing enclosure.

V.I.I.I. CONCLUSIONS

All methods for SLAM and localisation were successfully implemented in the bridge bearing enclosure. However, the real-world nature of the environment provided several challenges, such as: changes between the map and the current environment, difficult and varying lighting conditions and uneven terrains. These issues need addressing in order to achieve autonomous navigation for inspection. For all approaches considered here, improvements may be found by combining different methods and sensors to create a more robust approach, such as adding an IMU to Hector SLAM to account for uneven terrain. These changes will be considered in future work, as well as methods for performing the inspection of the bridge bearings.

REFERENCES

1. J. Park, J. Cho, H. Gil, J. Shin, Measurement and evaluation of thermal movements of existing bridges using a series of two-dimensional images, in: SHMII 2015 - 7th International Conference on Structural Health Monitoring of Intelligent Infrastructure, International Society for Structural Health Monitoring of Intelligent Infrastructure, ISHMII, 2015.

2. A. Niemierko, Modern bridge bearings and expansion joints for road bridges, Transportation Research Procedia 14 (2016) 4040–4049.

3. M. Aria, R. Akbari, Inspection, condition evaluation and replacement of elastomeric bearings in road bridges, Structure and Infrastructure Engineering 9 (2013) 918–934.

4. European Committee for Standardization, Structural Bearings Part 10 Inspection and maintenance. (2003).

5. A. Akutsu, E. Sasaki, K. Takeya, Y. Kobayashi, K. Suzuki, A comprehensive study on development of a small-sized self-propelled robot for bridge inspection, Structure and Infrastructure Engineering 2479 (October) (2017) 1–12.

6. N. H. Pham, H. M. La, Design and implementation of an Autonomous Robot for Steel Bridge Inspection, International Journal of Advanced Robotic Systems 10 (January) (2016) 556–562.

7. C.-h. Yang, M.-c.Wen, Y.-c. Chen, S.-c. Kang, An Optimized Unmanned Aerial System for Bridge Inspection, in: Automation in Construction, 2015.

8. H. Peel, S.Luo, A.G. Cohn and R. Fuentes, An improved robot for bridge inspection, in Proceedings of the International Symposium on Automation and Robotics in Construction (ISARC), 2017.

9. J. D. Mur-Artal, Raúl, Montiel, J. M. M. and Tardós, "ORB-SLAM: a Versatile and Accurate Monocular SLAM System," IEEE Trans. Robot., vol. 31, no. 5, pp. 1147-1163, 2015

10. G. Ponnu, J. George, and J. Skovira, "Real-time ROSberryPi SLAM Robot," Cornell University, 2016.S. Kohlbrecher, J. Meyer, T. Graber, K. Petersen, O. Von Stryk, U. Klingauf, Hector Open Source Modules for Autonomous Mapping and Navigation with Rescue Robots, RoboCup 2013: RoboCup 2013: Robot World Cup XVII (2013) 642–631.

11. S. Thrun, W. Burgard, D. Fox, Monte Carlo Localization, in: Probabalistic Robotics, 10th Edition, MIT Press, Massachusetts, 2006, Ch. 8.3, pp.250–263.

Navigation Testing for Continuous Integration in Robotics

Jaime Pulido Fentanes1, Christian Dondrup2, and Marc Hanheide1 1Lincoln Centre for Autonomous Systems, University of Lincoln, UK jpulidofentanes,mhanheide @lincoln.ac.uk
School of Mathematical & Computer Sciences, Heriot-Watt University, Edinburgh, Scotland, UK
c.dondrup@hw.ac.uk

ABSTRACT

Robots working in real-world applications need to be robust and reliable. However, ensuring robust software in an academic development environment with dozens of developers poses a significant challenge. This work presents a testing framework, successfully employed in a large-scale integrated robotics project, based on continuous integration and the fork-and-pull model of software development, implementing automated system regression testing for robot navigation. It presents a framework suitable for both regression testing and also providing processes for parameter optimisation and benchmarking.

I.INTRODUCTION

Robust long-term robot operation has many challenges that are yet to be overcome. Many of these challenges arise because in real-world deployments unexpected and unpredictable situations can harm robot performance. Some of these situations can only be dealt by constant software development and update, however, robotic systems are usually composed of many individual components, developed by multiple people, that particular in research environments, work mostly individually. This can lead to researchers modifying finely tuned parameters to fit one particular case but harming the robot's performance in other situations. It is for this reason, that systematic testing of the integrated robot system and test for regressions in the performance is critical.

Previous deployments[1] have proven that navigation failures are among the most critical problems impacting a mobile robot's overall autonomy. Navigation performance is usually affected by the respective performance of many different components, such as mapping, robust localisation in dynamic environments, path planning, and motion control. Looking for instance at the probably most popular robot navigation package "ROS move base"[*], there are more
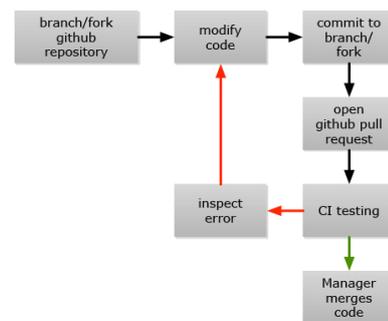
Figure 1. Work-flow.

than 50 parameters alone that affect navigation performance, even disregarding code changes and higher level autonomy functions. In an academic research environment where dozens of developers might be contributing to an integrated system, adopting established methodologies of software engineering and collaborative software development are key to ensure the high quality of the software required to facilitate long-term deployment (in the order of weeks and months) of robots in real-world environments.

II. CONTINUOUS INTEGRATION AND TESTING IN ROBOTICS

The proposed testing regime has been established in the context of the STRANDS[y]

---

project, which ambition as to develop autonomous mobile robots that run for weeks (a benchmark here was to run 120 days) without expert interventions[1]. As already proposed by earlier research on software engineering in robotics context[2], we adopted the paradigm of continuous integration (CI), successfully employed in many larger-scale software-intensive systems
(e.g. by Lacoste et al.[3]) and also in robotics[4], facilitated via a dedicated JENKINS CI server[z]. Replicating entire systems and testing them systematically has also been attempted by other researchers[5, 6], however, the embedding of full navigation testing in the software development work-flow is still rare in the robotics community. The general work-flow of software development captured

scenarios. These test scenarios are executed in the continuous integration server every time there is a change to the STRANDS navigation stack. If one of these tests should fail, the system's maintainer is notified and can access a report page where they can see what exactly produced the failure and take measures to solve possible issues. Fig. 2c shows the report page on the continuous integration server, this report is comprised of a video report on which a video of the simulated test for this version of the software can be seen, and a link to the console output log where the results of the navigation tests can be found[{]. It shall be noted that critical as well as supplementary scenarios are defined, with the first leading to rejection of any pull request of new code (a true critical
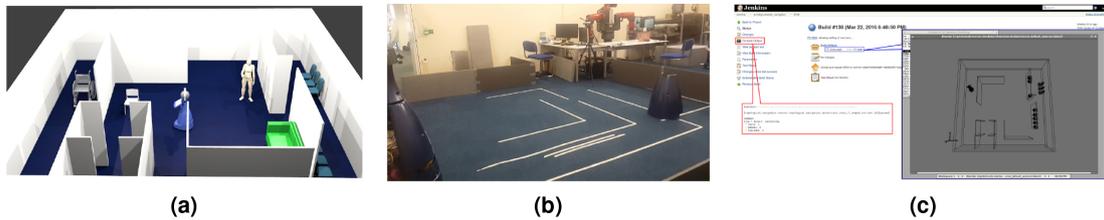
Figure 2. (a) Simulation environment. (b) Robot navigation testing arena at University of Lincoln. (c) Report page.

in Fig. 1 follows the "fork and pull" model[7], which is well integrated with continuous integration. Every so-called pull request in our system undergoes full system testing in simulation (using the "Morse" simulator[8]) through a number of defined navigation test scenarios, build on top of the rostest framework[9], and our own topological navigation[10]. However, the same tests can also be run in a real-world "test arena", to verify software commits also with a real robot.

III. NAVIGATION TEST SCENARIOS

We propose an implementation of specific and repeatable navigation tests[x] as regression tests in a software development environment support by CI paradigms. The aim to minimise regression of navigation behaviour by software updates, but also can be used to develop and benchmark new navigation components or settings, with this purpose in mind we have developed a series of test

regression), and the latter only being considered for performance analysis.

To successfully test the software the testing must be as realistic as possible, but at the same time tests have to be executed in a controlled environment where the conditions are as identical as possible every time. Additionally, tests should be run in an automated set-up where not only the robot should be able to move in the testing environment, but also the objects must move in a controlled manner. To achieve this we opted for the development of tests that could be performed in simulation and real-world system, with a transition as seamless as possible.

Simulated tests are executed in a tailored environment (figure 2a) where all the scenarios can be tested and the objects and robot position are part of the test definition. On the other hand, real-world testing requires a human operator and supervisor. A typical

---

§See https://github.com/strands-project/strands_navigation/tree/indigo-devel/topological_navigation/tests for the specification of our tests.

¶https://www.youtube.com/watch?v=2ROycER60t8

set-up for this kind of testing is modifying an open space using some kind of panels for each test as seen in figure 2b, resembling the simulated test arena. The test also in real-world utilise the same test definition as in simulation allowing to run entire scenarios automatically at the push of a button also in real-world.

I.V. DISCUSSION & CONCLUSION

Driven by demands of mid- to large-scale collaborative software development of robotic systems, we have proposed a framework for continuous integration focusing on automated testing of robot navigation. This framework has been productive in the EU STRANDS and ILIAD projects for more than 3 years, as has played an essential role to ensure robust system performance in real-world scenarios. The proposed work-flow has also been utilised to provide a framework for automated benchmarking of robotics algorithms[11], and will further be developed for testing full system capabilities, beyond navigation.

REFERENCES

1. Hawes, N. et al. The strands project: Long-term autonomy in everyday environments. IEEE Robotics Autom. Mag. 24, 146–156 (2017). DOI 10.1109/MRA.2016.2636359.
2. Lier, F., Schulz, S. & Lu¨tkebohle, I. Continuous Integration for Iterative Validation of Simulated Robot Models. In Proc SIMPAR, 101–112 (2012). DOI 10.1007/978-3-642-34327-8 12.
3. Lacoste, F. J. Killing the Gatekeeper: Introducing a Continuous Integration System. In 2009 Agile Confer- ence, 387–392 (IEEE, 2009). URL http://ieeexplore.ieee.org/document/5261054/ . DOI 10.1109/AGILE.2009.35.
4. Mossige, M., Gotlieb, A. & Meling, H. Testing robot controllers using constraint programming and continuous integration. Inf. Softw. Technol. 57, 169–185 (2015). URL http://www.sciencedirect. com/science/article/pii/S0950584914002080h ttp://linkinghub.elsevier.com/ retrieve/pii/S0950584914002080. DOI 10.1016/j.infsof.2014.09.009.
5. Ernits, J., Halling, E., Kanter, G. & Vain, J. Model-based integration testing of ros packages: A mo- bile robot case study. In Mobile Robots (ECMR), 2015 European Conference on, 1–7 (2015). DOI 10.1109/ECMR.2015.7324210.
6. Lier, F. et al. Towards Automated System and Experiment Reproduction in Robotics. In Proc IEEE Conf on Intelligent Robots and Systems (2016).
7. Gousios, G., Pinzger, M. & Deursen, A. v. An exploratory study of the pull-based software development model. In Proceedings of the 36th
8. International Conference on Software Engineering, ICSE 2014, 345–355 (ACM, New York, NY, USA, 2014). URL http://doi.acm.org/10.1145/2568225.2568260 . DOI 10.1145/2568225.2568260.
9. Lemaignan, S. et al. Simulation and HRI recent perspectives with the MORSE simulator, vol. 8810 (2014).
10. Foundation, O. S. R. rostest - ros wiki (2015). URL http://wiki.ros.org/rostest. Accessed: 2016-03-21.
11. Pulido Fentanes, J., Lacerda, B., Krajn´ık, T., Hawes, N. & Hanheide, M. Now or later? predicting and maximising success of navigation actions from long-term experience. In International Conference on Robotics and Automation (ICRA) (2015).
12. Marc Hanheide Toma´sˇ Vintr Keerthy Kusumam Tom Duckett, T. K. Towards automated benchmarking of robotic experiments. In ICRA Workshop on Reproducible Research in Robotics (2017).

SILICONE-BASED ULTRA-STRETCHABLE STRAIN SENSORS

Fabrizio Putzu[1], Kaspar Althoefer[1], Luigi Manfredi[2]

ABSTRACT

This paper presents the materials and methods used to produce polymer-based sensors. Stretchable sensors could be used to measure force, speed, pressure and can be applied in areas such as health monitoring. The procedure followed is easy and inexpensive, the outcome of it are sensors with high stretchability. These have been tested with an Instron® machine showing that good conductivity over a very broad range and high sensitivity can be achieved.

I. INTRODUCTION

Stretchable sensors find applications in several fields thanks to their easy fabrication and manufacturing process. High strain sensors can be worn and used as multifunctional sensors to measure, force, speed, pressure, acceleration, frequency or a wide range of health parameters. In addition, stretchable sensors can be used as feedback control for soft robots, allowing them to sense the surrounding environment.

II. MATERIALS AND METHODS

The material that has been used to produce the sensor prototypes is Ecoflex 00-30 by Smooth-On® (two- components, curable silicone polymer), and the moulder used has been designed with CAD software and then 3D printed. The fabrication of the sensor consists of the following steps:

i)two parts A and B, were mixed together using a mix ratio of 1:1 and degassed for 10 minutes, ii) subsequently the polymer was casted into the moulders and degassed again for 10 minutes more in order to avoid the presence of bubbles that can lead to a discontinuity in the material and could lead to the sensor fractures; iii) the moulder top part is carefully placed on the moulder base containing the degassed polymer mixture and it is put back in the oven at 60 °C, for 30 minutes; iv) after allowing the mixture to cure for the specified time, the sample was demoulded.

No mould release has been used as earlier trials showed that it

Figure 1 Stretchable Sensor attached to the Stretcher Machine

was unnecessary. To turn the moulded sample into a planar compliant sensor a small amount of graphite powder has been carefully applied as a uniform film on top of the silicone sample (Figure 1).

A specific 'stretcher' machine has been designed to validate the sensors performance, which allows the sensors to be precisely stretched while carrying out multi-meter readings, and identify the strain/elongation of the sensors, enabling their calibration. The electric connections were made with two rigid metallic plates glued to the two ends of

_____

[1]Fabrizio Putzu and Kaspar Althoefer are with Queen Mary University of London, f.putzu@qmul.ac.uk, k.althoefer@qmul.ac.uk,
[2]Luigi Manfredi is with Institute for Medical Science and Technology (IMSaT), University of Dundee, mail@luigimanfredi.com

Tab I: Stretchable sensors and their performance

Authors	Material	Elongation	Gauge Factor
Amjadi et al.	Graphite	50%	522-11344
Tadakaluru et al	Graphite	246%	12-346
Tadakaluru et al.	Carbon Nanotubes	620%	5-43

This paper outlines our approach to producing stretchable sensors.

the sensor. In order to allow the collection of the data, two thin wires have been attached to the metallic plates and to optimize the connection conductive epoxy has been used (Figure 1). The connection was essential to recording the output of the sensor; this allowed a multi-meter to be used to measure, the conductivity of the sensor at specific strains. A mid-range, among all the prototypes that have been created, starts from a value that was in the order of the Kilo-Ohm [KΩ] when the sensor was relaxed, reaching several Mega-Ohm [MΩ] when the sensor was completely stretched.

Several studies have been published in regard to stretchable sensors. Tadakaluru et al. and Amjadi et al., proposed to use polymers as stretchable sensors [1,2], while several

mechanical properties [15-23]. A comparison of these stretchable sensors is reported in Table I.

III. DATA COLLECTION

To collect the sensor data, an ADC converter (AD7714 from Analog Devices) and a microcontroller (Arduino UNO Board which uses ATmega328P microcontroller by Atmel) were used; as it is shown in Figure 2.

The sensor has been tested using a Wheatstone bridge configuration in order to reduce the noise and the temperature drift. The sensor has been attached to the circuit through the electric connection and at the same time, it has been connected to the Instron Machine by two dedicated 3D printed clamps (Figure 3)
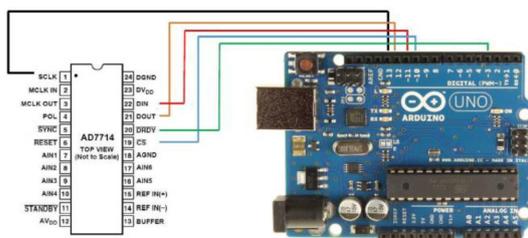
Figure 2 Circuit used to test the sensor; it includes an ADC converter and Arduino UNO board

Figure 3 Sensor test using Instron Machine

studies [3-7] proposed to embed graphene sheets on a flexible substrate to achieve high sensitive strain but only 5% of total stretchability. Carbon nanotube (CNT) on flexible substrates [8,9] have proved to have a gauge factor of maximum 2, non-linearity and large hysteresis. CNT has also been proved to have high performance, but low stretchability [3-7, 10-14]. Silver Nanowires (AgNWs) have been proposed for use in the manufacture of flexible electronics because of their excellent electrical conductivity and

I.V. RESULTS AND DISCUSSION

The main advantage of the proposed stretchable sensors is the simple manufacturing process and their inexpensiveness. They have a very high sensitivity and stretchability. The elongation value of these sensors is up to 900%. They also showed a good conductivity over a wide range. When a deformation is applied to the sensor resistance increases its value starting from $\simeq 40$ KΩ in a relaxed condition to 100 MΩ when the sensor prototype is stretched to

Figure 4 Multimeter reading

its maximum elongation. Additional work is obviously needed to reduce the output signal to noise ratio and to make the electrical connection more stable. They can be integrated in a soft robot by attaching these sensors on the external surface to measure the elongation and to implement a motion trajectory control by using a PID controller.

REFERENCES

1. Amjadi, M., Turan, M., Clementson, C. and Sitti, M. (2016). Parallel Microcracks-based Ultrasensitive and Highly Stretchable Strain Sensors. ACS Applied Materials & Interfaces, 8(8), pp.5618-5626.
2. Tadakaluru, S., Thongsuwan, W. and Singjai, P. (2014). Stretchable and Flexible High-Strain Sensors Made Using Carbon Nanotubes and Graphite Films on Natural Rubber. Sensors, 14(1), pp.868-876.
3. Jiang, H., Ren, Y. and Tao, Y. (2011). Microwire formation based on dielectrophoresis of electroless gold plated polystyrene microspheres. Chinese Physics B, 20(5), p.057701
4. Zeng, Z., Seyed Shahabadi, S., Che, B., Zhang, Y., Zhao, C. and Lu, X. (2017). Highly stretchable, sensitive strain sensors with a wide linear sensing region based on compressed anisotropic graphene foam/polymer nanocomposites. Nanoscale, 9(44), pp.17396-17404.
5. Hempel, M., Nezich, D., Kong, J. and Hofmann, M. (2012). A Novel Class of Strain Gauges Based on Layered Percolative Films of 2D Materials. Nano Letters, 12(11), pp.5714-5718
6. . Tuning the work function of graphene by ultraviolet irradiation. (2013). Applied Physics Letters, 102(18), p.183120.
7. Chun, S., Kim, Y., Jung, H. and Park, W. (2014). A flexible graphene touch sensor in the general human touch range. Applied Physics Letters, 105(4), p.041907
8. Le Cai, Song, L., Luan, P., Zhang, Q., Zhang, N., Gao, Q., Zhao, D., Zhang, X., Tu, M., Yang, F., Zhou, W., Fan, Q., Luo, J., Zhou, W., Ajayan, P. and Xie, S. (2013). Erratum: CORRIGENDUM: Super-stretchable, Transparent Carbon Nanotube-Based Capacitive Strain Sensors for Human Motion Detection. Scientific Reports, 3(1).
9. Park, S., Kim, J., Chu, M. and Khine, M. (2016). Highly Flexible Wrinkled Carbon Nanotube Thin Film Strain Sensor to Monitor Human Movement. Advanced Materials Technologies, 1(5), p.1600053.
10. Liu, C. and Choi, J. (2009). Patterning conductive PDMS nanocomposite in an elastomer using microcontact printing. Journal of Micromechanics and Microengineering, 19(8), p.085019.
11. I., Schulz, M., Lee, J., Choi, G., Jung, J., Choi, J. and Hwang, S. (2007). A Carbon Nanotube Smart Material for Structural Health Monitoring. Solid State Phenomena, 120, pp.289-296.
12. Lu, N., Lu, C., Yang, S. and Rogers, J. (2012). Highly Sensitive Skin-Mountable Strain Gauges Based Entirely on Elastomers. Advanced Functional Materials, 22(19), pp.4044-4050.
13. Xiao, X., Yuan, L., Zhong, J., Ding, T., Liu, Y., Cai, Z., Rong, Y., Han, H., Zhou, J. and Wang, Z. (2011). High- Strain Sensors Based on ZnO Nanowire/Polystyrene Hybridized Flexible Films. Advanced Materials, 23(45), pp.5440-5444.
14. Yang, X., Zhou, Z., Zheng, F. and Wu, Y. (2010). High sensitivity temperature sensor based on a long, suspended single-walled carbon nanotube array. Micro & Nano Letters, 5(2), p.157.
15. Kim, S., Lee, H., Na, S., Jung, E., Kang, J., Kim, D., Cho, S., Chae, H., Chung, H., Kim, S., Lee, B., Kim, K., Lee, S., Lee, H., Kim, H. and Lee, H. (2015). Enhancement of electrical conductivity of silver nanowires-networked films via the addition of Cs-added TiO2. Nanotechnology, 26(13), p.135705.
16. Kim, T., Canlier, A., Kim, G., Choi, J., Park, M. and Han, S. (2013). Electrostatic Spray Deposition of Highly Transparent Silver Nanowire Electrode on Flexible Substrate. ACS Applied Materials & Interfaces, 5(3), pp.788- 794.
17. Lee, J., Lee, P., Lee, H., Lee, D., Lee, S. and Ko, S. (2012). Very long Ag nanowire synthesis and its application in a highly transparent, conductive and flexible metal electrode touch panel. Nanoscale, 4(20), p.6408.
18. Liu, C. and Yu, X. (2011). Silver nanowire-

based transparent, flexible, and conductive thin film. Nanoscale Research Letters, 6(1), p.75.

19. Hu, L., Kim, H., Lee, J., Peumans, P. and Cui, Y. (2010). Scalable Coating and Properties of Transparent, Flexible, Silver Nanowire Electrodes. ACS Nano, 4(5), pp.2955-2963.

20. Korte, K., Skrabalak, S. and Xia, Y. (2008). Rapid synthesis of silver nanowires through a CuCl- or CuCl2-mediated polyol process. J. Mater. Chem., 18(4), pp.437-441.

21. Xu, F. and Zhu, Y. (2012). Highly Conductive and Stretchable Silver Nanowire Conductors. Advanced Materials, 24(37), pp.5117-5122.

22. De, S., Higgins, T., Lyons, P., Doherty, E., Nirmalraj, P., Blau, W., Boland, J. and Coleman, J. (2009). Silver Nanowire Networks as Flexible, Transparent, Conducting Films: Extremely High DC to Optical Conductivity Ratios. ACS Nano, 3(7), pp.1767-1774.

23. Ho, X., Cheng, C., Tey, J. and Wei, J. (2014). Biaxially stretchable transparent conductors that use nanowire networks. Journal of Materials Research, 29(24), pp.2965-2972

The impact of autonomous vehicles on traffic capacity at an intersection

Karam Safarov [*1], *Thomas Kent* [†2], *Eddie Wilson* [‡3], *Anthony Pipe* [§4], *and Arthur Richards* [¶5]

[1,2,5]*Department of Aerospace Engineering, University of Bristol, Bristol BS8 1TR, UK*

[3]*Department of Engineering Mathematics, University of Bristol, Bristol BS8 1UB, UK*

[4]*Faculty of Environment and Technology, University of the West of England, Bristol, BS16 1QY*

[1,2,3,4,5]*Bristol Robotics Laboratory, Bristol BS16 1QY, UK*

ABSTRACT

This research project aims to identify the impact of autonomous vehicles on road capacity. In particular, the project studies the flow of traffic at uncontrolled intersections using different decision-making policies. Analytical methods have identified bounds of position, time and speed of different classes of collision avoidance. These are being used to derive a range of simple but distinct avoidance policies. Next, a large-scale numerical simulation will be performed to study macro-scale flow effects. This data will be analysed further to predict the effect of the gradual increase of the autonomous vehicles on urban traffic scenarios.

I. INTRODUCTION

the number of vehicles deployed in urban traffic rises every year, the issue of traffic flow capacity limitations is becoming more prominent [10]. The gradual introduction of Autonomous Vehicles (AVs) can possibly reduce urban road capacity due to the trade-off between dynamics and comfort. The report by ATKINS demonstrated analysis of Connected Autonomous Vehicles (CAVs) on traffic flow in the UK [1]. They concluded that at a higher CAV market penetration, the traffic capacity improves.

Some researchers in their studies on AV assume that the market penetration of AVs is 100 percent[11, 20, 24, 27, 29]. However, an increasing number of studies demonstrate results on low AV market penetration deployed and its impact on urban road capacity [3, 4, 6, 8, 12, 14, 21, 30].In particular, the focus is on intersections, as they have significant implication on traffic

capacity and safety [5, 13, 17, 18, 19, 23, 32].As an example, according to Fortelle and Qian [7] more than one third of road accidents happen at intersections.

A great deal of the literature to date focuses on a centralised approach for intersection management [12, 18, 22, 26]. However, centralised system collapse can cause significant delays and accidents [18, 26, 28]. Distributed intersection management, on the contrary, is scalable, robust to failures, more reactive and can deal with the fairness problem [4, 5]. Despite that, such a system is prone to less consistent decision making and reduced efficiency. As a solution, a mix of centralised and distributed systems can have benefits of both [13, 23].

Uncontrolled intersections are common in UK, but have not been addressed in AV' studies in depth [31].

---

[*]karam.safarov@bristol.ac.uk

[†]thomas.kent@bristol.ac.uk

[‡]re.wilson@bristol.ac.uk

[§]Anthony.Pipe@uwe.ac.uk

[¶]arthur.richards@bristol.ac.uk

An obstacle avoidance occurs in the Time-Displacement-Velocity (TDV) space. The triple $\boldsymbol{x} = (t, s, v) \in \mathbb{R}_0^+ \times \mathbb{R} \times \mathbb{R}_0^+$, where t is time, s is displacement and v is velocity. The dynamics of the system has to satisfy:

$$\dot{s} = v, \ v \in [\underline{v}, \overline{v}], \ \dot{v} \in [\underline{a}, \overline{a}]$$

where, $\underline{v} \geq 0$, $\underline{a} \leq 0 \leq \overline{a}$. The trajectory $x(t) = (t, s(t), v(t))$ is dynamically feasible if and only if $\dot{s}(t) = v(t)$, $v(t) \in [\underline{v}, \overline{v}]$ and $\dot{v}(t) \in [\underline{a}, \overline{a}]$. The state $x(t_{end})$ is dynamically reachable for time $t \in [t_0, t_{end}]$, such that $x(t_0) = x_0$ and $x(t_{end}) = x_{end}$.
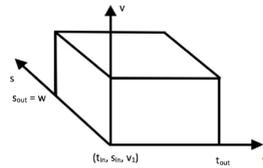
Figure 1: TDV space for two vehicles
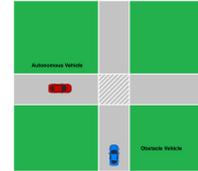
Figure 2: Two vehicles simulation

That is, those studies do not take into account low AV market penetration during early stages of the technology adoption [7]. Hence, data acquired in such studies is problematic to use for mixed traffic simulation studies. Our study is offering collision free decision making on-board AVs at the crossroad intersection, which potentially can offer a gradual improvement of the traffic flow with low level of penetration. Collision avoidance can be an issue for intersection management. The theoretical approach with provable safety can

III. SIMULATION AND RESULTS

The two fundamental actions which an AV can take when approaching an intersection with a single known obstacle are to either go ahead, that is pass the intersection before the other vehicle, or go behind and allow the vehicle to cross the intersection before the . They are demonstrated in the Figure 3 and 4. One suitable approach to allow scalability to multiple car simulations is to use behaviour trees. Whereby, each vehicle will hierarchically perform logical actions (or

Figure 3: Pass ahead

Figure 4: Pass behind

guarantee collision free crossing through reachability analysis [2, 7, 9, 15, 16, 25].

II. PROBLEM DEFINITION

We aim to identify the effect of deploying AVs on traffic capacity at an intersection. In our microscopic simulation, an AV and a human driven vehicle are crossing the uncontrolled crossroad intersection without colliding. The following analysis demonstrates that obstacle avoidance in Time-Displacement-Velocity (TDV) space can be developed for an AV. The TDV space will later be used to develop the numerical simulation of the collision avoidance at the intersection.

behaviours) to reach a their given goal. For example drive at nominal speed until a potential future collision is predicted, then switch the action of slowing down, allowing the other vehicle to pass, or maintaining a speed sufficient for passing the junction first.

I.V. CONCLUSION AND FUTURE WORK

Numerical simulation of two vehicles crossing a uncontrolled intersection has been developed in MATLAB to study its traffic capacity. Simple and robust control policies to avoid a collision at the crossing box were evaluated to study the speed profiles and

overall performance of the system. Next, large scale traffic simulation will be developed with low market penetration of AVs. Then, we will develop a more practicable model of the intersection environment by adding uncertainty to sensing.

Lastly, we will evaluate the simulation and validate it by comparing to existing simulation software and analyse a possibility of traffic throughput improvement with certain ways of deploying AVs into the urban traffic.

REFERENCES

1. Atkins. Research on the impacts of connected and autonomous vehicles (CAVs) on traffic flow Stage 1: Evidence Review. Technical Report March, 2016.

2. Leonardo Bruni, Alessandro Colombo, and Domitilla Del Vecchio. Robust multi-agent collision avoid- ance through scheduling. Proceedings of the IEEE Conference on Decision and Control, pages 3944– 3950, 2013. ISSN 01912216. doi: 10.1109/CDC.2013.6760492.

3. Danjue Chen, Soyoung Ahn, Madhav Chitturi, and David A. Noyce. Towards vehicle automation: Road- way capacity formulation for traffic mixed with regular and automated vehicles. Transportation Research Part B: Methodological, 100:196– 221, 2017.

4. Zhibin Chen, Fang He, Lihui Zhang, and Yafeng Yin. Optimal deployment of autonomous vehicle lanes with endogenous market penetration. Transportation Research Part C: Emerging Technologies, 72(October 2017):143–156, 2016.

5. Kurt Dresner and Peter Stone. A multiagent approach to autonomous intersection management. Journal of Artificial Intelligence Research, 31:591–656, 2008.

6. Daniel J. Fagnant and Kara Kockelman. Preparing a nation for autonomous vehicles: Opportunities, barriers and policy recommendations. Transportation Research Part A: Policy and Practice, 77:167–181, 2015.

7. Arnaud De La Fortelle and Xiangjun Qian. Autonomous driving at intersections : combining theoretical analysis with practical considerations. ITS World Congress 2015, (October):5–9, 2015.

8. Noah J. Goodall, Byungkyu (Brian) Park, and Brian L. Smith. Microscopic Estimation of Arterial Ve- hicle Positions in a Low-Penetration-Rate Connected Vehicle Environment. Journal of Transportation Engineering, 140(10), 2014.

9. Michael R Hafner, Drew Cunningham, Lorenzo Caminiti, and Domitilla Del Vecchio. Cooperative Colli- sion Avoidance at Intersections : Algorithms and Experiments. IEEE Transactions on Intelligent Trans- portation Systems, 14(3):1162–1175, 2013.

10. Fred L Hall and Kwaku Agyemang-Duah. Freeway capacity drop and the definition of capacity. Trans- portation research record, (1320), 1991.

11. Fu-sheng Ho and Los Angeles. Spacing and Capacity Evaluations for Different AHS Concepts. Proceed- ings of the American Control Conference Albuquerque, New Meixco, (June):2036–2040, 1997.

12. S. Ilgin Guler, Monica Menendez, and Linus Meier. Using connected vehicle technology to improve the efficiency of intersections. Transportation Research Part C: Emerging Technologies, 46:121–131, 2014.

13. Md Abdus Samad Kamal, Jun-ichi Imura, Akira Ohata, Tomohisa Hayakawa, and Kazuyuki Aihara. Co- ordination of automated vehicles at a traffic-lightless intersection. In 16th International IEEE Conference on Intelligent Transportation Systems-(ITSC), pages 922–927. IEEE, 2013.

14. Arne Kesting, Martin Treiber, Martin Schönhof, and Dirk Helbing. Adaptive cruise control design for active congestion avoidance. Transportation Research Part C: Emerging Technologies, 16(6):668–683, 2008.

15. Kyoung-dae Kim and P R Kumar. An MPC-Based Approach to Provable System-Wide Safety and Live- ness of Autonomous Ground Traffic. IEEE Transactions on Automatic Control, 59(12):3341–3356, 2014.

16. Hemant Kowshik, Derek Caveney, and P. R. Kumar. Provable systemwide safety in intelligent intersec- tions. IEEE Transactions on Vehicular Technology, 60(3):804–818, 2011.

17. Scott Le Vine, Alireza Zolfaghari, and John Polak. Autonomous cars: The tension between occupant experience and intersection capacity. Transportation Research Part C: Emerging Technologies, 52:1–14, 2015.

18. Scott Le Vine, Xiaobo Liu, Fangfang Zheng, and John Polak. Automated cars: Queue

discharge at signalized intersections with 'Assured-Clear-Distance-Ahead' driving strategies. Transportation Research Part C: Emerging Technologies, 62:35–54, 2016.

19. Joyoung Lee, Byungkyu Brian Park, Kristin Malakorn, and Jaehyun Jason So. Sustainability assessments of cooperative vehicle intersection control at an urban corridor. Transportation Research Part C: Emerging Technologies, 32:193–206, 2013.

20. Fangshu Lei, Yunpeng Wang, Guangquan Lu, and Daxin Tian. Travel time reliability affected by accident in freeway with connected vehicles. 17th International IEEE Conference on Intelligent Transportation Systems (ITSC), pages 51–56, 2014.

21. Michael W. Levin and Stephen D. Boyles. A multiclass cell transmission model for shared human and autonomous vehicle roads. Transportation Research Part C: Emerging Technologies, 62:103–116, 2016.

22. Zhixia Li, Madhav Chitturi, Dongxi Zheng, Andrea Bill, and David Noyce. Modeling Reservation-Based Autonomous Intersection Control in VISSIM. Transportation Research Record: Journal of the Trans- portation Research Board, 2381(August 2015):81–90, 2013.

23. Laleh Makarem, Minh Hai Pham, André-Gilles Dumont, and Denis Gillet. Micro-simulation modeling of coordination of automated guided vehicles at intersection. In Transportation research board 91st annual meeting, number EPFL-CONF-174790, 2012.

24. Edward Henry Pierowicz, John A and Pirson, B and Bittner, A and Lloyd, ML and Jocoy. Intersection Collision Avoidance Using ITS Countermeasures. 2000.

25. Xiangjun Qian, Jean Gregoire, Arnaud De La Fortelle, and Fabien Moutarde. Decentralized model pre- dictive control for smooth coordination of automated vehicles at intersection. Control Conference (ECC),

2015 European. IEEE, 2015, pages 3452–3458, 2015.

26. Hesham Rakha and Raj Kishore Kamalanathsharma. Eco-driving at signalized intersections using V2I communication. IEEE Conference on Intelligent Transportation Systems, Proceedings, ITSC, pages 341– 346, 2011.

27. Steven E. Shladover. Cooperative (rather than autonomous) vehicle-highway automation systems. IEEE Intelligent Transportation Systems Magazine, 1(1):10–19, 2009.

28. Weili Sun, Jianfeng Zheng, and Henry X. Liu. A capacity maximization scheme for intersection manage- ment with automated vehicles. Transportation Research Procedia, 23(2016):121–136, 2017.

29. Patcharinee Tientrakool, Ya Chi Ho, and Nicholas F. Maxemchuk. Highway capacity benefits from us- ing vehicle-to-vehicle communication and sensors for collision avoidance. IEEE Vehicular Technology Conference, pages 0–4, 2011.

30. Bart Van Arem, Cornelia J.G. Van Driel, and Ruben Visser. The impact of cooperative adaptive cruise control on traffic-flow characteristics. IEEE Transactions on Intelligent Transportation Systems, 7(4): 429–436, 2006. ISSN 15249050. doi: 10.1109/TITS.2006.884615.

31. Mark Vanmiddlesworth, Kurt Dresner, and Peter Stone. Replacing the Stop Sign : Unmanaged Intersec- tion Control for Autonomous Vehicles. Proc., Autonomous Agents and Multiagent Systems Workshop on Agents in Traffic and Transportation, Estoril, Portugal, pages 94–101, 2008.

32. Ismail H. Zohdy, Raj Kishore Kamalanathsharma, and Hesham Rakha. Intersection management for autonomous vehicles using iCACC. IEEE Conference on Intelligent Transportation Systems, Proceedings, ITSC, pages 1109–1114, 2012.

Motion Intent Recognition Using a Tactile Arm Brace

Thekla Stefanou[1] and Greg Chance Tareq Assaf Sanja Dogramadzi[2]
[1]BRL, University of Bristol, UWE
[2]BRL, UWE

I.INTRODUCTION

In this study we are looking at motion intent recognition using a tactile sensing system, with particular interest in stroke rehabilitation. During active-assisted training the paralysed limb is guided through a movement only after having detected visual or haptic cues of motion intent from the patient.

Based on previous work done [8], we introduce the tactile arm brace (TAB) with the aim of mimicing the recognition of movement intent in this therapist-patient interaction; potentially distinguishing between the different motions. In a robot assisted rehabilitation system the TAB would provide the control input.

A variety of sensors have been used in movement intent recognition systems. The well-established EMG controlled systems are yet to reach acceptable, consistent performance [2]. A different approach is force myography (FMG) [6], or tactile imaging, which has shown promising results. The contracting muscle shape changes that take place can be monitored on the skin surface and used as an indication of motion intent [3].

II.FOREARM TACTILE SIGNATURE

The study performed included 12 healthy participants. Wearing the TAB (Fig. 2c), the tactile sensor readings were recorded as the participant performed finger extension and gripping motions. A gripper device was built to monitor the force used. Eight force sensitive resistive sensors [7], were used on the brace.

III.DIGIT EXTENSION

During finger extension, Fig. 1a-1b, the digit extensors shorten and become thicker giving rise to higher contact forces on their associated sensors, S4 and S5. Concurrently, there are small changes within the wrist flexor muscles, S1 and S7, which move the wrist opposite to the fingers, tightening the digit extensor tendons. This was true across all 12 subjects.

I.V.GRIPPING

The flexor digitorum muscles, the largest group within the forearm, contract to produce gripping. As would be expected there is an increase on the forces between the TAB and the forearm when the gripper is pressed. Part of the challenge is a stroke survivor's muscle tone which can be as low as 5-10% [9] of their nominal strength [1], an average of 17N. Hence,
the grip force used during the trials was limited to that.

Some raw experimental data from one of the participants are presented on Fig. 2a. The contact forces perceived at each sensor location on the forearm brace , F_{Si}, (top) are plotted as the grip force changes, $F_{gripper}$, (bottom). Fig. 2b indicates the linear correlation between the raw brace forces as measured at each sensor point and the grip strength being used. Gripping motions in this trial appear to produce the largest force changes in the approximate locations of S3/S4, and presumably this is where the highest muscle activity occurs.

In proximity to the flexor muscles, S8 indicates the third highest contact force sensitivity. Good correlation between the gripping force and S3/S6 forces is related to the wrist extensors tightening the digit flexor tendons. Although   the linear relationship between gripping strength and each sensor readings was visible across all subjects there were variations in sensitivity.

(a) Relaxed. (b) Extended. (c) Forearm cross-section indicating the muscles involved in finger extension. (d) Normalised force distributions with the fingers extended & relaxed.

Fig. 1. Digit extension.

(a) Gripping force applied and the corresponding contact forces on the TAB. (b) Correlation between grip force and brace contact forces. (c) Performing gripping with the gripper, wearing the TAB.
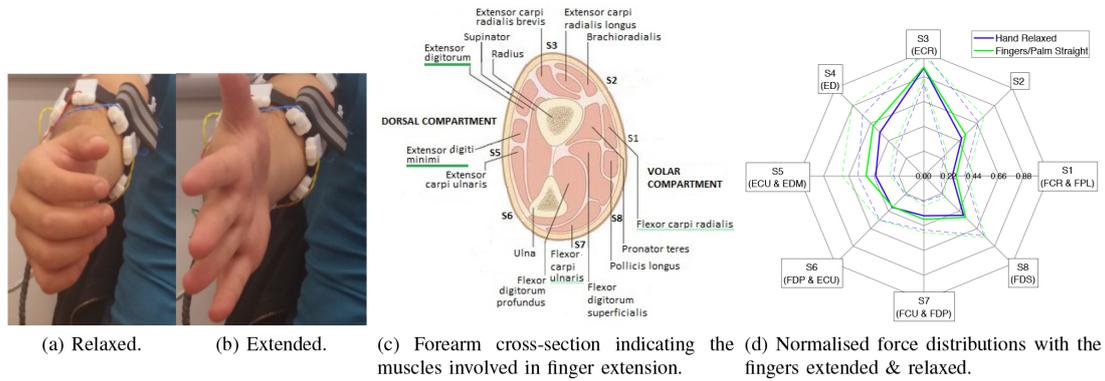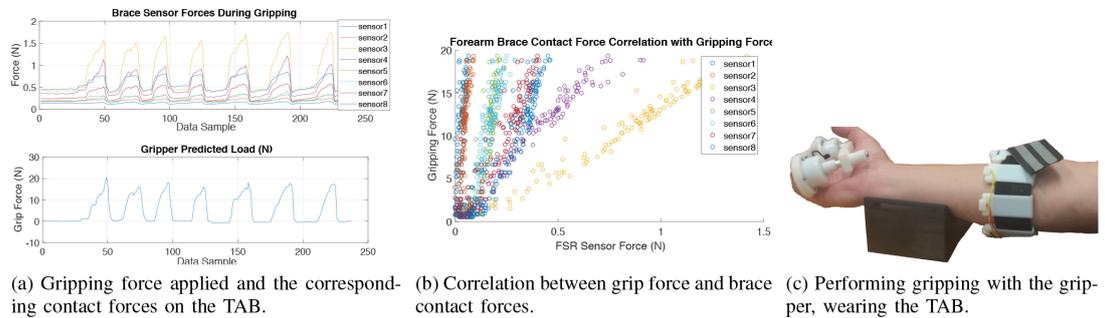
Fig. 2. Arm brace sensory response during gripping.

V. MOVEMENT INTENT PREDICTION

Linear regression analysis was performed around the TAB for each F_{Si}, to predict $F_{gripper}$. Certain forearm areas exhibited higher activity during power gripping, and hence sensitivity, than others; these were mainly in proximity to the muscles with the greater tension changes. The fitness of the individual regression models, was looked at using the coefficient of determination, R^2. The gripping intent recognition and grip force prediction was performed by favouring high R^2, 0.8, and grip sensitivity, 0.052N, of the individual sensor areas around the brace, as well as looking the consistency amongst participants. These tactile features captured by the arm brace during gripping were combined with the digit extension tactile features, to form the input of a motion intent prediction algorithm.

Further participant studies will be completed including subjects with movement difficulties. Four different types of grips (power, precision, tripod and pinch [5]) will be performed in addition to wrist extension/flexion. Thus, putting to the test the TAB's sensitivity and reliability and the system's ability to distinguish between closely related motions. Furthermore, the performance of the TAB will be measured against that of the Myo brace [4] in both healthy adults and stroke survivors with upper extremity impairment.

V.I. CONCLUSION

Using the TAB we are not only extracting the characteristic features for recognition of different types of motion intent but there is also an attempt to identify why certain features arise. This could potentially turn such system into a diagnostics tool for therapists.

REFERENCES

1. Richard M Dodds et al. "Grip strength across the life course: normative data from twelve British studies". In: PLoS One 9.12 (2014), e113637.

2. Dario Farina et al. "The extraction of neural information from the surface EMG for the control of upper- limb prostheses: Emerging avenues and challenges". In: IEEE Trans. Neural Syst. Rehabil. Eng. (2014).

3. Shunji Moromugi et al. "Muscle stiffness sensor to control an assistance device for the disabled". In: Artif. Life Robot. (2004).

4. Myo Gesture Control Armband — Wearable Technology by Thalmic Labs. URL: https://www.myo.com/ (visited on 11/24/2017).

5. Victor Hirsch Nordin, Margareta and Frankel. Basic biomechanics of the musculoskeletal system. Lippincott Williams & Wilkins, 2001.

6. Sam L Phillips and William Craelius. "Residual kinetic imaging: a versatile interface for prosthetic control". In: Robotica 23 (2017), pp. 277–282.

7. Measurement Specialties. FSR 402 Sensor Product Page. 2017. URL: http://www.interlinkelectronics.com/FSR402.php.

8. T. Stefanou et al. "Upper Limb Motion Intent Recognition Using Tactile Sensing". In: Accept. IEEE IROS 2017. 2017.

9. A Sunderland et al. "Arm function after stroke. An evaluation of grip strength as a measure of recovery and a prognostic indicator." In: J. Neurol. Neurosurg. Psychiatry (1989).

Antagonism in pneumatically-actuated, stiffness-controllable robot fingers

Agostino Stilli[1], Helge A. Wurdemann[2] and Kaspar Althoefer[3], Member IEEE.
[1]University College London, Department of Computer Science, Surgical Robot Vision Group
[2]University College London, Department of Mechanical Engineering, #SoftHapticsLab
[3]Queen Mary University of London, Advanced Robotics @ Queen Mary (ARQ), Mail:
k.althoefer@qmul.ac.uk

ABSTRACT

The capability to vary stiffness in flexible robotic fingers provides increased dexterity and manipulation capabilities – opening up a completely new approach to grasping a wide range of objects. The proposed robot finger concept marries the advantages of soft material robotics with the advantages of robot systems that are stiff and capable of handling high-payload objects. Is it widely accepted that most soft material robots such as those made from silicone rubber suffer from an inability to apply high forces to the environment they are in contact with, limiting their application. On the other hand, traditional non-compliant robot hands made of rigid components often require accurate information about the location of objects to be handled and advanced control strategies to achieve a good grasp – further, the range of objects is often limited, since a particular grasper architecture is often optimized for grasping a small set of objects. The proposed stiffness-controllable finger can approach the object in a low-stiffness state with all its advantages of compliance and can then adjust the stiff- ness adjusting to the shape of the object and requirements of the grasping task – once a grasp is established the stiffness can be ramped up considerably to lift heavy objects whilst not changing the assumed finger configuration. Hence, lifting heavy, but fragile objects becomes a possibility at low control cost. The proposed robot finger concept extends from existing robot fingers proposed elsewhere, because with its 2-DoF motion capability it can bend in different directions further enhancing the grasping capabilities of robot hands with which the pro- posed fingers is intended to be integrated – imagine a robot finger that can bend not only along one axis but in all directions around its longitudinal axis. The proposed concept provides the additional capability of massively extending from a collapsed state to a fully-extended state, even further enhancing the grasping and manipulation capabilities. This paper reports on the proposed robot finger concept highlighting its capability to bend in a multitude of directions, vary its stiffness and apply forces to the environment in a well-controlled fashion.

I.INTRODUCTION

The ability to change rapidly from a stiff to a soft configuration, mimicking natural limbs as for example octopus tentacles or elephant trunks, is very much desired by the modern robotics research community but difficult to achieve. Biology has clearly optimised its way of creating actuated limbs that are very difficult to recreate artificially. Nevertheless, robotic systems that are capable of adjusting their stiffness have been explored and developed by quite a few researchers attempting to realize robot systems applicable to areas such as human-robot interaction [2], minimally invasive surgery [3] as well as prosthetics [4]. The possibility to change the compliance of a joint, link or the entire
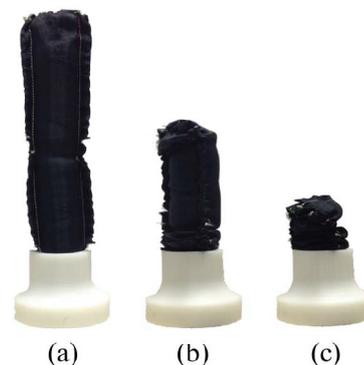
Figure 1 – Elongation capability of the antagonistically-actuated, stiffness-controllable robot finger in the fully elongated state (a), partially elongated state (b) and in the shrunk state (c).

robotic system can considerably enhance the capabilities in a wide range of manipulation tasks [5]

The concept of variable stiffness robots has advanced significantly over the last ten years or so with successful applications in industry, healthcare and entertainment. In the wide area of human-robot interaction, for example, achievements have been widespread developing solutions capable of adapting to the interaction with the human in a dynamic fashion and capable of undertaking collaborative tasks. In this context, hand/human-guided machine learning, where the robot hands "learns" how to perform a task while being steered by a human user clearly showed to be very positive [9]. In this context, it has been shown that robots that can alter from a soft compliant modality to a stiff mode, i.e., being capable of adjusting stiffness is of great benefit for those learning methods [10], [11].

II. MATERIALS AND METHODS

In this paper we investigate the behavior of the Inflatable Robot Finger concept, based on work presented in [1]. The proposed robot finger comprises a flexible sheath that is made from fabric. Important here is that the sheath fabric is capable of adapting to shapes and can fold when no pressure is applied. Since the outside sheath can contain the air inside and cannot expand past its default surface area, the stiffness of the chamber within the sheath and thus the robot finger's structure's can be varied significantly. The assembled prototype of the proposed system is shown in Figure 1 in a fully elongated state (a), partially elongated state (b) and in the shrunk state. The cables affixed to the outer sheath allow navigating the finger in different directions. Combining the two actuation means, based on air pressure, on the one hand, and cables, on the other hand, the pose of the robot finger can be altered and its stiffness controlled synchronously. This hybrid actuator method is inherently antagonistic. We take here inspiration from nature trying to imitate the functioning of animals such as the octopus with its antagonistically organized muscles. It is also noted that our robot finger lightweight and soft, and as such especially suited for the

interaction with soft and fragile objects.

The manipulator sheath is realized by fitting a cylindrical elastic bladder inside a similarly shaped outer fabric. The inside of the sheath is an airtight chamber that can be filled with air and the air pressure can be controlled over wide range. Multiple cables integrated with the outer sheath and fixed at the tip of the finger, allowing the structure to be navigated. Differently from the vast majority of variable stiffness robotic systems, where only a limited number of stiffness levels are achievable and stable, the stiffness of the inflatable finger can be changed and finely tuned over a wide range. Typically the manipulator is kept in a compliant state during steering and in a more rigid one when it is required to lock the body pose and to exert a high level of force during grasping – these two levels of stiffness can be customized according to objects and grasp requirements.

III. EXPERIMENTAL STUDY PROGRAMME

Exploiting the lessons learned from the analysis conducted in [1] applied to a robot manipulator, we investigate the robot finger's behavior in a comparable way to establish the finger's bending stiffness during different configurations. A number of tests have been performed to investigate the bending stiffness of the system and its performance when interacting with the environment. The configuration shown in Figure 2 have been extensively tested. Our analysis investigates
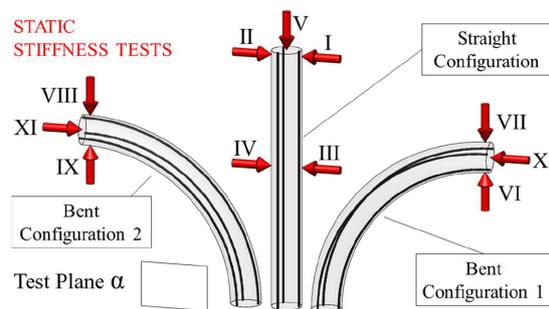
Figure 2 – Schematic of the test protocol to estimate the bending stiffness as a function of bending angle and chamber pressure [1].

the relationship between the bending stiffness of the robotic finger, the level of pressure inside the system, the tendon arrangement on the manipulator section and the body pose.

I.V.CONCLUSIONS AND FUTURE WORK

Extrapolating from the work presented in [1], we estimate a similar behavior for the proposed robot finger. It is noted that the bending stiffness of an inflatable, cylindrical structure is inversely proportional to the first power of the distance from the base. This result is different from that for beams made from a homogeneous elastic material which changes at the third power of the distance from the base. As a general rule, an increased bending stiffness can be achieved by raising the pressure in the inner chamber, as well as by increasing the area of the cross-section. The data from [1] also shows a low variance in the pose of the robot structure when being loaded and subsequently unloaded with a low hysteresis.

Future work will focus on integrating multiple of the inflatable, stiffness-controllable fingers with a base to achieve a highly dexterous robot hand. We will also explore the use of this technology for use as assistive systems in rehabilitation.

REFERENCES

1. Stilli, H. A. Wurdemann, and K. Althoefer, "Shrinkable, stiffness-controllable soft manipulator based on a bio-inspired antagonistic actuation principle," in IEEE International Conference on Intelligent Robots and Systems, 2014, pp. 2476–2481.
2. G. Tonietti, R. Schiavi, and A. Bicchi, "Design and Control of a Variable Stiffness Actuator for Safe and Fast Physical Human/Robot Interaction,"
3. Robotics and Automation, 2005. ICRA 2005. Proceedings of the 2005 IEEE International Conference on. pp. 526–531, 2005.
4. Sepetka, P. Pham, and E. T. Engelson, "Variable stiffness catheter." US Patent Office, 03-May-1994.
5. E. English and D. Russell, "Mechanics and stiffness limitations of a variable stiffness actuator for use in prosthetic limbs," Mech. Mach. Theory, vol. 34, no. 1, pp. 7–25, 1999.
6. Vanderborght, A. Albu-Schäffer, A. Bicchi, E. Burdet, D. G. Caldwell, R. Carloni, M. Catalano, O. Eiberger, W. Friedl, and G. Ganesh, "Variable impedance actuators: A review," Rob. Auton. Syst., vol. 61, no. 12, pp. 1601–1614, 2013.
7. S. Muench, J. Kreuziger, M. Kaiser, and R. Dillman, "Robot programming by demonstration (rpd)-using machine learning and user interaction methods for the development of easy and comfortable robot programming systems," in Proceedings of the International Symposium on Industrial Robots, 1994, vol. 25, p. 685.
8. J. Choi, S. Park, W. Lee, and S. C. Kang, "Design of a robot joint with variable stiffness," in Proceedings - IEEE International Conference on Robotics and Automation, 2008, pp. 1760–1765.
9. R. Ham, T. Sugar, B. Vanderborght, K. Hollander, and D. Lefeber, "Compliant actuator designs," IEEE Robot. Autom. Mag., vol. 16, no. 3, 2009.

Collaborative robot slip detection based on vibration analysis

Shane Trimble, School of Electronics, Electrical Engineering & Computer Science Queen's University Belfast Email: strimble08@qub.ac.uk

Wasif Naeem, School of Electronics, Electrical Engineering & Computer Science Queen's University Belfast Email:w.naeem@qub.ac.ukSeán McLoone, School of Electronics, Electrical Engineering & Computer Science Queen's University Belfast Email: s.mcloone@qub.ac.uk

ABSTRACT

Grasping between two cooperating robotic arms with a friction grip acting orthogonally to the surface to overcome tangential forces presents the matter of slip control. Modern smart collaborative robots have built- in joint torque sensing capability which prevents the need for additional external sensors when detecting slip, vital to create a feedback signal for slip control. This paper presents the preliminary findings of experimentation on a Baxter robot to investigate if these built-in torque sensors can be utilized for this purpose. The left shoulder joint torque values of the Baxter robot, S1, are recorded with and without slip taking place. Frequency domain analysis of both scenarios reveals differences in frequency components, showing that there is a substantial increase in magnitude from the 1.5 to 12 Hz range. A high-pass IIR filter is then applied to successfully identify slip in the time-domain, proving that it is a viable method for slip detection in real-time

I.INTRODUCTION

In recent years the robotics community has witnessed the introduction and growth of general purpose collaborative robots which can carry-out mundane and/or precise tasks similar to a traditional robot, but also have the ability to perform multiple jobs, in close proximity to other robots and humans [1], [2]. These robots minimise the work load on installation engineers, saving time and money. Also, a non-technical person can shift the robot from one task to another with minimal training and reprogramming of the robot.

A multi-purpose blank end-effector, Figure 1 (a), allows for a multitude of tasks to be carried out without the need for retooling for different jobs. This relies on the application of a normal force to an object and uses a combination of applied forces and friction to overcome gravitational and motion acceleration forces. Figure 1(b) shows the applied forces between two end-effectors attached to two separate manipulators working together to hold an object.

The manipulation of objects is typically accompanied by events such as slippage, between a robot's fingers or, in the case of general purpose end-effectors, two robotic arms. Humans can identify such events using a combination of superficial and deep mechanoreceptors [3]. In robotics, with more limited tactile sensing, such events can be hard to distinguish. In the field of robotic slip detection and control, much work has been done with single dexterous end-effectors [4], [5], [6], [7], [8]. Cooperating manipulators is also an active area of study [9], [10], [11], [12] and so the combination of the two on a collaborative robot is a natural extension to the field.

Baxter is a collaborative robot which is programmed through Robot Operating System (ROS), a set of libraries and tools built onto Ubuntu, which communicates through publishing/subscribing to/from *topics* The robot can be used safely around humans because it is able to sense forces on it's joints, something that will be used in this experiment to collect vibration data. For this experiment the topic in question is *gravity_compensation_torques/actual_ef*

fort, which reads the torque value of the joint motors in Nm and publishes at a rate of 95 Hz, similar to the 100 Hz sampling rate used in [7], but below the 400 Hz used in [13] & [14].

II. EXPERIMENT

Two blank end-effectors were 3D printed and attached to Baxter, as in Figure 1 (a) and were manipulated to a set of coordinates in order to grasp a flat piece of PVC sheeting, Figure 1 (c), with a 1kg weight attached, and the sheet was raised. In order to find the slip threshold, the shoulder (S0), elbow (E1) and
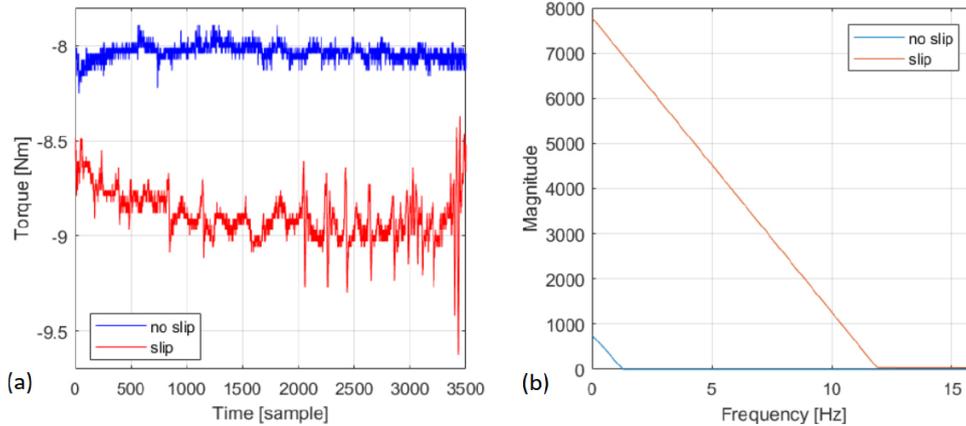
noise signal. Figure 2 depicts the time and frequency domain representation of both scenarios. Note the average difference of approximately 1 Nm between both time-domain signals, which is due to the robot independently determining the torque values when setting joint angles.

In order to identify slip in real-time, the Fourier transform of time data windows was found to have too high a latency, so a time domain filter needs to be designed. It can be seen that with no slip occurring, there are small components visible from 0 to 1.5 Hz,

Fig. 2. Slip and non-slip signals (a) time and (b) frequency domain representations.

wrist (W1) joint angles were tweaked until slippage occurs, where all 14 manipulator joint angles were recorded. The sheet was a again initialised to it's original position and

but when slip is taking place the 0 to 12 Hz range increases substantially, similar to [14]. From this information a 5th order, 2 Hz cutoff, high-pass Butterworth filter is applied to both signals, with the transfer function given in equation 1.

$$H(Z) = \frac{Y(Z)}{X(Z)} = \frac{0.899z^5 - 4.492z^4 + 8.899z^3 + 8.899z^2 + 4.492z - 0.8985}{z^5 - 4.786z^4 + 9.167z^- 8.783^2 + 4.209z - 0.8073}$$
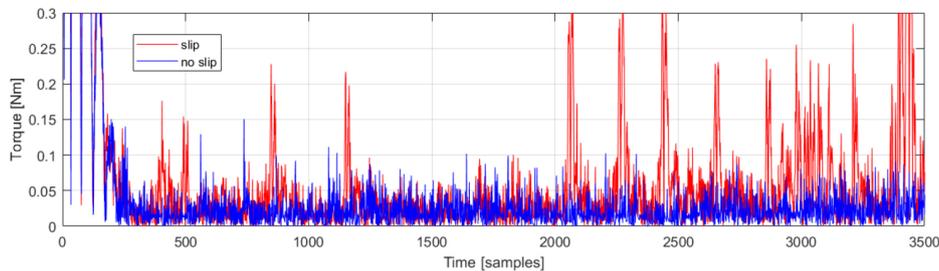
Fig. 3. Filtered non-slip signal and slip signal in the time domain

the joints set to these threshold values, with the *gravity_compensation_torques/actual__ef fort* topic for left joint S0 torque recorded on the ROS PC. The same process was repeated with no slip, giving a baseline

III. CONCLUSION

This experiment has successfully demonstrated that a slip event can be recognized between two manipulators on a

Baxter collaborative robot using the onboard force sensors. The near 4-fold difference in RMS allows a simple moving average calculation to be applied to time sample windows for slip classification.

REFERENCES

1. L. Johannsmeier and S. Haddadin, "A hierarchical human-robot interaction-planning framework for task allocation in collaborative industrial assembly processes," IEEE Robotics and Automation Letters, vol. 2, no. 1, pp. 41–48, Jan 2017.

2. S. Savazzi, V. Rampa, F. Vicentini, and M. Giussani, "Device-free human sensing and localization in collaborative human 2013;robot workspaces: A case study," IEEE Sensors Journal, vol. 16, no. 5, pp. 1253–1264, March 2016.

3. G. J. Gerling, I. I. Rivest, D. R. Lesniak, J. R. Scanlon, and L. Wan, "Validating a population model of tactile mechan-otransduction of slowly adapting type i afferents at levels of skin mechanics, single-unit response and psychophysics," IEEE Transactions on Haptics, vol. 7, no. 2, pp. 216–228, April 2014.

4. A. Aqilah, A. Jaffar, S. Bahari, C. Y. Low, and T. Koch, "Resistivity characteristics of single miniature tactile sensing element based on pressure sensitive conductive rubber sheet," in 2012 IEEE 8th International Colloquium on Signal Processing and its Applications, March 2012, pp. 223–227.

5. Saen, K. Ito, and K. Osada, "Action-intention-based grasp control with fine finger-force adjustment using combined optical- mechanical tactile sensor," IEEE Sensors Journal, vol. 14, no. 11, pp. 4026–4033, Nov 2014.

6. A. S. Al-Shanoon, S. A. Ahmad, and M. K. B. Hassan, "Re-gripping analysis based on implementation of slip-detection device for robotic hand model," in 2016 IEEE Region 10 Symposium (TENSYMP), May 2016, pp. 203–206.

7. M. Stachowsky, T. Hummel, M. Moussa, and H. A. Abdullah, "A slip detection and correction strategy for precision robot grasping," IEEE/ASME Transactions on Mechatronics, vol. 21, no. 5, pp. 2214–2226, Oct 2016.

8. A. Kent and E. D. Engeberg, "Robotic hand acceleration feedback to synergistically prevent grasped object slip," IEEE Transactions on Robotics, vol. 33, no. 2, pp. 492–499, April 2017.

9. Z. Xian, P. Lertkultanon, and Q. C. Pham, "Closed-chain manipulation of large objects by multi-arm robotic systems," IEEE Robotics and Automation Letters, vol. 2, no. 4, pp. 1832–1839, Oct 2017.

10. S. Erhart and S. Hirche, "Model and analysis of the interaction dynamics in cooperative manipulation tasks," IEEE Transactions on Robotics, vol. 32, no. 3, pp. 672–683, June 2016.

11. Z. Li, P. Y. Tao, S. S. Ge, M. Adams, and W. S. Wijesoma, "Robust adaptive control of cooperating mobile manipulators with relative motion," IEEE Transactions on Systems, Man, and Cybernetics, Part B (Cybernetics), vol. 39, no. 1, pp. 103–116, Feb 2009.

12. A. Lotfavar, S. Hasanzadeh, and F. Janabi-Sharifi, "Cooperative continuum robots: Concept, modeling, and workspace analysis,"

13. IEEE Robotics and Automation Letters, vol. 3, no. 1, pp. 426–433, Jan 2018.

14. R. P. Khurshid, N. T. Fitter, E. A. Fedalei, and K. J. Kuchenbecker, "Effects of grip-force, contact, and acceleration feedback on a teleoperated pick-and-place task," IEEE Transactions on Haptics, vol. 10, no. 1, pp. 40–53, Jan 2017.

15. D. Damian, T. H. Newton, R. Pfeifer, and A. M. Okamura, "Artificial tactile sensing of position and slip speed by exploiting geometrical features," IEEE/ASME Transactions on Mechatronics, vol. 20, no. 1, pp. 263–274, Feb 2015.

A Smart Contract Model for Agent Societies

Michele Tumminelli[1][0000-0002-8003-2533] and Steve Battle[1][0000-0002-7154-7869]

[1] University of West of England, Bristol, UK
michele2.tumminelli@live.uwe.ac.uk

ABSTRACT

This paper presents a solution to the exchange of services within an agent society. We explore an open delivery chain scenario in which autonomous drones offer and sub-contract delivery services to each other. Such agents are able to self-organize according to a chain of responsibility pattern. In such a heterogeneous agent society, it is crucial to define an approach that will guarantee accountability, responsibility, and ultimately trust in the execution of the service. The presented solution is based on smart contracts using a blockchain style of a distributed ledger.

Keywords: Blockchain, Smart Contract, Ethereum, Solidity.

I. INTRODUCTION

An agent society often called internet of agents [1] is an extension of the paradigm of the internet of things to autonomous systems. This society enables the coordination of heterogeneous autonomous agent systems within an open network. In this scenario, the autonomous agents cooperate and negotiate to solve their tasks. One issue is the establishment of trust between agents that need to exchange services; the solution needs to address the problems of responsibility, accountability, scalability and trust. Blockchain presents a new ap- proach to providing these capabilities. The implementation of smart contracts on top of a blockchain allows agents to commit to contracts and be accountable for delivering the agreed services.

The first section of this paper will present the agent society scenario; the second section will introduce the trust problem; the third section introduces the blockchain system; the fourth section will present the topic of smart contracts; the fifth section will explain trust systems and the sixth section will describe a possible sce- nario. In conclusion, future work is identified.

II. AGENT SOCIETY

One of the most interesting emerging topics is the internet of things, or industrial internet, especially when applied to autonomous connected devices. One simple example is a thermostat which allows a user to monitor and control the heating system of his house remotely and collect analytics. The internet of things is typically organised as a master-slave system where there is little or no autonomy at the edge of the network. The internet of agents [1] or agent society introduces intelligence and autonomy to the internet of things, extending it to the realm of autonomous agents which can independently cooperate and negotiate services to solve their tasks. The first characteristic of such systems is the open nature of the network and the heterogeneous implementation of the autonomous agents; this requires standardisation of the cooperation and negotiation protocols to allow interoperability. This may be solved by defining an ontology of contracts based on the Web Ontology Lan- guage (OWL) [2]. This ontology provides a common ground for agents to offer and request services, enabling sophisticated cooperation and negotiation. The services offered by an agent represent the specific physical capabilities an agent has available to it.

III. TRUST IN AGENT SOCIETY

In the kind of agent society defined above, it is essential to define the trust mechanism [3] on the basis of the exchange of services.

Agents need to authenticate themselves and pay for services. For physical services, there is a need to negotiate and commit to a physical task to be performed by an agent. There may be different approaches to payment, from free collaboration, one-off payments or subscriptions. The trust mechanism is critical since there may be serious implications if the service is not delivered as agreed. The agent requiring the service will publish a contract, and the service provider is able to bid for the contract and will commit to the contract via a deposit to guarantee the commitment or an insurance policy which covers the deposit. This is what happens typically in traditional society transaction. If the provider breaks the contract, it loses all or part of the deposit, whereas if it concludes the contract it takes the payment. To manage this trust mechanism, we need a platform which will act as a guarantor between requester and provider of the service in which the two-parties can trust each other, deliver on the contract, and execute the financial transaction.

I.V. BLOCKCHAIN

The blockchain is a distributed transactional database for managing financial transactions and smart contracts [4]. The system is based on a peer to peer network of nodes who maintain a records (blocks) of the transactions and the agreement mechanism within the nodes of the network provide the trust mechanism. The first implementation of blockchain which is widely used is the Bitcoin blockchain system for financial transactions. However, Bitcoin provides a limited capability for smart contracts. A more recent and general-purpose solution is based on the Ethereum [5] blockchain. Ethereum provides an embedded, isolated, secure and safe virtual machine which supports the execution of smart contracts. This solution is intrinsically secure and scalable by design. A third solution is represented by IOTA [6], it is a new type of cryptocurrency designed for the Internet of Things (IoT) which does not use blockchain technology but a Directed Acyclic Graph (DAG) technology which promises zero transaction cost. However, this technology is currently in beta and does not yet support smart contracts. Further investigation on the computational impact on the nodes is required.

V. SMART CONTRACTS

A smart contract is defined as executable code which automatically manages a transaction between parties. Ethereum contracts are coded in solidity [7], a high-level programming language similar to javascript which compiles to the Ethereum virtual machine. The smart contract is included in a blockchain transaction and is executed by the blockchain members in parallel comparing the results. Ethereum provides a separation of concerns between the logic of the contract, the security infrastructure, and the money transfer.

V.I. TRUST USING SMART CONTRACTS

As described above, the negotiation, bidding, payment, assurance and execution of these services depends on establishing mutual trust. Agents which need a service will emit a contract with the conditions of the executions and execution insurance. The provider agents are notified via a blockchain event of the creation of the contract. Agents acting in a particular area can register their presence on a service provider area contract which will provide notification services. Once the agent publishes the contract in the local area, the provider agents are free to bid for the contract by registering themselves and transferring the required deposit. Their reputations may be queried, and the winners and losers are notified. The contract governs the deposit, refunds the residual value of the contract to the customer agent and holds the value of the contract. Once the contract has been delivered, the smart contract will pay and refund the deposit to the supplier or manage the compensation to the customer agent and provide feedback to the provider reputation smart contract.

V.I.I. CONCLUSION AND FUTURE WORK

This paper presents a solution and business model to exchange services between agents. The mechanism of trust and contract guarantee is based on smart contracts using blockchain. This allows for the creation of a distributed scalable dual trust mechanism based on reputation and guarantees for the service requestor and provider agents. The next step is the design of detailed scenarios and to construct a prototype.

REFERENCES

1. Pico-Valencia, P., Holgado-Terriza, J.A.: Semantic agent contracts for internet of agents. In: Proceedings - 2016 IEEE/WIC/ACM International Conference on Web Intelligence Workshops, WIW 2016 (2017).
2. W3C: OWL 2 Web Ontology Language Document Overview (Second Edition), https://www.w3.org/TR/owl2-overview/.
3. Lu, A., Lu, G., Lu, J., Yao, S., Yip, J.: A review on computational trust models for multi-agent systems Title A review on computational trust models for multi-agent systems A Review on Computational Trust Models for Multi-agent Systems. Open Inf. Sci. J. 2, 18–25 (2009).
4. Christidis, K., Devetsikiotis, M.: Blockchains and Smart Contracts for the Internet of Things, (2016).
5. Ethereum White Paper, https://github.com/ethereum/wiki/wiki/White-Paper.
6. IOTA, https://iota.org
7. Solidity, https://solidity.readthedocs.io

In-situ Optical Characterisation of Nuclear Environments

Andrew West[a], Paul Coffey[a], Ioannis Tsitsimpelis[b], Michael Aspinall[b], Nicholas T. Smith[a], Malcolm J. Joyce[b], Philip A. Martin[a] and Barry Lennox[a]

[a]School of Electrical and Electronic Engineering, The University of Manchester

[b]Department of Engineering, Lancaster University, Bailrigg, LA1 4YR, Lancaster, UK

I. INTRODUCTION

Characterisation of materials is a key component in the planning and implementation of decommissioning of nuclear sites for both fission [1] and fusion [2]. Different waste may require different strategies for removal and treatment, prior to subsequent storage and disposal, which can result in increases in time and money if not considered before embarking on site decommissioning and remediation. Characterisation can include determination of elemental and chemical composition, radiometric properties, as well as identifying unexpected contamination be it radioactive or chemical. Furthermore, this information needs to be spatially resolved, so it informs stakeholders such as operations staff where hazards and materials are located.

Entry into a active area involves human workers wearing air-fed suits which are bulky and cumbersome. With a lack of rapid, lightweight scientific instruments for materials characterisation suitable for use

contaminated waste. This adds cost and time, as well as increased risk compared to in-situ analysis, and removing the spatial resolution of the measurements.

In both scenarios for current materials characterisation, there are the inherent risks involved with humans entering active environments, along with producing extraneous waste such as suits and tools that have to be safely disposed of. Furthermore, with large sites it may not be feasible for a worker to retrieve the number of samples required for effective characterisation, whilst access to some locations is so restricted for safety reasons that sample collection may be precluded completely. To minimise cost, time, and reduce risk whilst providing useful mapping and materials characterisation, it is proposed that a robot platform that can enter a site with a scientific payload capable of materials analysis, radiometric measurement, and physical mapping be developed.

Diagnostic	Purpose
LiDAR	3D laser scan mapping of environments
Camera	Operator vision and photogrammetry
Laser Induced Breakdown Spectroscopy (LIBS)	Elemental composition
Raman Spectroscopy	Chemical composition
CeBr scintilator	Gamma/neutron spectroscopy and dosimetry
Geiger Counter	Dosimetry, alpha, beta, gamma detection
Air quality sensors	Humidity, pH, volatile organic compounds

Table 1 – List of sensors and detectors that may be deployed to characterise hazardous environments

whilst wearing an air-fed suit, direct in-situ analysis is not usually undertaken. Typically, material samples are collected and analysed ex-situ in a lab environment, however the materials must be transported, stored and ultimately disposed of as possibly

To this end, a demonstration crawler robot has been built that utilises the commercially available Turtlebot 2. This robot has been modified to accommodate the various sensors required for it to be used as a proof of concept tool to investigate the capabilities

that deployed diagnostics offer when characterising and mapping environments, such as those found in the nuclear industry. The proposed scientific payloads are outlined in Table 1. To allow for 3D mapping of a space, LiDAR is preferred as it is not dependant on ambient light levels, however photogrammetry can also be used to build point clouds and meshes of the site. The 3D maps will provide a reference where other diagnostics information has been measured.

Laser Induced Breakdown Spectroscopy (LIBS) has been deployed as part of the Curiosity rover's ChemCam instrument [3], to determine the elemental composition of

the front of the robot, a QE-Pro spectrometer and a CW laser (max 350 mW) operating at 785 nm. Figure 1 shows an example spectra taken of the common calibration material silicon, with a peak at 520 cm^{-1} indicative of crystalline silicon bonds.

Diagnostic measurements require referencing to a physical position in the surveyed space. Figure 2(a) shows a high-resolution point cloud (pink) indicating a nearby wall as the robot approaches, visualised in real time through RVIZ [5]. Figure 2(b) demonstrates how RVIZ supports augmented reality, indicating the measurement point represented by a green marker superimposed on the
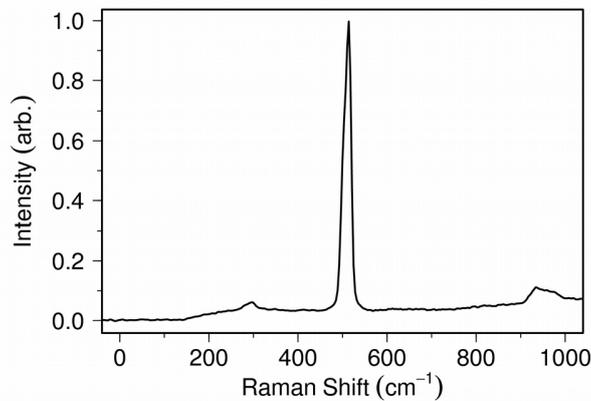
Figure 1 – Raman spectra of Silicon taken using the robot deployed instrumentation

Martian rocks. The same technique can be used to identify metals, concrete and possible radioisotopes [4]. Raman spectroscopy can identify chemical bonds, aiding in material classification compared to elemental composition alone. A Raman instrument was installed on a demonstrator robot, consisting of an Ocean Optics Raman probe mounted to

visual camera feed. Raman measurements (with the probe held in the orange mount), and any other collected data is tagged with spatial metadata.

Finally, radiometric data for alpha, beta, gamma, and neutrons can be achieved through lightweight detectors [6]. Mapping
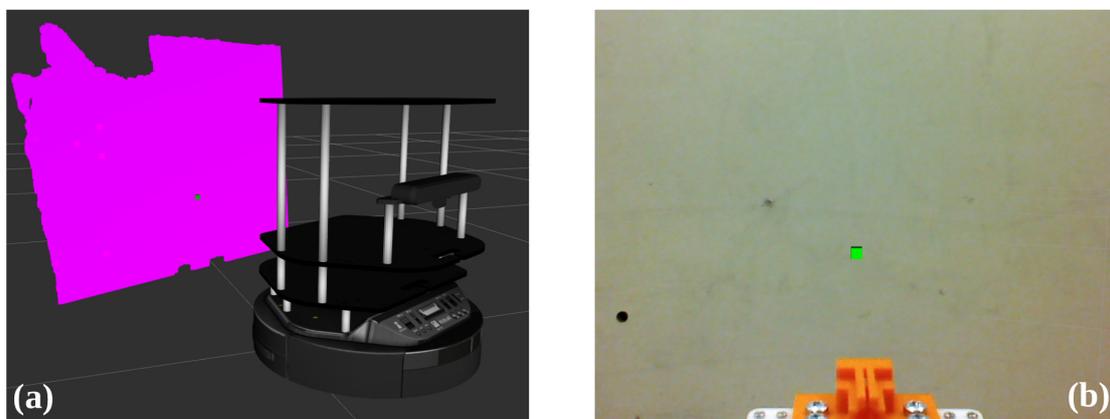
Figure 2 – (a) Target selection of the Raman diagnostic using RVIZ markers (green) with respect to a point cloud (pink), and (b) the augmented reality visual camera feed indicating the measurement point

of dosimetry is possible once again due to the spatial resolution offered by 3D mapping.

The use of CeBr scintillation gamma spectroscopy allows for identification of particular isotopes [7]. The synergy between the use of elemental, chemical, and radiometric information improves the confidence that can be associated with identifying materials and contamination, reducing risk, cost, and time during human lead exploration. These diagnostic measurements will be referenced to a full 3D LiDAR produced map, as visualised in real-time using RVIZ, and visualised post-measurement using a true 3D GIS (Geographical Information System) software.

REFERENCES

1. Nuclear Decommissioning Authority. Nuclear Decommissioning Authority Strategy: Strategy Effective from April 2016. TSO, 2016.

2. K. A. Wilson, and K. Stevens. Decommissioning planning for the Joint European Torus fusion reactor. In

3. 2007 Waste Management Symposia, 2007.

4. R. C. Wiens, et al. The ChemCam instrument suite on the mars science laboratory (msl) rover: Body unit and combined system tests. Space Science Reviews, 170(1), 2012.

5. A Lang, et al. Analysis of contaminated nuclear plant steel by laser induced breakdown spectroscopy.

6. Journal of Hazardous Materials, 345, 2018.

7. H. R. Kam, et al. RViz: a toolkit for real domain data visualization. Telecommunication Systems, 60(2), 2015.

8. F. G. A. Quarati, et al. Scintillation and detection characteristics of high-sensitivity CeBr3 gamma-ray spectrometers. Nuclear Instruments and Methods in Physics Research Section A: Accelerators, Spectrometers, Detectors and Associated Equipment, 729, 2013.

9. R. Jones, et al. On the design of a remotely-deployed detection system for reactor assessment at Fukushima Daiichi. In 2016 IEEE Nuclear Science Symposium, Medical Imaging Conference and Room-Temperature Semiconductor Detector Workshop (NSS/MIC/RTSD). IEEE, 2016.

Persuasive Robots for Motivation and Engagement (in Rehabilitative Therapies)

*Katie Winkle** January 31, 2018*

ABSTRACT

This paper gives an overview of current research being undertaken on human robot interaction (HRI) For social robots to be used as motivation and engagement tools in therapy. Socially assistive robots (SARs) provide assistance through social interaction. Past work in social HRI suggests that SARs can have an impact on engagement with health and wellbeing related activities. This work aims to further develop SAR interaction behaviours and artificial intelligence for task motivation and engagement, specifically considering the application of rehabilitative therapies which rely on patients undertaking self-led practice exercises.

I. INTORODUCTION

Socially assistive robots (SARs) are defined as those which provide assistance through their social interaction rather than providing physical aid [1]. Researchers are increasingly exploring the use of such robots in the domains of health, care and home support of older adults with ageing-related impairments (e.g. [2], [3] [4], [5]). It has been shown that social robots can have an impact on enjoyment and engagement with health and wellbeing related exercises/activities (e.g. [6], [7], [8], [9]).

Rehabilitative therapies increasingly rely on patient self-practice e.g. at home, typically in the form of an exercise programme to be undertaken without the therapist being present. Low adherence to such programmes is a known issue (e.g. [10], [11], [12]). We propose that SARs could be used to promote and facilitate such programmes with the patient and hence improve adherence. We are now working to identify the social cues and behaviours such a robot should employ.

II. STUDY WITH THERAPISTS

We conducted a study with therapists to explore the role of SARs in therapy and to generate a series of design implications for such SARs based on therapists' expert knowledge and best practices extracted from our results. The study consisted of focus groups, interviews and observations. Complete study design and analysis of the results is given in [13]. Key results included the importance of social interaction between the therapist and the patient, and the personalised approach to this that therapists take.

III. INTERACTION BEHAVIOUR & PERSONALISATION

Consideration of persuasion psychology in light of the findings from our study with therapists suggests we should that social human robot interaction design should target maximising peripheral persuasiveness as identified in the Elaboration Likelihood model of persuasion [14]. Peripheral persuasion is based very much on the social interaction and relationship between the message

_____

Bristol Robotics Laboratory, University of the West of England, Frenchay Campus, Coldharbour Lane, Stoke Gifford, Bristol BS16 1QY k.winkle@bristol.ac.uk

sender and receiver, and is typically employed when central persuasion, that which is based on reasoning and rationale, fails or is not enough. Further, the Theory of Planned Behaviour identifies user variables which should be

targeted by the robot persuasion strategies [15]. The relationship between therapist role, robot role, user behaviour and the

described psychological models is shown in Figure 1. This will inform our development and testing of robot behaviours, which will consider personalised social interactions, designed for maximum peripheral persuasion, and their impact on task engagement. This will be investigated with intermediary HRI experiments undertaken in the laboratory.
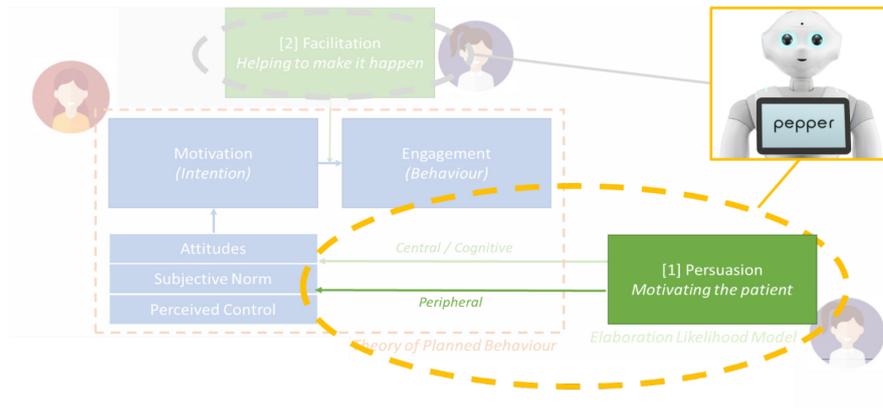
Figure 1: Role of robot system and associated psychological models for informing behaviour based on results from study with therapists and social psychology literature.
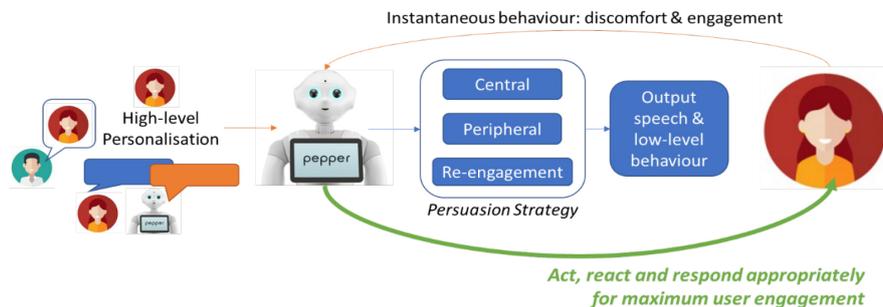
Figure 2: A cognitive architecture for informing robot behaviour should consider high level personalisation information as well as instantaneous user understanding in order to inform robot behaviour.

I.V. COGNITIVE ARCHITECTURE

Once initial behaviours have been developed and validated, a cognitive architecture will be developed in order to decide the robot's behaviour in real time. Imitating therapist behaviour this should incorporate high level personalisation settings with instantaneous user understanding in order to maximise user engagement in the requested task. This is depicted in Figure 2. Specific approaches have not yet been identified, but it is likely to involve a probabilistic approach

combining information in order generate probabilities for each possible action being the most appropriate. This could then also be combined with some instantaneous feedback mechanism for refinement. As an extension to this, the feasibility of using machine learning to adapt robot behaviour for improved/maintained impact over long term/multiple interactions will be investigated. The final system will be tested in a long term 'in the wild' study with real end users in order to evaluate real world effectiveness.

REFERENCES

1. Feil-Seifer and M. J. Matarić, "Defining socially assistive robotics," in *Rehabilitation Robotics, 2005. ICORR 2005. 9th International Conference on*, pp. 465–468, IEEE, 2005.

2. D. Kidd, W. Taggart, and S. Turkle, "A sociable robot to encourage social interaction among the elderly," in *Robotics and Automation, 2006. ICRA 2006. Proceedings 2006 IEEE International Conference on*, pp. 3972–3976, IEEE, 2006.

3. Montemerlo, J. Pineau, N. Roy, S. Thrun, and V. Verma, "Experiences with a mobile robotic guide for the elderly," in *AAAI/IAAI*, pp. 587–592, 2002.

4. H.-M. Gross, C. Schroeter, S. Mueller, M. Volkhardt, E. Einhorn, A. Bley, T. Langner, C. Martin, and M. Merten, "I'll keep an eye on you: Home robot companion for elderly people with cognitive impairment," in *Systems, Man, and Cybernetics (SMC), 2011 IEEE International Conference on*, pp. 2481–2488, IEEE, 2011.

5. M. Nani, P. Caleb-Solly, S. Dogramadzi, T. Fear, and H. van den Heuvel, "MOBISERV: an integrated intelligent home environment for the provision of health, nutrition and mobility services to the elderly," 2010.

6. K. Swift-Spong, E. Short, E. Wade, and M. J. Matarić, "Effects of comparative feedback from a Socially Assistive Robot on self-efficacy in post-stroke rehabilitation," 2015.

7. P. Gadde, H. Kharrazi, H. Patel, and K. F. MacDorman, "Toward Monitoring and Increasing Exercise Adherence in Older Adults by Robotic Intervention: A Proof of Concept Study," *Journal of Robotics*, vol. 2011, p. e438514, Oct. 2011.

8. A. Tapus, C. Tapus, and M. J. Mataric, "The use of socially assistive robots in the design of intelligent cognitive therapies for people with dementia," in *2009 IEEE International Conference on Rehabilitation Robotics*, pp. 924–929, June 2009.

9. R. Gockley and M. J. Mataric, "Encouraging physical therapy compliance with a hands-off mobile robot," in *Proceedings of the 1st ACM SIGCHI/SIGART conference on Human-robot interaction*, pp. 150–155, ACM, 2006.

10. S. D. O'Shea, N. F. Taylor, and J. D. Paratz, ". . . But watch out for the weather: factors affecting adherence to progressive resistance exercise for persons with COPD," *Journal of Cardiopulmonary Rehabilitation and Prevention*, vol. 27, pp. 166–174; quiz 175–176, June 2007.

11. R. Forkan, B. Pumper, N. Smyth, H. Wirkkala, M. A. Ciol, and A. Shumway-Cook, "Exercise adherence following physical therapy intervention in older adults with impaired balance," *Physical Therapy*, vol. 86, pp. 401–410, Mar. 2006.

12. M. Visser, R. J. Brychta, K. Y. Chen, and A. Koster, "Self-Reported Adherence to the Physical Activity Recommendation and Determinants of Misperception in Older Adults," *Journal of Aging and Physical Activity*, vol. 22, pp. 226–234, Apr. 2014.

13. K. Winkle, P. Caleb-Solly, A. Turton, and P. Bremner, "Social Robots for Engagement in Rehabilitative Therapies: Design Implications from a Study with Therapists," (In Press).

14. R. E. Petty and J. T. Cacioppo, "The Elaboration Likelihood Model of Persuasion," in *Advances in Experimental Social Psychology* (L. Berkowitz, ed.), vol. 19, pp. 123–205, Academic Press, Jan. 1986. DOI: 10.1016/S0065-2601(08)60214-2.

15. I. Ajzen, "The theory of planned behavior," *Organizational Behavior and Human Decision Processes*, vol. 50, pp. 179–211, Dec. 1991.

Design, Implementation and Experimental Evaluation of an IrisTK-Based Deliberative-Reactive Control Architecture for Semi-Autonomous Child-Robot Interaction in the Real-World Settings

Abolfazl Zaraki, Luke Wood, Ben Robins and Kerstin Dautenhahn
Adaptive Systems Research Group, School of Computer Science, University of Hertfordshire, UK
{a.zaraki, l.wood, b.robins, k.dautenhahn}@herts.ac.uk

I. MOTIVATION

A key challenge in the development of any autonomous robot is creating the ability for the robot to "reason", or understand the sensory information it is receiving, and plan the most appropriate action base on this input. This challenge becomes even more complex when operating in human-centred applications since the robot's reasoning relies on understanding human intention and social behaviours. In such situations, the robot should not only act as a reactive agent that simply displays a pre-defined set of behaviours without maintaining any internal state and without being aware of the status of the interaction. Instead, the robot should have the capacity to act as a deliberative agent that explores its behaviour space and predicts the effect of its reaction and displays an acceptable behaviour while taking into account the interaction scenario. The latter case is well suited for the development of autonomous robots and it may enable an acceptable Human-Robot Interaction (HRI) however, due to the performance requirements to facilitate such scenarios the implementation of a single module to deal with both the robot's planning and motor control is computationally expensive. Taking this into consideration it seems that a hybrid control architecture is most likely to provide the best solution when we develop an autonomous robot for real-world settings.

This paper summarizes the design, implementation and experimental evaluation of an IrisTK-based deliberative-reactive control architecture called "Sense-Think-Act" that gives some degrees of autonomy to the Kaspar robot [2][5] in Child-Robot Interactions (CRIs). As shown in Figure 1, the proposed architecture has three sub-systems that are fully interconnected via a TCP/IP network which deal with the robot's features from the perception system to the real-time action control system. The brain of the architecture, the "Think" layer, has been fully developed using the IrisTK [1] which is a powerful state chart-based toolkit for multi-party HRI designed for defining the interaction flow and developing autonomous systems. Although the architecture is technically capable of "fully autonomous" control over the robot's behaviour in a multi-party social interaction, due to the technical and ethical issues the robot must ask for the permission of human operator before displaying any behaviour to the interaction partners. For this reason, we have added a permission key to the architecture to keep the human in the control loop which prevents the possible ethical issues regarding the use of robots with human and particularly with vulnerable children. Besides, the permission key allows the human operator to take the control of the robot at any stage of interaction by overriding the robot's behaviour if it is needed. The developed architecture has been implemented on the humanoid robot Kaspar and evaluated in a trial with four children with Autism Spectrum Condition (ASC) at a local specialist secondary school in the UK.

We devised nine therapeutic games in which children individually play with the Kaspar robot (dyadic CRI) as well as two joint games in which children would play with the robot in pairs (triadic CRI). The games have been designed to encourage visual perspective taking (VPT) skills in children with autism [3][4]. For the purpose of evaluation, we tested the semi-autonomous Kaspar that we developed to play the same games that we have devised. The semi-autonomous Kaspar played four individual games with two children and also played a

supports any new module which is connected to the network even irrespective of programming languages which the module has been developed and also irrespective of the operation system that the module is functioning, this subsequently means they can easily be integrated into the architecture. One of the primary benefits to this architecture is potential for **scalability** allowing us to easily extend the architecture by adding new sensors/hardware devices and also new modules to the system.
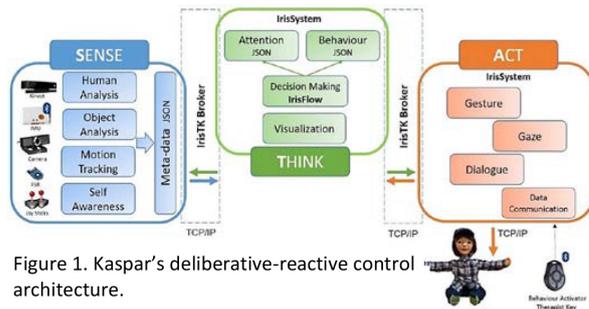
Figure 1. Kaspar's deliberative-reactive control architecture.

Figure2. Children are playing dyadic and triadic therapeutic games with semi-autonomous Kaspar.

joint game with a pair of children while a researcher was next to the robot to facilitate the interaction by evaluating the robot's behaviour and giving the final permission for the robot to display the behaviours recommended by the system. The preliminary results demonstrated the promising capabilities with regards to the architecture generating appropriate autonomous behaviours for the Kaspar robot to display which resulted in successful dyadic and triadic CRIs (Figure 2).

II. SYSTEM ARCHITECTURE

The architecture includes three **standalone layers** interconnected via a TCP/IP network (Figure 1). Each layer has a number of modules that process either the sensory data captured by sensors/hardware or the high-level information that are distributed to the network as "events" as standard JSON data packets. The layers and modules are **fully interconnected** and have the capacity to send and receive high-level information to the network. Thanks to the architecture's **modularity** and network structure the system is capable of **running on multiple devices** which allows handling the overall processing cycles for real-time applications, if required Since the architecture is **network-based** it is **platform independent** which means that it

In short, the architecture collects the sensory data and extracts high-level information and then streams the corresponding "events" as JSON packets to the network (Sense Layer). The central layer receives the JSON packets and evaluates which reactive behaviour is the most appropriate for the current situation taking into account the interaction status and high-level information, and then streams an action "event" (behaviour name) to the network and asks the robot to display that behaviour (Thinks Layer). The Act layer receives the action event from the network and moves the robot servos to display the behaviour on the permission of operator and returns the feedback/monitor "event" to the network to show that performing action has been completed.

Since the architecture communicates the high-level information in the JSON packets there are two main benefits. It facilitates a **real-time robot CRI** since data communication is so fast, and there is the potential to create the interaction log-file which includes all the distributed events during the interaction. This feature of the architecture is very important since allows **automatic data annotation** that is very helpful for post- processing the interaction data.

As discussed the Sense-Think-Act is a fully interconnected architecture in which means that the modules are connected to the same broker, they will receive all the distributed events over the network, however to reduce the computational costs, in each layer there is the possibility to subscribe only to the events that are necessary for that layer and dismiss all the other events.

II. EXPERIMENTAL EVALUATION OF THE SYSTEM WITH CHILDREN AT THE SCHOOL

We implemented the proposed architecture on the Kaspar robot and tested it at the school for two main reasons: to evaluate the real-time performance of the architecture in controlling the Kaspar robot in the real- world settings, and to find out if the architecture is capable of controlling the robot's behaviour in an autonomous and acceptable way in dyadic and triadic interactions with children. We installed the three layers of the architecture on the same laptop (Toshiba Tecra, Intel Core i7, 2.60 GHz, 16GB RAM) for the compatibility test as well as to check the overall real-time performance. Four children with autism with different levels of ability took part in the study and in total the data of 11 child-robot interactions were collected. As the results demonstrated, the architecture was able to provide robot control signals all the time in real-time without any latency which supports real-world applications. Besides, the "think" and "act" layers functioned correctly in all interaction sessions however due to the real-world relevant issues (lighting conditions, etc.) we got some issues in the object analysis module which we had to override the robot behaviour. Lastly, three layers of architecture and their modules were successfully operated in real-time on the same laptop.

I.I.I. FUTURE WORK

To have a reliable autonomous humanoid robot, compatible and robust to the changes of environmental factors (light, noise, etc.), we are integrating a long-range RFID technology to the architecture in order to replace the object and human motion analysis modules and we hope to have a more reliable and acceptable autonomous child-robot interactions.

ACKNOWLEDGMENTS

REFERENCES

1. G. Skantze, and S. Al Moubayed, "IrisTK: a statechart-based toolkit for multi-party face-to-face interaction," In Proceedings of the 14th ACM international conference on Multimodal interaction, pp. 69-76. ACM, 2012.
2. K. Dautenhahn et al., "KASPAR: A minimally expressive humanoid robot for human–robot interaction research," Applied Bionics and Biomechanics, vol. 6, pp. 369-397, 2009. [4] B. Robins and K. Dautenhahn, "Tactile interactions with a humanoid robot: novel play scenario implementations with children with autism," International Journal of Social Robotics, vol. 6, no. 3, pp. 397-415, 2014.
3. L. Wood, K. Dautenhahn, B. Robins, and A. Zaraki, "Developing child-robot interaction scenarios with a humanoid robot to assist children with autism in developing visual perspective taking skills". In Proceedings of the 26th IEEE International Symposium on Robots and Human Interactive Communication (Ro-Man), pages 1-6. IEEE, 2017.
4. Robins, K. Dautenhahn, L. Wood, and A. Zaraki, "Developing Interaction Scenarios with a Humanoid Robot to Encourage Visual Perspective Taking Skills in Children with Autism–Preliminary Proof of Concept Tests". In Proceedings of the 9th IEEE International Conference on Social Robotics (ICSR), pages 147-155, 2017.
5. L. Wood, A. Zaraki, M. Walters, O. Novanda, B. Robins, K. Dautenhahn, "The Iterative Development of the Humanoid Robot Kaspar: An Assistive Robot for Children with Autism". In Proceedings of the 9th International Conference on Social Robotics (ICSR), pages 53-63, 2017.

Motor Imagery Classification based on RNNs with Spatiotemporal-Energy Feature Extraction

Dan-Dan Zhang, Jian-Qing Zheng, Jahanshah Fathi, Miao Sun, Fani Deligianni and Guang-Zhong Yang, Hamlyn Centre for Robotic Surgery, Imperial College London, London, United Kingdom

ABSTRACT

With the recent advances in artificial intelligence and robotics, Brain Computer Interface (BCI) has become a rapidly evolving research area. Motor imagery (MI) based BCIs have several applications in neuro- rehabilitation and the control of robotic prosthesis because they offer the potential to seamlessly translate human intentions to machine language. However, to achieve adequate performance, these systems require extensive training with high-density EEG systems even for two-class paradigms. Effectively extracting and translating EEG data features is a key challenge in Brain Computer Interface (BCI) development. This paper presents a method based on Recurrent Neural Networks (RNNs) with spatiotemporal-energy feature extraction that significantly improves the performance of existing methods. We present cross-validation results based on EEG data collected by a 16-channel, dry electrodes system to demonstrate the practical use of our algorithm.

I.INTRODUCTION

Robotic control based on brainwave decoding can be used in a range of scenarios including patients with locked-in syndrome, rehabilitation after a stroke, virtual reality games and so on. In these cases, subjects may not be able to move their limbs. For this reason, the development of MI tasks based BCI is very important [1]. During a MI task, the subjects imagine moving a specific part of their body without initiating the actual movements. This process involves the brain networks, which are responsible for motor control similarly to the actual movements.

Decoding brain waves is challenging, since EEG signals have limited spatial resolution and a low signal to noise ratio. Furthermore, experimental conditions, such as subjects' concentration, prior experience with BCI, can bring confounds to the results. Thus far, several approaches have been proposed to classify MI tasks based data but their performances are limited even for the two-class paradigms that involve left and right hand MI tasks [2]. EEG-based BCI normally involves noise filtering, feature extraction and classification. Brain signals are normally analysed in cue-triggered or stimulus-triggered time windows. Related methods include identifying changes in Event Potentials (EPs), slow cortical potentials shifts, quantify oscillatory EEG components and so on [3]. These types of BCI are operated with predefined time windows. Furthermore, the inter- and intra-subject variability cannot be overlooked when finding suitable feature representation model.

Recently, Deep Neural Networks (DNNs) have emerged with promising results in several applications. Their adaptive nature allows them to automatically extract relevant features from data without extensive pre-processing and prior knowledge about the signals [4]. Convolutional Neural Networks (CNNs) have been used to classify EEG features by transforming the temporal domain into spatial domain [5]. However, the CNN structure is static and inherently unsuitable for processing temporal patterns. Furthermore, the trend in BCI is to reduce the number of channels and thus construct a sparse spatial representation of the signal, which impedes the effectiveness of CNNs. To deal with time series data, recurrent neural networks (RNNs) based on Long Short-Term Memory (LSTM) seems to be a better choice since they can preserve temporal

characteristics of the signal [6]. In this paper, we propose a novel approach to decoding multichannel EEG raw data based on RNNs and spatiotemporal features extracted from the EEG signal. Appropriate spatiotemporal feature extraction could play an important role in improving learning rate in these DNN. The presented results were based on an EEG dataset acquired using a dry, 16-channels, active electrodes g.tec Nautilus system. Although wet, active electrodes are the gold standard in EEG signal acquisition, they require long preparation times and the conductive gel to reduce skin-electrode impedance, which makes the subjects feel uncomfortable [7]. Dry electrodes make it easier to bring BCI systems from the laboratory to the patients' home but with the challenges of decoding low-quality signals. Therefore, there is a need for the development of more advanced methods for feature extraction and classification.

II.METHODS

Experimental Setup: EEG data were recorded from four healthy participants (one female, three males, 21-24 years old). During the experiment, the subjects were asked to complete a Graz-BCI MI task [8] for two-class (right/left hand, 20 trials/class). Subjects had no previous experience with BCI. A g.tec *Nautilus*, 16-channels dry, *g.Sahara* electrodes, EEG wireless acquisition system was used with active-electrodes placed on the subject's scale according to the standard 10-20 system.

Figure 1 (a) shows the original electrodes distribution, while Figure 1 (b) shows the mapping relationship of the spatial distribution of the feature graphs.

Feature Extraction based on spatiotemporal energy characteristics: Three feature representation methods were tested in the experiments. Figure 1 (c) shows the spatiotemporal feature graph.

The value of each pixel represents the normalized amplitude of a specific channel during a time epoch. Subsequently, short time Fourier Transform was used to extract Time-Frequency features as shown in Figure 1 (d), represented as a graph. The combination of spatiotemporal characteristics along with energy spectrum has provided the most effective classification features. To construct these features, the band power was used to track amplitude modulation at particular frequencies (8Hz-30Hz) related to motor intention, namely $m(7\text{ -}13Hz)$ and b (13 - $30Hz$) . In other words, the power spectral intensity was estimated for μ and β band, respectively as $E(m)$ and $E(b)$. Subsequently, the intensity ratio $p = E(m) / E(b)$ was used as a classification feature. After normalization, each pixel in the feature graph represents the ratio of energy in each time epoch of every channel, which provides information about the spatiotemporal distribution of energy. Finally, interpolation was utilized to smooth the energy spectral ratio graph, as shown in Figure 1 (f).
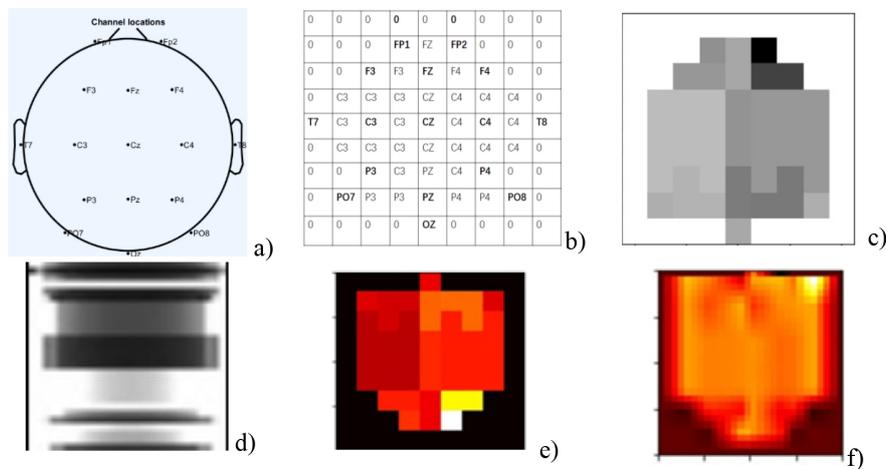
Figure 1. a) 16 channels EEG helmet electrodes distribution, b) spatial distribution of the feature graph, c) Spatiotemporal Feature Graph (ST-FG), d) Time-Frequency based features across channels and epochs (without spatial information), e) Spatiotemporal-Energy Feature Graph (STE-FG), f) Smoothed Spatiotemporal-Energy Feature Graph (STE-FG).

RNN Framework for Classification: A RNN based on LSTM is trained to learn features from the sequences of EEG data. LSTM units were employed to construct each RNN layer, since they are less sensitive to the gradient vanishing and exploding problems. The proposed approach is designed to preserve the spatiotemporal and energy information of EEG and to extract features that are less sensitive to noise within each channel.

III.RESULTS

The proposed method used has been compared with other common approaches used for motor imagery classification. The results have been summarised in Table 1. The first column shows results based on Common Spatial Pattern (CSP) for feature extraction and Support Vector Machine (SVM) for classification implemented in Matlab. To improve classification performance, the EEG signals have been pre-processed with a wavelet- based technique to preserve frequencies between 0.1 and 40 Hz and removed physiological noise related to eye blinks [9][10]. The proposed methods have also been evaluated against CNNs, while different features extraction methods are evaluated at the same time.

I.V.CONCLUSIONS

Our results show that the RNN classification method based on spatiotemporal energy characteristics outperforms both methods based on CSP/SVM and CNNs. Preserving the spatiotemporal information along with extracting energy features plays a critical role in the overall performance of MI tasks based data classification.

Table 1. Comparison for the classification accuracy of the motor imagery tasks.

	CSP/SVM	ST-FG/CNN	STE-FG/CNN	ST-FG/RNN	**STE /RNN**
01	56.5 %	50.9 %	60.1 %	62.5 %	**80.8 %**
02	54.5 %	54.4 %	56.3 %	72.3 %	**88.7 %**
03	52.7 %	55.0 %	57.8 %	`58.7 %	**75.6 %**
04	61.9 %	52.1 %	59 .0 %	60.5 %	**80.5 %**
Mean ± std	56.4±4.0 %	53.1±1.9 %	58.3±1.9 %	63.5±6.1%	**81.4 ±5.4%**

REFERENCES

1. Pfurtscheller, G, and L. D. S. Fh. "Event-related EEG/MEG synchronization and desynchronization: basic principles. " Clinical Neurophysiology 110.11(1999):1842-1857.
2. GüçlÜ, Umut, and K. L. Chu. "Evaluation of fractal dimension estimation methods for feature extraction in motor imagery based brain computer interface." Procedia Computer Science 3.1(2011):589-594.
3. Pfurtscheller, G, et al. "Graz-BCI: state of the art and clinical applications." IEEE Trans Neural Syst Rehabil Eng 11.2(2003):1-4.
4. D. Ravi, C. Wong, F. Deligianni, M. Berthelot, J. Andreu-Perez, B. Lo, G. Z. Yang, Deep Learning for Health Informatics, IEEE Journal of Biomedical and Health Informatics, 21(1), 2017.
5. Cecotti, H, and A. Graeser. "Convolutional Neural Network with embedded Fourier Transform for EEG classification." International Conference on Pattern Recognition IEEE, 2008:1-4.
6. Gers, Felix A., D. Eck, and J. Schmidhuber.

"Applying LSTM to Time Series Predictable through Time- Window Approaches." International Conference on Artificial Neural Networks Springer-Verlag, 2001:669-676.
7. Sun, Mingui, et al. "A low-impedance, skin-grabbing, and gel-free EEG electrode." 2012.4(2012):1992- 1995.
8. Pfurtscheller, G, et al. "Graz-BCI: state of the art and clinical applications." IEEE Trans Neural Syst Rehabil Eng 11.2(2003):177-180.
9. Khatun, Saleha, R. Mahajan, and B. I. Morshed. "Comparative analysis of wavelet based approaches for reliable removal of ocular artifacts from single channel EEG." IEEE International Conference on Electro/information Technology IEEE, 2015:335-340.
10. Bigirimana, A. D., N. Siddique, and D. Coyle. "A hybrid ICA-wavelet transform for automated artefact removal in EEG-based emotion recognition." IEEE International Conference on Systems, Man, and Cybernetics IEEE, 2017.

Poster Papers